TRIBO-ELECTROSTATIC SEPARATION OF SOUTH AFRICAN FINE COAL

Samson Oluwaseyi Bada

A Thesis submitted to the Faculty of Engineering and the Built Environment, University of the Witwatersrand, in fulfillment of the requirements for the degree of Doctor of Philosophy in Engineering.

Johannesburg, 2010

Declaration

I declare that this dissertation is my own unaided work. It is being submitted for the degree of Doctor of Philosophy in the University of the Witwatersrand, Johannesburg. It has not been submitted before for any degree or examination in any other University.

Signature: S.O Bada

……………………………..

May 2010

ABSTRACT

The need for the research into the tribo-electrostatic separation of South African high ash coal had increased significantly due to the depletion in the reserves of high grade coal, increase in SO_X and NO_X generation of low grade coal and increase in the South African power utility's coal burn rate. Wet coal beneficiation techniques have been reported for the beneficiation of South African fine coal, no info is available on dry beneficiation of South African coal using tribo-electrostatic technique. Hence, the dry coal beneficiation method which serves as an alternative approach to wet coal cleaning processes must be studied, importantly, for the coal producing countries such as South Africa (SA) where fresh water is scarce and precious.

This research presents an experimental study of rotary tribo-electrostatic separation (RTS) as an alternative approach for beneficiating steam coal mainly used in South African power plants. An RTS with an octagonal charger has been used in beneficiating eight types of South African coals with a feed coal ranging between 22% and 40% ash content. The cleaning potential of the coal samples was first evaluated using sink/float and kinetic froth flotation test with the -177 µm coal fraction and then using the rotary tribo-electrostatic separation in one and two stages. The RTS tests were conducted under different system parameters such as, applied charger potential, applied separating voltage, air injection velocity, particle feed rate, rotation speed of the copper plated rotor and splitter distances were investigated for their effects on the separation performance.

The two stage separation results with the -177 µm size fraction show the RTS reduced Majuba coal containing about 30.10% ash to a clean product of 14.30% and 19.46% ash at a combustible

matter of 15.10% and 53.02%, respectively. The calorific value for the feed coal was increased from 20.15 MJ/Kg to 27.48MJ/Kg with combustible matter of 11.10% after the second stage of separation while the single stage separation produced a clean coal product with 25.67 MJ/Kg, 16.10% ash and 29.23% combustible matter for Majuba coal. The RTS process reduced the ash content of the -177 µm coal fraction by nearly 14.92% for the Klipfontein coal and 12.21% for the Liketh Townlands coal, with corresponding combustible matter values of 10.73% and 8.90%, respectively. Total sulphur content was also reduced from 2.10% to 0.92% for the Klipfontein coal and from 2.81% to 0.40% for the Liketh Townlands coal at corresponding combustible recovery values of 5.74% and 8.90%, respectively.

Under the same operating condition, one stage of RTS separation produced a clean coal product with 14.80% ash at a combustible recovery of 28.24% from a coal feed with 22.12% ash for the Koorfontein coal. Cleaner coal of about 14.50% ash and 17.43% combustible matter was obtained at 0.6 cm away from the negative electrode, and 15.72% ash with 28.12% combustible matter at splitter position of 1.0 cm away from the negative electrode. The total Power loss model (P_t) was used to analyze the experimental data for the energy consumption or required for octagonal rotary charger at a surface tangential speed of 2500 rpm. The X-ray diffraction analysis of the feed, single and second stage coal products confirmed a reduction in the mineral content with an improvement in the organic composition for all coal samples.

The studies showed that rotary tribo-electrostatic separation (RTS) technique can be applied for effective dry coal cleaning of South African coal.

DEDICATIONS

This thesis is dedicated to God, my parents and Sisters

ACKNOWLEDGEMENTS

The thought that this research will be a success right from the start had filled my heart with such purpose and gave me the inspiration to strive so I can achieve success in all am attracted to. My life has been touched and influenced by so many people.

First, I am grateful to the Almighty God for granting me favour, intellect and capability to undertake this project. I would also like to sincerely acknowledge my supervisors, Prof R.M.S. Falcon and Mr L.M. Falcon, my deepest gratitude for their love, constant guidance, constructive suggestions, encouragement and financial support through my graduate program. Thank you for teaching me how to become a researcher.

Expressed appreciation is also due to Prof R.Q. Honaker and Dr Daniel Tao for their enormous time, insightful criticisms and patient encouragement aided in the completion of my experimental work at the University of Kentucky, USA. My gratitude also goes to Ms Blair and Mrs Gail Gordon, for being there for me at all times.

I also gratefully acknowledge the financial support by the South African National Energy Research Institute (SANERI), Mr Ed Thompson with the Department of Mining Engineering of the University of Kentucky and the Kentucky Geological Survey for granting permission to perform XRD analyses

Without the advice and encouragement from many relatives, friends and colleagues this thesis would not have been possible. Special thanks to my mom and dad, I do appreciate all you did. I would also like to thank my siblings, my sisters, Mr Omosehin, my nieces, OmoT and nephews.

Finally, to my close friends who have offered such precious emotional support that will never be forgotten. My thanks go especially to Magnus, Saka, Afolabi, Debbie, and Dayo,

LIST OF ACRONYMS

RSA	Republic of South Africa
SAC	South African Coal
FGD	Fluidized Gas Desulphurizer
FGX	Fluidized bed and a table concentrator
RTS	Rotary Triboelectrostatic separator
IGC	Inverse Gas Chromatography
ADMFBS	Air Dense Medium Fluidized Bed Separator
AED	Advanced Energy Dynamic
VFB	Vibrated Fluidized Bed
CFB	Conventional Fluidized Bed
HGMS	High Gradient Magnetic Separation
LOI	Loss on Ignition
LMT	Lithium Metatungstate
t_b	Breakthrough time at desired concentration (h)
V	Linear flow velocity of the feed to bed $(ml/\min)$
l	Volume of adsorbate (ml)

Table of Contents

Page

LIST OF TABLES

Table

LIST OF FIGURES

Figure **Page**

CHAPTER ONE

1.0 Introduction

1.1. Background and Motivation

The need for the research into the tribo-electrostatic separation of South African high ash coal had increased significantly due to the depletion in the reserves of high grade coal, and increase in the South African power utility's burn rate, which had risen at an annual rate of 4.5 %, from 88Mt in 1999 to 125Mt in 2007 (Piet and Moothoo, 2008). The republic of South Africa (RSA) is the fourth largest coal-producing country and the third largest exporter of coal, behind USA and Australia (Budge, 2000). South Africa (SA) is being ranked in the world as the second country that is heavily dependent on coal for generating electricity (WCI, 2008), and with its present consumption rate in utilizing coal to generate electricity, a mere 7 billion tons might remain by 2040 and future coal reserves is expected to be high in ash (Mbendi, 2004).

In 1982, the coal reserve in South Africa was estimated to be 50 billion tons. An estimated 74% of the 5.3 billion tons of coal mined in South Africa till 2003 came from Witbank and Highveld coalfields (Fauconnier, 2005). In addition, out of the 150 – 160 megatons of coal produced for the domestic market in 2000, approximately 92 megatons and 51 megatons were used by Eskom and Sasol respectively. The remainder was used by the cement, and other industries. A large proportion of SA seams are generally believed to contain a high content of ash, and difficult to wash. This is because it contains high Near Gravity Material which causes it to yield low calorific value product, making it unfavourable for effective utilization (Falcon and Falcon, 1983; Dieudonne, 2001). In addition, SA coals are renowned for being difficult to beneficiate because the mineral matter is so finely entrained within the organic matrix.

South African coal (SAC) are Gondwana in origin and are characterized by high levels of ash that are often finely disseminated throughout the coal matrix with thinner earth crust and lower coal rank (Falcon, 1986). Their nature is different to that of Northern hemisphere coals due to the conditions prevailing during the course of its formation and subsequent geological events (Falcon and Ham, 1988). These coals are difficult to clean, and their utilization in the power plants generated pollutants that cannot meet the Clean Air Act enacted by different governments to limit SO_X generation. The idea of using dry beneficiation techniques as an alternative approach for the beneficiation of SAC started from the uneconomical application of wet process for the beneficiation of coal in fine fraction (-600 μm). Hence, most of the coal beneficiation processes employed in SA are based on wet techniques, which introduces large quantities of potential pollutants. The estimated cost of handling/treating these pollutants constitutes a major disadvantage to many of these techniques (Lockhart, 1984). Moreover, the large quantity of water used or lost during coal preparation, costs associated with ancillary items, such as flotation reagents, thickeners, cyclones and filtration machines, coupled with the cost of managing and treating large quantities of aqueous slurries generated during wet beneficiation are some of the challenges facing this technique, irrespective of their market demand or the technical feasibility of the wet beneficiation techniques. In comparison, the dry beneficiation of coal has certain advantages over wet beneficiation such as dry handling of coal, less capital expenditure as it does not require thickener to settle the fines and tailing ponds to discharge the effluents and retention of high calorific value at the same coal quality product. Therefore, there is a need to conduct a detailed research using triboelectrostatic technique as an alternative approach in upgrading SAC relative to introduction of future Fluidized Gas Desulphurizer (FGD) plants in the post-utilization stage at power stations.

Recently, extensive research had been conducted on the development of high separation efficiency dry beneficiation techniques, with economical advantages and little engineering constraints. These techniques are based on the differences in the characteristics of the coal constituents such as specific gravity, grindability/friability, shape, size, magnetic susceptibility, electrical resistivity and frictional coefficient. Hence, with these differences in coal properties, equipment such as fluidized bed tribo-electrostatic separator, air dense medium fluidized bed separator, pneumatic tribo-electrostatic separator, pneumatic jig, pneumatic table, electrostatic sieve conveyor and Sortex machine applicable to different particle sizes, have been used to beneficiate coal (Gidaspow *et al.*, 1987; Cheng and Yang, 2003; Trigwell *et al.*, 2003b; Weitkämper and Wotruba, 2004; Biswal *et al*., 2005; Choung *et al*., 2006; Dwari and Rao, 2006; Dwari and Rao, 2008). The findings of Stencel *et al.* (1998) and Dwari and Rao (2008) on Indian coal and Northern hemisphere coal, respectively, show that dry beneficiation has the potential of separating pyrite and mineral matter from pulverized coal before being fed into the boilers. The success of this approach will definitely improve the existing boiler's efficiency, increase its life span, and improve the surrounding atmosphere. The cost of installing the dry process can be justified by the improved performance of the power station.

In this study, an innovative rotary tribo-electrostatic separator (RTS) developed at the University of Kentucky, USA, was used for the separation of organic matter from its mineral matter in coal. The equipment relies on differential charge imparted on the coal and mineral matter for effective separation in an electric field. This research presents the application of single-stage separation with middling recycling, as well as two stage separation under the optimum process conditions for maximum combustible recovery and improved calorific values using eight different coal samples. The total sulphur of the feed coal and cleaned coal from single and two stage separation were analysed along with the yield. The effects of applied charger potential, separation chamber voltage, feed rate, injection air velocity, tangential speed of the rotor, Co-flow velocity and splitter distances that determine the process separation efficiency were also investigated. The total sulphur of the feed coal and cleaned coal was analysed along with the particle distribution as a result of the applied voltage in separating the coal particles. The mineral and organic compositions in the feed, single stage and second stage coal products were characterized using the X-ray diffraction analysis to determine the effects of RTS separation. The performance curves generated were used to evaluate the separation performance for all samples. The washability test as well as the flotation rate test was also conducted to study the liberation attribute of the coal samples prior to the application of RTS. The performance curves obtained were used to evaluate the separation performance for all the samples. This investigation was worth conducting due to the depletion in the reserves of high grade coal and the fact that water demands will be a major problem for present and future developments in coal processing in South Africa.

1.2. Justification of the study

Several studies have been reported on wet beneficiation of coal both in South Africa and the world in general, but none have been recorded in the dry beneficiation of coal using electrostatic separator in this country as proposed. Due to the absence of studies on dry beneficiation, it is worthwhile to investigate the RTS system parameter as regards on its influence on the beneficiation of South African coal. Likewise, no work has been reported on the recovery of free ash and macerals separation of SAC using Tribo-electrostatic separator. Hence, this investigation was worth conducting due to the depletion in the reserves of high grade coal in South Africa, and the reproducibility in the cleaned coal product obtained from the RTS.

1.3. Problem Statement

The separation of coal components depends on the difference in the characteristics of the constituents of the run of mine. All the techniques employed in coal beneficiation for the removal of ash-bearing minerals in coal are based on the differences in physical characteristics of coal such as specific gravity, particle size, grindability/friability, surface and electrical properties. These physical properties also provide the means of carrying out the separation between the coal constituents, and therefore form the theoretical basis for the development of beneficiation techniques (Tsai, 1982). Recently, Dwari and Rao (2006) had applied fluidized bed tribo-electrostatic method for the cleaning of high ash non-coking coal and they found that the increase in the separation of the macerals from minerals depends on the applied electrode's voltage and other varying system parameters.

Despite the encouraging incentives from the dry beneficiation techniques as an alternative to wet processes for upgrading the quality of coal, there are still major challenges to be overcome. Problems such as inferior separation or low recovery, temperature and moisture content of the feed coal, particle charged saturation and greater attention to dust control which are easier to handle than slime, necessity for pre-screening into narrow size fractions, high sensitivity to changes in feed (charges, size, moisture, rate) are problems facing dry beneficiation application (Lockhart, 1984). These challenges are also applicable to some extent to wet methods. The inferior separation or low separation capacities noted under this approach are as a result of insufficient or inadequate liberation of the coal minerals from the organic coal matrix (Mazumder *et al.,* 1994), dampness that causes stickling and agglomeration of the particles of opposite polarities which mostly occurs in the charging chamber, and the particle build up on the surface of the electrodes as the applied separation potential increases. One of the approaches to overcome this problem is by crushing of coal fine to enable the pyrite to be liberated from the macerals group by the difference in their grindability (Tsai, 1982) and pre-heating of coal particles to remove the surface moisture prior to separation.

Perfect operating conditions are difficult to achieve in charging particles in the charging chamber and separating particles in the separating zone. The increase in the charger rotational speed in the charging chamber causes charge backflow or discharging due to the particle attaining its maximum charge density, thereby reduces the magnitude of charges imparted on the coal particle. This problem, along with low recovery and effective separation under this technique were optimized through the use of effective applied charging, separating potential and charger rotary speed at both single and two stage of separation by considering all others operating parameters for high separation efficiency.

1.4. Hypothesis

It is proposed that a novel dry beneficiation technique (RTS) is feasible for the removal of ash-forming minerals rather than reducing the sulphur content alone and also for improving the quality of the SA coal by taking into account the differences in the electrical characteristic of coal constituents, and also the process parameter such as splitter distance, feed rate, charger rotation speed, charging potential and separation potential. This result will form basis for further research in the separation of various coals from different deposits. Furthermore, the separation efficiency of the RTS and South African coal may differ significantly from those studied conducted with other dry techniques before due to the unique compositional and surface characteristics of the South African coal.

1.5. Aim and Objectives of the Research:

The aim of this study is to develop a cost effective and sustainable dry beneficiating processing route for separating South Africa coal organics from its minerals using a novel triboelectrostatic separator. This aim is expected to be achieved using these objectives;

i. To study the influence of mineralogy in determining optimal operating parameters for coal cleaned through single and second stage tribo-electrostatic method.

ii. To investigate the separation efficiency of this technique for improving the calorific value and reducing the total sulphur in the pulverized coal used in this study.

iii. To investigate the separation efficiency of this technique for cleaning pulverized coal as against froth rate test and sink/float technique.

iv. To establish whether varying the operating parameters will favour the separation of coal organics from coal minerals within the set-up.

v. To determine the optimum process conditions for maximum yield and high grade coal by running both single-stage and second stage separation tests.

1.6. Structure of the Thesis

The thesis starts from chapter one with an introduction outlining the importance of the research, motivation behind it, problem statement and the research objectives.

Chapter two covers the literature review of the charging mechanisms of triboelectrostatic separation and corona electrostatic separators, including models that explained how contact electrification can be achieved between two dissimilar particles.

The existing different techniques being utilized in dry beneficiation processes for separation of coal organics from its mineral matter, and the utilization of tribo-electrostatic separator is also discussed with detailed focus on the investigation reported by many researchers with regards to various operating parameters and the coal properties in chapter three. The application of other dry beneficiating techniques and other materials that can be beneficiated through the use of tribo-electrostatic techniques were also discussed under this chapter.

Chapter four discusses the detailed methodology and experimental techniques used for the characterization of the coal samples, tribo-electrostatic studies conducted, froth rate test, and sink/float analysis at different densities were discussed in details. The analytical techniques used in characterizing the feed and the cleaned products were thoroughly discussed and the results obtained from the particle size analysis also presented in this chapter.

Chapter five discusses the results obtained from the X-ray diffraction analysis for the single and two stage separation tests. The calorific values and total sulphur analysis conducted on the feed, single and two stage products are also stated in this section. The results from the proximate analysis of all the feed coal samples are presented, including the single and two stage tribo-electrostatic separation test, froth rate test and washability test.

The thesis is concluded in chapter six which contains the drawn conclusions and recommendations for future work.

CHAPTER TWO

2.0. Literature Survey (Mechanisms and theory of Tribo-charging)

The rapidly growing coal industry requires the development of new technologies and thorough improvement on the existing techniques in the area of dry beneficiation. Although many wet coal beneficiation techniques have been reported for the beneficiation of South African fine coal, scarce information on dry beneficiation of South African coal using tribo-electrostatic technique is not available. Wet coal separation techniques use water as separation medium, which necessitates the costly dewatering process and increases the transportation cost of the clean coal product to the power plant. The application of dry beneficiation technique has maintained a number of advantages over this approach, in terms of low energy consumption, no product dewatering, less environmental pollution, and its economical competitiveness since energy is not expended in drying fine coal, as coal being mainly used as fuel (Lockhart, 1984).

The differences in the surface electronic structure of the minerals from the organic phases in coal, and their electrical resistivities are responsible for particle electrostatic separation (Kelly and Spottiswood, 1989a), while the amount of charge exchanged between two contacting surfaces and the difference in their work functions and conductivities determines the degree of separation. Electrostatic separation of coal particles is based on the fact that coal constituents can be differently charged and separated when an external electric field is applied. The techniques of charging, along with other co-acting forces - such as centrifugal and gravitational forces, contributes to the effective separation of materials (Manouchehri *et al*. 2000). Inductive conduction, contact or friction (triboelectrification), and ion bombardment are three mechanisms often required in the charging of particles (Harper, 1967; Kelly and Spottiswood, 1989).

However, triboelectrification is predominately used in coal and minerals processing industry, due to its effective particle charging and separation efficiency. Developmental efforts in this regard have led to the design of a novel rotary charger, which was used in this study for higher charging magnitude and selectivity of particle charging. The schematic representation of the rotary separator is shown in page 63.

2.1. Electrostatic Processes:

The utilization of electrostatic separation techniques have been largely developed and employed in various fields for mineral beneficiation and for agricultural applications (Trigwell *et al.,* 2003; Butcher and Rowson, 1995; Dwari and Rao, 2007). The rotor-typed techniques, which use the induction of the corona charging, had been employed in separating raw materials into conductive and non-conductive materials based on their conductivity. Corona charging is applied in cases where there is a large difference in the work function of the material involved. Due to the similarity in the physical properties – such as in the work functions of the coal particles, the rotor-typed technique had been found ineffective for the separation of the ash components in coal. Triboelectrification, which is also influenced by the work functions of the materials involved, has been found to provide an alternative approach for charging and separating coal particles (Higashiyama and Asano, 1998; Soong *et al.,* 2001; Chen and Wei, 2003; Dwari and Rao, 2008). This mechanism enables increased charge magnitudes for effective separation of coal, and encourages more researches into dry beneficiation.

2.2. Charging Mechanisms

The three different electrostatic charging mechanisms involved in materials processing are discussed in this section.

2.2.1 Ion Bombardment

This process is one of the most efficient charging processes and can be applied in a consistent manner to charge particles and droplets either positively or negatively within a relatively short period of time, usually less than 1 sec. It can be applied to both insulating and conducting particles in a wide size range. Hence, ion bombardment of particles may be visualized by considering the conductor and non-conductor (dielectric) particles touching a grounded conducting surface. The difference in conductivities between the component particles in the materials is usually an essential pre-requisite for a successful separation. The bombarded particles are charged by feeding them through an atmosphere of charged gases. The charged gas is generated from a high-intensity electric field between the grounded roll electrode/metal and one or several electrodes connected to a high-voltage supply. Also, an increase in the distance between the electrodes, and the magnitude of the applied voltage increases the current generated and enhances particle separation efficiency (Lama and Gallo, 1976). Once the ion bombardment ceases, the insulating particles are held, or pinned, to the surface of the rotating roll electrode by the electric image force and the conducting particle loses its acquired charge to ground very rapidly. This is because there are no electrostatic forces to hold it to the conducting surface (Samuila *et al.,* 2005). In other words, the conducting particles are not affected by the corona field; they are charged by electrostatic induction in contact with the grounded roll and are attracted to the high voltage. If the electrostatic force is larger than the force of gravity or other forces tending to separate the dielectric particle from the conducting surface, the particle is held in contact with the surface (Knoll and Taylor, 1984).

2.2.2. Tribocharging and Contact

Tribocharging occurs through both the contact charging and friction charging mechanisms by utilizing the differences in the surface electronic structure of the particles involved. In both cases, the mechanical processes that produce the charges on the materials are sliding, rolling or milling, impact and vibration of the surface at contact, separation of solid–solid, solid–liquid, and liquid–liquid surfaces, and deformation leading to charge distribution at stress points (Mazumder *et al.*, 2006). In the case of a rotary charger, which was used for this study, the particles are charged due to the collision between the cylindrical charging chamber, particle-particle contact and the rotating charger octagonal copper plated surface. This action known as tribo-electrification causes the transfer of negative charges (electrons) from the surface of one particle to another, with two different polarities within the particles. The magnitude of tribo-electric charge exchanged between two contacting surfaces will depend upon their relative speed, residence time, the difference in their work function, and on the pressure between the surfaces in contact. Also, as the pressure increases, the area or the number of contact points increases, leading to a very high surface charge density.

2.2.3. Induction Charging

This is the process by which static field is used in charging particles. An uncharged particle comes into contact with a charged surface such as plate or screen, an electric field, and assumes the same polarity and potential of the contacted surface. These particles are then considered to have become polarised whether they were conductive or dielectric (Dyrenforth, 1978). Under this influence, a conductive particle will become an equipotential surface by redistributing the charge almost instantaneously via the grounded rotor. The particles will therefore acquire a charge opposite to that of the high-voltage electrode generating the electric field (Inculet, 1984). However, a dielectric particle will become polarized so that the side of the particle away from the charged surface develops the same polarity as the surface and will remains polarised due to its inability to effectively redistribute electrons (Dyrenforth, 1978). For this reason, non-conducting particles have no net charge and so are neither attracted nor repelled by the field.

Electrostatic separation between conductor and dielectric is usually accomplished by means of a single electrode whose charge is opposite to that of the charged plate, and whose particles are of different charges which lead to attraction towards the electrode. The movement of conducting particles within the electric field can lead to electrostatic separation of the conductor and non-conductor (dielectric) particles. Effective separation of the particles components can only be achieved in conductive induction through large differences in particle conductivity or work function. Knoll and Taylor (1984) reported that the forces generated by induction separation are generally weaker than that of ion bombardment due to less particle charging, which reduces the process efficiency

2.3. Electrostatic Approach:

The electrostatic methods, which are utilized in the industry, can be classified into two: (i) corona separation, and (ii) tribo-electrostatic separation. These methods utilize the differences in the physical properties of organic coal and those of the inorganic (impurities). The corona electrostatic method utilizes a rotating drum with a small diameter of pointed electrode that provides corona discharge. The other category of electrostatic separation process is tribo-electrostatic separation, which separates particles based on the difference in their electronic surface charge, and various components within the particle.

Electrostatic separation techniques are dependent on the difference in the electrical resistivities and differences in the electronic surface structure of the mineral from the organic phases in coal (Kelly and Spottiswood, 1989a). This phenomenon enables the two charged phases to develop and maintain their charges and be deflected towards one of two opposite electrodes. Hence, with the application of various operation parameters on the separator the separation efficiency of the coal particles can be improved. Each separation technique requires different charging methods to generate opposite polarities needed to effect a separation and several theories have been put forward to predict the amount of charge transferred between surfaces in contact. In this study, tribo-electrostatic technique which involves particle charging by contact or friction with other particles will be explored to separate coal organics (macerals) from coal minerals in order to improve the quality of pulverized coal used in generating electricity in SA power plant.

2.3.1. Theory of Corona Electrostatic

The separation of particles using an electrostatic separator involves the charging of particles in a medium, and under a dynamics state. The charged coal particles make contact with the rotating, grounded roll-surface. Simultaneously, a separating force acts on it based on its inherent physical and electrical properties, before separating out at different angles. The intensity of the electric field is responsible for this action. There are two forces acting on particles in an electrostatic separator. The electrostatic force (F_e) on a charge q in an electric field of intensity E, is the force responsible for the action between the charged particle and the electrodes. On the other hand, the separating force between two isolated small charges q_1 and q_2 in electrostatic separator is known as the image force. This is the force of attraction between the charged particle and the grounded surface. The forces are given as,

$$F = Q.E, \qquad (2\text{-}1)$$

Where Q is the total charge and E is the electric field intensity at a point r in space. F is the vector sum of all the forces, which is given by Coulomb's law as

$$F = K\frac{q_{1.}\ q_2}{r^2}. \qquad (2\text{-}2)$$

In this case, r is the distance between the charges and K is a dimensionless constant, with magnitude $1/(4\pi\varepsilon)$, where ε is the permittivity of the space between charges q_1 and q_2. The knowledge of the relative conductivity of the particles involved is very important because if the particles are of the same sign after being charged they will repel each other. In the vicinity of an arbitrary test charge (q^1), the electric field experienced by this charge $F/(q^1)$ is given by,

$$\frac{F}{q^1} = \frac{q_{1.}\ q_2}{4\pi\varepsilon r^2 q^1} \qquad (2\text{-}3)$$

As the magnitude of the test charge q^1 increases, the resultant electric field it experiences due to fixed charges q_1 and q_2 decreases, and vice versa. The limiting case is obtained, for the electric field intensity E at a distance r from an isolated point charge, when the magnitude of q^1 corresponds to a unit test charged q_1.

In the case whereby the grounded surface is a rotor, then the centrifugal force F_c acting perpendicular to the surface is given as,

$$F_c = \left(1/6\right) \pi d_v^3 \rho_s \omega^2 R , \qquad (2\text{-}4)$$

and the gravitational force F_g is given by

$$F_g = \left(1/6\right) \pi d_v^3 \rho_s g , \qquad (2\text{-}5)$$

where d_v is the particle diameter, ρ_s is the density of the particle, ω is the rotor angular velocity, and R is the rotor radius.

The maximum charge (Q_m) that can be imparted on a particle in the corona field is given by

$$Q_m = K_f \, S_p \, E_i = 4 \, K_f \, \pi r^2 E_i \qquad (2\text{-}6)$$

(Mora, 1958; Barthelemy and Mora, 1960)

Where S_p , is the surface area of the particle and is equal to $4\pi r^2$ for a spherical particle with radius r. E_i represents the ionic field intensity, while K_f is a function of the dielectric constants of the medium and particle and also of particle shape (e.g., for free space $K_f = K\varepsilon_0$) and K is a function of the shape and dielectric constant of the particle)

2.3.2. Theory of tribo-electrostatic separation

In a rotary electrostatic separator, particles are charged by contact or friction with other particles, the wall of the cylindrical chamber and the rotary charger copper plated surface. Due to contact between particles, electrons (charge) are transferred from the surface of one particle to the other until the energy of electrons acquired at the interface of each particle is equalised. This effect was as a result of the ability of the material to donate or accept electrons when it is in dynamic contact with other material. The net charge attained by the material in tribo-electrification depends on the work function difference between the particles in contact, and the measure of the relative affinity for electrons of the material is known as work function, which is the energy to move an electron from the surface to infinity. In this investigation a rotary copper plated rotor was utilized as the charger in the tribo-electrification of the coal particles, and with a work function value between that of the coal and its mineral matter to create different polarity for effective particle separation. The particle with higher affinity for electrons gains electrons (i.e., lower Fermi level or higher work function) and charges negatively, while the particle with lower affinity loses electrons (i.e., higher Fermi level or lower work function) and charges positively. After electrification, the coal particles are subjected to an electric field in the separating zone that deflects the particles toward either a positive or negative electrode according to the magnitude and polarity of their charge. For effective separation, the electric field and the particle flow within the separating zone must be stable and uniform.

The magnitude and the polarity of the charge transfered between two dissimilar materials are controlled partly by their surface chemistry (Trigwell, 2003; Trigwell *et al*. 2003a; Sharma *et al.* 2004). Hence, the electron transfer during particle/particle charging is due to the inherent surface properties of the materials rather than its bulk properties. The work functions of various materials can be measured by Ultra-violet photoelectron spectroscopy in air, while their surface composition determined by X-ray photoelectron spectroscopy (Mazumder *et al.,* 2006). The donating-accepting affinities of pharmaceutical powder have also been investigated using inverse gas chromatography (IGC) and the results showed a correlation between the charges generated in tribo-electrification studies and acid/base parameters established by IGC (Ahfat *et al.,* 2002). Contact electrification had also been explained in terms of acid-base interaction between surfaces involving protons in the case of Bronsted acids-bases or electrons in the case of Lewis acids-bases, where the surface acidity and basicity are related to surface acceptor and donor electronic states, and to work functions (Dwari and Rao, 2008).

The concept of charge accumulation, charge transfer between two materials, particle trajectories in separating zone and the maximum charge acquired by a particle after tribo-charging can be estimated or investigated through the established models instituted by different researchers (Cho, 1964; Harper, 1967; Frankal, 1968; Masuda and Iinnoya, 1978; Ohara, 1988; Castle, 1997; Sharmene Ali *et al*., 1998; Greason, 2000; Wu *et al.,* 2003, Castle *et al*., 2004). In addition, a fundamental approach known as Hertzian theory was also used in describing the relationship between charging speed and the particle charging magnitude by Fan and Zhu, (1998).

Cluster model was used by Yoshido *et al*. (2006) to investigate the contact charging mechanism of polymer particles. The experimental data were obtained from the charges caused by the impact between a single polymer particle and a metal plate, which were measured and recorded. The polymer-metal charge transfer was further investigated in terms of a first-principle calculation to discuss these experimental results. The result obtained from the model shows that the calculated binding energies of the polymers were comparable to that of the experimental results and are of good correlation. Harper equation was also developed in measuring the triboelectric charged available on a particle after contacting another particle or a tribocharger by investigating the maximum charge acquired by metallic powders (Harper, 1967). The experimental results obtained by Mehta *et al*. (1994 and 1996) yielded good agreement with the estimated result from the Harper equation on mineral grains measurement.

The most commonly adopted models to understand the charge transfer process are surface state model and molecular-ion-state model. Surface state model was used by Castle, (1997) to investigate the magnitude of charge acquired when two insulators with different work functions exchange their charges during contact. Gady and Reifenberger (1997) and Gady *et al.* (1998) also studied contact electrification using atomic force microscope technique. The results obtained showed a consistent qualitative expectation of contact charging based on tribo-electric series of common materials. In addition, the observed contact electrification was also found to be consistent with electronic charge transfer between materials, rather than an ionic or material transfer mechanism. The most common models adopted in understanding the contact electrification phenomena of charge transfer or migration on the surface are discussed below.

2.3.2.1. Cartesian coordinate system

The particle trajectory within the separating zone was discussed using a Cartesian coordinate system. The electric field and the particle flow within the system are assumed to be uniform while, the drag force on the particles is assumed to be stokes drag only, with Brownian motion considered to be negligible.

From Figure 2-1, the Y –axis represented the particle velocity, which is assumed to be constant at initial conditions, $\frac{d\bar{x}}{dt} = 0$ and $\frac{d\bar{y}}{dt} =$ initial velocity when $t = 0$

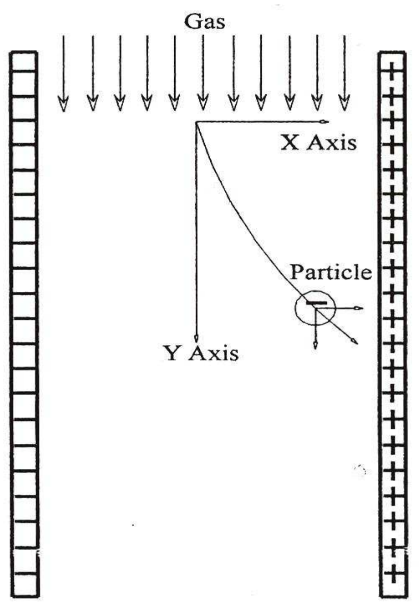

Figure 2-1. Cartesian system representing the separating zone

With an applied high voltage connected to the two vertical poles representing the positive and negative electrodes, the electric field created will accelerate the particles horizontally. The horizontal deflection of the particles toward the electrodes is being influenced by the electric field while, the residence time for particle travel through the separation zone is being controlled by the particle vertical motion.

Electrostatic force (F) resulting from the interaction of the electric field (E) with a charged particle (q), regardless of the material of the particle, is given by

$$F = qE \tag{2-7}$$

The horizontal displacement, $\overline{x}$ of the motion of a particle is governed by;

$$m\frac{d^2\overline{x}}{dt^2} = \overline{E}q \tag{2-8}$$

The mass is being represented by m, $\overline{x}$ the horizontal displacement vector, and t the time.

Equation (2-2) can be rewritten as;

$$\frac{d^2\overline{x}}{dt^2} = \overline{E}\left(\frac{q}{m}\right) \tag{2-9}$$

The particle specific charge known as charge to mass ratio is represented by $\left(\frac{q}{m}\right)$, and it is very important during the determination of the motion of particles during separation processes. In case the resistance of air and viscosity (η), are being considered, the horizontal motion (deflection) of the moving spherical particle of radius r is given by:

$$m\frac{d^2\overline{x}}{dt^2} + 6\pi\eta\, r = \overline{E}\, q \tag{2-10}$$

Or

$$\frac{d^2\overline{x}}{dt^2} + 6\pi\frac{\eta}{m}r\frac{d\overline{x}}{dt} = \overline{E}\frac{q}{m} \qquad (2\text{-}11)$$

The solution to equation (2-11), gives the speed of the particle as a function of time

$$\frac{d\overline{x}}{dt} = \frac{\vec{E}\,q}{6\pi\eta\,r}\left(1 - e^{\frac{t}{m/6\pi\eta r}}\right) \qquad (2\text{-}12)$$

The particle deflection in the separation zone is determined by particle charge and applied electric field intensity as shown in equation (2-12).

Assuming that $t >> \frac{m}{6\pi\eta\,r}$ or $t \to \infty$, the final horizontal speed of particle is:

$$\left(\frac{d\overline{x}}{dt}\right) horizontal = \frac{\vec{E}\,q}{6\pi\eta\,r} \qquad (2\text{-}13)$$

The terminal horizontal speed is independent of the mass under the condition set above. However, since time t is in the range of milliseconds, the mass therefore play an important role in the determination of the particle's motion and the resultant trajectory (deflection), which affects the separation performance of the charged particles.

2.3.2.2 Gauss's law

The maximum charge imparted on a particle through friction can be explained through this theory. Assuming an imaginary particle with a surface area (S) drawn around a uniform density of charge, the component of the electric field that is perpendicular to the surface is proportional to the total charge enclosed (Crosss, 1987).

$$E = \frac{\Sigma q}{S\varepsilon_0\varepsilon_r} \qquad (2\text{-}14)$$

Where Σq the sum of charges enclosed by the surface , ε_0 the permittivity of free space (8.8×10^{-12} F/m) and ε_r the relative permittivity of the particle.

The maximum charge density imparted on a particle before air ionizes it in an electric field can be calculated from equation (2-14). From Gauss's law, the total charge enclosed is the surface density of charge, Q_s (C/m^2), multiplied by surface area of the particle,

$$\Sigma q = Q_s\, S \qquad (2\text{-}15)$$

Substituting equation (2-15) into equation (2-14);

$$E = \frac{(Q_s\, S)}{(S\varepsilon_0)} = \frac{Q_s}{\varepsilon_0} \qquad (2\text{-}16)$$

The maximum charge density ($Q_{\max}$), with the unit (C/m^2), where C is the amount of charge transported in one sec by a steady current, and can be obtained by rearranging equation (2-16)

$$Q_{\max} = E\,\varepsilon_0 \qquad (2\text{-}17)$$

The limit of particle charging in a rotary cylindrical chamber used for this study can be obtained from the Gauss's law in figure (2-16).

The surface of the rotary charger is $2\pi L r_1 + 2\pi L r_2$, since only one half of the chamber is occupied by particles, then the volume of the side area of the chamber that was occupied with particles is equation (2-18), while the other half of the chamber is being ignore.

$$\frac{1}{2}\left(\pi r_2^2 L + \pi r_1^2 L\right) \qquad (2\text{-}18)$$

The maximum particle specific charge is given by;

$$\left(\frac{q}{m}\right)_{\max} = \frac{4E_b\varepsilon_0}{w\left(r_2 - r_1\right)} \qquad (2\text{-}19)$$

2.3.2.3. Surface state model

The theory stated that, the exchange of charges between two materials occurs at the surface, and the charges being proportional to the difference between the two materials surface work functions (Lowell and Rose-Innes, 1980; Schein *et al.,* 1992; Castle 1997). Under the surface state theory, there are two limits called low density and high density limit. The charge flows from the surface of the material with lower work function to that of higher work function until the work functions equalized.

$$\sigma = e\,N\,(\phi_1 - \phi_2). \qquad (2\text{-}20)$$

Provided the density of the surface states per unit energy per unit area is low and given by N, the resulting charge density (σ), can be written as equation (2-20), where e $(=-1.6\times 10^{-19}\ C)$ is the electron charge.

In the high density limit, the charge exchanged between two materials is large enough to raise the energy and equalized the states of the insulator of the larger work function to that of the insulator with the smaller work function such that the effective Fermi levels of each are equal. Therefore, a potential difference V_C, is established between two metal interfaces, with corresponding Fermi levels when different work functions ϕ_{M1} and ϕ_{M2} $(\mathrm{e}V)$, are brought into contact and then separated. The contact potential difference is given by

$$V_C = \frac{(\phi_{M1} - \phi_{M2})}{e}. \qquad (2\text{-}21)$$

The charged transfer Q, during the contact in equation (2-21) is:

$$Q = CV_C = C\,\frac{(\phi_{M1} - \phi_{M2})}{e}, \qquad (2\text{-}22)$$

where C, is called the capacitance for plane condenser, and its unit is the Farad (F) is represented as,

$C = \frac{\varepsilon_o A}{Z}$, where A the effective area of contact, Z is the separation at contact, ε_o is the permittivity of free space $= 8.85 \times 10^{-12}\ Fm^{-1}$.

and for a sphere shape particle with radius R, the capacitance is:

$$C = 4\pi\varepsilon_0 R \tag{2-23}$$

Then, the charges transfer Q equals to

$$Q = \frac{\varepsilon_o A}{Z} V_C , \tag{2-24}$$

While the surface charge density that can be generated during contact between two bodies is,

$$Q = \frac{Q}{A} = \frac{\varepsilon_O}{Z} \frac{(\phi_{M1} - \phi_{M2})}{e}. \tag{2-25}$$

The capacitance C decreases when two bodies are separated after contact, and Q also decreases until charge exchange by tunneling ceases. Harper (1951) showed that at about 1 nm cut-off distance, the tunnelling current is abrupt and for a sphere plane geometry,

C is given by,

$$C = 4\pi\varepsilon_0 r\left\{0.577 + 0.5\left(\frac{2r}{z}\right)\right\}, \tag{2-26}$$

where r represents the radius of sphere and z, the distance at which tunnelling ends. Combining equations (2-22) and (2-26), the charge transfer during contact between the bodies can be written as,

$$Q = 4\pi\varepsilon_0 r\left\{0.577 + 0.5\left(\frac{2r}{z}\right)\right\} \frac{(\phi_{M1} - \phi_{M2})}{e}. \tag{2-27}$$

Hence, the charge density equal,

$$\frac{Q}{A} = \frac{\varepsilon_O}{r} \left\{0.577 + 0.5\left(\frac{2r}{z}\right)\right\} \frac{(\phi_{M1} - \phi_{M2})}{e}. \tag{2-28}$$

This theory had been found to be in a semi-quantitative agreement with the experimental data acquired by using the tunnelling cut-off distance of z = 1 nm. In addition, from the investigation conducted on real materials with rough surfaces by Lowell (1975), the result shows that the capacitance can be better estimated by taking into account the fact that most of the two surfaces involved are separated by much larger distances when closest point of separation is at 1 nm, and he also found that tunnelling current actually ceases at z = 100 nm.

2.3.2.4. Hertzian theory

The relationship between charging speed and particle charging behavior is based on the contact force between the particles and the rotary charger. The logarithmic linear theoretical approach between particle charging and charging speed had been observed by Gupta *et al.* 1990, while

Ban *et al*. 1994, also reported a linear relationship between particle charging and particle speed in a copper tube charger. According to Hertzian theory, the contact area (A_C) depends on the compressional force and the material properties of the particles and the charger provided that the normal pressure is not affected by the existence of the tangential traction and the resulting displacement.

$$A_C = \pi \left(\frac{3}{4} F_Z \frac{r^*}{E^*} \right)^{\frac{2}{3}} \tag{2-29}$$

Where A_C represents the contact area, r^* is the relative radius, F_Z is the normal collision force, and E^* is the contact modulus defined by equation (2-30).

$$\frac{1}{E^*} = \frac{1-v_1^2}{E_1} + \frac{1-v_2^2}{E_2} \tag{2-30}$$

$$\frac{1}{r^*} = \frac{1}{r_1} + \frac{1}{r_2} \tag{2-31}$$

From equation (2-30), E_1 and E_2 represents the Young's modulus of the particle and charger material respectively; r_1 and r_2 are the radius of the particles and charger; and v_1 and v_2 are the Poisson's ratios of particle and charger material, respectively.

The maximum impart force F_Z between the particle and the charger as stated by Hertz theory can be described in equation (2-32), where m^* is the relative mass and U_r is the relative speed between the particle and charger.

$$F_{ZM} = \frac{4}{3} E^* \sqrt{r^*} \left(\frac{15 m^* U_r^2}{16 E^* \sqrt{r^*}} \right)^{\frac{3}{4}} \qquad (2\text{-}32)$$

$$\frac{1}{m^*} = \frac{1}{m_1} + \frac{1}{m_2} \qquad (2\text{-}33)$$

In a rotary charger system, the radius of the charger is much greater than that of the particles, and the charger mass also greater than that of the particles ($r_1 << r_2$ and $m_1 << m_2$, hence $r^* = r_1$ and $m^* = m_1$

Therefore, substitute r^* in equation (2-29) for r_1, and m^* in equation (2-32) as m_1

$$A_C = \pi \left(\frac{3}{4} F_Z \frac{r_1}{E^*} \right)^{\frac{2}{3}} \qquad (2\text{-}34)$$

$$F_{ZM} = \frac{4}{3} E^* \sqrt{r_1} \left(\frac{15 m_1 U_r^2}{16 E^* \sqrt{r_1}} \right)^{\frac{3}{4}} \qquad (2\text{-}35)$$

From equation (2-35), the maximum impact force is proportional to $U_r^{\frac{3}{2}}$, hence, the higher the relative speed of the rotary charger the higher the contact force and contact area between the particles.

2.3.2.5. Local (intrinsic) model

This model explained the transfer of charges between metal and an insulator (e.g. polymer) based on the material's inherent energies and positions. The transfer of charges between materials was associated to that in a molecular structure by Shinohara *et al*. (1976). The author suggested that electron donating polymers enhance positive charging while electron accepting polymers enhance negative charging. From the investigation conducted by Gibson, (1975; 1984) on charge transferred in polymers and organic solids (Q/m = charge/mass), it was observed that the charge transferred is exponentially proportional to the energy difference of the donor and acceptor states. Therefore, the following relationships were established by Gibson, (1975; 1984) using Hemmet σ function and molecular energy level.

Considering positive charging,

$\ln(Q/m)\,\alpha\, E_{HOMO} - E_A$ and (2-36)

$E_{HOMO} = - m_1\sigma_x + b_1$

Thus, $\ln(Q/m)\,\alpha - E_A - m_1\sigma_x + b_1$

For negative charging,

$\ln(Q/m)\,\alpha\, E_D - E_{LUMO}$, and

$E_{LUMO} = - m_2\sigma_X + b_2$

Thus, $\ln(Q/m)\,\alpha\, E_D + m_2\sigma_x - b_2$,

Where $m_1, m_2, b_1,$ and b_2 are constants, while E_A and E_D are the acceptor and donor level of the metal, respectively. This theory had been observed by Pochan *et al*. (1980) and found that the transfer of electrons between a metal and a polymer is a function of either the work function of the metal when the polymer is charged negatively or the Fermi energy of the metal when the polymer is charged positively.

2.3.2.6. Ion Conduction model

This model had supported the fact that, contact electrification is due to the transfer of ions from one surface to the other, and also said to be responsible for transferring ions located on the surface of one material to another due to crystal lattice defects (Ruckdeschel and Hunter 1977; Kornfield, 1976). The migration of ions from one surface to another under this model is being aided by the energy possesses by the ion at a defined temperature to skip to the neighboring stable position so that the charge is transferred from one material to the other. The transfer of ions under water adsorption for waste removals, polymer dissociation, polymer additives and plasticizers, are similar to the mechanism of charge exchange.

2.4. Summary

The separation efficiency of an electrostatic separator can be enhanced through detail knowledge of its charging mechanism. Tribo-electrostatic separation of particles can be improved by increasing particles charge and separation potential provided the particles are not charged saturated. The concept of contact electrification, charge transfer between two materials, particle trajectory in the separating zone and maximum charge magnitude acquired by the material can all be estimated through different models, provided both faraday cup and an electrometer is connected to the separator to determine the particles charge magnitude.

CHAPTER THREE

3.0. Electrostatic Separation Techniques for coal Beneficiation

Dry beneficiation relies on the differences in the components physical and chemical properties for effective separation. The effective separation of coal organics from its mineral matter depends on the type of separator, and the properties of the coal involved. Due to the variation in the properties of coal such as electrical, particle size and moisture content, beneficiation techniques responded with different separation efficiency. There has been a tremendous research and development in the area of dry coal beneficiation processes. Notable advances are made by Choung *et al.* (2006) on dry coal preparation using air dense medium fluidized bed separator (ADMFBS). However, more researches and development are required to increase the separation efficiency of this process as compared to the same type of coal with the same size range under wet beneficiation. The application of electrical conductivity of particles under the influence of a very high potential have received significant attention in recent years. This technique utilizes the inherent differences in the coal components considering the particles friction charging, electrical conductivity and dielectric constant properties (Manouchehri *et al*., 2000a; 2000b).

The material electro-physical properties determine the way in which the particles can be endowed with charges, either by conductive induction or tribo-electrification or corona-electrostatic charging mechanism. The three major macerals in coal are vitrinite formed by carbonisation of cellulose, liptinite, formed from noncellulose materials such as resins and seeds, and inertinite from charred plant remains. The evaluation of charges acquired by the electrostatically beneficiated coal samples had been investigated by Inculet and co-workers (1982). They found through petrographic analysis that the macerals present in the samples were endowed with different charge polarities, with vitrinite charged positively and inertinite charged negatively. Lockhart, (1984) investigated the conductivity of coal, and found coal to be generally less conducting than mineral matter, except perhaps in the case of brown coal that has a high water content and also often high ion content. Previous investigations conducted had shown that pyrite possesses the most conducting mineral found in coal. While, clean coals are generally charged positively and ash forming minerals or high-ash coals charge negatively (Lockhart, 1984; Alfano *et al*., 1988). These properties had enabled the separation of coal and encourage more researches into dry beneficiation. The two electrical separation methods that had been used for the cleaning of coal are tribo-electrostatic method and corona electrostatic process (Butcher and Rowson, 1994; Dwari and Rao, 2007), with both techniques discussed below.

3.1. Corona-electrostatic separation

The corona electrical separator usually consists of an induction charging electrode, which charges the particles as it passes through an electric field generated by a high voltage electrode. This technique is also known as the strongest electrostatic separator (Butcher and Rowson, 1994; Dwari and Hanumantha, 2007). The separating capability of the particles depends on the difference in their polarity and the amount of charged acquired by the particles. Conductive particles are charged by induction within a short time depending on their conductivity, while it takes longer for non-conductive particles to acquire induction charge on their surface. The technique of using ion bombardment in charging and separating minerals is the most common and strongest method of charging particles for electrostatic separation. It has been employed in recovering of copper and plastic materials from power cable, removal of stalks from tea leaves, separation of metals from glass, ceramics, plastics, and polymers, and also for removing contaminants from grains and processed foods (Moore, 1973; Hayakawa *et al*., 1985; Taylor, 1988; Higashiyama and Asano, 1998). In the mineral processing industry, the commercial applications of corona separation are in the concentration of heavy minerals (rutile, zircon, illmenite, monazite) from beach sands and alluvial, and separation of zircon and TiO2 phases during the processing of heavy mineral concentrates derived from heavy mineral sands (Yongzhi, 1992 and Worobiec *et al.,* 2007).

The earliest application of corona technique regarding coal cleaning was in the beneficiation of coal in the size range 1700 – 400 μm by Mukai *et al*. (1967), where coal product of 2.5 – 3% ash level enriched in vitrinite was obtained with recoveries of 96 – 98% relative to washability curves. The reduction in the coal ash level and maceral separation was conducted by Olofinskii *et al.* (1959), using corona-chamber with tribo adhesive-drum, and fluidized-bed electric separators for beneficiation, size classification, and dust recovery for coal. The result reveals that particle size and coal density were responsible for the separation of the coal constituents, with coarse and fine fractions having different mineral and maceral contents. The Advanced Energy Dynamics (AED) conducted an extensive test in cleaning particles down to 37 μm size, and the result shows that more ash-forming mineral and more sulphur can be removed compared to any conventional beneficiation method, with higher recoveries and removal of 65 to 89% of ash particles at an appreciably lower costs (Lockhart, 1984). The electrostatic separation of pyrite from coal using corona roll separator was conducted on Moira Pottery coal, UK, at various atmospheric conditions, various feed pretreatment, particle size and different relative humidities by Butcher and Rowson, (1995). The authors found that ash reduction of 50.64% can be achieved under compressed air atmosphere using particle of -500 + 300 μm size fraction as compared to 19.07% under ambient condition on the same size range. In addition, both results obtained under the nitrogen and carbon dioxide atmospheric condition were found comparable with results achieved under standard conditions.

However, there appears to be a limitation regarding this application for coal beneficiation. The closeness in the work function of coal constituents had favoured the application of tribo-electrostatic technique for coal cleaning due to its effectiveness in separating particles with little difference in conductivities. In addition, there is also a limitation for separation of particles below a few hundred micrometers regarding the utilization of corona technique for separating fine coal (Higashiyama and Asano, 1998).

3.2. Tribo-electrostatic Method

Pulverized coal has long been used as fuel for power plants. The beneficiation of pulverised coals used in conventional boilers of thermal power plants by tribo-electrostatic separation would be a satisfactory solution to the environmental pollution caused by the fly ash particulates, NO_x and SO_x emissions. Therefore, fundamental research that are presently been conducted on tribo-electrostatic separation and their present status is reviewed below, for future references.

The diversity in particle charging reflects the variety in different types of tribo-electrostatic separator that have been reported in the literature. The electrical separation with tribo-charging technique has been found as a great potential for coal cleaning in fine sizes. Tribo-electrostatic separation of coal and its tribo-charging characteristics have been investigated by many researchers with successful results reported on the separation of mineral matter from coal (Mukherjee *et al*., 1987; Nifiku *et al.*, 1989; Ban *et al*., 1993a, 1993b; Higashiyama *et al*., 1998;

Trigwell *et al*. 2003b; Dwari and Rao, 2008; Dwari and Rao, 2009). There have been some recent development in this direction but they are yet to achieve commercial status in coal industry (Hower *et al*., 1997; Dwari and Rao, 2007; Dwari and Rao, 2008). Tribo-charging of coal particles can be conducted in a separator using a cyclone, a rotating cone/cylinder or fluidized bed and a charging tube. The process occurs as a result of impacts between the particles by contact or friction with other particles or with a third material, usually the walls of a container or copper plated rotor, followed by transport or freefall through an electric field that deflected the particles according to the magnitude and sign of their charge (Gidaspow *et al*., 1984; Masuda *et al.*, 1984; Finseth *et al.*, 1993; Higashiyama *et al*., 1998).

The test conducted by Masuda *et al.* (1984) using a cyclone charger **(**Fig 3-1) shows that the positively charged coal was deflected towards a negative electrode and the negatively charged ash particles or ash forming minerals was deflected towards a positive electrode. The result obtained shows a reduction in the coal ash content from 15.2% to 7.1% with coal recovery of 90%. This finding can also be supported by the investigation conducted by (Lockhart, 1984; Alfano *et al*., 1988), where it was found that clean coals are generally charged positively and ash forming minerals or high-ash coals charge negatively. This property is responsible for coal separation and encourages more researches into dry beneficiation. The potential and separation efficiency of copper tribocharger considering different set conditions such as velocity, concentration of coal in air and separator voltage were investigated in a separator using a tribo-charging pipe by Finseth *et al.* (1993). The author found that the tribo-electrostatic beneficiation method using a tribo-charging pipe (Fig 3-2), had efficiently produced a clean coal product with 2.1% ash and 0.6% sulphur from a feed coal with 24.4% ash content and 1.4% sulphur at a recovery rate of 38.8%.

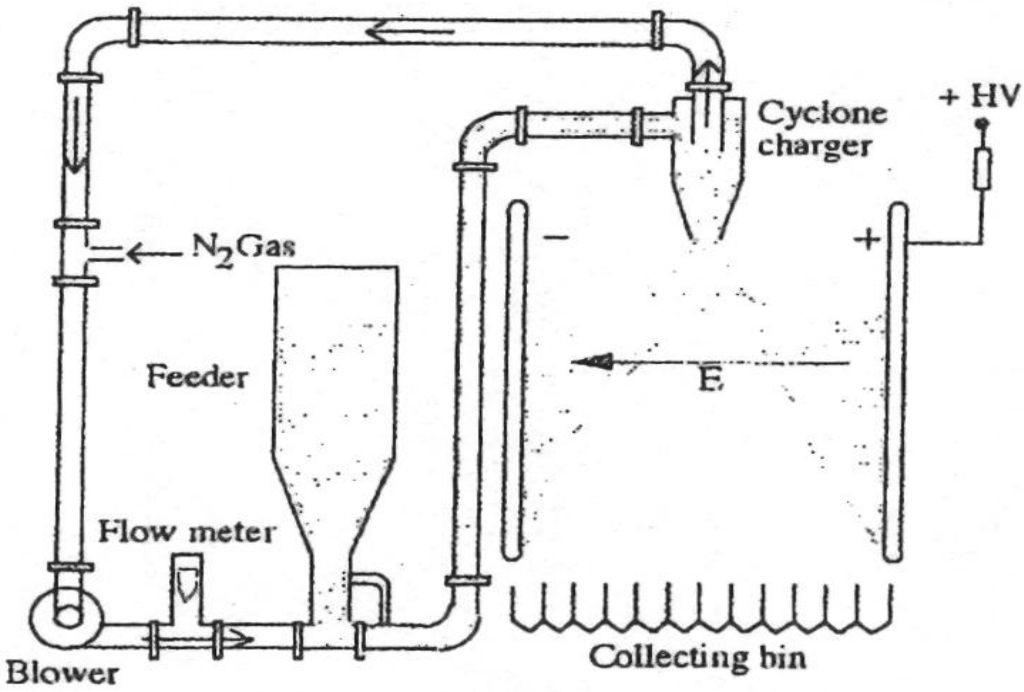

Figure 3-1 Schematic representation of electrostatic cyclone charger for coal cleaning.

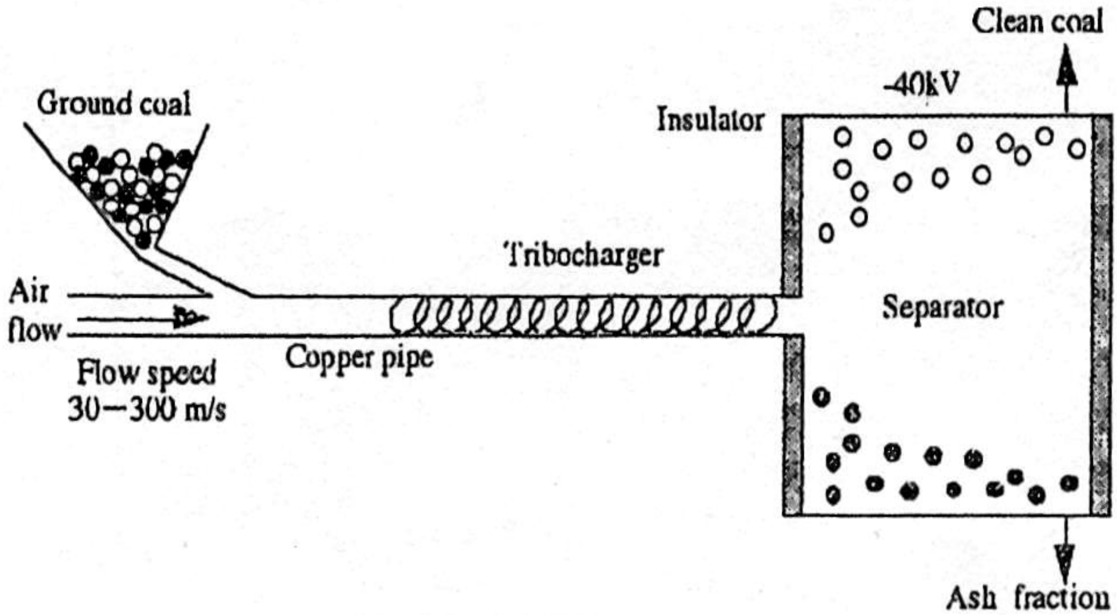

Figure 3-2 Schematic representation of electrostatic separation with tribocharging pipe.

The electrostatic separator in (Fig 3-3) was developed at the Virginia Technology, USA. The separator is made up of a drum shaped electrodes, which increases the electric field within the system and also used in cleaning the surface of the electrode. In addition, the separator has a chamber for creating laminar airflow, flow straighteners to reduce the turbulence flow within the system, along with heat source and a splitter unit. The investigation conducted on the three coal samples shows that the run of mine sample has the best separation efficiency at the optimum operating voltages of 40-50 KV, with a maximum throughput of 30 kg/hr. In Figure 3-4, the vertical-belt separator developed by the Advanced Energy Dynamic (AED, 1987), was utilized in the separation of coal from impurities. The Vertical-belt separator has the following characteristic feature: flat, parallel and stationary electrodes to maintain the charges imparted on them and the electric field intensity within the system. The movement of the belt in opposite directions leads to the transportation of the coal particles, and stirring up of the particles, which later lead to the creation of a turbulent flow within the set up. The test conducted on Lower Kittaning and Illinois no 6 coal, USA, (-44 um) size fraction shows a reduction in the ash content of the feed coal in the range of 50-60% and pyritic sulphur between 20-75%, with calorific value increases by 62-81% Btu.

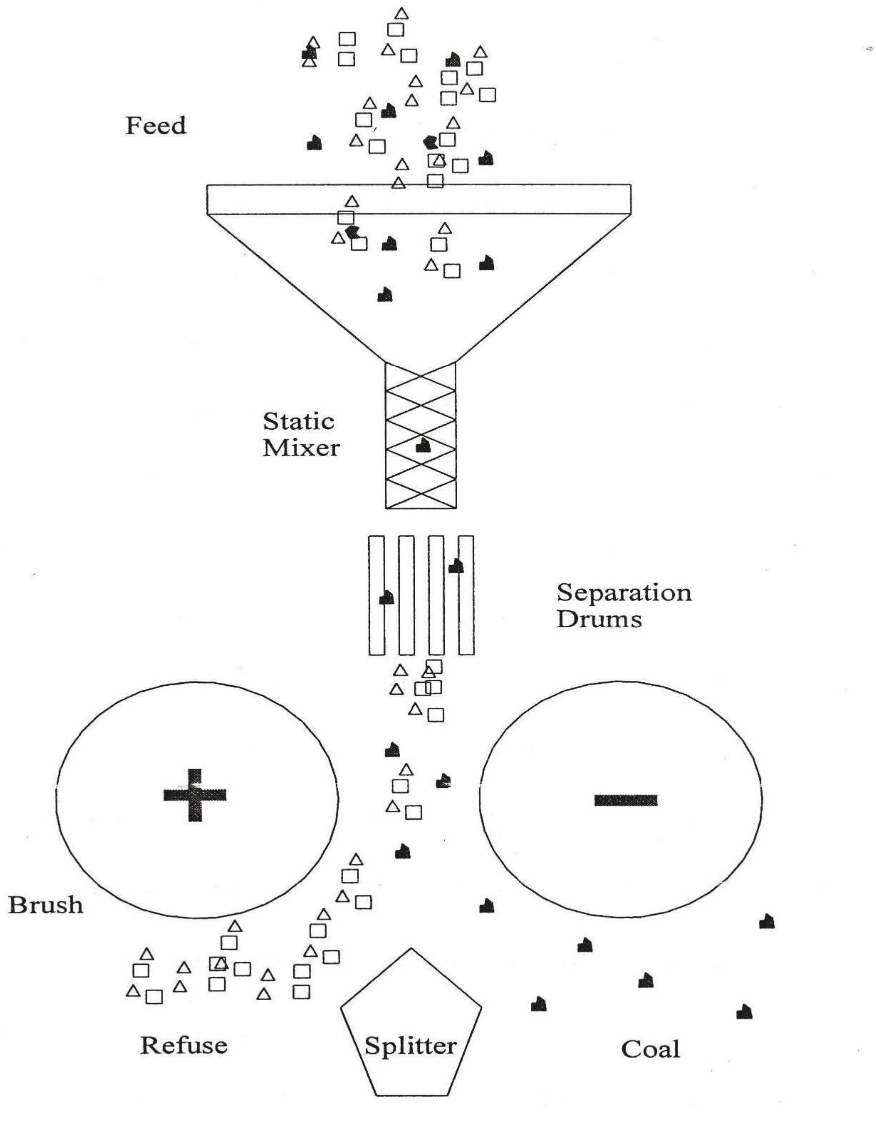

Figure 3-3 Schematic representation of a bench scale tribo-electrostatic separator (Chandrasekhar, 1998)

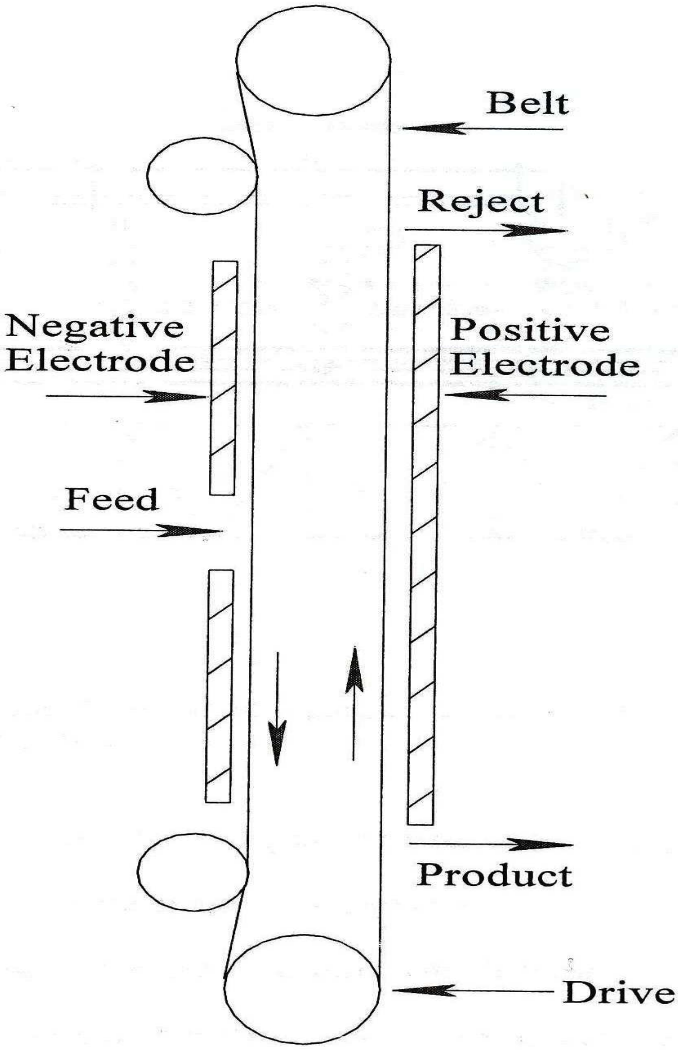

Figure 3-4 Schematic representation of AED’s continuous UFC belt separator (AED, 1987)

Dwari and Rao, (2006) also investigated the effect of different tribo-charger on high ash non-coking Indian thermal coal with particle size -300 + 210 um, constant voltage of 15 KV and tribo-charging time of 5 min. Copper was found to have the best separation efficiency among the tribo-charger tested for and this was due to its high electrical conductivity. The result obtained by these authors on the electrification of coal shows a clean coal collected at the negative bin with 18% ash from 43% feed coal. While, the washability test conducted on feed coal of 43.2% ash was reduced to clean coal with only 25% ash and about 65% yield. The removal of pyritic sulphur from fine ground coal was conducted in an electrostatic sieve conveyor by Gidaspow *et al.* (1987). The result obtained showed that the separation efficiency of this technique can be attributed to the grinding of the coal fine to -40 μm size, which was responsible for the liberation of the pyrite from the coal with a pyritic sulphur reduction of 2.4% to 0.86% after a five stage sieve conveyor. The Pre-combustion cleaning of coal by triboelectric separation of minerals was examined by Trigwell *et al.* (2003b). The author reported that the triboelectric separation of minerals from coal was a viable beneficiating method. Petrographic and X-ray analysis of the feed and cleaned coal shows the reduction in the sulphur and ash content for Pittsburgh No. 8 and Illinois No. 6 coal samples. Fine coal samples were found to yield cleaner coal product, with the Pittsburgh samples showing a greater reduction for both sulphur and ash as compared to the Illinois feed and cleaned coal.

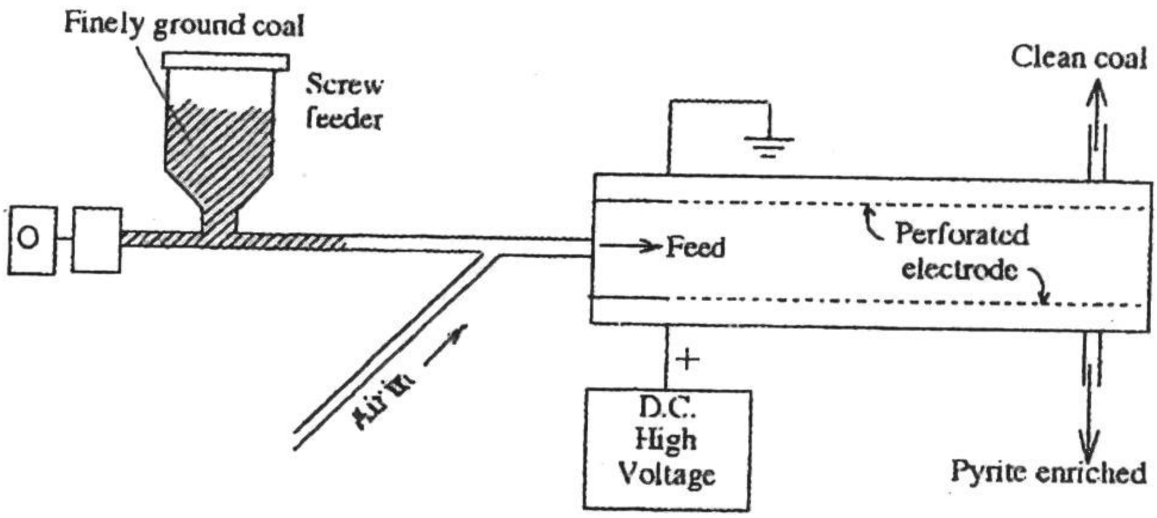

Figure 3-5 Schematic representation of electrostatic sieve conveyor (Gidaspow et al. 1987).

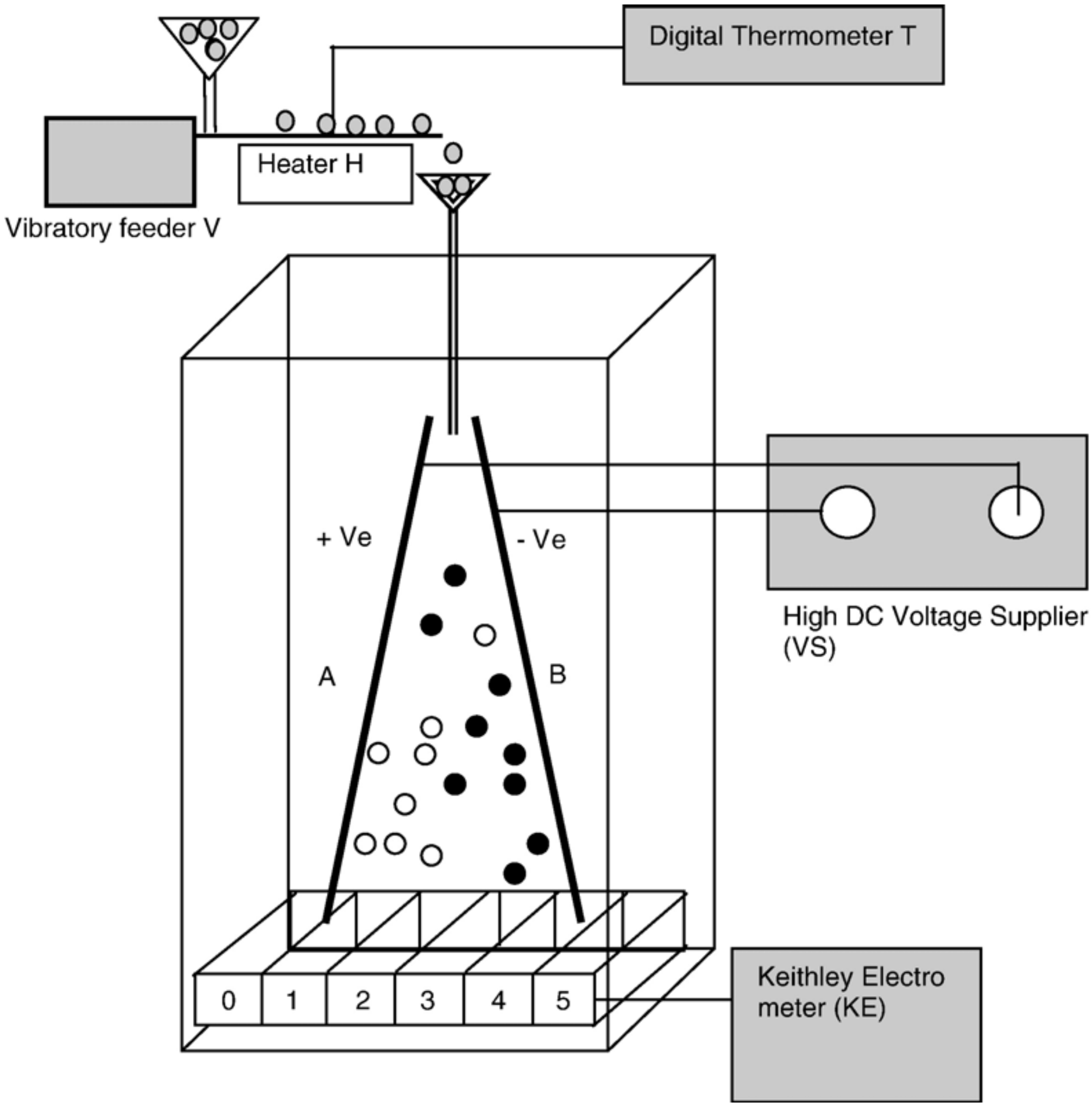

Figure 3-6 Tribo-electrostatic (Dwari and Rao, 2006).

Inculet *et al.* (1980) uses fluidized bed tribo-charger for the beneficiation of coal. The result obtained shows that the ash was successfully removed from the coal with an improved calorific value. In addition, the result obtained for both recovery and ash content of the cleaned product are comparable to that obtained from the wet beneficiation processes. Lewowski (1993) also studied the electrostatic desulphurisation of Polish steam coals and the result shows that the technique can be used in separating coal constituents. A newly built cylindrical fluidised bed tribo-charger with internal baffles, made up of copper metal had been use to beneficiate an Indian thermal coal sample from Ramagundam coal mines, India, by Dwari and Rao (2009). The authors found that the coal particle size, tribo-charging time, voltage, gas flow rate and residence time of fluidization all played a role in the separation of the coal from its minerals. They reported a reduction in the ash content of coal from 43% to 18% for -300 μm particle size with about 30% yield at 10 KV and 60 sec tribo-charging times. Hence, a yield of 67% was also obtained but with a moderately reduced 33% ash. The washability studies conducted on this sample also shows a clean coal of 25% ash with 65% yield. Dwari and Rao (2008) also investigated the potential of a fluidized bed tribo-charger (Fig 3-7) with internal baffle system (FTB) for the beneficiation of non-coking coal from Hingula block of Talcher coal field. The effect of particle size on the separation potential of two size fractions, -75 mm and -1 mm were investigated. The result showed a reduction in feed coal containing 39.39% ash to a clean coal of 25% ash for -75 mm size fraction and 17% ash with 85% yield for -1 mm size fraction. It was observed that the non-liberation of coal at -75 mm was responsible for its higher ash content. Experimental result obtained at 15 KV and 30 sec tribo-charging times from the same separator also revealed that it is possible to achieve a clean coal of about 15.6% ash from 25% feed coal with 69% yield.

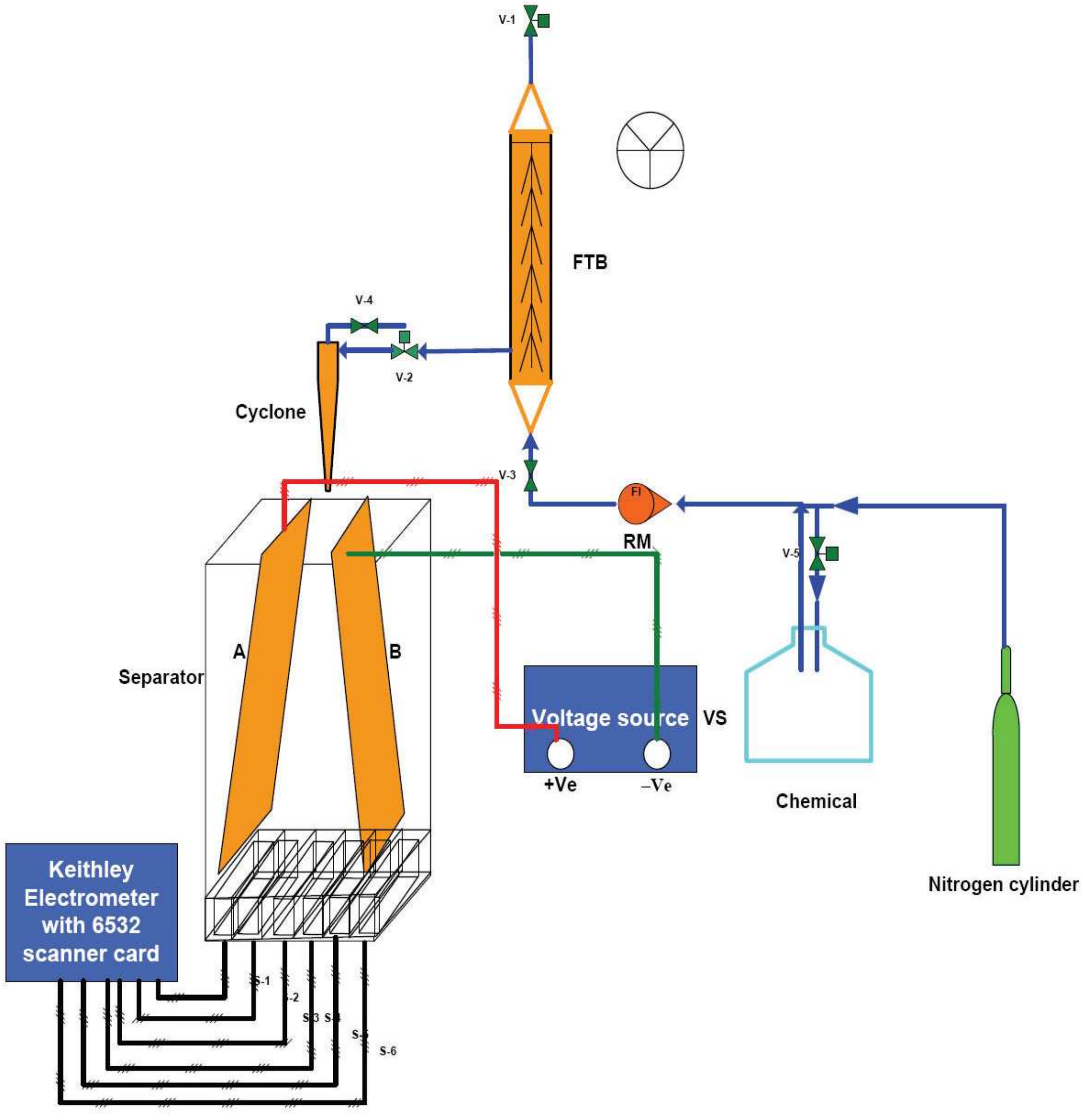

Figure 3-7 Schematic representation of fluidized bed tribo-electrostatic separator (Dwari and Rao, 2008).

The separation efficiency for both tribo-electrostatic process and a bench scale fuel oil agglomeration technique was investigated by Hower *et al.* (1997) and their result compared with each other. The authors found that the bench scale tribo-electrostatic separator provided a better separation in comparison to bench scale fuel oil agglomeration technique for the three eastern Kentucky and two iIllinoise coals. The result shows clean coals enriched with vitrinite and vitrinite-enriched microlithotypes while inertinites, liptinites, and minerals were present in the tailings. From the petrography analysis conducted, similar coal evaluated by this technique shows different separation efficiency due to the differences in their moisture content, with the degree of charging being reduced at higher moisture content, along with the separation efficiency but it is not clear whether the driest materials had the best charging properties (Mazumder *et al.*, 1995; Kwetus, 1994). The result reported by Mazumder *et al.* (1995) had shown that the resistivity of coal particles depended upon their moisture and ash content and therefore, different types of coal will have different resistivity.

Studies had been conducted on how to modify or alter the surface energetic structure of fine coal in order to improve its separation efficiency. The work function values between the particles after tribo-electrification, relative humidity of coal and temperature of the coal material are expected to be affected for possible increase in coal separation from its minerals. Dwari and Rao, (2009) had proposed to treat fine coal in the vapour of acidic and /or basic organic solvents in the fluidised bed tribo-charger, with the result from this investigation expected for presentation in their future publication. The increase in coal separation efficiency after chemical pre-treatment was investigated by Zhou and Brown (1988). They utilized the vapours of different organic chemicals such as methyl acetate, acetone and acetic acid under dry nitrogen atmosphere in the fluidised-bed tribo-charging medium for improving the charging capability of the coal.

The surface treatment performed on the coal samples with particle size between 75 and 150 μm had shown an improvement of separation to some degree. Trigwell *et al.* (2003) studied the influence of acetone, ammonia and sulphur dioxide vapours on the charge properties of coal exposed to these chemical. They found beneficiation to be slightly enhanced using acetone than using ammonia, with ammonia found to be detrimental to beneficiation, and So_2 as a non effective conditioning agent.

Mazumdar *et al*. (1995) suggested that there are several fundamental factors associated with tribocharging and separation processes which had been hindering its commercial implementation to date. The effects of the coal surface composition on work function and under different tribocharger such as copper, stainless steel, aluminium, nylon was evaluated using X-ray photoelectron spectroscopy and UV photoelectron spectroscopy by Trigwell *et al.* 2001. The investigation showed that the work functions for the samples varied considerably as a function of the samples surface composition, while the actual work function for the samples can differ from their expected values due to the alteration in their surface composition upon exposure to different environment. Therefore, since it has been a broad understanding that electron transfer during frictional charging is surface property dependent rather than bulk properties and the magnitude of charge and polarity transferred between two dissimilar materials was controlled partly by the surface chemistry (Ruckdeschel and Hunter, 1975; Trigwell, 2003; Trigwell *et al*., 2003a; Sharma *et al.,* 2004; Mazumder *et al.,* 2006), then, numerous investigations had to be conducted on coal in order to the best processing route for its separation considering the stated factors abov

3.3. Other Dry Beneficiation Techniques:

The simplicity, as well as the ease of operation had influenced the research into dry coal beneficiation process as an alternative approach to the existing wet techniques for the separation of coal organic from its inorganic. There are many research reports that had been reported on the development of different dry beneficiation techniques for cleaning coal. And all these methods utilize the physical and electrical characteristic of coal and other operating parameters within the set-up in separating the coal organic from its minerals to achieve the required cleaned product, and some of these methods are discussed below**.** These processes are found to be environmentally safe with the potential of removing pyrites and ash from the coal, and could also make flue gas desulphurization unnecessary in a power plant (Higashiyama *et al.*, 1998).

3.3.1. Air Dense Medium Fluidized Bed (ADMFB)

The application of ADMFB for cleaning coal was first investigated by the Chinese for the beneficiation of 50 ~ 6 mm size fraction coal, with a capacity of 50 ton/h, and 700,000 ton/year output (Cheng and Yang, 2003). This is an efficient coal-separation method, which uses a gas–solid fluidized bed as the separating medium rather than air used in a conventional air jig or shaking table separation method. In order to attain high separation efficiency with this technique, stable dispersion fluidization and micro-bubbles must be achieved within this system. Cheng and Yang, (2003) found that the beneficiation of coal with different density ranges from 1.3 to 2.2 g/cm^3 and 50-6 mm size fraction with ADMFB can compared favourably with the best existing wet heavy medium beneficiation process. In addition, coarser particles greater than 50 mm can also be beneficiated by increasing the bed height. Vibrated air-dense medium fluidized bed was also investigated by the same authors, and they found that 6-0.5 mm fine coal with a feed ash of

16.57% can be reduce to 8.35% with yield up to 80.20%. This was achieved through the investigation on the effects of the system operating parameters. Luo *et al.* (2000) also conducted an investigation on the vibrated air-dense medium fluidized bed. The result obtained also supported the fact that various system parameters enhanced better separation of the coal constituents. The reduction in the size of the medium solids and the supply of the bed with mechanical vibration energy enhanced a better gas–solid interaction as a result of a better-dispersed fluidized bed, giving the Vibrated fluidized bed (VFB) better fluidization qualities compared to simple bubble conventional fluidized bed (CFB).

Choung *et al*. (2006) also utilizes Air Dense Medium Fluidized Bed (ADMFB) for the separation of coal organics from its inorganic. This research was initiated due to the challenges facing the coal industry, the emissions of NO_X and CO_2 by the power station and the degradation in some coal beneficiated by wet preparation. The separation efficiency of ADMFB for cleaning coal fines smaller than 6 mm was studied by varying the system operating parameters such as feed rate, fluidized air velocity and the size of the medium solids by Choung *et al*. (2006). The author reported that the decrease in the magnetite size was responsible for the increase in the separation efficiency of coal in 5.66 × 3.35 mm size fractions. The result showed an ash rejection from 14% to 6% at 90% yield. The introduction of Vibrated fluidized bed has reduced the effect of high viscosity and back mixing found in the CFB during the separation of fine coal < 6 mm by strengthening the contact between the gas and solid phase. Zhenfu *et al*. (2008) utilizes VFB for the beneficiation of fine coal < 6 mm, under different technological and operating conditions. The result obtained from the investigation shows an Epm value of 0.07 ton/m^3 for the VFB, compared to wet jig with an Epm value of 0.11 ton/m^3. The Epm is known as the Ecart Probable Moyen or probable mean error which is defined below as;

$$EPM = \left(\frac{RD_{75} - RD_{25}}{2} \right) \quad (3\text{-}1)$$

Where RD_{75} is the relative density corresponding to a partition coefficient of 75 and RD_{25} is the relative density corresponding to a partition coefficient of 25

Chen *et al*. (2003) developed a fluidized bed with uniform and stable density condition. The stability of this bed density was found to be the key to the high separation efficiency of the technique. The bed utilizes magnetite powder and silica as the medium solids and found suitable for separating high density coal with feed greater than 1.5 g/cm^3. In order to meet customer's product requirements for coal lesser than 1.5 g/cm^3, the operating conditions for this bed were investigated. A Pilot test was performed on coal feed with particle size 6-50 mm by Zhen-fu *et al.* (2007) using magnetic pearls of certain size distribution as the medium, the test produces clean coal with low ash content. The result showed that at a separation of 1.44 g/cm^3, coal with an ash content of 13.95% and a tailing ash content of 56.82% can be obtained. The stable density and uniform condition achieved during this test was as a result of the optimal technological approach and operating conditions set, which meet the requirements of low density coal cleaning with high performance. Yang *et al.* (2002) utilizes vibrated fluidized bed to extracts fine coal from coarse coal by entrainment of an ascending airflow. The ash contents of fine coal products obtained from this process were 2-3% lower than those of the same size fractions in feed for most cut-size of 6, 3, 2, 1, or 0.5 mm tested. From the pilot and commercial test conducted, the authors had proved that this new technology provides a practical solution to the difficult task of sizing moist raw coal at sizes below 6 mm for producing lower ash fine coal from raw coal for blast furnaces or pulverized coal firing boilers.

Kretzschmar *et al.* (2008) utilizes a dense medium fluidized bed separator with a naturally occurring magnetite to beneficiate South African Coal. The test was conducted on a discard coal and high ash Waterberg coal with particle size between 15 – 35 mm, in order to determine the process optimal operating conditions, fluidizing characteristic of the bed and the efficiency of the separator. The investigation shows that the continuous test conducted for the high ash Waterberg coal at a flow rate of 18 kg/hr, separation density of 2.00 g/m^3 achieved an Ep value of 0.0462, with an Ep value of 0.0458 achieved for the discard samples under the same conditions. The authors concluded that the Ep values for the continuous test regarding Waterberg coal can be compared to that obtained from the traditional wet separation techniques.

3.3.2. Jig

The technique utilizes the differences in the density between coal and its associated minerals for beneficiating coal. The air jig is designed in a closed structure to distribute air uniformly through a vibrating bed with the same principle as the air tables. The separation of this technique is based on an air pulsing flow, which moves all the materials in the same direction to produce a stratification of fed particles. Weitkämper and Wotruba (2004) designed a new air jig for beneficiating feedstock 5–50 mm coal sizes. The equipment operates both under a pulsed air flow and constant air flow. These operating conditions serve as an advantage over all the existing fabricated jigs. The authors reported that a clean coal with an ash percentage lower than 20% can be obtained from a feed coal with 52% ash content under this process.

The elimination of pyrite nodules and liberation of clays from candiote coal was evaluated by Sampaio *et al*. (2008) using the dry jigging method. The result showed a reduction in sulphur from 1.8% to 0.7%, (about 50% drop) in feed content. The ash reported to the tailings also moved up to 60%, which is comparable to the result obtained from their sink and float analysis with an ash content above 45% in the clean coal. The Department of Trade and Industry, United Kingdom (DTI, 2004; Dwari and Rao, 2007) reported the fabrication of FGX compound dry cleaner separator, which had already been employed in over 95 plants throughout China. This equipment produces multi-products of clean coal, middlings, and refuse. It has been reportedly utilized for beneficiating -80 mm raw coal with more than 75% ash content removal, but with lower efficiency for the -6 mm size range, and less efficient than wet processing.

3.3.3. High-Gradient Magnetic Separation (HGMS)

Magnetic separation of coal has been applied to the problem of removing sulphur and ash from coal prior to combustion in the power stations. The studies conducted on coal and its product is primarily on pyrite removal due to the importance of sulfur reduction in putting a limit to the amount of SO_X emissions from the coal. A novel dry approach introduced by Oda *et al.* (1983) using a high-gradient magnetic separator combined with a fluidized bed was investigated for the evaluation of cleaning pulverized coal. The ash percentage of coal was found to be effectively reduced by 44.40% ash at a low-coal recovery rate of 74.50% after 5 to 8 passes. Saeid *et al*. (1992) at optimum fluidization applied magnetic separator under intensified magnetic field for effective coal desulphurisation and ash removal. The result obtained showed an ash analysis of processed samples demonstrating a significant ash reduction at lower ranges (-2 mm), with a 40% reduction in the - 500 + 106 μm size fraction. The authors also found that only the ash was removed during the wet test, with total sulphur removal being in the order of 10% achieved from the dry method. Researchers also implied that better liberation of coal through grinding will improve the efficiency of HGMS combined with a gas stream.

Air magnetic pearls fluidized bed and magnetically stabilized fluidized bed was utilized by Fan *et al*. (2005) to beneficiate 50 to 6 mm coarse coal and 6 to 0.5 mm fine coal. The separation efficiency of this process was found to depend on the uniformity and stability of the bed, which resulted into weak back mixing of medium solids and small bubbles within the bed. The result obtained showed an ash analysis of processed feed coal of 50 to 6 mm size, with ash of 21.48% reduced to a clean coal of 9.80% ash with an Ep value of 0.05. While, an Ep of 0.066 was obtained for the beneficiation of 6 to 0.5 mm fine coal under the Air magnetically stabilized fluidized bed.

The difference in the coal magnetic properties has lead to various research being conducted in order to increase the magnetic susceptibility of very weakly paramagnetic pyrite prior to magnetic separation. Microwave energy had been used in treating coal to facilitate the change of FeS_2 into FeS (pyrrhotite) for increased magnetic processing efficiency, and with the combination of other methods such as selective dielectric heating and iron carbonyl treatment investigated by (Zavitsanos *et al.,* 1978; Zavitsanos *et al.*, 1982; Butcher and Rowson 1995; Cicek *et al.,* 1996). Cicek *et al.* (1996), on the test for the desulfurization of coals by flash pyrolysis prior to the magnetic separation of coal constituent also resulted into better separation. The author converted pyrites into iron sulfides based on the temperature of pyrolysis by improving the paramagnetic characteristics of the coal. In addition, the result shows that after the beneficiation of -100 um particle size, 35% of the sulfur reduction was achieved by flash pyrolysis while, magnetic separation further improved the reduction to 48%. The study on the sulfur and ash removal from low-rank lignite coal by low temperature carbonization and dry magnetic separation was investigated by Celik and Yildirim (2000). The result proved to be successful but there was a serious concern regarding air pollution by sulfur removal during low-temperature carbonization.

There appear to be an improvement in the magnetic susceptibility potential of coal for HGMS beneficiation technique, at least for pyrite removal, but much work has to be done to improve this technique and to evaluate technical and economic feasibility of the whole process for coal cleaning.

3.4. Other Material Beneficiated by Tribo-electrostatic Techniques

Power generation, combined with the magnitude of green house gas (GHG) in the 21^{st} century had lead to a very high demand in producing an environmentally clean and cost effective fuel for the generation of electricity in the world. The introduction of low-NO_x burners had been very effective in the reduction of NO_x although, they often increase the quantity of carbon in the coal combustion by-products. However, due to the limitation in the utilization of this by-product, new research has been conducted using Tribo-electrostatic techniques for the separation of high LOI ash from the unburned carbon for its utilization in the cement industries. In addition, the disposal of waste plastic in an incinerator had resulted in the formation of unacceptable emissions of gases such as nitrous oxide, sulphur oxides, and hazardous HCl gases which pollute the environment and shorten the life of incinerators. Hence, this had also lead to research into the application of tribo-electrostatic separator for recycling mixed plastics due to its ability for separating different types of material (Li *et al.*, 1999; Manouchehri, 2000).

There are many research reports on work that have been carried out in the field of dry beneficiation using Tribo-electric techniques for the separation of quartz from feldspar, PVC removal from mixed plastics, fly ash from both coal combustion and coal mixed with biomass, phosphate rock from silica sand, separation of silica from a synthetic mixture consisting of charcoal and silica, and rubber from fabric, zircon from rutile, phosphorus and silica from iron ore, mineral matters from oil shales, and diamond from gangue (Gupta *et al.*, 1993; Soong *et al.*, 2000; Park *et al.*, 2007; Mazumder *et al.*, 2006). These researches had been successfully demonstrated in laboratory experiments, pilot plant studies, and in some cases commercial plants (Gidaspow, 1987; Ralton, 1961). Five minerals from different mineral groups with similar crystallography and structure, such as the feldspar group (albite and anorthite), the pyroxene group (augite and enstatite), the olivine group (forsterite, ilmenite and quartz) were selected as the samples representative of those found in lunar soil. The mixtures were separated after subjected to beneficiation tests using analytical triboelectrostatic separator (Li *et al.*, 1999).

Dry electrostatic beneficiation of silica from a synthetic mixture consisting of charcoal and silica with a particle size of approximately 37 μm was carried out by Gupta *et al.* (1993). The separation test was conducted in a batch laboratory electrostatic separator, and the result obtained showed that the efficiency of the electrostatic separator is strongly dependent on the hydrodynamic conditions such as gas velocity, electric field strength, and particle concentration in carrier gas. They found agglomeration of the fine particles as the limiting factor in achieving a higher separation and proposed particle loading of 45.36 g of solids per 453.59 g of air as a solution to this problem. The authors also investigated the beneficiation of an Indiana-New Albany oil shale, with a particle size of less than 5 μm. The carbonaceous matter acquired a positive charge while the mineral matter including pyrites charged negatively. The charge discrepancy provided the driving force for the separation, and the utilization of shale rock for oil production after the removal of mineral matter and pyrites from the shale. The depletion in the high grade deposits of phosphate rock and increasing demand for phosphate had lead to the research into the electrostatic beneficiation of low grade rocks containing various impurities. Phosphate beneficiation using electrostatic method was conducted by Zafar *et al*. (1996) in order to reduce the cost of washing, desliming, and eliminating problems relating to water shortage. The results showed that the concentrates can be obtained with fairly good recoveries, depending on the extent to which the ore can be liberated.

A tribo-electrostatic separator was utilized by Li *et al*. (1999) to investigate the fundamentals of tribo-electrification and the potential of applying these fundamentals to separate ilmentite from a mixture of five samples representing minerals typical of those found in lunar regolith with a particle size ranges from + 200 to – 140 mesh (75 μm to 106 μm). In addition, this research was conducted in order to ascertain the possibility of extracting oxygen for human use on the moon after the separation of ilmentite from the mixture of closely related minerals as that found in lunar regolith (space). The parent mixtures and data obtained from the investigation were evaluated using optical microscopy to determine to what extent the mixtures are separated. The result obtained showed that the work function of ilmenite was higher than, but very close to copper, and that the concentration of ilmenite production in all tests was 2 or 3 times more pure than in its parent mixtures. The authors concluded that from this investigation, the dry tribo-electrostatic separation technology has potential as a simple and effective method for extracting selected minerals from physical mixtures.

Park *et al*. (2007) reported the use of bench scale tribo-electrostatic separator for the removal of PVC from mixed plastics (polyvinyl chloride/polyethylene terephthalate). The authors investigated the charge polarity and charge density of PET and PVC on charging materials and various factors such as air velocity (the impact of collision or contact), mixture ratio, and the effect of relative humidity on charge efficiency were tested. The PVC and PET particles were found to be charged negatively and positively, respectively due to the difference in the work function of plastics in tribo charger of the fluidized-bed, and are separated by means of a splitter through an oppositely charged electric field. The best results were obtained at 20 KV with a tribo charger material made of PP (polypropylene), at a relative humidity below 30%, air velocity of over 10 m/s and with PVC rejection and PET recovery of 99.60% and 98.10%, respectively. The test result had shown that, the deviation between the measurements was negligible and the reproducibility was very good (±1%).

The elimination of wet cleaning, subsequent drying and processing of accompanying aqueous solution had lead to the investigation and utilization of two different types of tribo-electrostatic separators, parallel plate and louvered plate separators for the separation of fly ash derived from both coal combustion and the combustion of coal mixed with 10 wt% biomass by Soong *et al*. (2001). Thermogravimetric analyser and microscopic image analysis of the image was conducted to evaluate the parent samples and fractions collected after separation for ash and fixed carbon contents. The results obtained showed that the simple parallel plate separator is able to provide separation on fly ash derived from the combusted coal. However, in the case of fly ash derived from combustion of coal mixed with 10 wt% biomass, the parallel plate separator provided a poor quality separation. This was as a result of more carbon particles trapped within and attached to larger ash particles in biomass fly ash than that of coal combustion fly ash. The significance of surface moisture as one of the parameters affecting the separation efficiency of carbon-rich and ash-rich products derived from coal combustion fly ash was investigated by Cangialosi *et al.* (2006). The effect of humidity and particle surface moisture had been shown to be very important as the particle size of the ash decreases. Particles with size greater than 75 μm are found to be nearly unaffected whereas particles smaller than 45 μm experienced up to a four-fold change in their separability upon changing their surface moisture contents, degree of liberation and charging steps. They found that the increase in separation capability of ash having smallest particle size can be achieved upon heating.

3.5. Concluding observations

Both tribo-electrostatic and corona electrostatic method had been reported in the literature for mineral beneficiation and agriculture application. Several studies have shown that corona electrostatic techniques are basically used in separating raw materials with large difference in conductivity. Hence, the tribo-electrostatic techniques, which is a cheaper process compared to wet beneficiation processes are found to be more applicable in charging materials with little difference in conductivities. Moreover, its charging mechanism had been responsible for its ability to separate ash forming minerals from pulverized coal, and separation of reusable plastics material from plastic mixture. South African coal was beneficiated through the application of a Rotary tribo-electrostatic separator in this study. The influence of the system parameters such as charging voltage, separating voltage, injection air velocity and splitter distance were investigated in order to find an optimum process route regarding coal separation, and the results obtained have shown that the RTS also has a high separation efficiency similar to the Fluidized bed tribo-electrostatic separator.

CHAPTER FOUR

4.0. Material and Methods

4.1 Materials

In this chapter, various experimental procedures adopted in the beneficiation of South African fine coal from its mineral will be presented. The chapter is divided into three major parts. This part listed the materials used in this research and also made mentioned of the test methods employed. The tribo-electrostatic separation experiments were performed on eight different coal samples from South Africa, i) Liketh Townlands coal, ii) No. 4 Seam from Khutala colliery, iii) No. 2 seam from Khutala colliery, iv) Koornfontein coal, v) Klipfontein coal, vi) Majuba coal, vii) Polmaise coal, and viii) New Vaal coal. The samples were first milled in a hammer mill, and then pulverized to -177 µm and then separated to (177 X 74) and (-177) µm size fractions. Representative fractions at -177 µm were prepared for tribo-electrostatic separation and froth flotation test. A kinetic froth flotation test was carried out in a 4-litre Denver mechanical flotation cell under the following conditions: impeller speed: 1200 rpm; SNF Flomin F-100C froth dosage: 15 ppm; and fuel oil # 2 collector dosage: 910 g/ton. The sink/float was conducted at (177 X 74) µm for all samples and tribo-electrostatic test was also conducted at the same size fraction for Klipfontein and Liketh Townlands coal.

4.2. Equipment

Bruker-AXS D8 Discover X-ray diffractometer, LECO Thermo Gravimetric Analyzer (TGA-701) for proximate analysis, Petrographic analyses (Zeiss Universal Microscope), LECO S632 analyzer, CILAS (1092), Leco (AC-500) Bomb calorimeter, Electronic weighing balance, A 4-liter Denver cell, Hammer mill, Pulverizer, Hydrometer, Sieves, Sieve shaker, Rotary triboelectrostatic separator, (Glassman DC voltage power supply, Thermo-anemometer, Vibratory feeder, Vacuum, and Product bin)

4.2.1. Rotary tribo-electrostatic separator

The rotary tribo-electrostatic separator (RTS) developed at the University of Kentucky, USA, (2006) has the following characteristic features (Figure 4-1): 1), a rotary rotor mounted in a cylindrical chamber, with a copper plated surface for contacting and creating differential charges on particles; 2) a chamber comprised of both an inlet for receiving the particles and an outlet for discharging the particles; 3) a power source connected to the chamber's wall and the rotor, providing an electric potential to the rotary charger; 4) a separation zone consisting of two electrodes with a fixed distance between them, where charged particles from the charging chamber are deflected towards the negative or positive electrodes depending on the charge acquired; and 5) an adjustable splitter connected to three cyclones or air bags for collection of different products including, macerals and ash forming minerals. The air flow within the separating compartment is monitored and regulated using a thermo-anemometer and gate valve connected to the nozzle under the collecting bin.

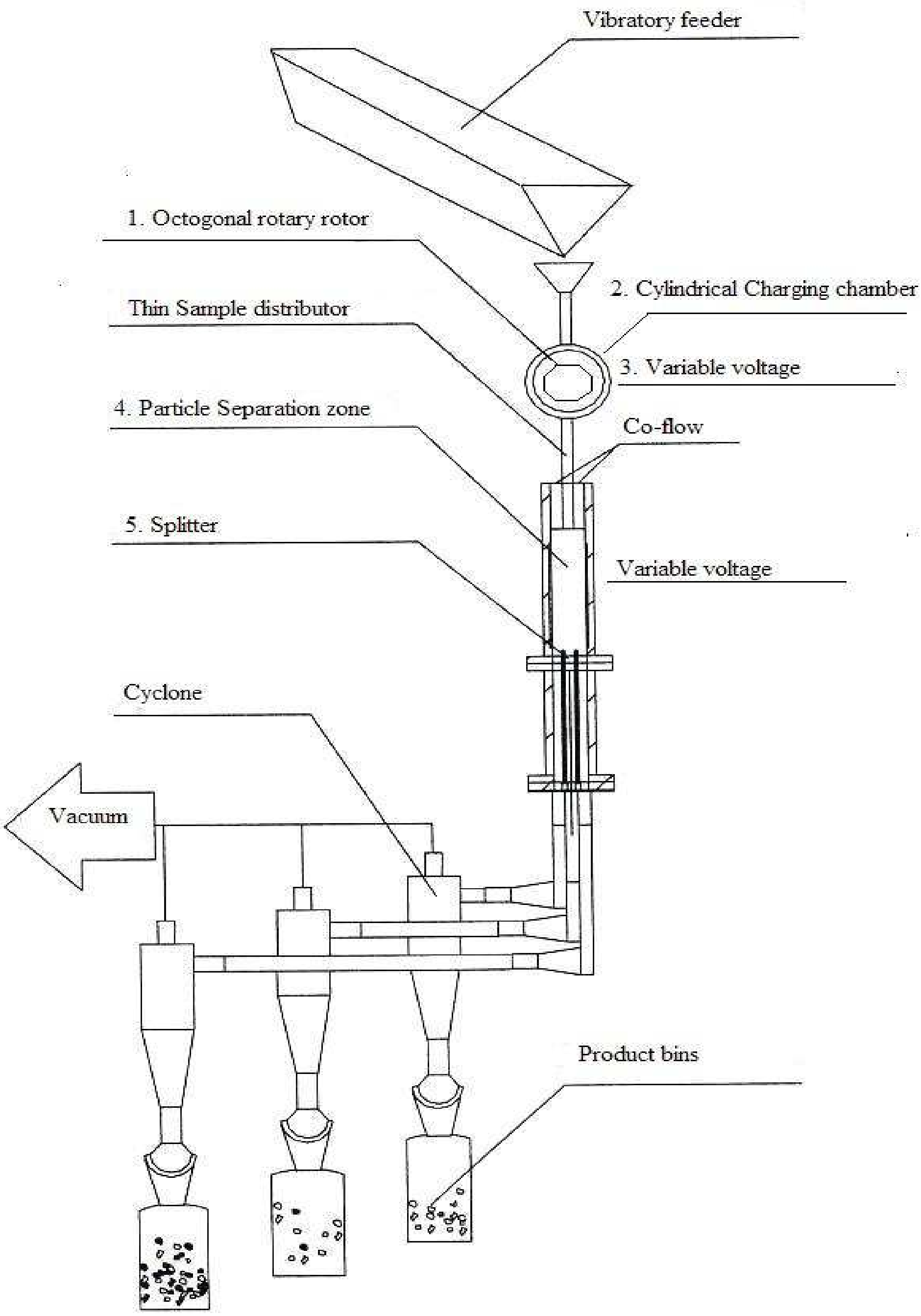

Figure 4-1. Schematic representation of a pneumatic tribo-electrostatic separator with an octagonal rotary rotor.

The innovative rotary tribo-electrostatic separator developed at the University of Kentucky, USA was used for the separation of coal organic from its mineral matters. The differential charge imparted on the coal and its mineral matter for effective separation in an electric field was created by a positively charged electrode and a second electrode connected to the ground. Thus, any mineral matter within the coal was charged negatively in the charging chamber and subjected to an attractive force from the positive electrode, while the coal organic (charged positively) are subjected to a repulsive force from the same positive electrode. The grounded electrode also provides a surface for the collection of the positively charged particles without interfering in the repulsion or attraction of the particle from the electrode. Coal particles were deposited on both electrodes after passing through a high strength electric field at the separating zone, and those that passed through the separation zone into the bins were collected and analyzed to determine the separator efficiency.

4.3. Experimental Procedure

4.3.1. Mineralogical Methods Used For the Classification of Feed Coal

The techniques needed for the characterization of coal requires the knowledge of its origin, maceral and mineral composition, and physical properties such as the particle size, phase composition and proximate analyses. In order to obtain a best possible result from the characterization of the coal a combination of Bruker-AXS D8 Discover X-ray diffractometer and CILAS (1092) particle size distribution analyser were used by employing standard procedures.

4.3.2. Proximate Analysis

The proximate analysis was carried out with a Leco Thermo Gravimetric Analyser (TGA-701). Approximately 1 g of coal sample was used for the analyses in determining the inherent moisture, fixed carbon, ash content and volatile matter present in the coal. The TGA was operated under N_2 atmosphere for moisture and volatile matter analysis with the end temperature of 107 ^{0}C and 950 ^{0}C, respectively. The ash analysis was carried out under low oxygen atmosphere and at an end temperature of 750 ^{0}C. The result obtained with -177 µm coal fractions are presented in Table 5-1, which shows high ash and low moisture contents for all samples.

4.3.3. Particle Size Distribution Analysis

The coal sample particle size distribution was determined using a laser particle size analyzer CILAS (1092) with a measuring range of 0.04 to 500 µm. It utilizes both Mie algorithms and Fraunhofer diffraction of light formed by particles with a diameter larger than the incident laser beam wavelength. A combination of multiple lasers and optical filter, lens and photo detector coupled with a computer loaded with SizeExpert software enables one to compute the particle size distribution from the diffraction data and store it as cumulative value percentage against the particle diameter (µm).

Table 4-1. Particle size distribution for feed coal

Coal sample	Particle Size D_{90} (µm)	Particle Size D_{50} (µm)	Particle Size D_{10} (µm)
Klipfontein	127.40	68.20	4.87
Liketh Townlands	122.00	49.32	7.82
Polmaise	92.02	54.25	5.28
Majuba	102.69	44.01	3.19
New Vaal	106.95	46.08	3.51
Koorfontein	119.56	65.04	8.03
Khutala seam 2	106.45	34.66	5.00
Khutala seam 4	104.72	34.90	4.51

4.3.4. X-ray Diffraction Analysis

The identification of the mineralogical constituents of the coal was performed with the X-ray diffraction analysers for the qualitative evaluation of the common and predominant phases within the coal. The phase identification of the representative coal powder samples was carried out using a Bruker-AXS D8 Discover X-ray diffractometer with a rotating Cu-anode. The diffractometer was operated at 40 kV and 40 mA, over the range of 2θ from -2^o to -70^o at a scan speed of 1 deg/min and the identification was conducted with DIFFRAC^{PLUS} suite software. The diffractogram (Figure 5-1 to 5-8) shows the X-ray diffraction pattern for the feed coal, single pass and two stage cleaned coal products.

4.3.5. Total Sulphur Analysis

The total sulphur in feeds and products was analyzed with LECO S632 analyzer, which has the capability to operate at up to 1,450^{o} C with an analyzing time between 60 – 120 seconds. The proximate analysis was conducted with LECO Thermo Gravimetric Analyzer (TGA-701). The ash was analyzed under oxygen atmosphere and the volatile matter and moisture under nitrogen atmosphere.

4.3.6. Heat Content Analysis

The calorific value which is known as the measure of the heat content of coal was determined using a Leco (AC-500) bomb calorific, with a window based operating system. The system uses an electronic thermometer with an accuracy of 0.0001 ^{0}C to measure the temperature every six seconds, with the results obtained within 4.5 to 7.5 minutes.

4.3.7. Tribo-electrostatic Test

The coal samples used for the tribo-electrostatic experiment were kept in an oven at 54 ^{0}C overnight to remove the surface moisture prior to separation. For each test, 100 g of the representative samples were fed through a vibration feeder and then transported pneumatically at different air flow velocities into a cylindrical charging chamber of 18 cm in diameter. The tests were conducted at single and two stage separation process as shown in Figure (4-2 and 4-3), with variable separating voltage DC power supply employed to study the effect of electric field created in the separating zone which was found to have considerable effects on the separating efficiency of the coal particles. Other parameters such as applied charger potential, tangential speed of the rotor, splitter distances, air injection velocity and Co-flow were also investigated.

The feed coals were fed and transported pneumatically into a cylindrical charging chamber, and imparted with positive and negative charges. The positively charged particles are deflected towards the negative electrode (R plate), while the negatively charged particles are attracted towards the positive electrode (L plate) and the uncharged particles fall in-between the two electrode and collected as a middling. The middling was then fed into the separator for further separation and the three products collected were further analyzed. Regarding the two stage test, the three products collected from the single stage test under the same splitter distance were subjected to further cleaning to generate more finely separated products. The feed and products were analyzed for ash composition, phase composition, total sulphur and calorific value. The performance curves generated were used to evaluate the separation performance for all samples.

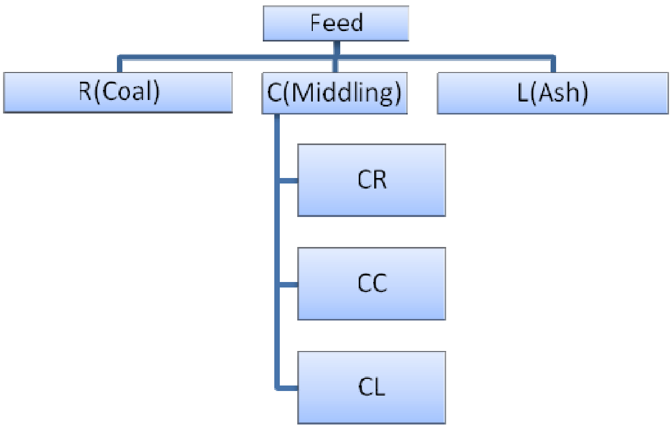

Figure 4-2. Flowsheet for single and middling re-cycled stage process

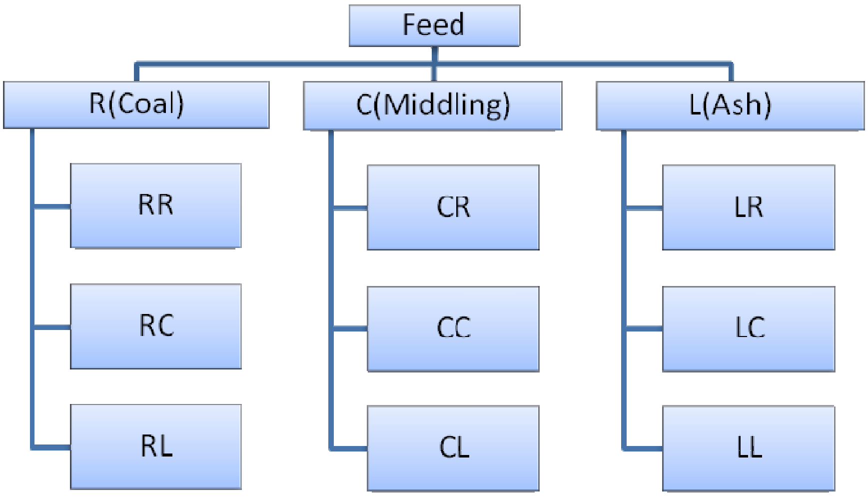

Figure 4-3. Flowsheet for two stage process

4.3.8 .Washability and Froth rate test

Following standard sampling procedure, the washability study was conducted with the (177 X 74) µm size fraction by the sink/float technique at 1.4 and 1.8 relative density (R.D) using lithium metatungstate (LMT) solution. The float and sinks fractions collected after each test were filtered, and dried at 54 ^{0}C, weighed and detailed analysis conducted. The incremental froth flotation test was conducted with -177 µm size fraction in a 4-litre Denver cell under the following conditions, impeller speed: 1200 rpm; froth dosage: 15 ppm; and collector dosage: 910 g/ton. The result obtained from both test was used as standard for evaluating the performance of the electrostatic techniques by providing basis and background information for comparing the separation performance of the results obtained from the electrostatic separator.

4.4. Concluding observations

High ash and low moisture contents samples were utilized in this study. The particle size utilized for the tribo-electrostatic and washability test were -177 µm and 177 X 74 µm, respectively. Samples were subjected to single and two stage tribo-electrostatic separation processes to determine the optimum process conditions for maximum cumulative yield and product grade. The extent of sulphur reduction for the feed and cleaned coal product obtained after the single and two stage test was determined by sulphur analysis using a Leco analyser. Change in mineralogical composition was determined using XRD before and after triboelectrostatic separation.

CHAPTER FIVE

5.0 Results and Discussion

Available literature in the cleaning of coal fly ash through the separation of unburned carbon from the fly ash indicates that the cylindrical rotary tribo-electrostatic separator had been employed for coal fly ash cleaning Tao *et al.* (2009). In this research, the newly developed octagonal rotary tribo-electrostatic separator was utilized for the first time in cleaning and separating coal organics from its coal minerals. There are many factors affecting the efficiency of a tribo-electrostatic separator, and different material responded to tribo-electrification based on their origin, particle size, material properties and system operational parameters. The effect of particle size at (-177) µm and (177 X 74 µm was investigated for Klipfontein and Liketh Townlands at single and two stage separation processes. Other parameters, such as rotary charger rotation speed, injection air velocity, separating voltage and feed rate were also evaluated to maximize coal beneficiation for all the eight samples used in this study.

The froth rate and washability tests were conducted to investigate the cleaning potential of the coals and the results obtained were compared with those obtained from the tribo-electrostatic test. The data reported from the rotary tribo-electrostatic separation were generated with the single and two stages of separation, and the separation efficiency was evaluated based on grade and percentage of cleaned product recovered. In addition, the separation efficiency was also evaluated based on the total sulphur reduction, improved calorific value and mineral reduction in cleaned coal products. The performance curves at different operating parameters are also presented to illustrate and evaluate the separation performance for all coal samples.

5.1. Analytical test results on all coal samples

The results of the analysis on the feed coals were presented in Table 5-1, It shows the proximate results for all the feed coal used in this study, and Figure 5-1 to 5-8 shows the mineralogical composition of the feed coal and products obtained from the tribo-electrostatic test, While Table 5-2 and 5-3 shows the rank, maceral composition and microlithotype particle analysis conducted on the feed and products obtained from the tribo-electrostatic test. The extent to which the feed coal can be cleaned after single and two stage separation were summarized in Table 5-5 and 5-6.

Table 5-1. Proximate results for feed coal

Coal sample	Fixed carbon %	Volatile matter %	Moisture %	Ash %
Klipfontein	42.03	20.57	1.59	35.81
Liketh Townlands	44.97	20.71	2.82	31.50
Polmaise	42.88	20.76	3.28	33.08
Majuba	43.69	23.01	3.19	30.10
New Vaal	33.64	20.08	7.51	38.77
Koorfontein	52.35	24.04	3.03	20.58
Khutala seam 2	44.66	22.28	1.21	31.85
Khutala seam 4	38.91	22.88	1.20	37.46

5.1.1. XRD Analysis

The diffractograms from Figure 5-1 to Figure 5-8 shows the X-ray diffraction pattern for particles smaller than 177 µm. It can be observed that the coal consists mostly of crystalline minerals such as quartz, kaolinite, and organic hump. The intensity of quartz and Kaolinite is very strong in the feed coal compared to the cleaned single pass and second pass coal products obtained after separation, which is characteristic of a high ash Southern Hemisphere coal. With Majuba coal (Figure 5-1) the feed shows a lower organic hump with high mineral matter compared to a much larger hump in the cleaned product. The increase in the organic hump of the cleaned products indicates lower mineral matter which can be seen in all the coal tested. Organic hump corresponds to the quantity of the organic present in the coal since organic matter behaves like an amorphous material to X-rays (Hutton and Mandile, 1996).

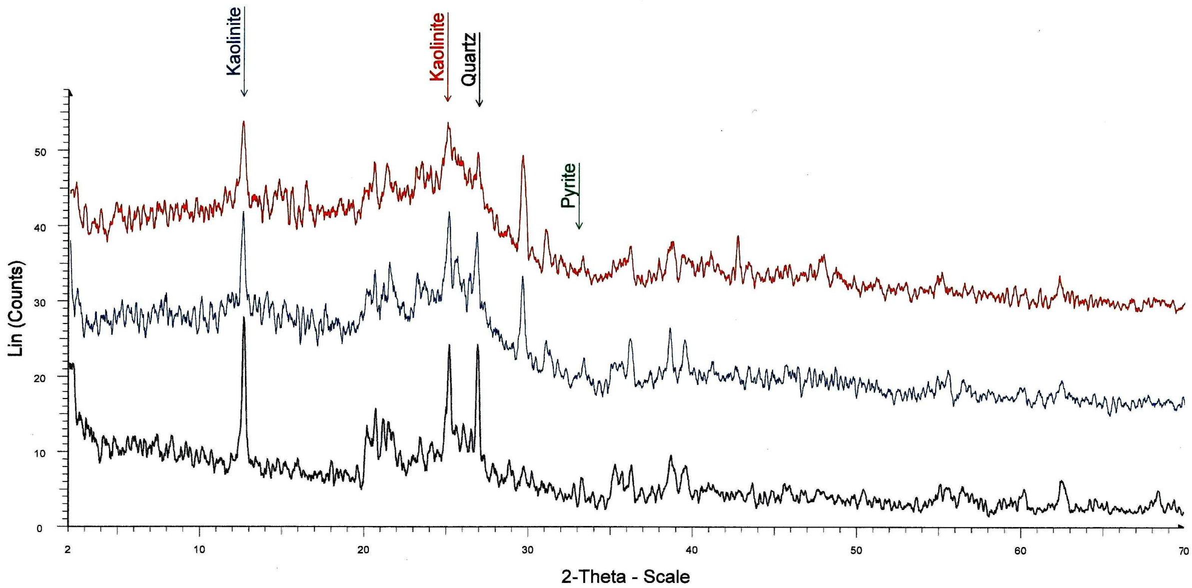

Figure 5-1. X ray diffraction pattern Majuba feed (below), cleaned single pass product (middle) and cleaned second pass coal product (above) after Tribo-separation

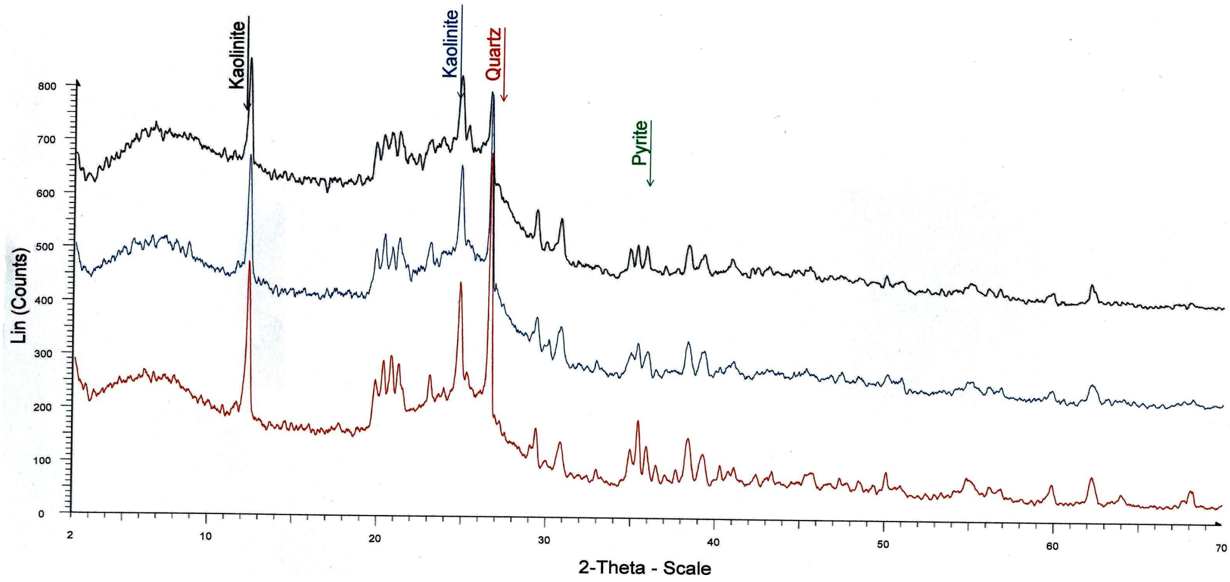

Figure 5-2. X ray diffraction pattern Koorfontein feed (below), cleaned single pass product (middle) and cleaned second pass coal product (above) after Tribo-separation

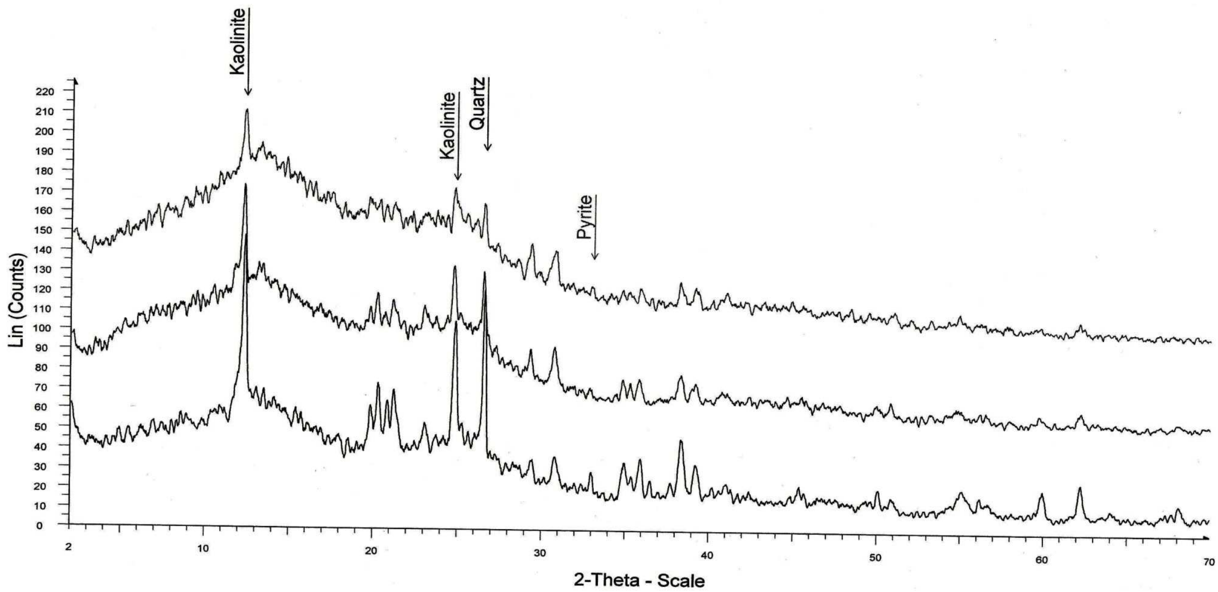

Figure 5-3. X ray diffraction pattern of Khulata 2 seam feed coal (below), cleaned single pass product (middle), and cleaned second pass product (above) after Tribo-separation

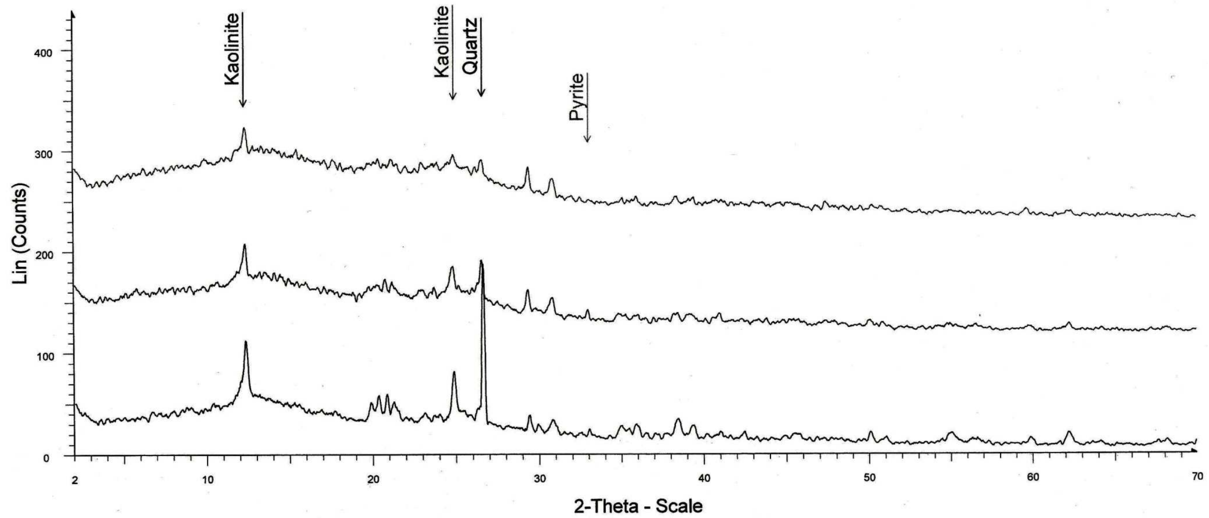

Figure 5-4. X ray diffraction pattern of Khulata 4 seam feed coal (below), cleaned single pass product (middle), and cleaned second pass product (above) after Tribo-separation

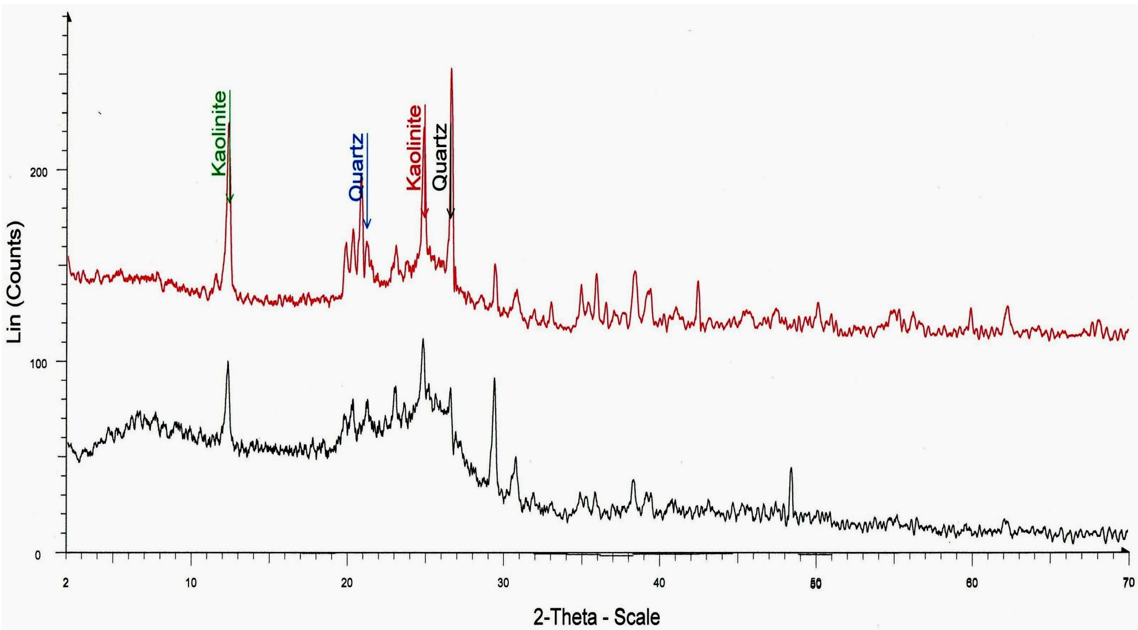

Figure 5-5. X ray diffraction pattern of Liketh Townlands feed (above) and cleaned coal (below) after Tribo-separation

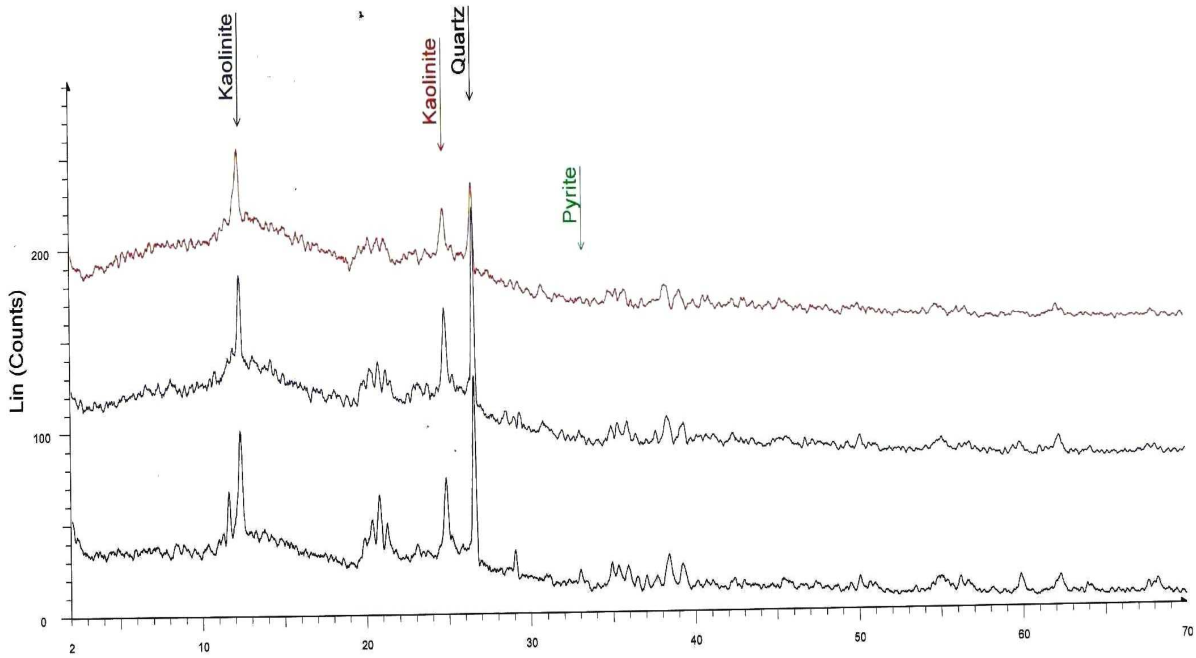

Figure 5-6. X ray diffraction pattern of Polmaise feed coal (below), cleaned single pass product (middle), and cleaned second pass product (above) after Tribo-separation

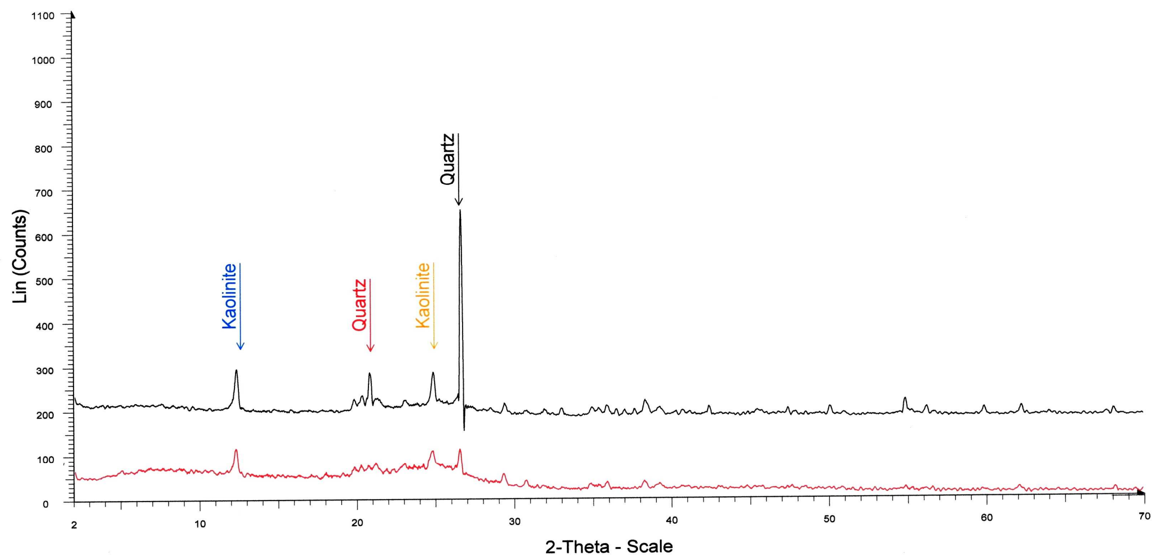

Figure 5-7. X ray diffraction pattern of Klipfontein feed (above) and cleaned coal (below) after Tribo-separation.

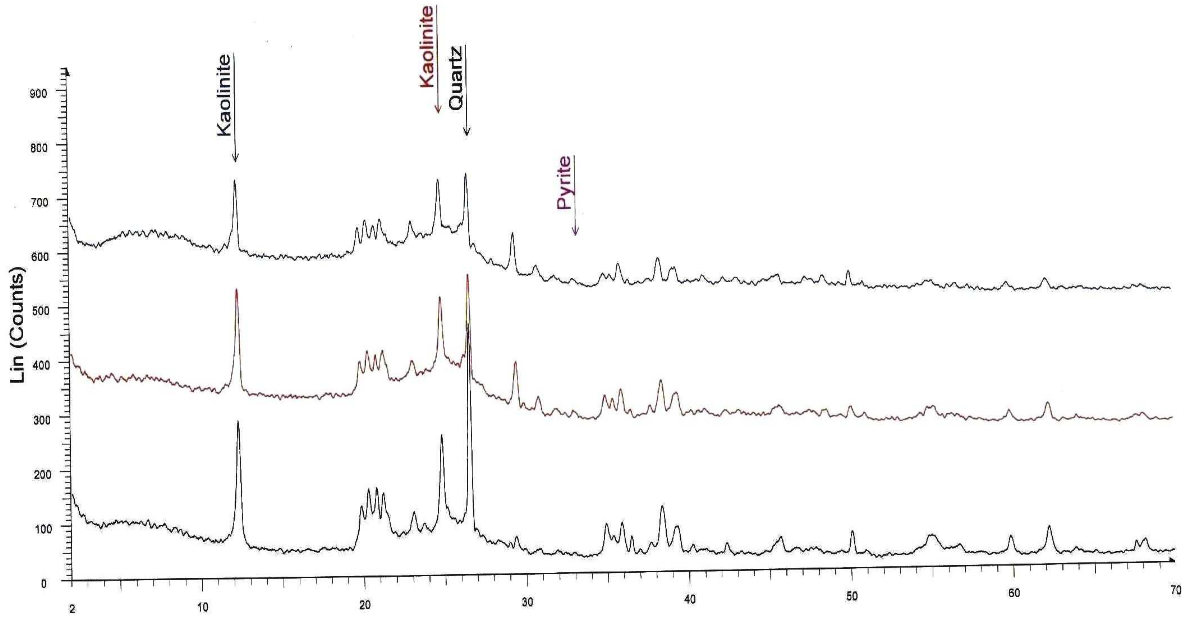

Figure 5-8. X ray diffraction pattern of New Vaal feed coal (below), cleaned single pass product (middle), and cleaned second pass product (above) after Tribo-separation

5.1.2. Petrographic Analysis

Petrographic composition in terms of the maceral and microlithotype analysis provided some information regarding the extent to which the coal was cleaned using tribo-electrostatic separation technique. Cleaned coal products obtained from the single and two stage separation, along with the feed were subjected to a combined maceral and microlithotype analysis. The results obtained were presented in Table 5-2 and 5-3. Particles charged positively in the charging chamber and collected from the negative plate electrodes shows a high vitrinite composition compared to the feed coal. From table 5-2, the total vitrinite in the Khutala No.2 seam coal feed accounted for 15% and increasing to 53% after the two stage test with the total inertinite decreased to 37% from 63%. In terms of the mircolithotype analysis, the pure vitrinte particles showed a remarkable increase from 11% in the feed up to 34% in the two stage product. Same trend were followed by Koorfontein and Klipfontein coal in regards to the reduction in the visible mineral in the feed. The change in mineral concentration down to 6% after the two stage cleaning for Koorfontein coal was accompanied by a less marked change of maceral composition, with vitrinte content increasing to 36%. This is an evident that the vitrinite was more concentrated in the clean product with the support from the lower ash content from two stage test results obtained in Table 5-5 .

Table 5-2. Maceral composition and mineral matter for Khutala No. 2 seam, Khutala No. 4 seam Koorfontein and Klipfontein coals processed through triboelectrostatic separation

SAMPLES (-177) um	**MACERAL ANALYSIS (% BY VOLUME AND MINERAL MATTER BASIS)**			
	VITRINITE	**LIPTINITE**	**INERTINITE**	**VISIBLE MINERAL**
Khutala 2 seam (feed)	**15**	**3**	**63**	**19**
Khutala 2 seam (Single stage test)	**39**	**3**	**50**	**8**
Khutala 2 seam (Two stage test)	**53**	**3**	**37**	**7**
Khutala 4 seam (feed)	**21**	**3**	**51**	**25**
Khutala 4 seam (Single stage test)	**34**	**2**	**51**	**13**
Khutala 4 seam (Two stage test)	**54**	**3**	**34**	**9**
Koorfontein (feed)	**23**	**3**	**64**	**10**
Koorfontein (Single stage test)	**31**	**2**	**60**	**7**
Koorfontein (Two stage test)	**36**	**2**	**56**	**6**
Klipfontein (feed)	**17**	**2**	**61**	**20**
Klipfontein (Single stage test)	**18**	**2**	**66**	**14**
Klipfontein (Two stage test)	**17**	**2**	**71**	**10**

Table 5-3. Microlithotype – particle analysis for Khutala No. 2 seam, Khutala No. 4 seam, Koorfontein and Klipfontein coals processed through triboelectrostatic separation

Samples (-177) um	Pure Vitrinite %	Pure Liptinite %	Pure Inertinite %	Organic Intermediates %	VISIBLE MINERALS %	
					Carbominerite	Mineral rich
Khutala 2 seam (feed)	11	0	26	21	23	19
Khutala 2 seam (Single stage test)	25	0	35	27	10	3
Khutala 2 seam (Two stage test)	34	0	31	25	8	2
Khutala 4 seam (feed)	12	0	30	20	19	19
Khutala 4 seam (Single stage test)	22	0	33	27	14	4
Khutala 4 seam (Two stage test)	40	0	25	24	8	3
Koorfontein (feed)	15	0	40	25	14	6
Koorfontein (Single stage test)	20	0	43	25	8	4
Koorfontein (Two stage test)	25	0	41	26	7	1
Klipfontein (feed)	11	0	35	22	21	11
Klipfontein (Single stage test)	12	0	44	21	16	7
Klipfontein (Two stage test)	14	0	57	14	9	6

5.2. ***Washablity and froth rate test***

The washability and froth flotation studies were conducted to evaluate or delineate the cleaning potential of the coal samples utilized in this study prior to their separation in RTS, and the results obtained from both tests are shown in Figure 5-9 and 5-10. For the froth rate test, the coal particles are collected between 15 to 360 seconds for analysis, while the washability test was conducted at a relative density of 1.4 and 1.8 RD. It can be seen in Fig. 5-10 that a clean coal of 6.80% ash with a combustible recovery of 20.99% was obtained at 1.4 RD for Klipfontein coal while a clean coal of 7.51% ash was produced at 1.4 RD with a combustible recovery of 15.02% for New Vaal coal. The results obtained from the sink/float analysis were far better as compared to the froth flotation test in Figure 5-9 which resulted in a clean froth product of 18.30% ash at 3.60% combustible recovery after 15 seconds for the New Vaal coal and another clean product of 22.20% ash at 22.42% combustible recovery was also collected after 60 seconds. A clean froth product of 20.63% ash with 10.75% combustible matter was obtained for the Klipfontein coal, while the Koornfontein coal shows the best separation and responses to froth flotation. It was quite obvious that the coal samples utilized in this study were difficult to clean by froth flotation as shown by low recovery and high ash percentage cleaned coal product obtained. This supports the alternative cleaning processes such as tribo-electrostatic separation.

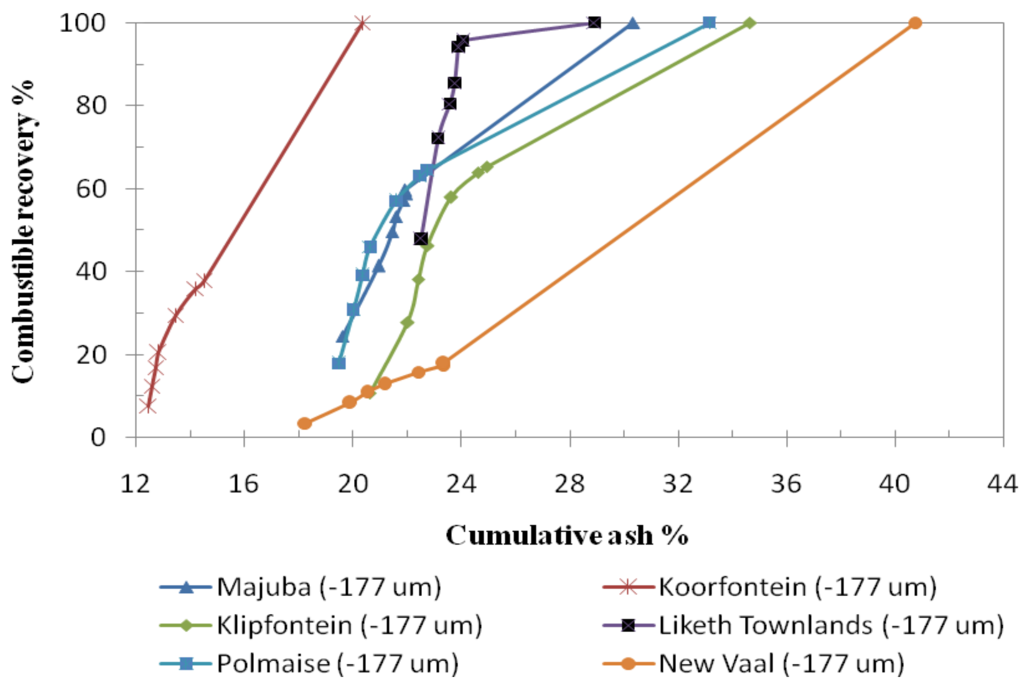

Figure 5-9. Combustible recovery/cumulative ash curve obtained using "froth flotation rate test" at 910 g/ton, 15 ppm and 1200 rpm.

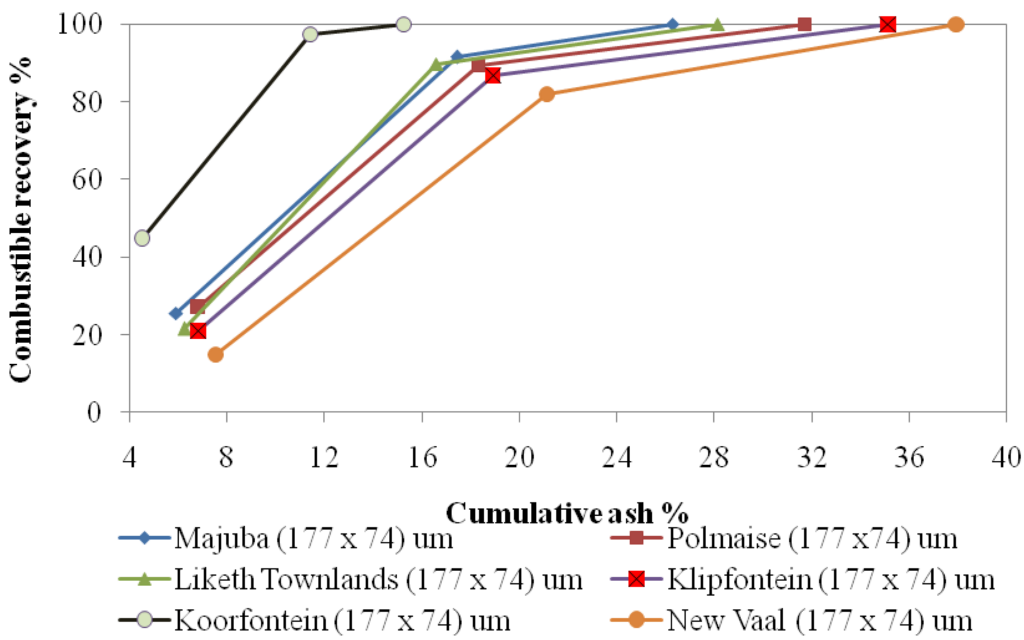

Figure 5-10. Performance washability curve for six coal samples at relative density: 1.4 and 1.8

5.3. ***Effect of particle size on tribo-electrostatic separation***

Figure 5-11 and 5-12 presents the experimental results for the effect of particle size on the grade and cumulative yield of clean product obtained from the two stage separations conducted using an octagonal rotary charger electrostatic separator. The investigation was performed on Klipfontein coal at (177 x 74) µm and (-177) µm size fraction, and the same fractions were also investigated for Liketh Townlands coal. Figure 5-13 and 5-14 shows another set of investigation conducted under single and two stage separation on both coal samples at (177 X 74) size fraction. All tests were conducted at constant charging voltage: 0 KV; separating voltage: 12.5 KV; air velocity: 2.5 m/sec; rotary speed of 2500 rpm and splitter positioned at 0.6 cm from the negative electrode. The results obtained as presented in Figure 5-11 and 5-12 that coarser particles with lower ash clean product and better separation compared to the result obtained from the finer particles. Cleaner coal product of 9.80% ash was obtained for the Liketh Townland coal at (177 x 74) µm compared to 12.60% ash product obtained for (-177) µm in Figure 5-4. The result obtained in Figure 5-3 for Klipfontein coal also followed the same trend, with a cleaner product ash of 11.10% attained at (177 x 74) µm and 14.90% obtained at (-177) µm size fraction.

Results obtained on Klipfontein coal are presented in Figure 5-13 for the single and two stage separation with (177 x 74) µm size fraction. The results reveal a clean product of 17.30% ash with a yield of 14.70% from a feed coal of about 35% ash was obtained under the single stage of separation. The second stage of separation further reduced the clean coal ash to 15.50% ash product with 10.90% yield and 11.10% ash product with 3.40% yield. From Figure 5-14, Liketh Townlands coal with a feed coal of 30% ash was also reduced to 15.11% ash after single stage separation, and further reduced to a clean product of 9.87% ash under second stage separation. It is noticed that all data generated from two stage of separation are at the upper part of the single stage separation curve, showing better separation and recovery for both coal tested.

The result from the (177 x 74) µm size fraction for all samples tested can be attributed to higher charge density imparted by the rotary charger on this size fraction as compared to (-177) µm coal fraction. Fine particles are known to be more attracted to the charging surfaces after being charged due to the large differences in surface charge relative to the mass of the particle. The reduction in the charge densities imparted on this coal fraction might be attributed to the decrease in the field intensity within the charging chamber by the sticking of these particles on the rotary charger and the decrease in the particle-wall chamber contacts. The increase in higher ash products obtained from the (-177) µm size fractions in this study seems to be in an agreement with the result obtained by Yoon *et al.* (1997a; 1997b) on the cleaning of fine coal with a bench scale Tribo electrostatic separator (TES) unit equipped with tribocharger.

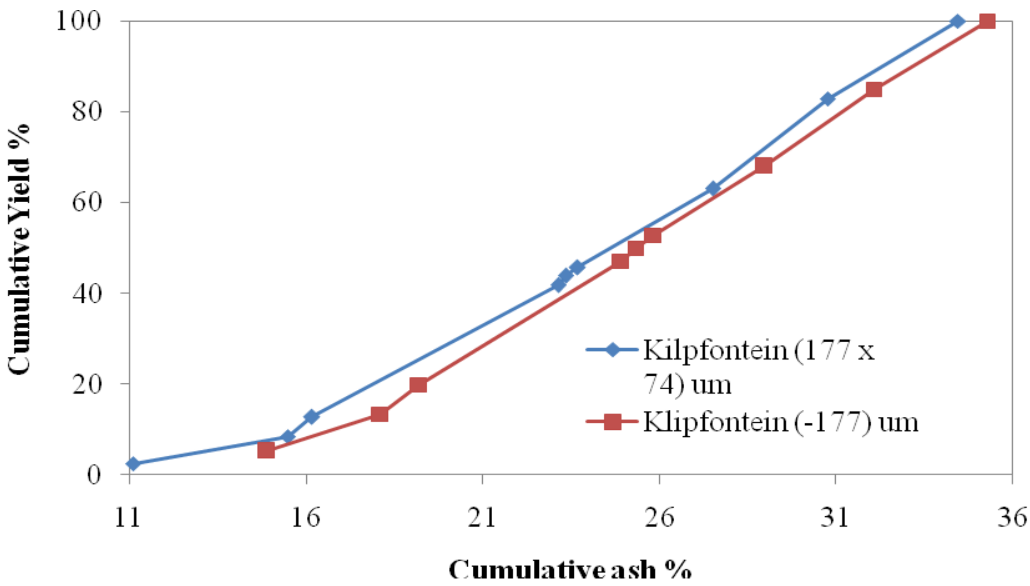

Figure 5-11. Effect of particle size on grade and recovery of Klipfontein coal at constant charging voltage: 0 KV; separating voltage: 12.5 Kv; air velocity: 2.5 m/sec; and rotary speed of 2500 rpm.

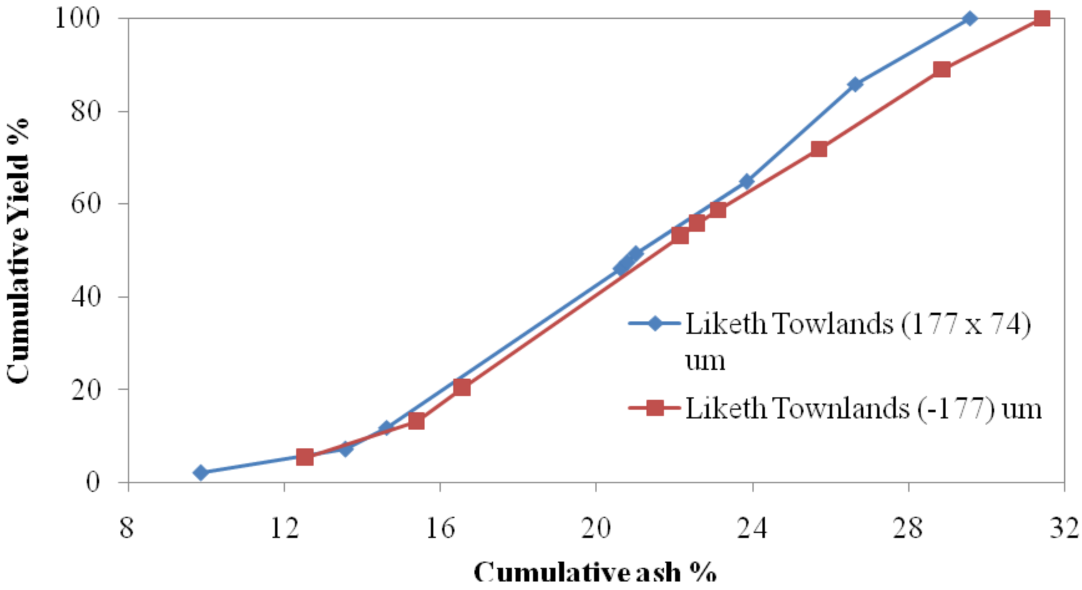

Figure 5-12. Effect of particle size on grade and recovery of Liketh Townlands coal at constant charging voltage: 0 KV; separating voltage: 12.5 Kv; air velocity: 2.5 m/sec; and rotary speed of 2500 rpm.

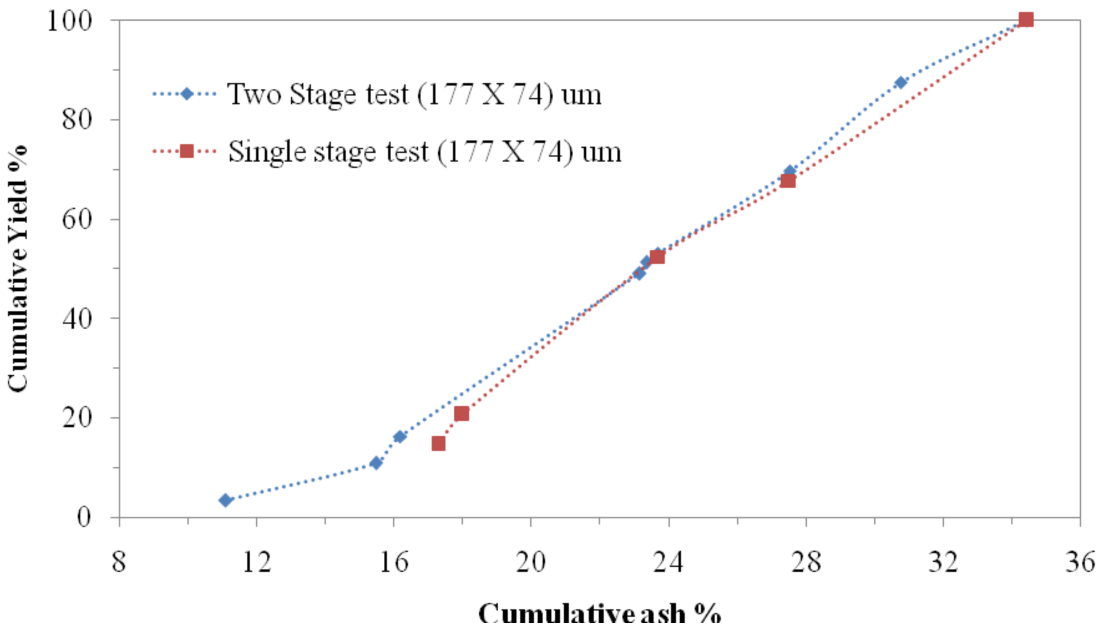

Figure 5-13. Single and two stage test on Klipfontein coal at constant charging voltage: 0 KV; sseparating voltage: 12.5 Kv; air velocity: 2.5 m/sec; and rotary speed of 2500 rpm.

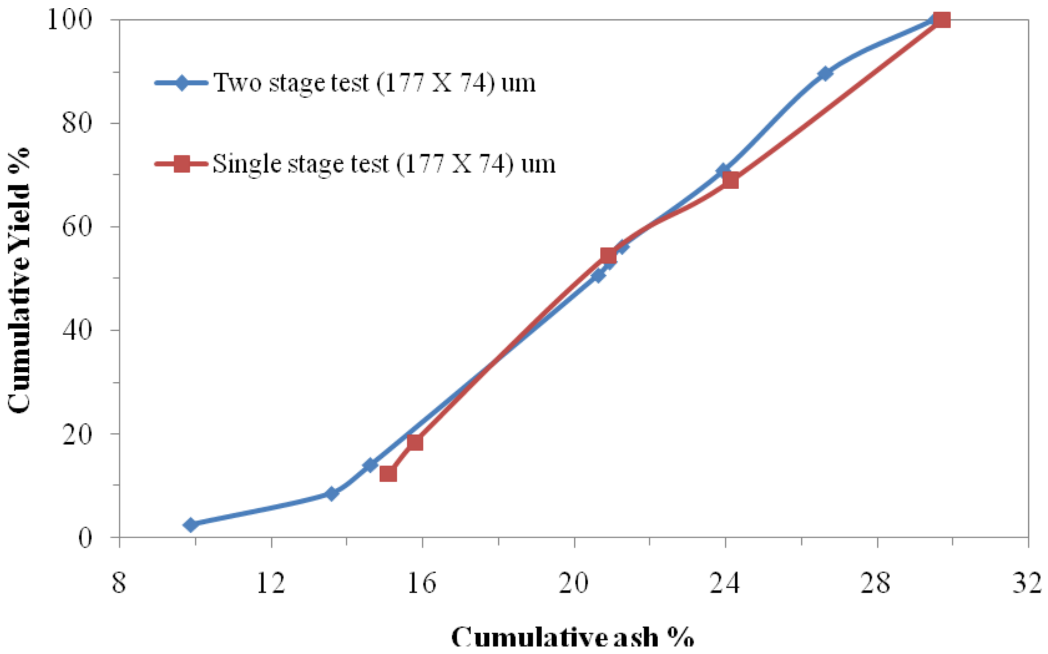

Figure 5-14 Single and two stage test on Liketh Townlands coal at constant charging voltage: 0 KV; sseparating voltage: 12.5 Kv; air velocity: 2.5 m/sec; and rotary speed of 2500 rpm.

5.4. *Effects of splitter position*

The study provides information on the position of the splitters which is very important for the efficiency of the triboelectrostatic separator and also influences the grade and recovery of the coal product. The product splitter position was adjusted to achieve different splits of clean coal products, middlings and tailings. For instance, when the splitter was tilted more toward the negative electrode, a cleaner coal product was collected at the expense of combustible recovery. This resulted in the shift of the data point to lower left corner along the combustible recovery vs. Ash curve and also changes the shape and position of the curve as shown in Figure 5-15. Two stage separation tests were conducted with Klipfontein coal at four different splitter settings to optimize the positions of the splitters for high grade product recovery. Tests were investigated at a constant injection gas velocity of 2.5 m/s, applied charging potential of 5.0 KV, separation chamber voltage of 22.5 KV, and rotating speed of 3000 rpm**.** The outlet air velocities through the three nozzles were maintained at 6.1 m/sec. As shown in Figure 5-15, a product of 24.46% ash was obtained when the splitter was 0.6 cm from the negative electrode and 2.7 cm away from the positive electrode. The decrease in ash from 35.12% to 24.32% was at the expense of combustible matter recovered. For example, the combustible matter recovered was 61.24% for the Klipfontein coal when the splitter was located 1.5 cm from the negative electrode. This was in agreement with the result reported by Soong *et al.* (1998) on the tribo-electrostatic separation of Slovakian coal and also confirms the information provided by Kelly and Spottisword (1982) on the influence of splitter position over grade and recovery.

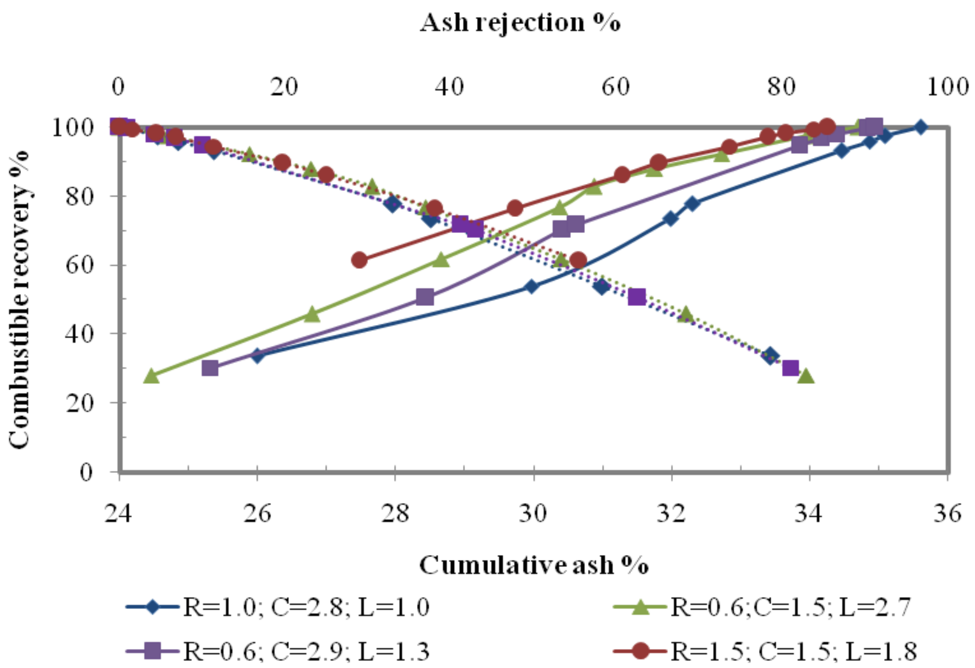

Figure 5-15. Effect of splitter distance on grade and recovery of Klipfontein coal at constant charging voltage: 5 KV; sseparating voltage: 22.5 Kv; air velocity: 2.5 m/sec; and separating voltage: 12.5 Kv.

5.5. Comparing the effect of splitter distance on single and two stage separation

The effect of splitter distance on single and two stage separation was investigated. Results obtained as presented in Figure 5-16 reveals that second stage test had a better separation in terms of ash reduction and product quality recovered. The application of both single and two stage test can only be economically justified, based on the product quality obtained and the end utilization. The clean coal products, middlings and tailings obtained during the test were achieved by varying the splitter position at R=0.6; C=1.5, & L=2.7 cm and R=1.0; C=1.5 & L=2.3 cm for both samples, respectively. Single and two stage separation was conducted on Majuba coal at a constant injection gas velocity of 1.9 m/s, applied charging potential of 1.5 KV, separation chamber voltage of 12.5 KV, and rotating speed of 2500 rpm**.** For Majuba coal in Figure 5-16, the single stage curve for a splitter positioned at 0.6 cm from the negative electrode shows a clean coal product of 14.70% ash from a feed coal of 30.10% ash, which is closer to the clean product of 13.30% ash obtained from the two stage test at 1.0 cm away from the negative electrode. The ash % in the clean coal product further increased to 15.90% as the splitter was adjusted to 1.0 cm away from the negative electrode. However, two stage separation processes still shows greater reduction of high ash from the feed coal. The two stage test result shown in Figure 5-16 for the same coal shows the splitter positioned 0.6 cm from the negative electrode, with a clean coal product of 11.10% ash and 5.90% combustible matter collected, while the increase in the combustible matter from 5.90% to 9.20% at 1.0 cm away from the negative electrode was at the expense of the cleaned product collected. The same trend was observed from Koornfontein coal, as shown in Figure 5-17, a clean product of 9.98% ash and combustible matter of 3.51% was obtained when the splitter was 0.6 cm from the negative electrode and 11.70% cleaned ash product was collected at 1.0 cm away from the negative electrode for two stage test. While under single pass test, a clean coal of 13.10% ash and combustible matter of

11.30% was obtained when the splitter was 0.6 cm from the negative electrode and 14.20% cleaned ash product was collected at 1.0 cm away from the negative electrode.

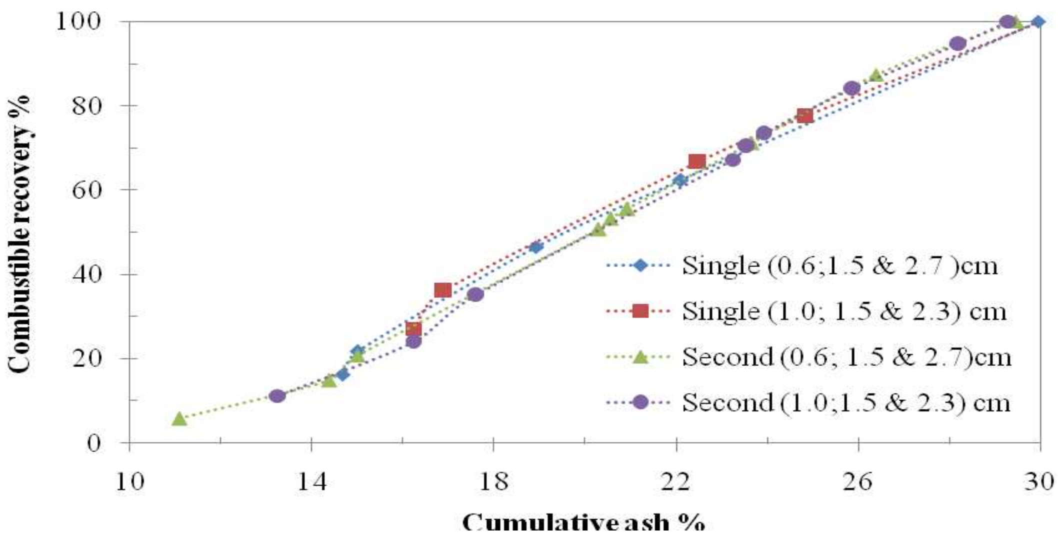

Figure 5-16. Effect of splitter distance on single and second stage test on Majuba coal at a constant charging voltage: 1.5 KV; separating voltage: 12.5 KV; air velocity of 1.9 m/sec and rotary speed of 2500 rpm.

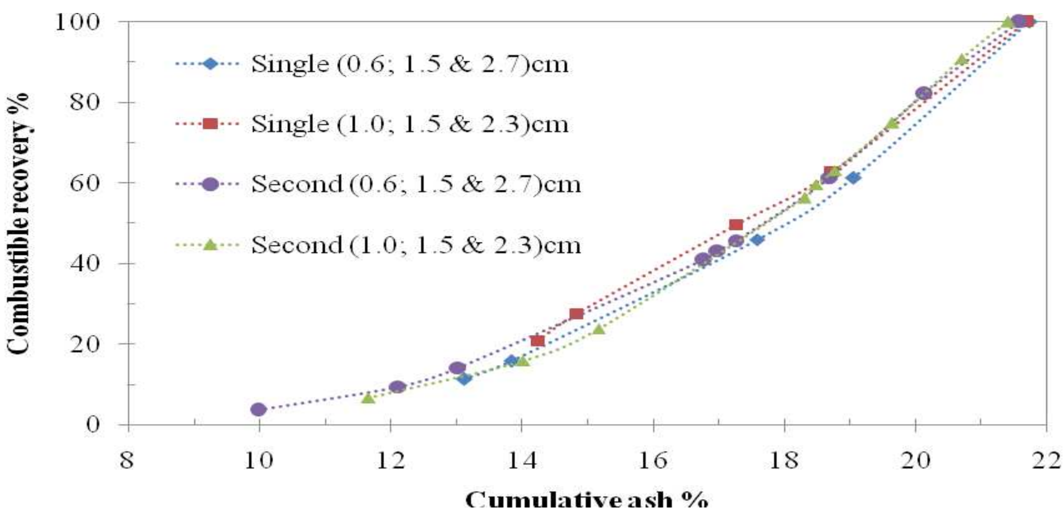

Figure 5-17. Effect of splitter distance on single pass and second stage test on Koornfontein coal at a constant charging voltage: 1.5 KV; separating voltage: 12.5 KV; air velocity of 1.9 m/sec and rotary speed of 2500 rpm.

Khutala No. 2 seam coal was also subjected to tribo-electrostatic separation at two different splitter set-ups and the result was presented in Figure 5-18, the test was conducted under the single stage separation process. Splitter positions were set at 0.6 cm and 1.0 cm away from the negative electrode. Cleaner coal of about 14.50% ash and 17.43% combustible matter was obtained when the splitter was moved 0.6 cm away from the negative electrode. In addition, 15.72% ash with 28.12% combustible matter was obtained when the splitter position was shifted 1.0 cm away from the negative electrode. The result shows that a cleaner coal product can be obtained as the splitter is being position closer to the negative electrode.

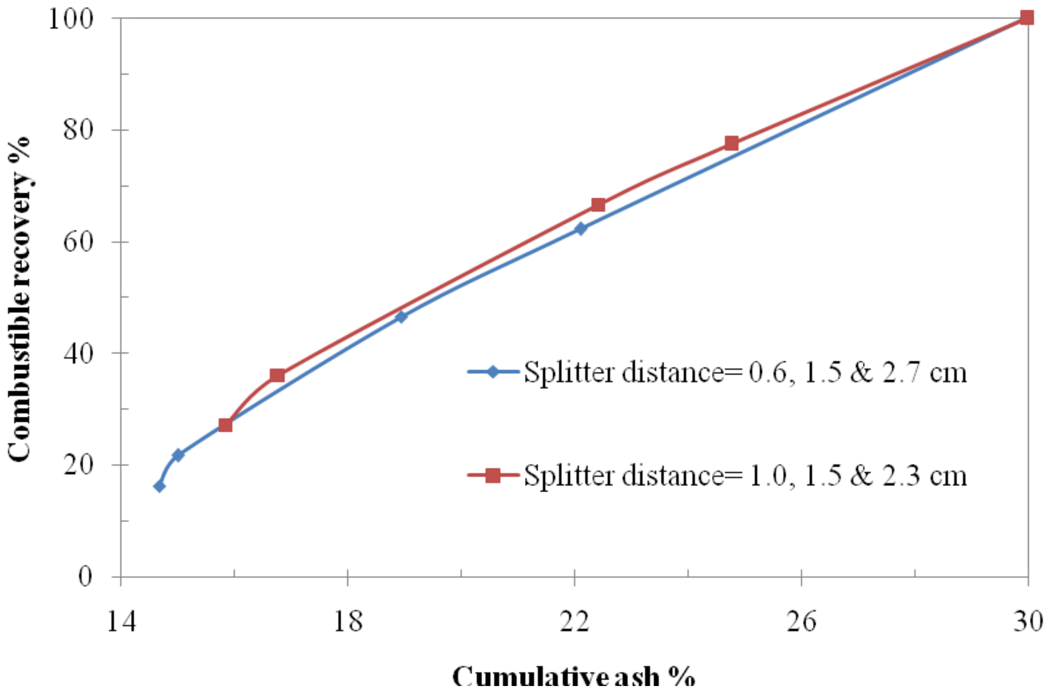

Figure 5-18. Effect of splitter distance on Khutala No. 2 seam coal at a constant charging voltage: 0 KV; separating voltage: 12.5 KV; air velocity of 1.9 m/sec and rotary speed of 2500 rpm.

5.6. *Effect of charger rotation speed*

A second stage separation test was conducted by varying the tangential speed of the octagonal rotary charger electrostatic separator. The charging of particles with a copper plated material has been proven to be the best material for imparting both positive and negative charges on coal particles and for effective tribo-charging of carbon powders and quartz (Dwari and Rao, 2006; Dwari and Rao, 2009). The results obtained for the cleaning of Klipfontein, Liketh Townlands, Majuba, Khutala No. 2 and 4 seams are presented. Figure 5-19, shows the RTS separation data obtained with the Klipfontein coal at four different charger rotation speeds. In these tests, the charger was subjected to zero electric potential and the external potential applied to the separation chamber was 22.5 kv. The feed rate was maintained at approximately 12 g/min with one splitter set at 0.6 cm away from the negative electrode and the other at 2.7 cm apart from the positive electrode. As shown in Figure 5-19, a clean coal product with 14.52% ash was produced from a feed coal of about 35.23% ash at 2500 rpm and 2.5 m/sec air velocity with a yield of about 10.14%. More so, cleaner products of 24.36% and 27.26% ash were also obtained at about 60.09% and 80.16% cumulative yield, respectively. As the rotating speed increased, the separation curve shown in figure 5-19 did not change significantly. Although the curve obtained at 3000 rpm appeared to be away from the other curves, a careful examination indicates that the shift was caused mainly by the slight changes in feed ash.

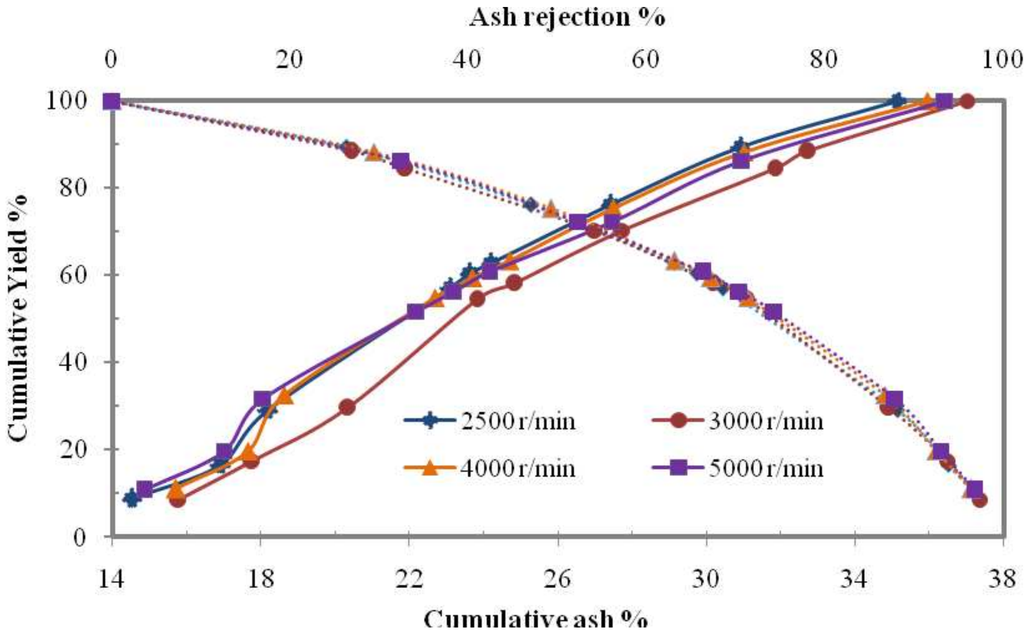

Figure 5-19. Effect of charger rotation speed on grade and recovery for Klipfontein coal at constant splitter distance: R=0.6; C= 1.5 & L= 2.7 cm; charging voltage: 0 Kv; separating voltage: 22.5 Kv and air velocity of 2.5 m/sec

Figure 5-20 and 5-21 show the separation data generated with the Liketh Townlands and Majuba coal as a function of charger rotation speed, respectively. A clean coal product of 12.53% ash was produced from the feed coal of about 31.40% ash at a cumulative yield of about 8.26% at 2500 rpm for Liketh Townlands coal. Under the same test condition, cleaner coal products with 16.40% ash and 29.22% yield, and 20.43% ash and 57.11% yield was produced, respectively. The cumulative yield also increased to approximately 48.41% at a clean coal ash of 20.33%, as shown in Figure 5-12. The highest grade product obtained in Figure 5-13 for Majuba coal was produced at 2500 rpm when the clean coal reached the lowest ash content of 11.10% from a feed coal of about 30.10% ash. At 4000 rpm, clean coal product with 15.80% ash and 31.12% yield was also obtained at 1.9 m/sec air velocity.

As the rotary charging speed increases, the number of contacts and impact force also increases, therefore, high charge transfer is expected. The charges might reach a maximum whereby charge backflow or discharging might occurred as the particles reaches a plateau. This can be noted in all the figures, which indicate the separation performance was not significantly affected by the rotation speed in the range of 2500 and 5000 rpm.

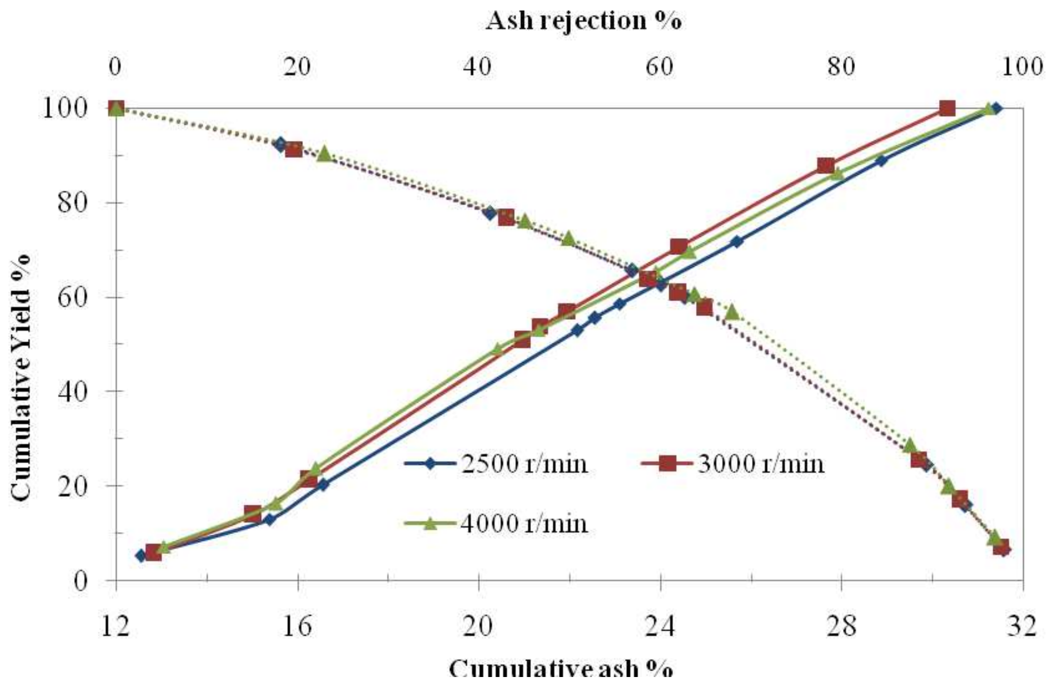

Figure 5-20. Effect of charger rotation speed on grade and recovery for Liketh Townlands coal at constant splitter distance: R=0.6; C= 1.5 & L= 2.7 cm; charging voltage: 0 Kv; separating voltage: 22.5 Kv and air velocity of 2.5 m/sec

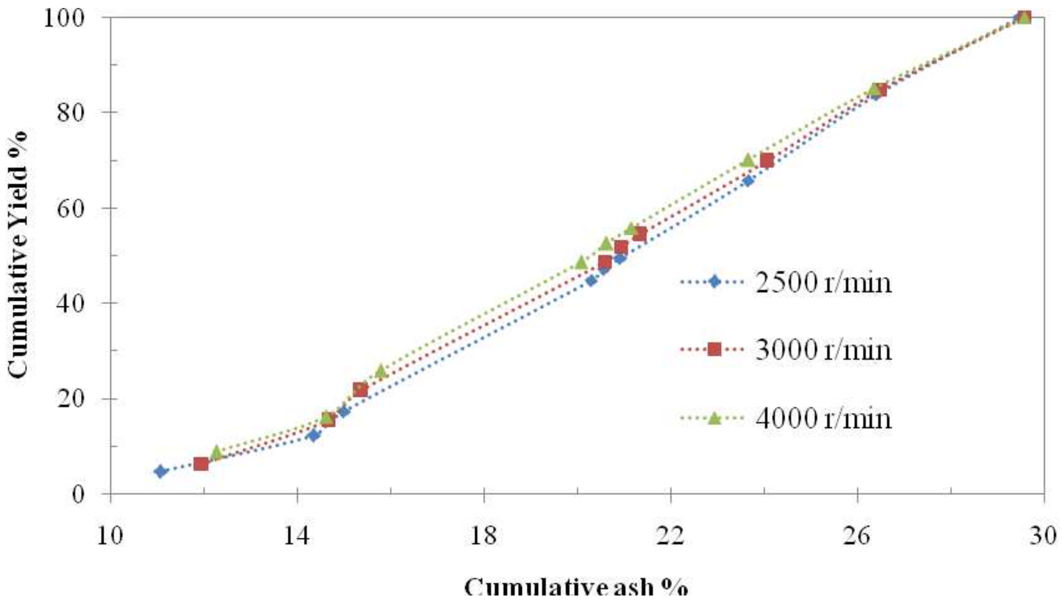

Figure 5-21. Effect of charger rotation speed on grade and recovery for Majuba coal at constant splitter distance: R=0.6; C= 1.5 & L= 2.7 cm; charging voltage: 0 Kv; separating voltage: 12.5 Kv and air velocity of 1.9 m/sec

The second stage test as shown in Figure 5-22 and 5-23 for Khutala No. 2 seam and 4 seam also shows that the cleanest coal can be produced at 2500 rpm as compared to other rotating speed tested. For the two coals, the splitter was positioned at 0.6 cm from the negative electrode with the cleanest coal product of 8.90% ash and 10.63% ash obtained at 2500 rpm for Khutala 2 seam and 4 seams, respectively. While, a clean coal product with 16.30% ash and 25.71% yield was obtained at 4000 rpm for Khutala No. 4 seam coal. Higher recovery was observed at higher rotation speed for Khutala No. 4 seam coal as compared to the result obtained for Khutala No. 2 seam, which shows almost the same curve pattern but with the cleanest product obtained at 2500 rpm at a given product ash for all the coal samples. The cumulative yield vs. cumulative ash curve as presented in Figure 5-19 and 5-20 also provides further evidence that high rotation speed results in slightly better separation since the curve moves towards the upper right corner as the rotation speed increases. Nevertheless, in all the Figures it can be seen that the coal cleaning performance is not strongly affected by the rotation speed in the test range. This is possibly because particles almost reached the maximum charge density at the rotation speed of 2500 rpm and thus further increase in charger rotation speed had little effect on charging efficiency. Inculet (1984) stated that as the particle reaches its charge limit, charge backflow or discharging occurs.

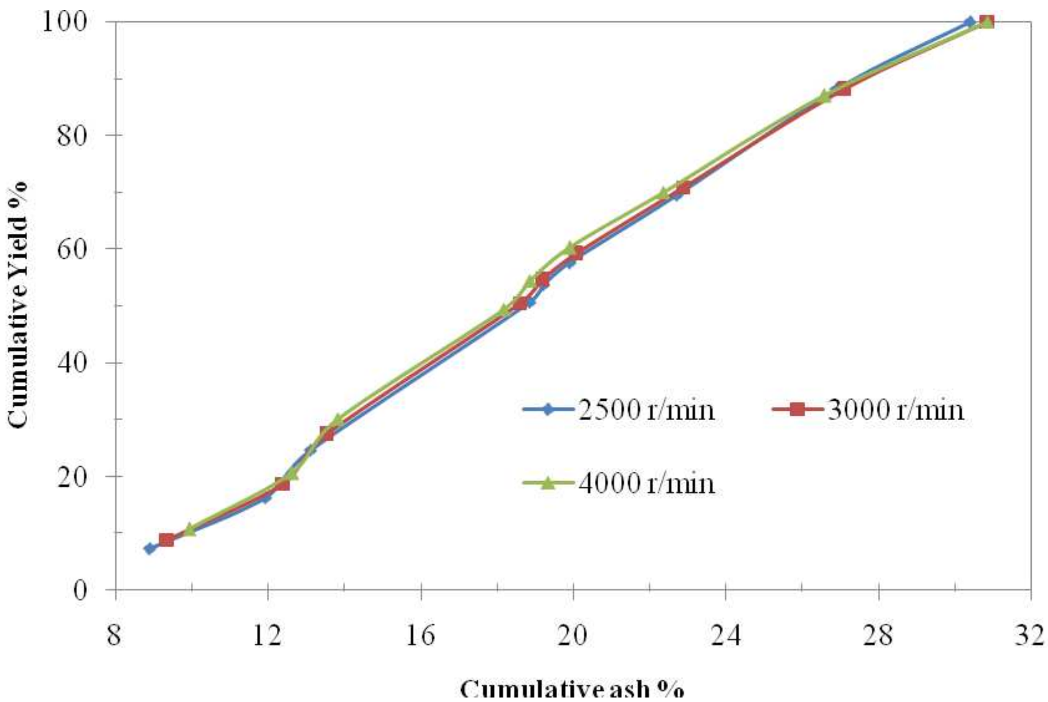

Figure 5-22. Effect of charger rotation speed on grade and recovery for Khutala No. 2 seam coal at constant splitter distance: R=0.6; C= 1.5 & L= 2.7 cm; charging voltage: 0 Kv; separating voltage: 12.5 Kv and air velocity of 1.9 m/sec.

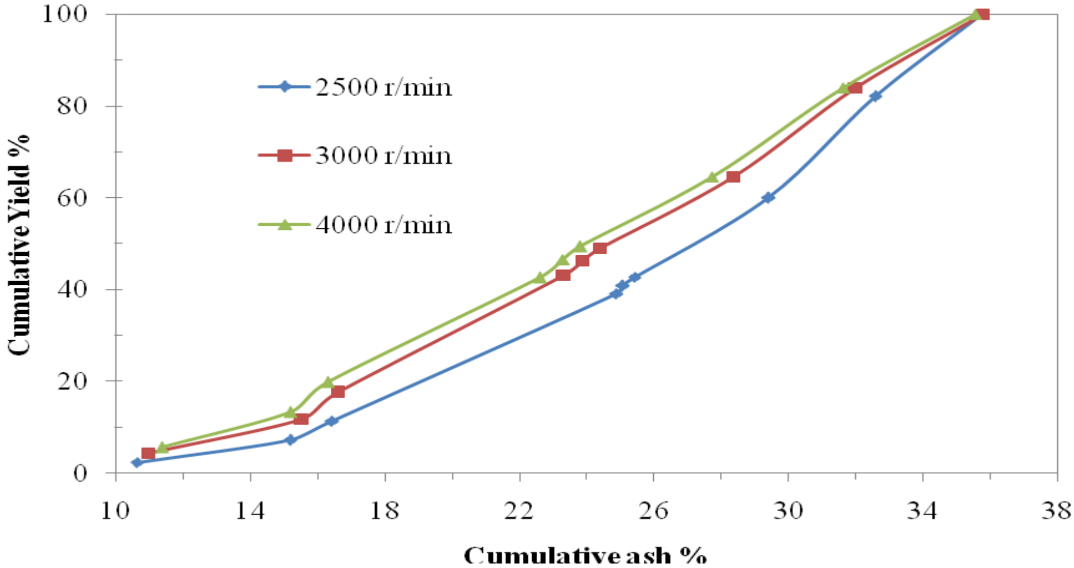

Figure 5-23. Effect of charger rotation speed on grade and recovery for Khutala No. 4 seam coal at constant splitter distance: R=0.6; C= 1.5 & L= 2.7 cm; charging voltage: 0 Kv; separating voltage: 12.5 Kv and air velocity of 1.9 m/sec

5.7. ***Effect of charging potential***

Particles are fed into the cylindrical charging chamber where the rotor is positioned to prevent the coal particles from falling into the separating zone without making contact with the copper plated surface of the octagonal rotor and the inside wall of the chamber. The potential of the rotary charger of the RTS was controlled as one of the means of enhancing particle charging and subsequent separation efficiency by applying an electric field to the charger. The application of an external applied voltage or zero potential may allow an increase in the charge density imparted on the coal particles depending on the material or coal type tested. Figures 5-24 shows the coal beneficiation results obtained under different charging potentials with Klipfontein coal.

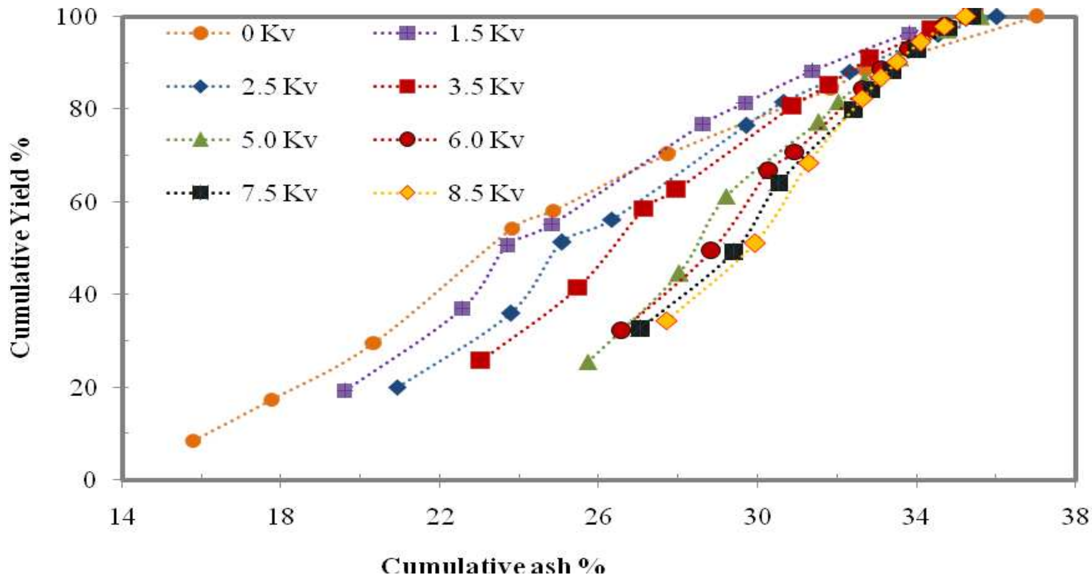

Figure 5-24. Effect of charging voltage on Klipfontein coal at a constant splitter distance, air velocity, feed rate and separating voltage

The test was conducted under two stage separation conditions and the average feed rate was maintained at 12 g/min and the rotary charger operated at a speed of 3000 rpm with the splitters set 0.6 cm from the negative electrode and 2.7 cm from the positive electrode. The charging potential varied from 0 to 8.5 KV with the Klipfontein coal. Figure 5-23 shows the clean coal ash decreased for a given yield as the applied charging potential was lowered, indicating lower charging potential was preferred for this particular coal. For instance, the cleanest coal of 27.70% ash was generated with a cumulative yield of approximately 36.44% from a feed of 36.02% ash at a charging potential of 8.5 KV. At zero charging potential, a clean coal with the same ash content was produced with a cumulative yield of nearly 70.12%. The result is in contrast with the findings reported from the separation of quartz from phosphate, where the increase in external voltage was found to be more efficient in the charging and separation of phosphate from quartz (Tao and Jiang, 2006). The variation can be attributed to the coal particles used in this research being charged saturated at zero potential compared to the magnitude of charge that can be acquired by phosphate particles.

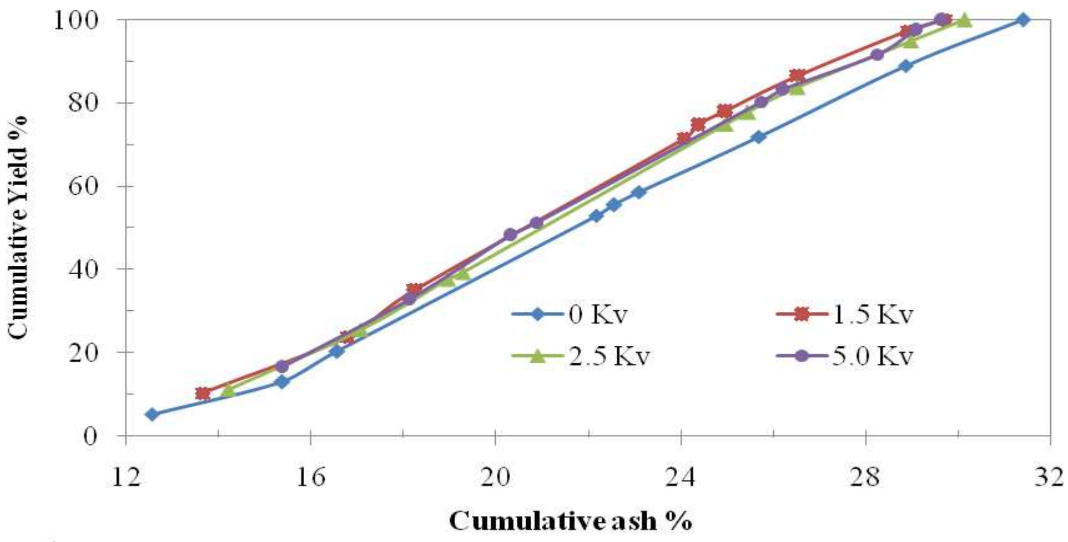

Figure 5-25. Effect of charging voltage on Liketh Townlands coal at a constant splitter distance, air velocity, feed rate and separating voltage

Figure 5-25 shows the effect of different charging voltage from 0 KV to 5.0 KV at a separating voltage of 12.5 KV for the cleaning of Liketh Townlands coal. Results obtained as presented in Figure 5-25 also indicates that cleaner coal products can be produced at lower charging potential, with the cleanest clean coal ash of 12.62% obtained from a feed of 31.50% ash at zero charging potential with a yield of 7.12%. Further increase in the charging potential to 5.0 KV produces a clean coal product with 15.40% ash and yield of about 18.04%. This also indicated that lower charging voltage or zero charging potential was preferred for the entire coal sample investigated. The same trend was also observed in Figures 5-26 and 5-27 for Koornfontein coal and Khutala No. 4 seam coal, respectively.

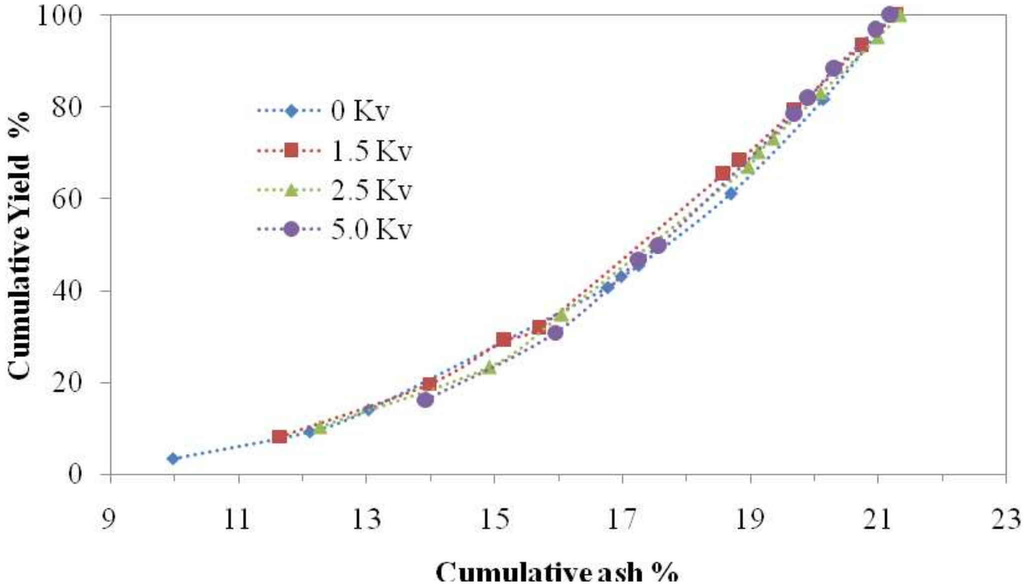

Figure 5-26. Effect of charging voltage on Koornfontein coal at a constant splitter distance, air velocity, feed rate and separating voltage

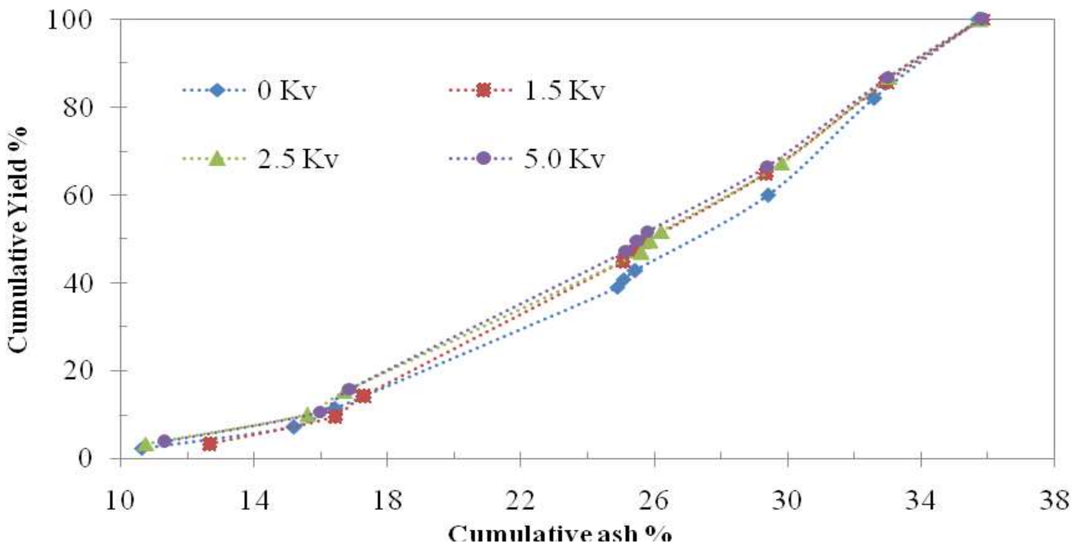

Figure 5-27. Effect of charging voltage on Khutala No. 4 seam coal at a constant splitter distance, air velocity, feed rate and separating voltage

The cleanest coal product of approximately 9.03% ash was also obtained from a feed coal of about 22.12% ash at 0 KV charging voltage compared to the cleanest product of 13.93% ash with a yield of 16.20% obtained when the potential was increased to 5.0 KV in Figure 5-26. The same trend was also observed when Khutala No. 4 seam coal in Figure 5-27 was subjected to different charging voltage, with the highest grade product obtained at zero charging voltage at the expense of the cumulative yield. The cumulative yield vs. cumulative ash curve is almost identical for the entire sample tested, indicating that the charging potential had little effect on the separation for this coal sample. In addition, it can be concluded that the particle/particle, copper plated rotor and the chamber wall are more effective in inducing charges for the separation of the coal tested compared to an applied external voltage.

5.8. Effect of separating voltage on single and second stage test

The external electric field strength and the charge magnitude control the particle trajectory in the separation zone. Clean coal with different grades can be obtained by varying the applied potential in order to regulate the field intensity within the separating zone. The increase in the separation voltage is expected to produce clean coal products with better separation and grade. However, the electric field intensity and the coal grade decreases for this separator as the applied potential increases due to particle build-up on the surface of the two electrodes. The potential of an external applied separation voltage in enhancing the separation efficiency and setting the best separation potential for the single stage test on Majuba and Koornfontein coal was investigated. The second stage test conducted on Majuba coal was carried out at 1.5 KV charging voltage, separation voltage ranging from 10 to 20 KV, air velocity of 1.9 m/s and splitter distance of 0.6 cm from the negative electrode. While, Polmaise coal and Khutala No. 4 seam coal were separated at zero charging voltage, separation voltage varying from 10 to 25 KV, air velocity of 2.5 m/s, splitter distance of 0.6 cm from the negative electrode and rotary charger operated at a speed of 2500 rpm.

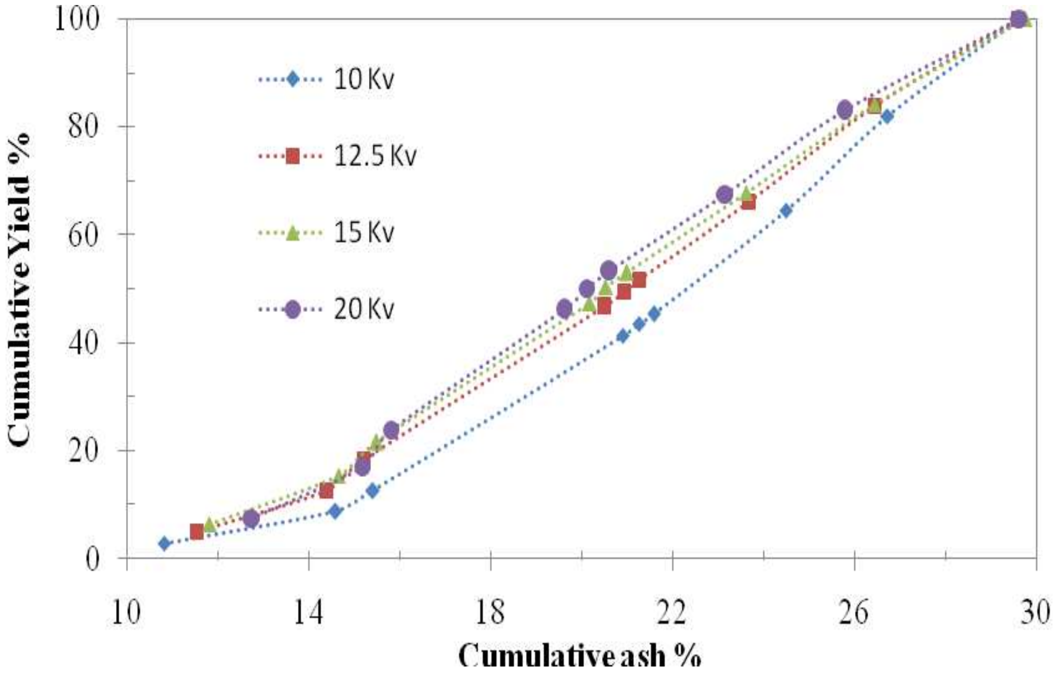

Figure 5-28. Effect of separating voltage on Majuba coal under two stage test at a constant splitter distance, air velocity, feed rate and separating voltage

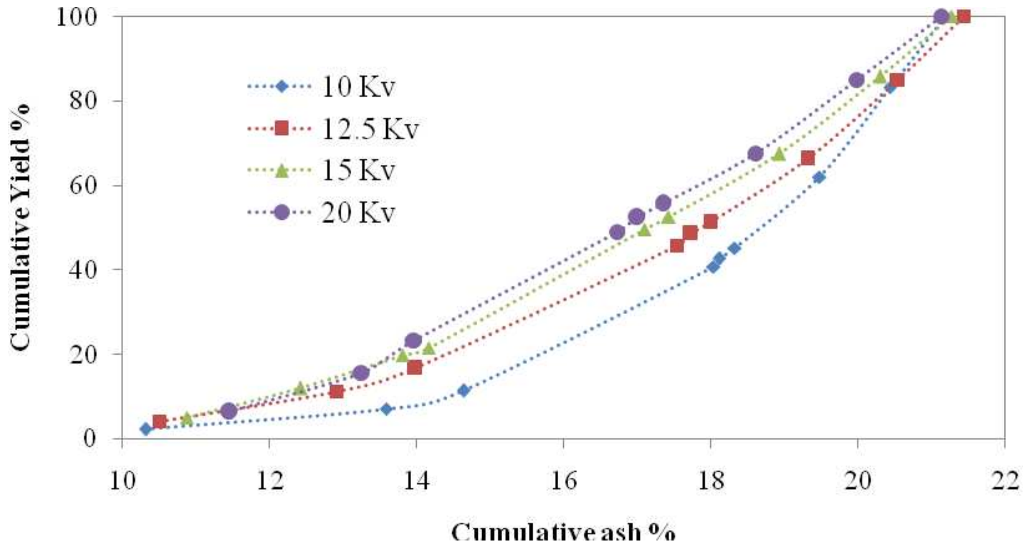

Figure 5-29. Effect of separating voltage on Koornfontein coal under two stage tests at a constant splitter distance, air velocity, feed rate and separating voltage

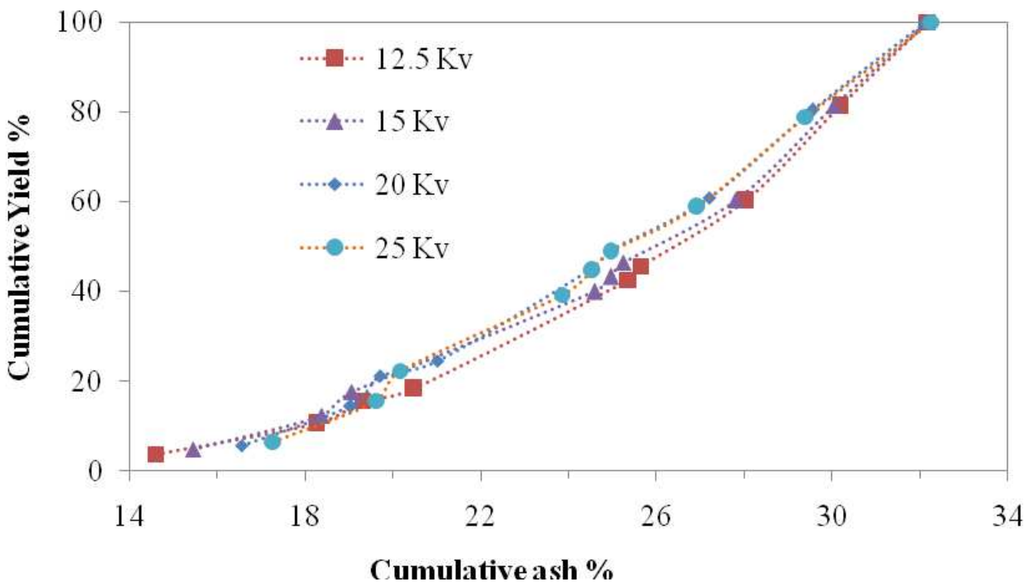

Figure 5-30. Effect of separating voltage on Polmaise coal under two stage test at a constant splitter distance: R=0.6; C= 1.5 & L= 2.7 cm; charging voltage: 0 Kv; air velocity of 2.5 m/sec and rotary speed of 2500 rpm.

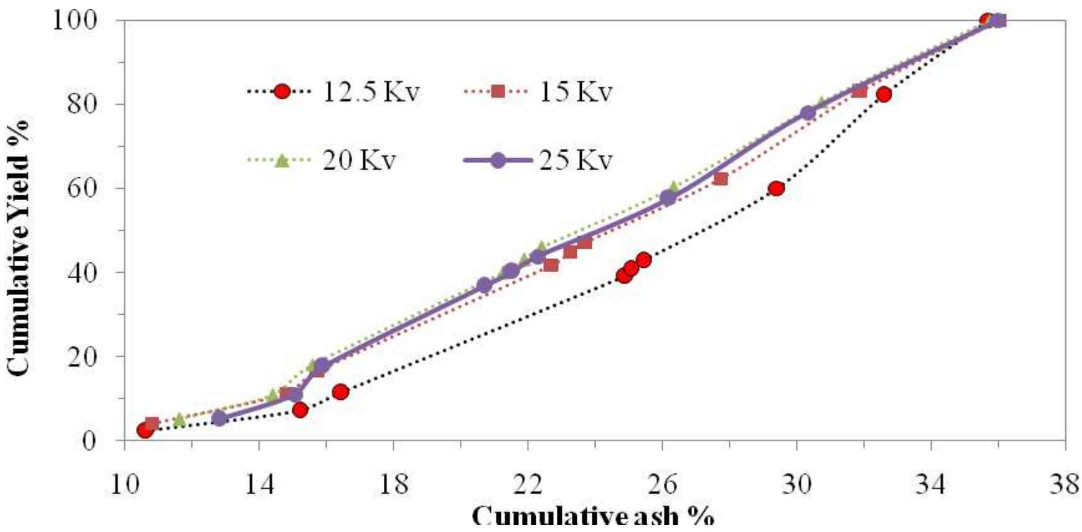

Figure 5-31. Effect of separating voltage on Khutala No. 4 Seam coal under two stage at a constant splitter distance: R=0.6; C= 1.5 & L= 2.7 cm; charging voltage: 0 Kv; air velocity of 1.9 m/sec and rotary speed of 2500 rpm.

The results obtained from the two stage tests are shown in Figures 5-28, 5-29, 5-30 and 5-31 for Majuba coal, Koornfontein Polmaise coal and Khulata No. 4 seam, respectively. Coal products with the highest grade were obtained at the lowest applied potential with better separation generated as the potential increases for the entire test. This was observed in all the tests as the potential increases to 20 KV the curve can be seen moving to the upper right of the plot, showing better separation than the products obtained at 10 KV, 12.5 KV and 15 KV. It should be pointed out that higher separation voltages may increase the ash content in the cleanest fraction of coal products. For example, the lowest ash value of 10.80% was increased to 12.74% as the potential increased from 10 KV to 20 KV with the Majuba coal at the two stage of separation. In addition, ash % for Khutala No. 4 seam clean product further increased from 10.60 % to 12.81 % as the potential applied increases from 12.5 KV to 25 KV in Figure 5-31. Similar observation was made by Dwari and Rao (2006) with the separation of an Indian thermal coal. This is mainly because the higher separation potential diverted more coal particles to the clean coal or increased cumulative yield.

The plots for the single pass test with middling recycling are presented in figures 5-32, 5-33 and 5-34, respectively. Separating voltage varied from 12.5 KV to 20 KV was used in separating Majuba coal at 1.5 KV charging voltage, while Koornfontein coal was separated at 10 and 12.5 KV separating voltage and zero charging voltage. The cumulative ash % vs. cumulative yield curves in Figure 5-32 for Majuba single pass test reveals an ash content of 16.09% at a cumulative yield of about 29.12%. Second stage test in Figure 5-33 shows a product ash of 9.98% and 13.12% ash with a cumulative yield of 3.21% and 11.30%, respectively for Koornfontein coal. Hence, another coal product with 17.58% ash with a combustible recovery of 46% was also obtained for Koornfontein coal under the single stage test in Figure 5-32.

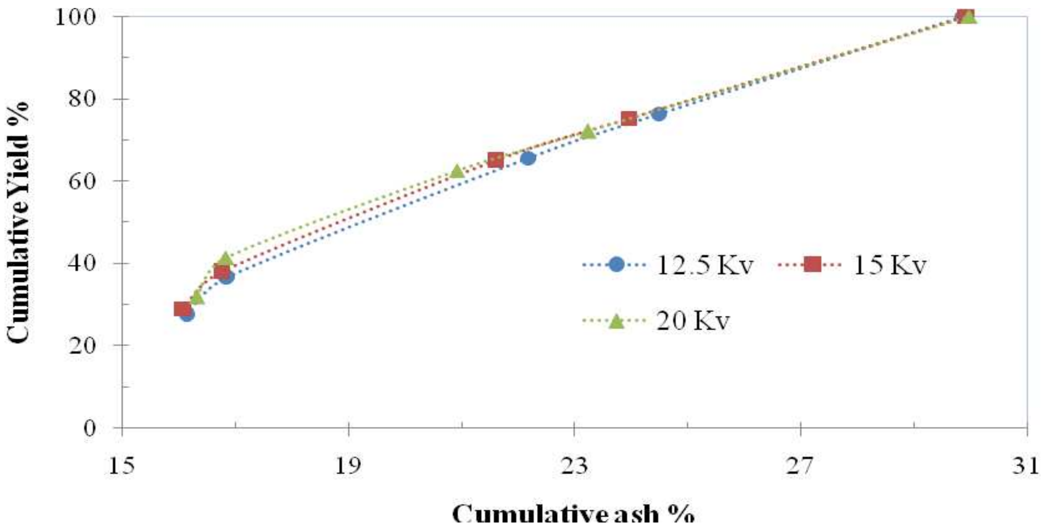

Figure 5-32. Effect of separating voltage on single pass and middling re-cycled Majuba coal at a constant splitter distance: R=0.6; C= 1.5 & L= 2.7 cm; charging voltage: 1.5 Kv; air velocity of 1.9 m/sec and rotary speed of 2500 rpm.

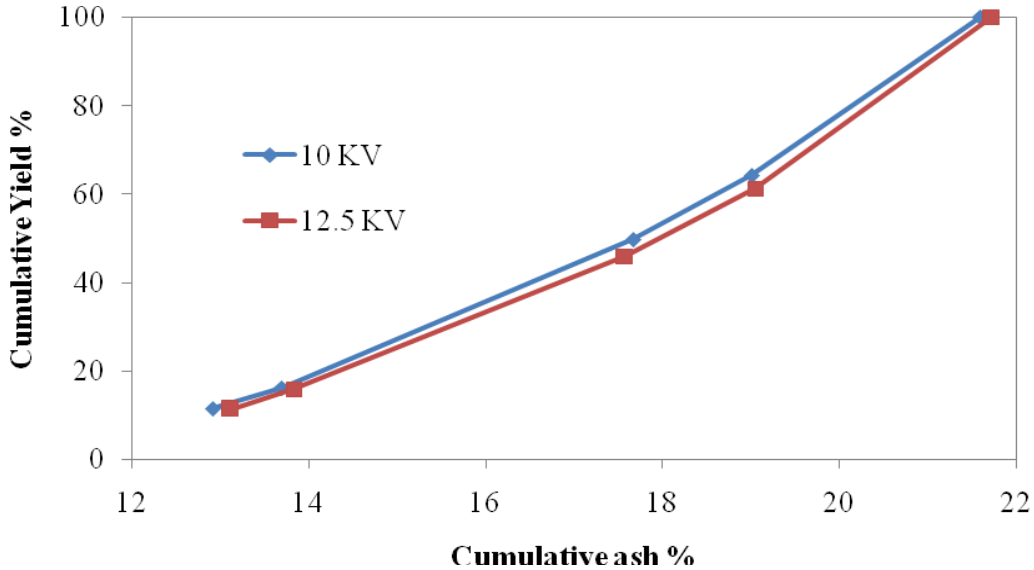

Figure 5-33. Effect of separating voltage on single pass and middling re-cycled Koornfontein coal at a constant splitter distance: R=0.6; C= 1.5 & L= 2.7 cm; charging voltage: 0 Kv; air velocity of 2.5 m/sec and rotary speed of 2500 rpm.

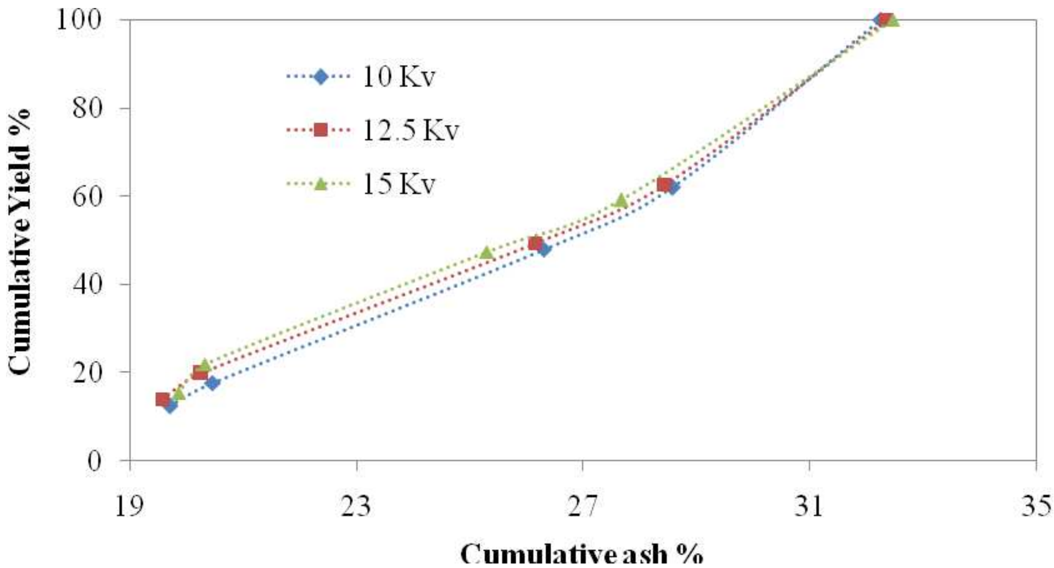

Figure 5-34. Effect of separating voltage on single pass and middling re-cycled Polmaise coal at a constant splitter distance: R=0.6; C= 1.5 & L= 2.7 cm; charging voltage: 0 Kv; air velocity of 2.5 m/sec and rotary speed of 2500 rpm.

The separation of Polmaise coal also followed the same trend as those observed during the separation of Majuba and Koornfontein coal, with the highest grade product obtained at 10 KV was 19.70% ash product with a yield of 10.52% from a feed coal of about 33.23% in Figure 5-34. Both single and second stage test indicated that better separation can be achieved depending on the required grade and percentage yield required. The calorific values and total sulphur obtained from both tests as shown in Table 5-4, indicate that better separation with high grade products can only be obtained after multistage test but at the expense of recovery.

Table 5-4. Triboelectrostatic separation results on Majuba and Koornfontein coal

Coal Sample	Majuba Feed	Single Pass	Second Pass	Koornfontein Feed	Single Pass	Second Pass
Calorific Value (MJ/Kg)	20.149	25.669	27.479	24.53	25.815	28.30
Total Sulphur (%)	2.35	0.924	0.725	2.10	0.775	0.680
Ash (%)	30.10	14.67	10.76	22.12	12.92	11.11

5.9. ***Effect of air injection velocity***

The injection flow velocity of particles through a tribo-electrostatic separator is an important parameter for determining the system separation efficiency. The air flow rate through the separator determines the extent of the contact force between the particles and the turbulence force required in promoting particle-particle contact, particle-wall and particle-octagonal rotary surface collision. The number of contacts between the particles and the copper plated rotary surface could be enhanced by the air flow rate which also determines the residence time of the particles within the cylindrical charging chamber and the separating zone of the RTS. The separation efficiency as a function of injection air velocity on the product's grade was conducted using two stage separation, where the clean coal products from the single pass test are used as a feed during the two stage separation process. Figure 5-35 shows the effect of injection flow velocity on -177 µm Majuba coal. The coal was fed into the separator under different injection air velocities, ranging from 1.3 m/sec to 2.5 m/sec, constant rotary speed of 2500 rpm, separation chamber voltage of 12.5 KV, and applied charging potential of 1.5 KV.

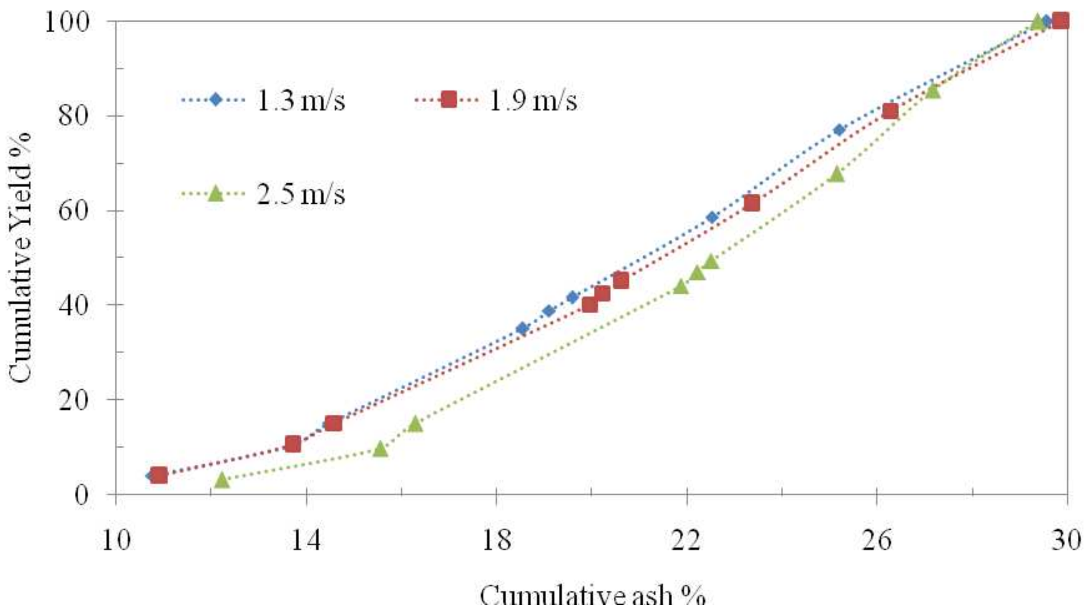

Figure 5-35. Effect of air injection velocity on Majuba coal at a constant splitter distance, feed rate, charging voltage and separating voltage

The increase in injection velocity is known to increase the particle/particle interaction, turbulent flow, tribo-charging time, and the particle specific charges, but in this investigation, higher air injection flow had been found to reduce the particle separation efficiency. This might be as a result of reduction in the particle residence time in the charging chamber, thereby reducing the number of contacts between particle/particle and particle/octagonal surface of the rotor, thereby reducing the particle's charge density. The ash content in Majuba coal was reduced from a feed coal of 30.10% ash to 10.76% ash at 1.3 m/sec. Under the same conditions, a clean coal product of 18.54% ash with a cumulative yield of 40.70% was obtained, and as the air injection velocity increases to 2.5 m/sec the product ash also increases to 12.21 %.

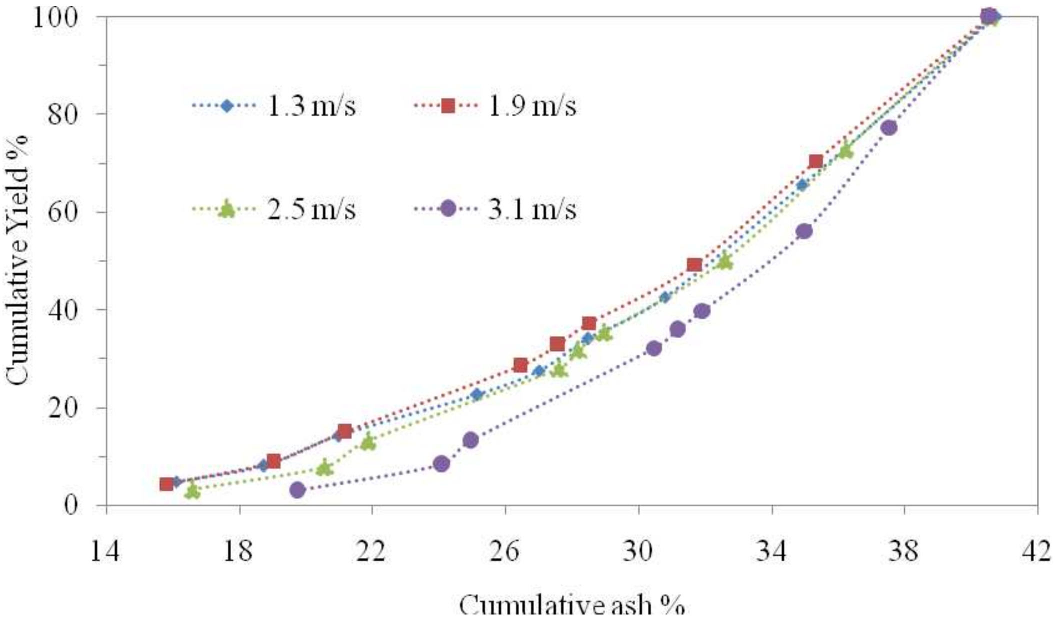

Figure 5-36. Effect of air injection velocity on New Vaal coal at a constant splitter distance, feed rate, charging voltage and separating voltage

Figure 5-36 shows the results obtained for the separation of New Vaal coal using the octagonal rotary charger of the RTS. The test was conducted under different injection air velocities, ranging from 1.3 m/sec to 3.1 m/sec, constant rotary speed of 3000 rpm, separation chamber voltage of 12.5 KV, and applied charging potential of 0 KV. A significant effect of the injection flow rate was observed between 1.3 m/sec and 3.1 m/sec. Cleaned coal product with 15.8% ash was obtained at 1.9 m/sec, while at 3.1 m/sec a product with 19.74% ash was obtained under the same test conditions. As the injection velocity increases, the grade and separation efficiency for all the curves in Figure 5-36 from 1.3 m/sec to 3.1 m/sec also reduces. This might be as a result of reduction in the particle residence time in the charging chamber and the separating zone, thereby decreases the contact number and magnitude of charges acquired by the particles from each other and the copper rotary surface. At 1.3 m/sec and 1.9 m/sec, the separation shows little variation with changes in injection air velocity, and this shows that changes in injection velocity within 1.3 m/sec and 1.9 m/sec do not have significant influence on the New Vaal coal separation within the velocity range.

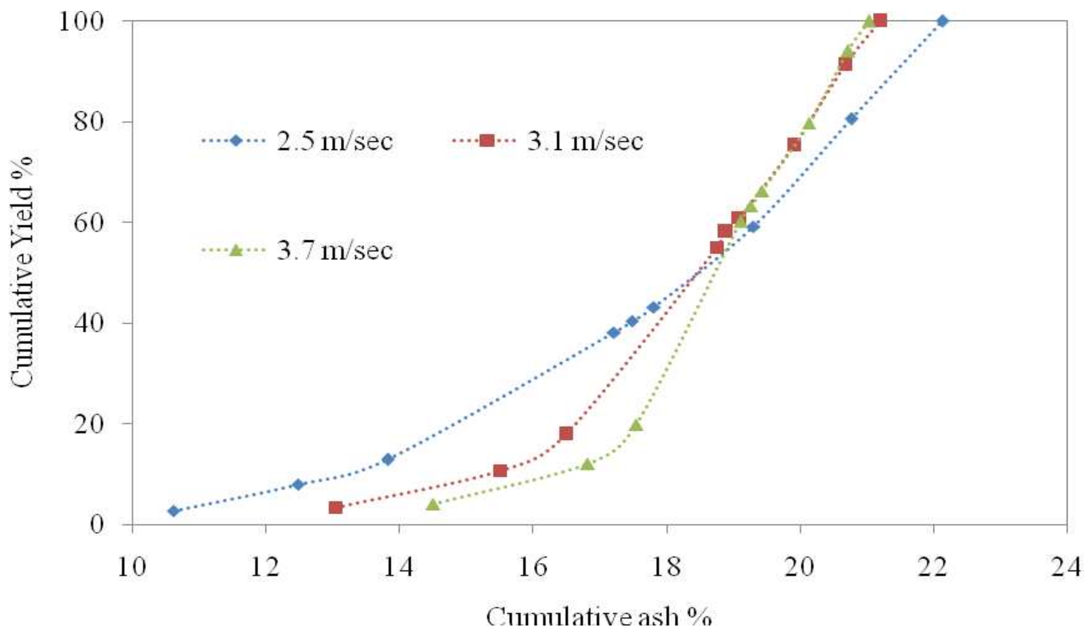

Figure 5-37. Effect of air injection velocity on Koornfontein coal at a constant splitter distance, feed rate, charging voltage and separating voltage.

The separation of Koornfontein coal also followed the same trend as that observed during the separation of New Vaal coal in Figure 5-36 but with changes in pattern as the cumulative ash product obtained was above 18% under different air injection velocity. For the best separation of coal macerals from its inorganic component within the Koornfontein coal, the injection velocity was varied from 2.5 m/sec to 3.7 m/sec, constant splitter distance, and rotary speed of 2500 rpm, charging voltage of 0 KV, and separating voltage of 12.5 KV. At low air injection velocity of 2.5 m/sec, a grade of 10.62% ash product was obtained from a feed of 22.12% ash. Hence, further increases in the air velocity to 3.7 m/sec yield a product with 14.51% ash and 4.12% combustible matter. This result shows that increasing the flow velocity for particle's transportation reduces both residence time in the charging chamber and the separation zone, thereby increasing the ash content at 3.7 m/sec. As the separation proceeds, better separation was noticed at 3.7 m/sec with about 19.13% ash product. This might be as a result of substitution between the particle-particle contact charging and the rotary surface contact charging. Since at higher air velocity, rotary charging surface tends to dominate over the particle–particle charging mechanism.

5.10. Effect of feed rate

The -177 µm coal samples were subjected to tribo-charging in the octagonal rotary chamber at different feed rate, and the result do reveals that the particles do respond differently to tribo electrostatic separation under different feed rate. The Cumulative ash % vs. Cumulative yield % curve representing the effect of coal feed rate on grade and recovery for Majuba, Klipfontein, Koornfontein and Khutala No. 4 seam coal are shown in Figure 5-38, 5-39, 5-40 & 5-41. All tests were conducted at 1.5 KV charging voltage, 12.5 KV separation voltage, 1.9 m/s injection velocity, 2500 rpm rotary speed, and splitter distance of 0.6 cm away from the negative electrode for Majuba coal. A significant reduction was observed in the ash content of the feed coal as the feed rate increases from 12 g/min to 24 g/min as shown in Figure 5-37 for Majuba coal. The results obtained show a feed coal of 30.10% ash being reduced to 10.50% ash product at 24 g/min, compared to 11.10% ash product obtained at 12 g/min for the same coal sample. The same figure also indicates that a cleaner coal product of 18.90% ash and 46.20% yield can be produced at a feed rate of 24 g/min. These results are similar to those obtained by Tao *et al.* (2009) on the dry coal fly ash cleaning using rotary triboelectrostatic separator, where the authors found that the increase in yield and ash reduction are less sensitive to the feed rate with a rotary electrostatic separator due to its efficient charging mechanism under the set conditions.

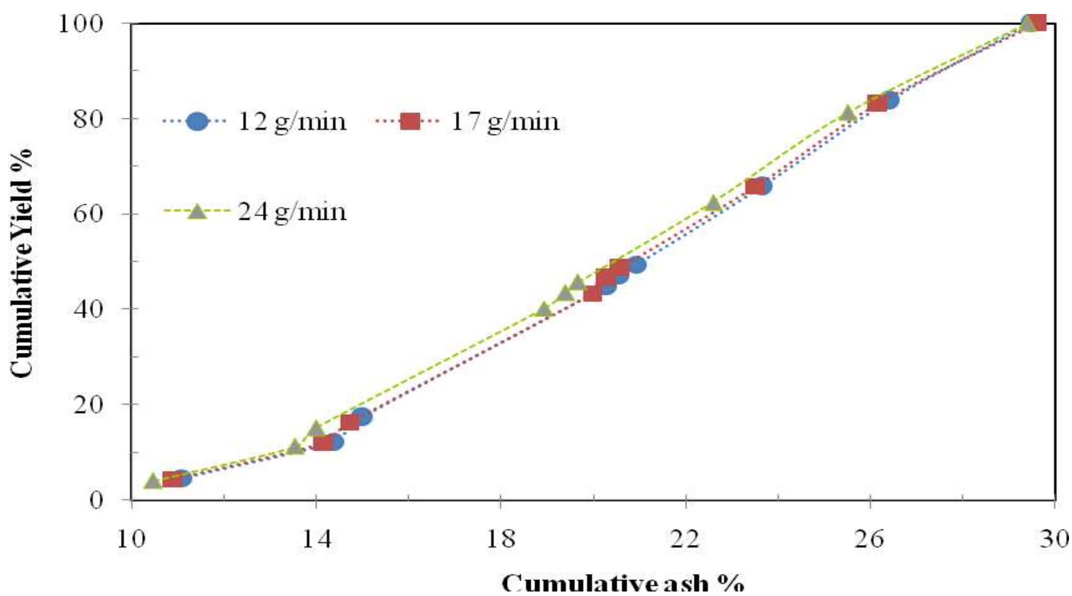

Figure 5-38. Effect of particle feed rate on Majuba coal at a constant charging voltage: 1.5 KV; separating voltage: 12.5; air velocity of 1.9 m/sec and rotary speed of 2500 rpm.

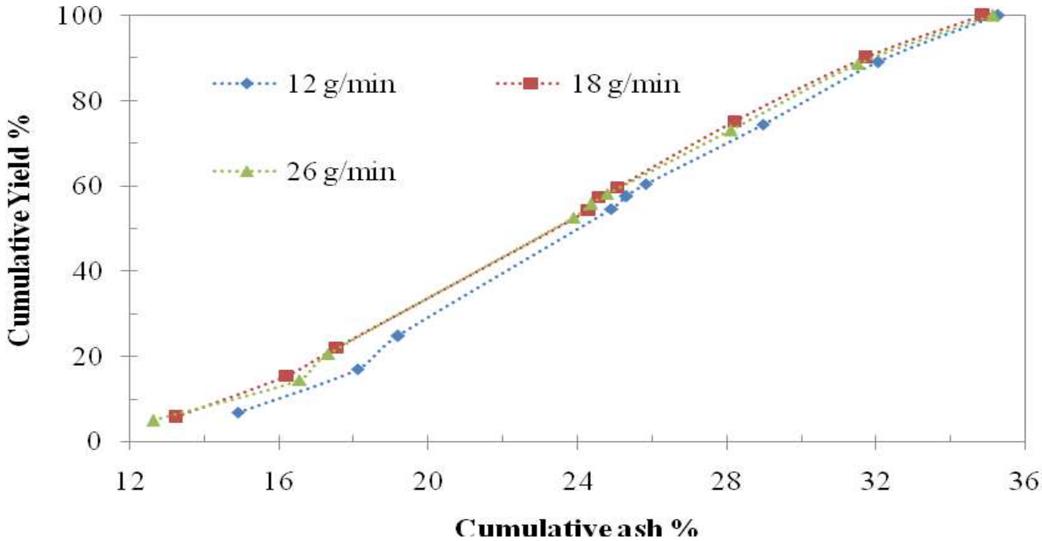

Figure 5-39. Effect of particle feed rate on Klipfontein coal at a constant charging voltage: 0 KV; separating voltage: 12.5; air velocity of 2.5 m/sec and rotary speed of 2500 rpm.

Further experimental tests conducted also show Klipfontein coal being subjected to tribo-charging at 12 g/min, 18 g/min and 26 g/min feed rate. The test was conducted at zero charging voltage, 12.5 KV separation voltage, 2.5 m/s injection velocity, 2500 rpm rotary speed, and splitter distance of 0.6 cm away from the negative electrode. The result as shown in Figure 5-39 illustrate that the separation performance for the RTS was actually improved as the feed rate increases. At a feed rate of 12 g/min, a feed ash of about 35.40% ash was reduced to 14.90% with a yield of 6.90 %. However, a higher feed rate of 26 g/min produces a clean coal of 12.60 % ash with a yield of 5.02 % under the same test condition. The increase in the particle concentration in the charging chamber which generated more intensive particle\particle collisions might be responsible for an enhanced particle charging and better separation at higher feed rate.

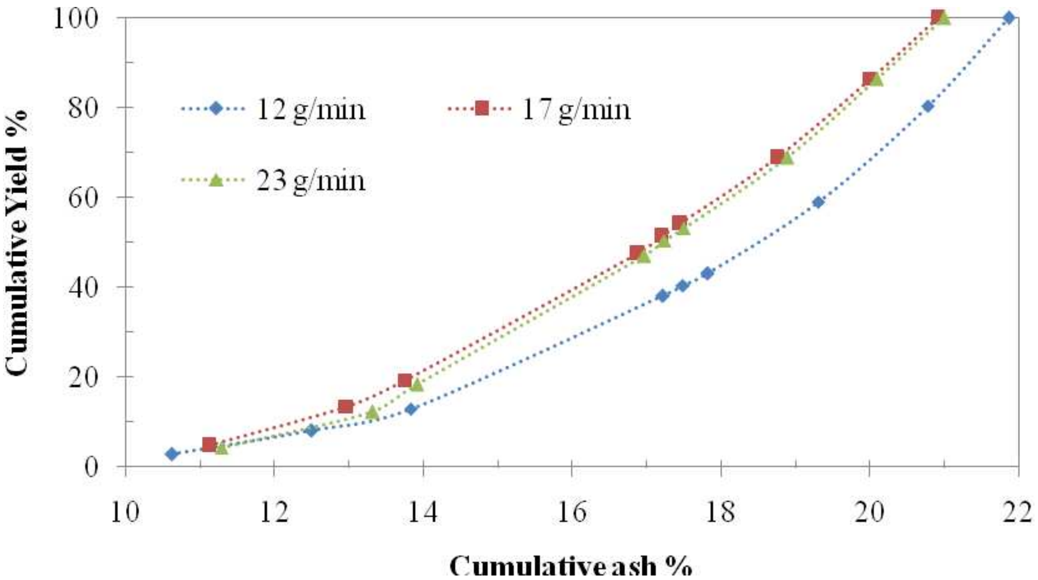

Figure 5-40. Effect of particle feed rate on Koornfontein coal at a constant charging voltage: 0 KV; separating voltage: 12.5; air velocity of 2.5 m/sec and rotary speed of 2500 rpm.

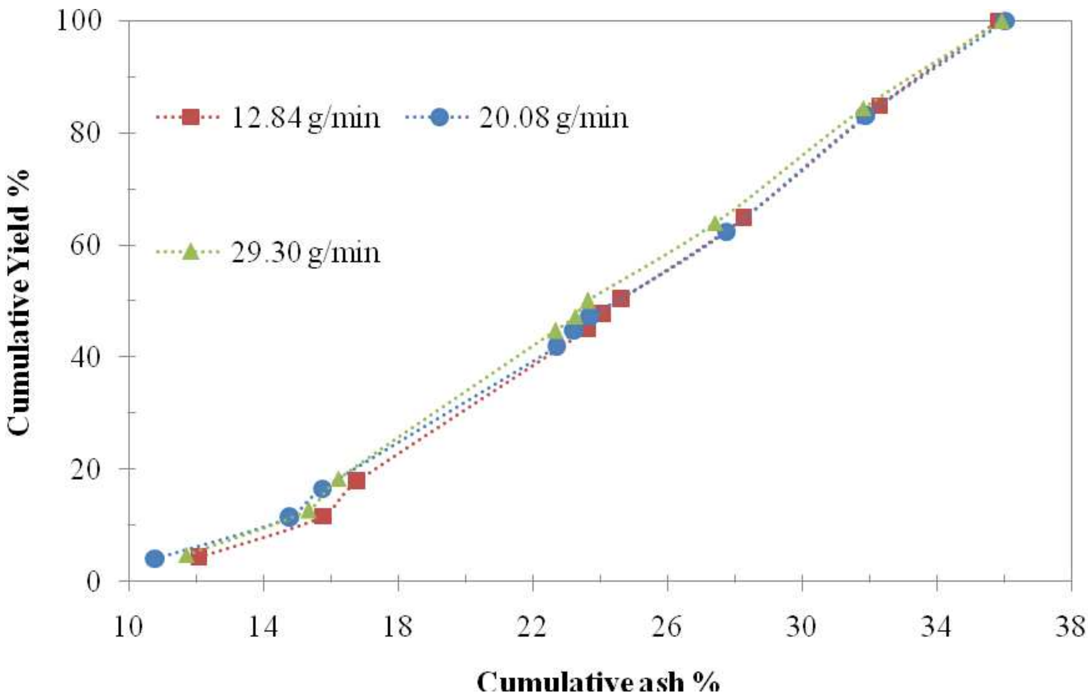

Figure 5-41. Effect of particle feed rate on Khutala No. 4 seam coal at a constant charging voltage: 0 KV; separating voltage: 12.5; air velocity of 1.9 m/sec and rotary speed of 2500 rpm.

Figure 5-40 shows the separation data generated with the Koornfontein coal at 0 KV charging voltage, 12.5 KV separation voltage, 2.5 m/s injection velocity, 2500 rpm rotary speed, and splitter distance of 0.6, 1.5 and 2.7 cm as a function of particle feed rate. The cleanest coal product produced from a feed of 22.12% ash was 10.62% at a feed rate of 12 g/min. As the feed rate increases better separation was noticed at 17 g/min and 23 g/min, with the feed rate of 17 g/min having the best separation. Similar trend was also observed for Khutala No. 4 seam coal as shown in Figure 5-41, with better separation achieved at a feed rate of 29.03 g/min compared to 12.84 g/min feed rate. Two mechanisms might be responsible for the discrepancy in the separation of Koorfontein coal as compared to that of Majuba coal. The cleanest coal product obtained at a feed rate of 12 g/min might be attributed to the role of particle/wall charging, which is responsible for charging particle at lower load rate than the particle/particle charging. While, at higher load rates particle tend to be charged by the particle/particle mechanism. The increase in the particle-particle collisions at higher feed rate, which could give rise to more coal particles being charged positively in the rotary chamber might be responsible for better separation of the Majuba coal and Klipfontein coal from its inorganic. This result was in agreement with the result reported by (Yoon *et al.* 1997a; 1997b) on the testing of a dry triboelectrostatic separator for fine coal cleaning, and also indicates the important of particle-particle collisions in tribo-charging.

5.11. *Effect of Co-flow*

Separation efficiency for Khutala No. 2 seam coal, Khutala No. 4 seam coal and Majuba coal were evaluated based on the grade and recovery of the coal products generated. The effect of co-flow rate was assessed in order to maximize coal cleaning. Co-flow also known as the flow straighteners are provided for sweeping away the particles drawn to the surface of electrodes, and to reduce the turbulence flow by forming smooth co-flow of gas parallel to the feed stream upon entering the separation zone. The airflow within the separation zone is expected to be laminar so that the charged particles are only deflected by the action of the electric field which is of comparable strength to the drag force.

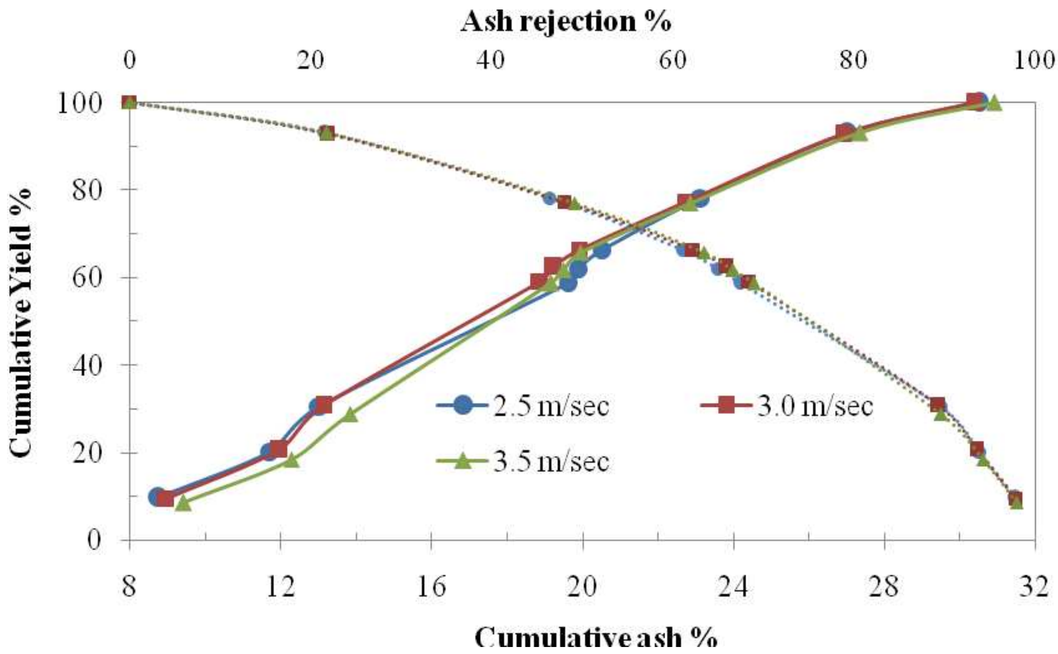

Figure 5-42. Effect of Co-flow on Khutala No. 2 seam coal at constant air velocity: 1.9 m/sec; charging & separating voltage: 0 KV & 12.5 KV; and different outlet velocity of 1100 ft/min, 1300 ft/min & 1500 ft/min.

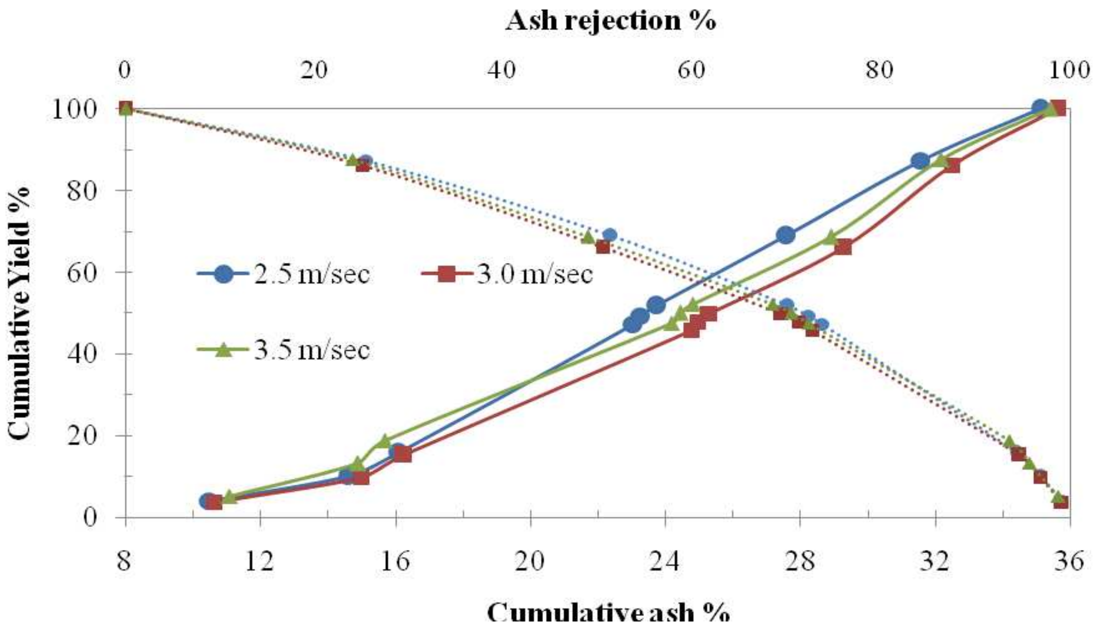

Figure 5-43. Effect of Co-flow on Khutala No. 4 seam coal at constant air velocity: 1.9 m/sec; charging & separating voltage: 0 KV & 12.5 KV; and different outlet velocity of 1100 ft/min, 1300 ft/min & 1500 ft/min.

The test on Khutala No. 2 seam, Khutala No. 4 seam coal, and Majuba coal were performed at a constant injection velocity of 1.9 m/sec, varied outlet velocity of 1100 ft/min, 1300 ft/min and 1500 ft/min. The effect of co-flow speeds of 2.5 m/sec, 3.0 m/sec and 3.5 m/sec are presented in Figure 5-42 for Khutala 2 seam coal. The highest grade product was obtained at the lowest co-flow velocity of 2.5 m/sec with a product ash of 8.75%, and 9.75% yield from a feed coal of about 30.51% ash. At 3.5 m/sec co-flow velocity, another coal product with 9.41% ash was also obtained for Khutala No. 2 seam coal under the same two stage test. The same trend was also observed for Khutala No. 4 seam coal in Figure 5-43 with the highest grade coal product obtained at 2.5 m/sec co-flow velocity. The result shows that for the range of co-flow velocity tested the effect of co-flow are found to be limited, with the 2.5 m/sec and 3.0 m/sec co-flow velocity for Majuba coal in Figure 5-44 generating almost the same product grade. It can be observed that at 2.5 m/sec co-flow velocity for the three coals presented, the results shows that at 1100 ft/min outlet velocity the highest quality coal products were obtained which might be as a result of decrease in turbulence flow caused by the smooth stream of air within the separation zone as the outlet velocity decreases. Similar result was also observed by Tao *et al*. (2009), where an increase in co-flow velocity unfavourably affected the separation capacity of the cylindrical rotary separator.

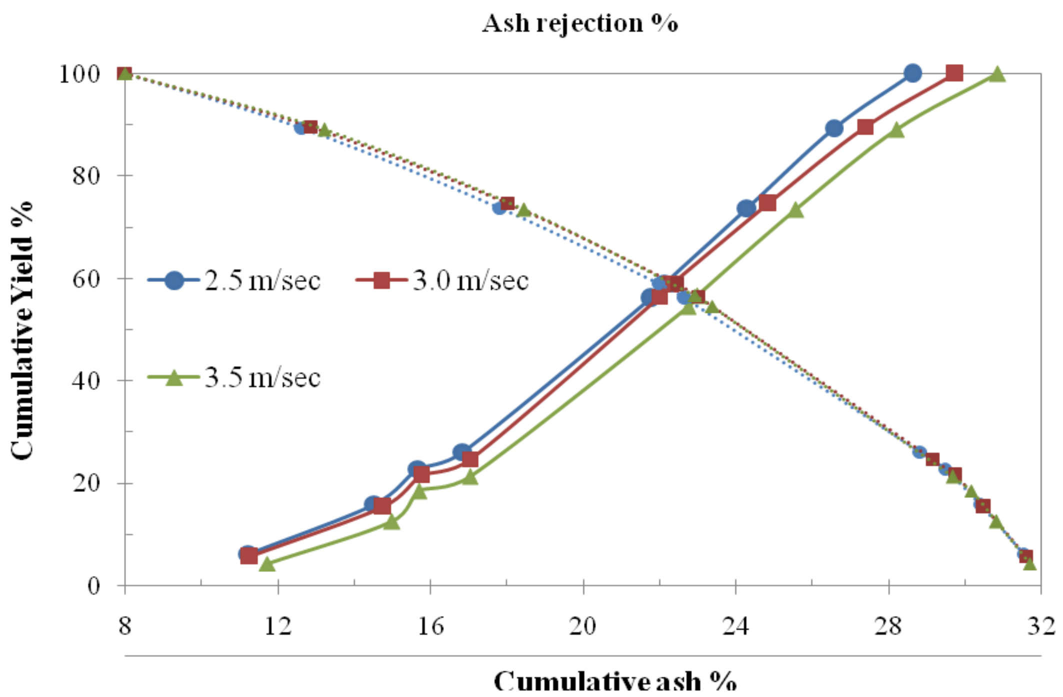

Figure 5-44. Effect of Co-flow on Majuba coal at constant air velocity: 1.9 m/sec; charging & separating voltage: 1.5 KV & 12.5 KV; and different outlet velocity of 1100 ft/min, 1300 ft/min & 1500 ft/min.

5.12. Theoretical Energy Used by Octagonal Rotary Charger

Tribo-electrification occurs as a result of relative motion and exchange of charges between particles, with the imparted charges being maintained. Bearing friction and transported gas within the separator are responsible for the energy utilized by the octagonal rotary charger. The heat energy generated due to the action of the bearing friction increases the temperature of both the lubricant and neighbouring parts. While, the power utilized by the journal bearing, that is, a simple bearing in which the shaft rotates in the bearing with a layer of grease separating the two parts can be established from equation 5-1 (Spotts, 1985).

$$P_b = fPld \frac{1}{2} d \frac{2\pi n}{60} \quad \textbf{(5-1)}$$

Where P_b is the power loss in watt, and P is assumed as the unit load measured in (N/m^2) on the bearing over an estimated journal area ld . l (m) is the length in axial direction, d (m) represents the diameter of the journal. Total force on the bearing is Pld (N), frictional force is $fPld$ (N), and f is the coefficient of friction. While, the friction moment is $fPld\left(\frac{d}{2}\right)$ (Nm), and $2\pi n$ representing the number of radians turned by the shaft per minutes.

The energy consumption by gas friction was also established from (Spotts, 1985), and the fluid motion is being accomplished by slip or shear force between the fluid particles throughout the entire height of the fluid. According to Newton's law, the shearing stress τ (N/m^2) in the fluid varies directly with velocity U and inversely with the fluid height h .

$$\tau = \mu \frac{U}{h} = \frac{F}{A} \quad (5\text{-}2)$$

Where μ is known as the coefficient of viscosity, A is the area of the rotary charger which can be represented as $2S^2\left(1+\sqrt{2}\right)$ for octagonal rotary charger used in the experiment,

$$F = \mu \frac{AU}{h} \quad (5\text{-}3)$$

Substituting A (m^2**)**, known as the octagonal surface area of the rotary charger into equation 5-3 to obtained equation 5-4, where S (m) is the side length of rotary charger; h (m) is the distance between the rotary chamber and the surface of the copper plated octagonal charger.

$$F = \mu \frac{2S^2\left(1+\sqrt{2}\right)U}{h} \tag{5-4}$$

Power loss $P_g = F_g U = \mu \dfrac{2S^2\left(1+\sqrt{2}\right)\left(\dfrac{2\pi n}{60}\right)^2}{h}$ (5-5)

$$P_g = \mu \frac{2S^2\left(1+\sqrt{2}\right)\left(4\pi^2 n^2\right)}{60^2 h} \tag{5-6}$$

Therefore, the total power loss P_t is,

$$P_t = P_b + P_g = fPld\ \frac{1}{2} d\ \frac{2\pi n}{60} + \mu \frac{2S^2\left(1+\sqrt{2}\right)\left(4\pi^2 n^2\right)}{60^2 h}$$

$$P_t = P_b + P_g = fPld\ ^{2}\frac{\pi n}{60} + \mu \frac{2S^2\left(1+\sqrt{2}\right)\left(4\pi^2 n^2\right)}{60^2 h} \tag{5-7}$$

The total power used by the octagonal rotary charger in the present study was calculated from equation (5-7),

L, The length of the rotary charger = 0.1025 m

f, Coefficient of friction for ball bearing = 0.0015

n, Rotary charger speed used = 2500 rev/min

D, Diameter of an octagonal rotor for the test = 0.0974 m

l, Length of the shaft = 0.2032 m

d, Diameter of the shaft = 0.0160 m

ρ, Density of copper rotary charger = 8960 kg/m^3

h, Distance between the rotary chamber and the surface of the copper plated octagonal charger = 0.0936

S, Side length of rotary charger used = 0.035 m

μ, Coefficient of viscosity = 1.8 X 10^{-5}

$$P_t = P_b + P_g = fPld^2 \frac{\pi n}{60} + \mu \frac{2S^2\left(1+\sqrt{2}\right)\left(4\pi^2 n^2\right)}{60^2 h}$$

$$P_t = 0.0015 \text{ x } 6.84 \text{ x } 0.2032 \text{ x } (0.0160)^2 \frac{3.14 \text{ x } 2500}{60} +$$

$$1.8 \text{ x } 10^{-5} \frac{2(0.035)^2\left(1+\sqrt{2}\right)\left(4 \text{ x } 3.14^2 \text{ x } 2500^2\right)}{60^2 \text{ x } 0.0936}$$

P_t = 6.9828 x 10^{-5} + 0.0779

P_t = 0.078 watt

The energy consumption or required for octagonal rotary charger at a surface tangential speed of 2500 rpm is 0.078 watt.

Since the rpm is constant for a given trial, therefore the power rating is expected to be constant throughout the test. The total power utilized by 0.1 kg of coal in this test was 0.078 watt and for 1 ton of coal, the power utilized was 780 ton/watt. This was found to be lower than that provided from the coal plants utilizing DMS and flotation technique per ton. The energy consumed by the DMS and Float flotation range from 8,000 to 15,000 Watt h/ton, which varied according to the rating of the motors, processing equipment, length of the conveyor and type of coal utilized

5.13. Summary of the Calorific and Sulphur Analysis Results

The current results on the utilization of triboelectrostatic separator to determine the process optimum condition for maximum ash reduction and product's recovery, and the factors responsible for effective separation can be determined from both single and two stage results shown in Table 5-5 and 5-6. The preliminary data obtained for both separation stages indicates that single stage triboelectric separation is effective in producing cleaned coals, but cleaner, higher grade with lower total sulphur content products are obtainable under two stage of separation but at the expense of the coal particle recovered.

Table 5-5: Second Stage Tribo-electrostatic Test Results

Coal (-177 µm)	Feed Ash content (%)	Calorific value (MJ/Kg)	Total sulphur	Second Pass (Cum. Ash) %	Cum. Wt %	Calorific value (MJ/Kg)	Total sulphur
Liketh townlands	31.30	21.313	1.740	12.20	8.90	27.730	0.351
Khutala 2 Seam)	30.40	20.872	1.610	8.90	9.60	29.438	0.718
Khutala 4 Seam	36.00	18.126	1.590	10.94	6.01	28.183	0.873
Majuba	30.00	20.149	2.35	14.67	9.83	27.497	0.725
New Vaal	40.45	16.585	1.000	16.10	4.95	24.657	0.705
Polmaise	32.35	19.995	2.51	15.27	6.37	27.451	0.750
Klipfontein	36.00	21.735	1.90	14.52	8.49	27.023	0.565
Koorfontein	22.00	24.530	0.884	9.98	3.06	28.350	0.510

Table 5-6: Single Stage Tribo-electrostatic Test Results

Coal (-177 µm)	Feed Ash content (%)	Calorific value (MJ/Kg)	Total sulphur	Single Pass (Cum. Ash) %	Cum. Wt %	Calorific value (MJ/Kg)	Total sulphur
Liketh townlands	31.30	21.313	1.740	14.64	17.11	26.853	0.513
Khutala 2 Seam)	30.40	20.872	1.610	14.64	25.66	26.952	0.809
Khutala 4 Seam	36.00	18.126	1.590	18.18	17.36	25.160	1.02
Majuba	30.00	20.149	2.35	10.76	5.83	25.669	0.924
New Vaal	40.45	16.585	1.000	22.83	14.06	22.234	0.915
Polmaise	32.35	19.995	2.51	19.57	13.54	25.636	1.100
Klipfontein	36.00	21.735	1.90	17.42	19.58	25.955	0.896
Koorfontein	22.00	24.530	0.884	13.12	11.30	27.233	0.685

5.14. Concluding observations

The separation performance of the RTS with SA coal is dependent on the operating parameters such as tangential speed of the rotor, injection flow velocity, feed rate, separating potential and feed rate, compared to other electrostatic separator where their performance are found to be very sensitive to changes to feed rate change. The mineralogical studies, along with the total sulphur analysis and heat content test shows the important of two stage separation over single stage of separation. The zero charging potential applied to the charging chamber also resulted into product with the highest grade, which might be as a result of particle charged saturation and backflow as the applied charging potential increases.

On the basis of test work done to date, the original pilot scale test equipment and process were critically assessed and further developments have been drawn up in order to design an improved pilot scale separator for test work in South Africa.

The key aspects of the new design (Figure 5-45) herein are as follows:

a. A Keithley electrometer with a 6522 scanner card for the measuring of the charge magnitude imparted on coal particles to determine the potential at which the particles are charge-saturated.

b. Collecting bins made in the form of Faraday cups.

c. The surface electrodes should be replaced with grid electrodes to mitigate the effect of particle build up and increase the separation efficiency at higher separation voltage.

d. Sample distribution in the feed system should be reduced from the initial 45.72 cm to 15.24 cm to reduce the time taken for particles passing through the charging chamber to the downstream separating zone.

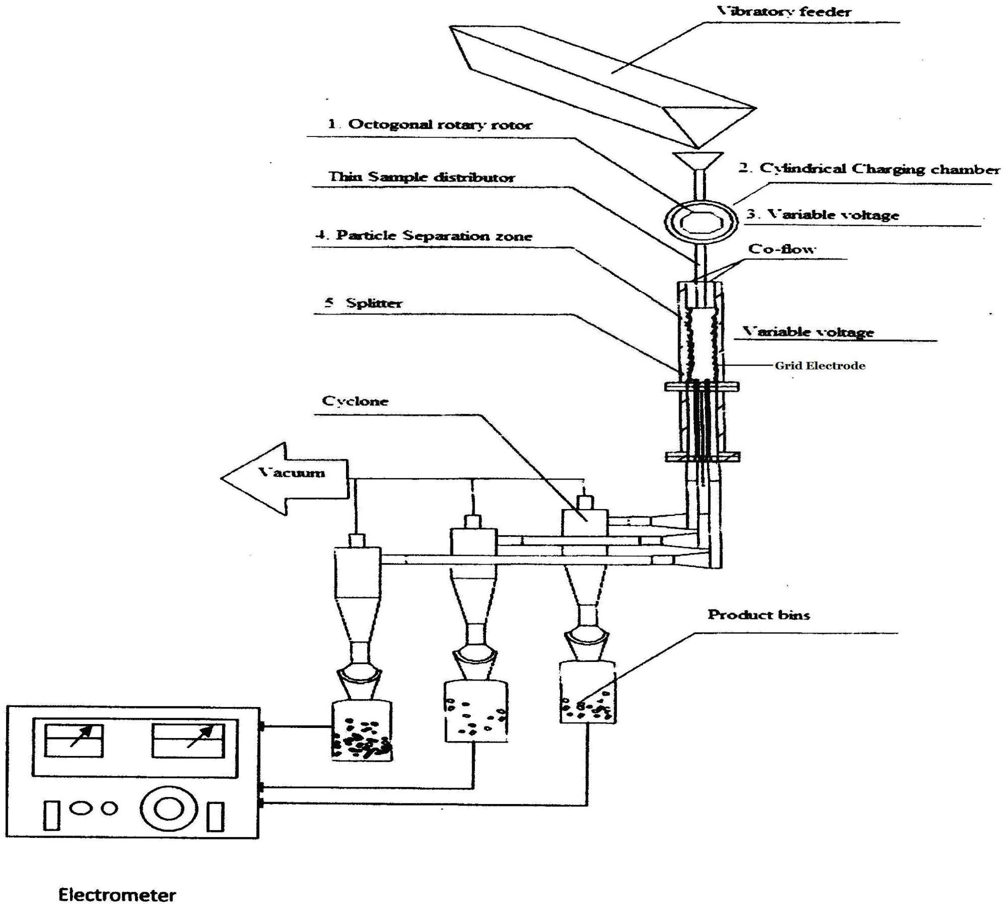

Figure 5-45. Schematic representation of an upgraded pneumatic triboelectrostatic separator with an octagonal rotary rotor.

CHAPTER SIX

6.0. Conclusions, Benefits and Recommendations

6.1. Conclusions

The research focuses on the feasibility of the Tribo-electrostatic separator (RTS) for the separation of South African fine coal organics from the mineral components using different electric field strengths which are generated within the separation zone. Optimum process conditions for maximum combustible recovery and yield were determined by running both single-stage and second stage separation tests. Operational parameters that determined the process separation efficiency were investigated. The results obtained under different separation parameters on single and two stage separation tests were analysed to determine the extent of beneficiation, change in coal characteristics and the potential application of the RTS technology for beneficiating South African fine coal. The kinetic froth flotation tests and sink/float tests were conducted on six different fine coals to evaluate the cleaning potential of the coals for separation using conventional methods.

A model for determining the energy consumption (watts) for an octagonal rotary charger was established based on the energy created by the bearing and the gas friction.

The following observations are drawn from the outcomes of this research:

1. The data on the electrostatic separation of South African coal samples has shown that the RTS technique can be applied for effective dry coal cleaning. The RTS separation

technique was more effective in separating South African coals tested in this research than the current kinetic froth flotation methods in upgrading South African coals.

2. The X-Ray Diffraction (XRD) has revealed that South African coals contained high concentrations of quartz, kaolinite and pyrite and the organic component was enriched in the clean coal products obtained from single and two-stage RTS separation tests compared to the feed.

3. Better separation with the cleanest coal products was achieved but at the expense of the recovery of the combustible matter by using the two-stage separation rather than the single- stage separation. The cleanest coal product of 10.82% ash at a combustible recovery of 3.61% was obtained from Majuba feed coal with 30.10% ash from the second stage of separation. Further cleaning also resulted in a clean product of 14.28% ash and a combustible recovery of 10.60%, and a clean coal with 16.09% ash was produced at a combustible recovery of 29.23% from one stage of separation.

4. Cleaner coal products are obtained as the splitter is positioned at 0.6 cm away from the negative electrode than when shifted 1.0 cm away from the negative electrode. The single stage separation test of Khutala 2 seam coal at 0.6 cm and 1.0 cm from the negative electrode resulted in a clean coal of 15.20% ash and 22.14% combustible matter when the splitter was 0.6 cm from the negative electrode, and 17.37% ash product with 36.20% combustible matter when the splitter position was shifted 1.0 cm from the negative electrode

5. The coal grades were shown to decrease in quality for this type of separator as the applied potential increases as a result of the increase in electric field intensity created within the separating zone and thereby resulted into particle build-up on the surface of the two electrodes. Two stage tests conducted on Majuba coal at 1.5 KV charging voltage and air velocity of 1.9 m/s shows the increase in the ash content of the product obtained from 10.80% to 12.74% as the potential increased from 10 KV to 20 KV. The same trend also applied to Khutala 4 seam coal with ash content increasing from 10.60% to 12.81% as the potential that was applied increased from 12.5 KV to 25 KV.

6. A higher potential of 22.5 KV in the separation chamber resulted in better separation recovery of 8.40% clean coal product and13.90% ash content. While, a clean coal product of 13.18% ash was achieved with a recovery of 3.91% at the lowest potential of 12.5 KV. For a given ash in a product, the combustible recovery was up to 20 % higher at 22.50 KV than at 10 KV for the Liketh Townlands coal and 18.32% higher for the Klipfontein coal. The coarser sized coal provided a cleaner product relative to the tailings since the minerals in the tailings, such as clay, were liberated and, being smaller in size than the coal particles, accumulated in the finer sized fraction and thereby increased the ash content in that fraction.

7. The external voltage applied to the charging chamber shows that the separation curves are essentially similar for all the coal samples tested apart from zero potential where the lowest ash products were obtained for all the samples tested. This shows that an external potential should not be applied to the rotary charger for the coal tested due to the higher ash products obtained between 1.5 KV to 5.0 KV. However in future tests the potential of

the particles reaching a saturated point still needs to be determined from the upgraded RTS.

8. The RTS process is efficient in rejecting sulphur in the coal samples tested in this study. It reduced sulfur content from 2.09 % to 0.93% at a combustible recovery of 5.74% with the Klipfontein coal at 0 KV charging voltage, 10 KV separating voltage and 3000 rpm rotary speed. Liketh Townlands sulfur content was also reduced from 1.73% to 0.27% at 8.90% combustible recovery at 0 KV charging voltage, 12.5 KV separating voltage and 5000 rpm rotary speed.

9. The RTS process is very effective in increasing the calorific value of coals tested in this study. The calorific value for the Majuba feed coal was increased from 20.15 MJ/Kg to 27.48 MJ/Kg after the second stage of separation while the single stage separation produced a clean coal product with 25.67 MJ/Kg, 16.10% ash and 29% combustible recovery for the Majuba coal. The same applied to Polmaise coal where a calorific value of 19.99 MJ/Kg was increased to 25.64 MJ/Kg and 27.45 MJ/Kg after the single and two-stage separation process respectively.

10. The effect of feed rate on several coals tested using RTS has indicated a strong dependence of separation performance on particle-to-particle collisions. More significant reduction in the ash content was observed as the feed rate increased from 12 g/min to 24 g/min for Majuba coal. Feed coal of 30.10% ash was reduced to 10.50% at 24 g/min, as compared to 11.10% at 12 g/min. In addition, due to the increase in the better grade of clean coal products obtained at higher feed rate under RTS, it would appear that this

separator can be scaled up for commercial applications due to its efficient charging mechanism under controlled feed rates.

11. The octagonal separator demonstrated a better particle separation for the (177 x 74) µm than the (-177) µm size fraction. The results obtained for Liketh Townland and Klipfontein coal indicate that lower ash, cleaner product and better separation is achieved using coarser sized particles compared to the result obtained from the finer particles. This result can be attributed to higher charge density imparted on (177 x 74) µm coal fraction, while the higher ash product obtained from the (-177) µm size fractions can be attributed to the decrease in the field intensity within the charging chamber by the sticking of fine particles onto the rotary charger and the decrease in the particle-to-wall chamber contacts.

12. The theoretical model developed based on the bearing and gas friction within the octagonal rotary charger can be used to calculate the cost of energy expended after each tests had been conducted at different parameter setups. This has shown that the total energy used by an octagonal rotary rotor with 0.0974 diameter and at 2500 rpm is 0.078 watt.

13. On the basis of test work done to date, the original pilot scale test equipment and process were critically assessed and further developments have been drawn up in order to design an improved pilot scale separator for test work in South Africa.

6.2. Benefits

In terms of future potential applications of RTS technologies, the following processes and industries are listed as potential beneficiaries:

1. In terms of power generation, beneficiation of the fine milled products between the mill and boiler would lead to a considerably improved quality of coal fed into the boilers. This would result in less coal required to provide the same energy output.

2. Providing lower ash coal would increase the efficiency of all pulverized fuel fed kilns in the cement industry or blast furnaces in the metallurgical industry.

3. The use of cleaner coal would lead to improved environmental conditions through the reduction of emissions of CO_2, SO_x, NO_x, and lower the quantities of combusted ash for disposal.

4. Higher efficiencies in coal utilization would lead to reduced unburned carbon content obtained in fly ashes. This in turn would lead to low carbon ash products which have high value as mineral admixtures for cement in the manufacturing of a concrete.

5. Beneficiating pulverized coal could also open up opportunities for using specific gasification technologies that have not been suitable in South Africa to date due to their high ash content and relatively low reactivity. This specifically refers to the Koppers Totzek gasifiers which were installed for the manufacture of ammonia in the 1980's in South Africa but which were found to be totally unsuitable to South African coals due to the factors listed above.

6. In terms of advanced carbon products, beneficiating high ash coal to very low ash content products would open up opportunities to obtain ultra clean coal which could be used in the manufacture of nanotubes, carbon fibres, and micronized coal. The latter can substitute for oil or gas in certain power stations and as transport fuels.

7. Alternative uses for the RTS process have already been shown, for example, in the beneficiation of phosphate from its host rock concentrate. This process has been found to be more efficient and cost effective that the current conventional processes that include, relative to flotation and leaching, washing and desliming, and drying.

In summary, South Africa is known to have low grade coal in its remaining reserves and the value of using such coal has been limited by poor washability, high sulphur content, high unburned carbon and inefficiency in most conventional utilisation processes. Conventional beneficiation processes are unable to reduce the ash content in most run-of-mine coals due to the size limitations in coarse sized processes and difficulty in separating ultra fine coal from minerals in fine coal separation. The RTS process has been shown to beneficiate such difficult fine material to very high efficiencies and most importantly, without the utilization of water in the cleaning process. This could open the door to significant commercialization of Triboelectrostatic techniques in future, not only for coal but also for other base metals in Southern African region.

6.3. Recommendations

The main focus of the present study was to determine the feasibility of cleaning South African fine coal through dry beneficiation using Tribo-electrostatic process. The RTS has proved to be an alternative approach in coal separation with great potential for improvement in the recovery of cleaned products. Emphasis was placed on the system parameters such as applied charger potential, separation chamber voltage, rotation speed of the copper plated rotor, injection flow speed, co-flow, feed rate and splitter distances. Results have indicated that further experimental studies on the charging mechanism and the magnitude of charges imparted on particles is needed to fully understand the importance of different electric field intensities in tribo-electrostatic separation processes. The following is therefore recommended for future study:

1. The construction of a new novel octagonal tribo-electrostatic separator consisting of three collecting bins in the form of Faraday cups and a Keithley electrometer with a 6522 scanner card for the measuring of the charge magnitude and polarity of the charges imparted on the coal particle are needed to better understand the influence of an applied potential difference in coal separation. The charge magnitude (Q) acquired by the coal particles from each of the bins will need to be calculated knowing the voltage (V) measured from the Keithley electrometer and (C) from the Faraday cup.

2. Particle build-up was noticed along the surface of the two electrodes used in this experimental work as the separation potential increases from 10 KV to 25 KV, thereby decreasing the quality of coal product obtained. In order to mitigate this effect, a grid

electrode, spaced apart from the chamber body is recommended as a possible alternative form of separating electrode~~s~~.

3. The study on the influence of the system parameters such as charger rotary speed should be investigated further by measuring the charge magnitude of coal particles obtained using a Keithley electrometer at different rotary charger speeds and different charging potential. Emphasis should be placed on the speed at which the particles become charge saturated once they are charge at zero potential.

4. More experimental studies should be conducted on the froth flotation of SA fine coal to evaluate and compare the cost and effectiveness of the RTS for fine coal separation.

5. A computer model should also be developed for simulating the performance of the separator in order to lead to forecasting commercial viability of the process.

References:

Advanced Energy Dynamics, Inc. (1987). Final Report Advanced Physical Fine Coal, DOE Contract No. DE-AC22-85PC81211

Ahfat, N. M., Buckton, G., Burrows, R. and Ticehurst, M. D. (2000). An exploration of Interrelationships between contact angle, inverse phase gas chromatography andtriboelectric charging data. *European Journal of Pharmaceutical Sciences*, Vol. 9, 271-276.

Alfano, G., Carbini, P., Ciccu, R., Ghiani, R. and Zucca, A. (1988). In: Progress in Triboelectric Separation of Minerals, (E. Forssberg, Ed.), Proceedings of the XVI IMPC, Stockholm, Sweden. Amsterdam, pp. 833-844.

Ban, H., Schaefer, J. and Stencel, J. (1994). Particle tribocharging characteristics relating to electrostatic dry coal cleaning. *Fuel*, Vol. 73, 1108-1115.

Ban, H., Schaefer, J. and Stencel, J. (1993a). Size and velocity effects on coal particle triboelectrification and separation efficiency. In: Proceedings of International Pittsburgh Coal Conference, *Pittsburgh.* PA, pp. 138–143.

Ban, H., Yang, J., Schaefer, J., Saito, K. and Stencel, J. (1993b). Measurement of charge and charge distribution on coal and mineral matter during electrostatic dry coal cleaning. In: Proceedings of International Conference on Coal Science. *Banf,* AB, Canada, 1, pp. 615–618.

Barker, O.B. and Barker & Associates. (1999). A techno-economic and historical review of the South African Coal Industry in the 19^{th} and 20^{th} Centuries. *Bulletin 113*, Johannesburg, South Africa.

Barthelemy, R.E. and Mora, R.G. (1960). Electrical high tension minerals beneficiation: principles and technical aspects, *Proceedings of V IMPC*, London, IMM. pp. 757-773

Biswal, S.K., Das, S.P., Reddy, P.S.R. and Misra, V.N. (2005). Prospect of beneficiation of high ash non-coking coals. *In: Engineering Trends in Mineral Processing and Extractive Metallurgy*, New Delhi, India, pp. 61-71.

Budge, G., Brough, J., Knight, J., and Baker Process. (2000). Review of the Worldwide Status of Coal Preparation Technology. Page 23, Report No. Coal R199 DTI/Pub URN00/1205.

Butcher, D. A. and Rowson, N. A. (1995). Electrostatic separation of pyrite from coal. *Magnetic and Electrical Separation*, Vol. 6, pp. 19–30.

Cangialosi, F., Notarnicola, M., Liberti, L., Caramuscio, P., Belz, G., Gurupira Z.T. and Stencel, J.M. (2006). Significance of surface moisture removal on triboelectrostatic beneficiation of fly ash, *Fuel*, Vol. 85, 2286–2293.

Castle, G. P. S. (1997). Contact charging between insulators. *Journal of Electrostatics*, Vol. 40 & 41, 13–20.

Castle, G. S. P., Inculet, I. I., Sines, G. S. and Schein, L. B. (2004). Contact charging between metals revisited. *IEEE Transactions on Industrial Applications*, Vol. 40(5), 1226–1230.

Celik, M. S. and Yildrim, I. (2000). A new physical process for desulphurization of low rank coals. *Fuel*, Vol. 79, 1665–1669.

Chandrasekhar, P. (1998). Design and Testing of a Triboelectrostatic Separator for Cleaning Coal, *Master's Thesis.* Virginia Polytechnic Institute and State University.

Chen, Q. and Wei, L. (2003). Coal dry beneficiation technology in China: The state-of the-art China. *Particuology*, Vol. 1(2), 52–56.

Cheng, Q. and Yang, Y. (2003). Development of fly beneficiation of coal in China. *Journal of*

Coal Preparation, Vol. 23, 3-12.

Cho, A. Y. H. (1964). Contact charging of micron-sized particles in intense electric fields. *Journal of Applied Physics*, Vol. 35, 2561–2564.

Choung, J., Mak, C. and Xu, Z. (2006). Fine Coal Beneficiation using an Air Dense Medium Fluidized Bed. *International Journal of Coal Preparation and Utilization*, Vol. 26:1, 1-15.

Cicek, B., Bilgesu, A. Y., Senelt, M. A. and Pamuk, V. (1996). Desulphurization of coals by flash pyrolysis followed by magnetic separation. *Fuel Processing Technology*, Vol.46, 133–142.

Cross, J.A. (1987). Electrostatic: Principles, Problems and Applications, Adam Hilger, Bristol, England, pp. 17-19 and 273-248.

Department of Trade and Industry, UK, (2004) Available at: http://www.dti.gov.uk/files /file20079.pdf ?pubpdfdload=02%2F786. Accessed, September 2009.

Dieudonne, V., Hewitt, S. and Wyk, D.N. (2001). Jigging the South-Africa coals – a new challenge. *Mintek*, Randburg, South Africa.

Dwari, R.K. and Rao, H.K. (2006). Tribo-electrostatic behaviour of high ash non coking Indian thermal coal. *International Journal of Mineral Process*, Vol. 81, 93-104.

Dwari, R.K. and Rao, H.K. (2007). Dry Beneficiation of coal – A review. *Mineral Processing and Extractive Metallurgy*, Vol. 28, 177-234.

Dwari, R.K. and Rao, H.K. (2008). Characterising Electron Transfer Mechanism in Tribo Electrification of pyrite through Contact Angle Measurements. *The Open Mineral Processing Journal*, Vol. 1, 6-17

Dwari, R.K. and Rao, H.K. (2008). Non-coking coal preparation by novel triboelectrostatic method. *Fuel*, Vol. 87(17-18), 3562-3571

Dwari, R.K. and Rao, H.K. (2009). Fine coal preparation using novel tribo-electrostatic separator. *Minerals Engineering*, Vol. 22(2), 119-127

Dwari, R.K. and Rao, H.K. and Somasundaran,P. (2009). Characterisation of particle tribo-charging and electron transfer with reference to electrostatic dry coal cleaning. International Journal of Mineral Processing. Vol. 91(3-4), 100-110.

Falcon, L.M. and Falcon, R.M.S. (1983). The application of Coal Petrography to Certain Beneficiation Techniques on South African Coal. *Geological Society of South Africa*, Vol.7, 137-148.

Falcon, R.M.S. (1986). A brief review of the origin, formation, and distribution of coal in South Africa, Anhaeusser C.R. and Maske, S. (Eds), (1986). In: Mineral Deposits of Southern Africa, Vol. I and II, *Geological Society of South Africa*, Johannesburg, 1986, page 1879-1898.

Falcon, R.M.S. and Ham, A. J. (1988). The characteristics of Southern African coals. *Journal of the South African Institute of Mining and Metallurgy*, Vol. 88(5), 145-161.

Fan, L.S. and Zhu, Ch. (1998). Principles of Gas-Solid Fluidization. Cambridge University Press, New York (1998).

Fan, M., Chen, Q., Zhao, Y., Tao, D., Zhenfu, L., Tao, X., Yang, Y., Jiang, X. and Zhu, J. (2005). Coal Ash beneficiation and Utilization in coal separation process. *Conference proceeding, World Coal Ash*, April 11-15, Lexington, Kentucky, USA, 2005.

Fauconnier, C. (2005). The future of The South African Coal Mining Industry. Kumba Resources Limited, Waterberg, South Africa.

Finseth, D., Newby, T. and Elstrodt, R. (1993). Dry electrostatic separation of fine coal. In: Processing and Utilization of High Sulfur Coals, (V. B. K. Parekh, and J. G. Groups, Eds.), Amsterdam *Elsevier*, pp. 91–98.

Frankal, D. R. (1968). Electrostatic energy in a semiconductor surface space-charge layer. *Surface Science*, Vol. 9, 73–86.

Gady, B. and Reifenberger, R. (1998) Contact electrification studies using atomic force microscope techniques. *Journal of Applied Physics*, Vol. 84 (1), 319-322.

Gady, B. and Reifenberger, R., Rimai, D. S. and DeMejo, L. P. (1997). Contact electrification and the interaction force between a micrometer-size polystyrene sphere and a graphite surface. *Langmuir* 13, 2533-2537.

Gibson, H. W. (1975). Linear free energy relationships. V. Triboelctric charging of organic solids. *Journal of American Chemical Society*, Vol. 97, 3832–3833.

Gibson, H. W. (1984). Control of electrical properties of polymers by chemical modification. *Polymer*, Vol. 25, 3–27.

Gidaspow, D., Wasan, D., Saxena, Y.T. Gupta, R. and Mukhenjee, A. (1984). Electrostatic Desulphurization of Coal in Fluidized Beds and Convectional Fluidized and Fluid Particle system. *AIChE symposium Series No. 255*, Vol. 83, pp 74-85.

Gidaspow, D. (1987). Separation of pyrites from Illinois coals using electro-fludized beds and electrostatic sieve conveyors. In: Proceedings of the Second International Conference on the Processing and Utilization of High Sulfur Coals II, Carbondale, IL.

Gupta, R. Gidaspow, D. and Wasan T. (1993). Electrostatic separation of powder mixture based on the functions of its constituents. *Powder Technology*, Vol. 75, 79-87.

Greason, W. D. (2000). Investigation of a test methodology for triboelectrification. *Jourrnal of Electrostatics*, Vol. 49, 245–256.

Harper, W. R. (1951). The voltage effect as a cause of static electrification. *Proceeding of the Royal Society London A. Math. Phys. Sci*. 83–103.

Harper, W. R. (1967). Contact and Frictional Electrification. Oxford, UK: Clarendon

Hayakawa, S., Sakaguchi, E. and Yamashita, R. (1985). Conditions of Suited for separation of tea stems by electrostatic separator. *Journal of Institution of Agriculture Machine*, Vol. 47, 107-112.

Higashiyama, Y. and Asano, K. (1998). Recent progress in electrostatic separation technology. *Particulate science and technology*, Vol. 16(1), 77-90.

Hower, J.C., Hang, B., Schaefer, J.L. and Stencel, J.M. (1997). Maceral/microlithotype partitioning through triboelectrostatic dry coal cleaning. *International Journal of Coal Geology*, Vol. 34, pp. 277-286.

Hutton, A. C., and Mandile, A. J. 1996. Quantitative XRD measurement of mineral matter in Gondwana coals using the Rietveld method. *J. African Earth Sci*. 23(1): 61-72.

Inculet, I. I., Quingley, R. M., Bergougnou, M. A. and Brown, J. D. (1980). Electrostatic beneficiation of hat creek coal in the fluidized state. *CIM Bulletin*, Vol. 73, 51–61.

Inclet, I.I., Quingley, R. M. Bergougnou, M.A. and Brown, J.D. (1982). Electrostatic beneficiation of hat creek coal in the fluidized state. *CIM Bulletin*, 73, pp 51-61.

Inclet, I.I., Bergougnou, M.A. and Brown, J.D. (1982). Electrostatic beneficiation of Coal. Physical cleaning of coal-present and developing methods. (Y. A. Liu, Ed.), New York Marcell Dekker, pp. 87-131.

Inculet, I. I. (1984). Electrostatic Mineral Separation, England, UK: Research Study Press Ltd, pp. 153.

Kelly, E. G. and Spottiswood, D. J. (1989a). The theory of electrostatic separations: A review. Part I. Fundamentals. *Minerals Engineering*, Vol. 2(1), 33–46.

Knoll, F. S. and Taylor, J. B. (1984). Advances in Electrostatic Separation. *SME Preprint*, page 84–71.

Kornfield, M. I. (1976). Frictional electrification. *Journal of Physics D: Applied Physics*, Vol. 9, 1183–1192.

Kretzschmar, S., Pocock, J. and Loveday, B. (2008). Dry Benenficiation of coal using an air dense-medium fluidized separator. Proceedings, *Industrial Fluidization South Africa*, November 19-20, Johannesburg.

Kwetus, B.A., (1994). Contact electrification of coal and minerals. Journal of Electrostatics, Vol. 32, pp. 271-276.

Lama, W.L. and Gallo, C.F. (1976). The Sparking Characteristics of needle to plane coronas. IEEE Transactions on Industry Application, Vol. IA(12), pp 288-293

Lewowski, T. (1993). Electrostatic desulphurisation of Polish steam coals. *Coal Preparation*, Vol. 13, 97–105.

Li, T.X., Ban, H., Hower, J.C., Stencel, J.M. and Saito, K. (1999). Dry triboelectrostatic separation of mineral particles: a potential application in space exploration. *Journal of Electrostatics*, Vol.47, 133-142.

Lockhart, N.C. (1984). Dry Beneficiation of Coal- Review Paper. *Powder Technology*, Vol. 40, 17-42.

Lowel, J. (1975). Contact electrification of metals. *Journal of Physics D: Applied Physics*, Vol. 8, 53–63.

Lowell, J. and Rose-Innes, A. C. (1980). Contact electrification. Advances in Physics, Vol. 29(6), pp. 947–1023.

Luo, Z., Chen, Q. and Tao, X. (2000). Formation mechanism of vibration fluidized bed (VFB). *Journal of China University of Mining & Technology*, Vol. 29, 230–234.

Manouchehri, H.R., Hanumantha Rao, K. and Forsberg, K.S. (2000a). Review of electrical separation methods. Part 1: *Fundamental aspects. Mineral and Metallurgical processing*, Vol. 17 (1), pp. 23-36.

Manouchehri, H.R., Hanumantha Rao, K. and Forsberg, K.S. (2000b). Review of electrical separation methods. Part 1: Practical consideration. *Mineral and Metallurgical processing*, Vol. 17 (3), pp. 139-166.

Masuda, H. and Iinoya, K. (1978). Electrification of particles by impact on inclined metal plates. *AIChE Journal*, Vol. 24, 950–956.

Masuda, S., Taraguchi, M., Takashashi, T. and Haga, K. (1984). Electrostatic Beneficiation of Coal Using a Cyclone-Tribocharger. *IEEE Transactions of Industry Applications*, Vol. 1A-19.

Mazumder, M.K., Tennal, K.B. and Lindquist, D.P. (1994). Electrostatic beneficiation of coal. In Proceeding of the Tenth Annual Coal Preparation, Utilization and Environmental Control Contractors Conference, pp. 18-21.

Mazumder, M. K., Tennal, K. B. and Lindquist, D. A. (1995). Triboelectric separation of coal from mineral impurities. In Proceedings of the Annual Meeting of the Electrostatic Society of America, Morgan Hill, CA: Laplacian, pp. 59–70.

Mazumder, M.K., Sims, R.A., Biris, A.S., Srirama, P.K., Saini, D., Yurteri, C.U., Trigwell, S. De, S. and Sharma, R. (2006). Twenty-first century research needs in electrostatic processes applied to industry and medicine. *Chemical Engineering Science*, Vol. 61, 2192 – 2211.

Mbendi Profile: South Africa Coal Mining – Over view. (2004). www.mbendi.co.za/i-ndy/ming/coal/af/sa/p0005.htm (Accessed, 22 February 2008).

Mehta, R.K., Misra, M., and Nelson, M. (1994). Triboelectrification assisted air classification process for removal of radionuclides from contaminated soils. *Presented at the Annual Conference on Contaminated Soils*. October 17-20, pp. 12

Mehta, R.K., Chatterjee, I., and Misra, M. (1996). Simultaneous grinding and triboelectrification of coal following by separation in an electrocentrifugal field. *SME Annual Meeting*, March 11-14, pp. 12

Moore, A.D. (1973). Electrostatic and its application. Wisley Publisher, New York.

Mora, R.G. (1958). Study of Electrical Concentration of Minerals, *Thesis*. Mass. Inst. Tech.

Mukai, S., Ishikawa, T. and Wakamatsu, T. (1967). Study on the Electrostatic Concentration of low ash coal in corona discharge field. *Society of Mining Engineers AIME Transaction*, 238, page 205.

Mukherjee, A., Gidaspow, D. and Wasan, D. T. (1987). Surface charge of Illinois coal and pyrites for dry electrostatic cleaning. *American Chemical Society, Division of Fuel Chemistry*, Vol. 32(1), 395–407.

Nifuku, M., (1989). Static electrification phenomena in pneumatic transportation of coal. *Journal of Electrostatics,* Vol. 23, 45–54.

Oda, T., Kunisue, Y. and Masuda, S. (1983). Pulverized coal beneficiation by dry high gradient magnetic separation process. *IEEE Transactions on Magnetics*, Vol. 19(5), 2121–2123.

Ohara, K. (1988). A method of exponential function analysis of contact and frictional electrification curves. *Journal of Electrostatics,* Vol. 20, 319–326.

Olofinskii, N. F. (1957) Electric corona separation of coal fines and certain minerals. Moscow. Translated by Israel Program for Scientific Translations, 1969.

Park, C.H., Jeon, S.J. and Park, J.K. (2007). PVC removal from mixed plastics by triboelectrostatic separation. *Journal of Hazardous Material*, Vol. 144, 470-476.

Piet Viljoen and Jeanie Moothoo. 2008. Eskom gets nervous over SA's coal production. http://www.miningmx.com/news/energy/720032.htm. Accessed, April 2009.

Pochan, J. M., Gibson, H. W., Bailey, F. C. and Hinman, D. F. (1980). Space-charge effects of semiconductive coatings on triboelectric charge exchange. *Journal of Electrostatics*, Vol. 8, pp. 183.

Ralston, O. C. (1961). Electrostatic Separation of Mixed Granular Solids, Amsterdam, Elsevier.

Ruckdeschel, F. R. and Hunter, L. P. (1975). Contact electrification between insulators: Phenomenological aspects. *Journal of Applied Physics*, Vol. 46(10), 4416–4430.

Ruckdeshel, F. R. and Hunter, L. P. (1977). Thermionic return currents in contact electrification. *Journal of Applied Physics*, Vol. 48(12), 4898–4902.

Saeid, A.M., Butcher, D.A. and Rowson, N.A. (1992). Coal desulphurisation and ash removal in intensified magnetic fields. *Magnetic and Electrical Separation*, Vol. 4, 107-116.

Sampaio, C.H. Aliaga, W., Pacheco, E.T., Petter, E. and Wotruba, H. (2008). Coal beneficiation of Candiota mine by dry jigging. *Fuel Processing Technology*, Vol. 89, 198-202.

Samuila, A., Urs, A. and Iuga, A. (2005). Optimization of Corona Electrode Position in Roll-Type Electrostatic Separators. *IEEE Transactions on Industry Applications.* Vol. 41(2), 527-534.

Schein, L. B., Laha, M. and Novotny, D. (1992). Theory of insulator charging. *Physical Letter A*, Vol. 167, 79–83.

Sharma, R., Trigwell, S., Sims, R.A. and Mazumder, M.K. (2004). Modification of electrostatic properties of polymer powders using atmospheric plasma reactor. In: Mittal, K.L. (Ed.), Polymer Surface Modification: *Relevance to Adhesion*, Vol. 3, VSP, AH Zeist, The Netherlands, p. 25.

Sharmene Ali, F., Adnan Ali, M., Castle, G. S. P., and Inculet, I. I. (1998). Charge exchange model of a disperse system of spherical powder particles. *Institute of Electrical and Electronics Engineers*, Vol. 3, 1884–1890.

Shinohara, I., Yamamoto, F., Anzai, H. and Endo, S. (1976). Chemical structure and electrostatic properties of polymers. *Journal of Electrostatics*, Vol. 2, 99–110.

Soong, Y., Link, T. A., Schoffstall, M. R., Turčániová, Ľ., Baláž, P., Marchant, S., and Schehl, R. R. 1998. Triboelectrostatic Separation of Mineral Matter from Slovakian Coals. Acta

Montanistica Slovaca Ročnik 3: 393-400.

Soong, Y., Link, T. A., Schoffstall, M. R., Gray, M. L., Fauth, D. J., Knoer, J. P., Jones, J. R. and Gamwo, I. K. (2001). Dry beneficiation of Slovakian coal. *Fuel Processing Technology*, Vol. 72(3), 185–198.

Soong, Y., Schoffstall, M.R. and Link, T.A. (2001). Triboelectrostatic beneficiation of fly ash. *Fuel*, Vol. 80, 879-884.

Spotts, M.F. (1985). Design of Machine Elements, Prentice-Hall, Inc., Englewood Cliffs, New Jersey, page 435.

Stencel, J. M., Schaefer, J. L., Ban, H., Li, T. –X., and Neathery, J. K. 1998. Triboelectrostatic Cleaning of Coal In-line Between Pulverizer and Burners at Utilities. *International Journal of Coal Preparation and Utilization*, Vol. 19(1), 115-129.

Tao, D., and Jiang, X. (2006). *Electrostatic Particle Charger, Electrostatic Separation System, and Related Methods*. Publication number.: US 2006/0213760 A1. Lexington: Kentucky.

Tao, D., Mao-ming, F. and Jiang, X. (2009). Dry coal fly ash cleaning using rotary triboelectrostatic separator. *Mining Science and Technology*. Vol. 19, 642–647.

Taylor, J.B. (1988). Separation of granular materials. *Conference record IEE Annual Meeting*, Vol. 23, 1741-1759.

Trigwell, S. (2003). Correlation between surface structure and tribocharging of powders. Doctoral Dissertation, University of Arkansas at Little Rock, USA.

Trigwell, S., Mazumder, M. K. and Pellissier, R. (2001). Tribocharging in electrostatic beneficiation of coal: Effects of surface composition on work function as measured by xray photoelectron spectroscopy and ultraviolet photoelectron spectroscopy in air. *Journal of Vacuum Science and Technology*, Vol.19A (4), pp. 1454-1459.

Trigwell, S., Grable, N., Yurteri, C.U., Sharma, R. and Mazumder, M.K. (2003a). Effects of surface properties on the tribocharging characteristics of polymer powder as applied to industrial processes. *IEEE Transactions on Industry Applications*, Vol. 39 (1), 79–86.

Trigwell, S., Tennal, K.B., Mazumder, M.K. and Lindquist, D.A. (2003b). Precombustion cleaning of coal by triboelectric separation of minerals. *Particulate Science and Technology*, Vol. 21(4), 353–364.

Tsai, S.C. (1982). Fundamental of Coal Beneficiation and Utilization. Elsevier Scientific Publishing Company, New York, U.S.A.

Weitkämper, L., and Wotruba, H. (2004). Recent development in the dry cleaning of coal. In Proceedings of Mineral processing Technology, Bhubaneswar, India: *Allied*, pp. 539–546.

World Coal Institute. 2008. Coal in Electricity Generation. www.worldcoal.org/resources/coal-statistics/. Accessed February 2009.

Worobiec, A., Anna Stefania, E., Potgieter-Vermaak, S. Sawlowicz, Z., Spolni, Z. and Van Grieken, R. (2007). Characterisation of concentrates of heavy mineral sands by micro-Raman spectrometry and CC-SEM/EDX with HCA. *Applied Geochemistry*, Vol. 22, 22078–2085

Wu, Y., Castle, G. P. S., Inculet, I. I., Petigny, S. and Swei, G. (2003). Induction charging on freely levitating particles. *Powder Technology*, Vol. 135–136, pp. 59–64.

Yang, G. H., Zheng, D. C., Zhou, J. H., Zhao, Y. M. and Chen, Q.R. (2002). Air classification of moist raw coal in a vibrated fluidized bed. Minerals Engineering, Vol. 15, 623–625.

Yongzhi, L. (1992). Electrostatic separation study and practice of fine particles rutile. Proceedings, 1st International Conference. *Modern Process Mineralogy and Mineral Processing*, Beijing, pp. 385-390.

Yoong R.H., Yan, E.S., Luttrell, G.H. and Adel, G.T. (1997a). POC-Scale Testing of a Dry Triboelectrostatic Separator for Fine Coal Cleaning. *6th Quarter Technical Progress Report*, DE-AC22-95PC95151.

Yoong R.H., Yan, E.S., Luttrell, G.H. and Adel, G.T. (1997b). POC-Scale Testing of a Dry Triboelectrostatic Separator for Fine Coal Cleaning. *7th Quarter Technical Progress*

Report, DE-AC22-95PC95151.

Yoshida, M., Li, N., Shimosaka, A., Shirakawa Y. and Hidaka, J. (2006). Experimental and theoretical approaches to charging behaviour of polymer particles, *Chemical. Engineering Science.* Vol. 61(7), pp. 2239–2248

Zafar, I.Z., Anwar, M.M. and Pritchard, D.W. (1996). Innovation in beneficiation technology for low grade phosphate rocks. *Nutrients Cycling in Agroecosystems*, Vol. 46, 135-151.

Zavitsanos, P.D., Golden, J.A., Bleiler, K.W. and Kinkead, K.W. (1978). Coal Desulfurization Using Microwave Energy. *EPA-600/7-78-089*, US Environmental Protection Agency, Office of Research and Development, prepared by General Electric Co. Washington, D.C.

Zavitsanos, P.D., Jacobs, I.S. and Golden, J.A. (1982). Tracking pyritic sulfur in the microwave desulfurization of coal. *Journal of Applied Physic.* Vol. 53, 2730-2732.

Zhen-fu, L., Jiang-feng, Z., Mao-ming, F. Yue-min, Z. and Xiu-xiang, T. (2007). Low density dry coal beneficiation using an air dense medium fluidized bed. *Journal of China University of Mining and Technology*, Vol. 17 (3), 306-309.

Zhenfu, L., Fan, M., Zhao, Y., Tao, X., Chen, Q. and Chen, Z. (2008). Density-dependent separation of dry fine coal in a vibrated fluidized bed. *Powder Technology*, Vol. 187(2), 119-123.

Zhou, G. and Brown, D. (1988). Coal surface conditioning for electrostatic separation. Canadian *Journal of Chemical Engineering*, Vol. 66, pp. 858–863.

Appended Papers

Paper 1

Bada, S, Falcon, L.M. and Falcon, R.M.S. (2009). The potential of electrostatic separation in the upgrading of South African fine coal prior to utilisation. Conference: 14th Southern African Coal Science and Technology Conference – Indaba 2009: Clean Coal Technology. 11-12 March 2009, Johannesburg

Submitted for Publication

Paper 2

Bada Samson, Tao Daniel, Honaker Rick, Falcon Lionel, Falcon Rosemary (2010). Parametric study of electrostatic separation of South African fine coal. *Mining Science and Technology*. Vol 20, 0535-0541.

Published

Paper 3

S. O. Bada, D. Tao, R. Q. Honaker, L. M. Falcon and R. M. S. Falcon. (2010). A study of rotary triboelectrostatic separation of South African fine coal. *International Journal of Coal Preparatio n and Utilization.* Vol 30 (2): 154-172.

Published

APPENDIX A

APPENDIX A

Washability, Froth rate and Tribo-electrostatic studies Data

Table A.1. Sink and float data for Polmaise coal (177 X 74) µm at different relative density

Relative Density Fraction	Weight %	Ash content %	Cum Float (clean coal) Wt %	Cum Float (clean coal) Ash %	Combustible Recovery %
Float 1.40	19.76	6.81	19.76	6.81	26.95
1.40-1.80	54.96	22.42	74.72	18.29	89.38
Sink 1.80	25.28	71.3	100.00	31.69	100
Total	100	31.69			

Table A.2. Sink and float data for Majuba coal (177 X 74) µm at different relative density

Relative Density Fraction	Weight %	Ash content %	Cum Float (clean coal) Wt %	Cum Float (clean coal) Ash %	Combustible Recovery %
Float 1.40	19.97	5.9	19.97	5.9	25.49
1.40-1.80	61.77	21.16	81.74	17.43	91.55
Sink 1.80	18.26	65.88	100.00	26.28	100
Total	100	26.28			

Table A.3. Sink and float data for Liketh Townlands coal (177 X 74) µm at different relative density

Relative Density Fraction	Weight %	Ash content %	Cum Float (clean coal) Wt %	Cum Float (clean coal) Ash %	Combustible Recovery %
Float 1.40	16.50	6.22	16.50	6.22	21.53
1.40-1.80	60.84	19.39	77.34	16.58	89.77
Sink 1.80	22.66	67.56	100.00	28.13	100
Total	100	28.13			

Table A.4. Sink and float data for Klipfontein coal (177 X 74) µm at different relative density

Relative Density Fraction	Weight %	Ash content %	Cum Float (clean coal) Wt %	Cum Float (clean coal) Ash %	Combustible Recovery %
Float 1.40	14.61	6.8	14.61	6.8	20.99
1.40-1.80	54.87	22.12	69.49	18.90	86.88
Sink 1.80	30.51	72.1	100.00	35.13	100
Total	100	35.13			

Table A.5. Sink and float data for Koorfontein coal (177 X 74) µm at different relative density

Relative Density Fraction	Weight %	Ash content %	Cum Float (clean coal) Wt %	Cum Float (clean coal) Ash %	Combustible Recovery %
Float 1.40	39.70	4.48	39.70	4.48	44.73
1.40-1.80	53.51	16.5	93.21	11.38	97.43
Sink 1.80	6.79	67.95	100.00	15.22	100
Total	100	15.22			

Table A.6. Sink and float data for New Vaal coal (177 X 74) µm at different relative density

Relative Density Fraction	Weight %	Ash content %	Cum Float (clean coal) Wt %	Cum Float (clean coal) Ash %	Combustible Recovery %
Float 1.40	10.04	7.51	10.04	7.51	14.97
1.40-1.80	54.56	23.61	64.60	21.11	82.14
Sink 1.80	35.40	68.7	100.00	37.96	100
Total	100	37.96			

Table A.7. Froth rate data for Polmaise coal (-177) µm at 15 ppm and 1200 rpm

Sample (Time) sec	Fractional Yield (Wt) %	Ash content %	Cumulative Weight %	Cumulative Ash content %	Combustible Recovery %
15	14.88	19.49	14.88	19.49	17.92
30	10.90	20.76	25.78	20.03	30.84
45	7.12	21.58	32.90	20.36	39.19
60	5.87	22.29	38.77	20.66	46.02
120	9.90	25.29	48.68	21.60	57.09
240	5.77	29.82	54.44	22.47	63.15
360	1.40	33.27	55.84	22.74	64.54
Tailings	44.16	46.32	100.00	33.15	100
Total	100.00	33.15			

Table A.8. Froth rate data for Majuba coal (-177) µm at 15 ppm and 1200 rpm

Sample (Time) sec	Fractional Yield (Wt) %	Ash content %	Cumulative Weight %	Cumulative Ash content %	Combustible Recovery %
15	21.30	19.61	21.30	19.61	24.58
30	15.20	22.85	36.50	20.96	41.41
45	7.56	23.89	44.06	21.46	49.67
60	3.29	23.37	47.35	21.59	53.29
120	3.59	25.32	50.94	21.86	57.14
240	1.53	25.61	52.47	21.97	58.77
360	0.72	20.60	53.19	21.95	59.59
Tailings	46.81	39.86	100.00	30.33	100
Total	100.00	30.33			

Table A.9. Froth rate data for Koorfontein coal (-177) µm at 15 ppm and 1200 rpm

Sample (Time) sec	Fractional Yield (Wt) %	Ash content %	Cumulative Weight %	Cumulative Ash content %	Combustible Recovery %
15	7.05	12.49	7.05	12.49	7.75
30	4.39	12.78	11.44	12.60	12.56
45	4.07	13.06	15.51	12.72	16.99
60	3.13	13.52	18.64	12.86	20.40
120	8.62	14.82	27.26	13.48	29.61
240	6.17	17.55	33.43	14.23	36.00
360	1.87	19.99	35.30	14.53	37.88
Tailings	64.70	23.53	100.00	20.35	100
Total	100.00	20.35			

Table A.10. Froth rate data for Liketh Townlands coal (-177) µm at 15 ppm and 1200 rpm

Sample (Time) sec	Fractional Yield (Wt) %	Ash content %	Cumulative Weight %	Cumulative Ash content %	Combustible Recovery %
15	43.93	22.53	43.93	22.53	47.88
30	22.79	24.34	66.72	23.15	72.14
45	8.12	27.22	74.84	23.59	80.45
60	4.89	26.31	79.73	23.76	85.52
120	8.20	25.33	87.93	23.90	94.14
240	1.56	33.03	89.49	24.06	95.60
Tailings	10.51	70.27	100.00	28.92	100
Total	100.00	28.92			

Table A.11. Froth rate data for Klipfontein coal (-177) µm at 15 ppm and 1200 rpm

Sample (Time) sec	Fractional Yield (Wt) %	Ash content %	Cumulative Weight %	Cumulative Ash content %	Combustible Recovery %
15	8.85	20.63	8.85	20.63	10.75
30	14.48	22.88	23.33	22.03	27.84
45	8.87	23.46	32.21	22.42	38.24
60	6.92	24.33	39.13	22.76	46.25
120	10.40	26.99	49.53	23.65	57.87
240	5.84	32.83	55.37	24.62	63.87
360	1.56	37.01	56.93	24.96	65.38
Tailings	43.07	47.47	100.00	34.65	100
Total	100.00	34.65			

Table A.12. Froth rate data for New Vaal coal (-177) µm at 15 ppm and 1200 rpm

Sample (Time) sec	Fractional Yield (Wt) %	Ash content %	Cumulative Weight %	Cumulative Ash content %	Combustible Recovery %
15	2.58	18.27	2.58	18.27	3.56
30	3.66	21.07	6.24	19.91	8.44
45	1.96	22.57	8.20	20.55	11.00
60	1.52	24.66	9.72	21.19	12.93
120	2.33	27.57	12.05	22.42	15.78
240	1.46	30.82	13.51	23.33	17.48
360	0.35	24.31	13.86	23.36	17.93
Tailings	86.14	43.55	100.00	40.75	100
Total	100.00	40.75			

Table A.13. Charging voltage experiments data for Khutala No. 2 seam coal from second stage Tribo-electrostatic test at **0 KV**, 1.9 m/sec air velocity & 12.5 KV separating voltage

Product collected	Fractional Yield (Wt) %	Ash content	Cumulative Weight %	Cumulative Ash content (%)	Combustible Recovery	Ash rejection %
1	6.90	10.48	6.90	10.48	8.87	97.62
2	10.52	17.04	17.42	14.44	21.40	91.71
3	8.05	17.39	25.47	15.37	30.95	87.10
4	32.74	27.07	58.21	21.95	65.23	57.89
5	3.25	28.89	61.46	22.32	68.55	54.80
6	2.16	31.67	63.62	22.64	70.66	52.55
7	13.04	39.06	76.66	25.43	82.08	35.76
8	14.43	42.38	91.09	28.12	94.01	15.61
9	8.91	53.17	100.00	30.35	100	0.00
Total	100.00	30.35				

Table A.14. Charging voltage experiments data for Khutala No. 2 seam coal from second stage Tribo-electrostatic test at **1.5 KV**, 1.9 m/sec air velocity & 12.5 KV separating voltage

Product collected	Fractional Yield (Wt) %	Ash content	Cumulative Weight %	Cumulative Ash content (%)	Combustible Recovery	Ash rejection %
1	6.74	10.42	6.74	10.42	8.69	97.69
2	9.65	16.19	16.40	13.82	20.33	92.57
3	7.93	17.21	24.33	14.92	29.78	88.09
4	32.52	26.55	56.85	21.57	64.14	59.78
5	2.35	30.71	59.19	21.94	66.48	57.41
6	3.69	32.97	62.89	22.58	70.04	53.42
7	13.88	38.61	76.77	25.48	82.30	35.84
8	14.56	42.96	91.33	28.27	94.25	15.32
9	8.67	53.89	100.00	30.49	100	0.00
Total	100.00	30.49				

Table A.15. Charging voltage experiments data for Khutala No. 2 seam coal from second stage Tribo-electrostatic test at **2.5 KV**, 1.9 m/sec air velocity & 12.5 KVseparating voltage

Product collected	Fractional Yield (Wt) %	Ash content	Cumulative Weight %	Cumulative Ash content (%)	Combustible Recovery	Ash rejection %
1	6.34	9.59	6.34	9.59	8.26	98.01
2	9.33	15.78	15.67	13.27	19.58	93.20
3	7.85	17.41	23.52	14.65	28.92	88.73
4	2.83	26.27	26.35	15.90	31.92	86.30
5	31.71	26.34	58.07	21.60	65.58	58.98
6	2.66	30.15	60.73	21.98	68.26	56.35
7	13.82	38.87	74.55	25.11	80.43	38.79
8	15.87	42.27	90.42	28.12	93.62	16.85
9	9.58	53.80	100.00	30.58	100	0.00
Total	100.00	30.58				

Table A.16. Charging voltage experiments data for Khutala No. 2 seam coal from second stage Tribo-electrostatic test at **5 KV**, 1.9 m/sec air velocity & 12.5 KVseparating voltage

Product collected	Fractional Yield (Wt) %	Ash content	Cumulative Weight %	Cumulative Ash content (%)	Combustible Recovery	Ash rejection %
1	5.96	9.28	5.96	9.28	7.80	98.01
2	8.75	15.91	14.71	13.22	18.40	93.20
3	7.52	16.75	22.23	14.42	27.43	88.73
4	31.23	25.92	53.46	21.14	60.79	86.30
5	3.21	27.57	56.68	21.50	64.15	58.98
6	2.87	29.57	59.55	21.89	67.06	56.35
7	13.65	38.36	73.20	24.96	79.19	38.79
8	16.58	41.71	89.77	28.05	93.12	16.85
9	10.23	53.36	100.00	30.64	100	0.00
Total	100.00	30.64				

Table A.17. Separating voltage experiments data for Khutala No. 2 seam coal from second stage Tribo-electrostatic test at **12.5 KV**, 1.9 m/sec air velocity & 0 KV charging voltage

Product collected	Fractional Yield (Wt) %	Ash content	Cumulative Weight %	Cumulative Ash content (%)	Combustible Recovery	Ash rejection %
1	7.30	8.90	7.30	8.90	9.56	97.86
2	9.00	14.39	16.31	11.93	20.63	93.60
3	8.32	15.44	24.62	13.12	30.74	89.37
4	26.18	24.27	50.81	18.86	59.22	68.46
5	3.04	25.22	53.84	19.22	62.48	65.94
6	3.78	29.59	57.62	19.90	66.31	62.26
7	11.99	36.21	69.62	22.71	77.30	47.97
8	18.63	42.59	88.25	26.91	92.67	21.86
9	11.75	56.55	100.00	30.39	100	0.00
Total	100.00	30.39				

Table A.18. Separating voltage experiments data for Khutala No. 2 seam coal from second stage Tribo-electrostatic test at **15 KV**, 1.9 m/sec air velocity & 0 KV charging voltage

Product collected	Fractional Yield (Wt) %	Ash content	Cumulative Weight %	Cumulative Ash content (%)	Combustible Recovery	Ash rejection %
1	7.14	9.03	7.14	9.03	9.33	97.88
2	9.22	15.11	16.36	12.46	20.58	93.30
3	8.37	16.19	24.73	13.72	30.65	88.84
4	26.84	24.88	51.56	19.53	59.62	66.88
5	3.50	26.15	55.07	19.95	63.34	63.87
6	3.43	29.63	58.49	20.52	66.80	60.53
7	11.87	36.91	70.36	23.28	77.56	46.12
8	17.98	42.21	88.34	27.13	92.49	21.16
9	11.66	55.17	100.00	30.40	100	0.00
Total	100.00	30.40				

Table A.19. Separating voltage experiments data for Khutala No. 2 seam coal from second stage Tribo-electrostatic test at **20 KV**, 1.9 m/sec air velocity & 0 KV charging voltage

Product collected	Fractional Yield (Wt) %	Ash content	Cumulative Weight %	Cumulative Ash content (%)	Combustible Recovery	Ash rejection %
1	8.66	9.85	8.66	9.85	11.24	97.21
2	9.64	15.47	18.30	12.81	22.97	92.32
3	8.45	15.83	26.75	13.76	33.20	87.94
4	22.66	24.63	49.41	18.75	57.79	69.66
5	3.98	26.01	53.39	19.29	62.04	66.27
6	4.53	28.68	57.93	20.02	66.69	62.01
7	11.91	36.89	69.84	22.90	77.51	47.62
8	17.34	42.06	87.18	26.71	91.97	23.73
9	12.82	56.51	100.00	30.53	100	0.00
Total	100.00	30.53				

Table A.20. Separating voltage experiments data for Khutala No. 2 seam coal from second stage Tribo-electrostatic test at **25 KV**, 1.9 m/sec air velocity & 0 KV charging voltage

Product collected	Fractional Yield (Wt) %	Ash content	Cumulative Weight %	Cumulative Ash content (%)	Combustible Recovery	Ash rejection %
1	9.25	10.11	9.25	10.11	12.00	96.95
2	9.29	15.68	18.54	12.90	23.29	92.20
3	9.04	16.19	27.58	13.98	34.22	87.42
4	20.29	24.17	47.88	18.30	56.41	71.42
5	4.42	25.85	52.30	18.94	61.14	67.69
6	5.32	27.80	57.62	19.76	66.68	62.86
7	11.05	36.47	68.68	22.45	76.81	49.72
8	16.92	41.47	85.60	26.21	91.09	26.82
9	14.40	57.10	100.00	30.66	100	0.00
Total	100.00	30.66				

Table A.21. Air velocity experiments data for Khutala No. 2 seam coal from second stage Triboelectrostatic test at **1.3 m/sec,** 0 KV charging voltage & 12.5 KV separating voltage

Product collected	Fractional Yield (Wt) %	Ash content	Cumulative Weight %	Cumulative Ash content (%)	Combustible Recovery	Ash rejection %
1	9.30	9.76	9.30	9.76	12.14	97.06
2	9.47	15.53	18.76	12.67	23.71	92.30
3	9.16	16.25	27.92	13.84	34.81	87.49
4	21.53	24.10	49.45	18.31	58.46	70.70
5	4.22	27.34	53.67	19.02	62.90	66.96
6	5.75	31.02	59.42	20.18	68.63	61.19
7	10.24	36.07	69.66	22.52	78.11	49.24
8	18.07	43.91	87.73	26.92	92.78	23.55
9	12.27	59.32	100.00	30.90	100	0.00
Total	100.00	30.90				

Table A.22. Air velocity experiments data for Khutala No. 2 seam coal from second stage Triboelectrostatic test at **1.9 m/sec,** 0 KV charging voltage & 12.5 KV separating voltage

Product collected	Fractional Yield (Wt) %	Ash content	Cumulative Weight %	Cumulative Ash content (%)	Combustible Recovery	Ash rejection %
1	7.30	8.90	7.30	8.90	9.56	97.86
2	9.00	14.39	16.31	11.93	20.63	93.60
3	8.32	15.44	24.62	13.12	30.74	89.37
4	26.18	24.27	50.81	18.86	59.22	68.46
5	3.04	25.22	53.84	19.22	62.48	65.94
6	3.78	29.59	57.62	19.90	66.31	62.26
7	11.99	36.21	69.62	22.71	77.30	47.97
8	18.63	42.59	88.25	26.91	92.67	21.86
9	11.75	56.55	100.00	30.39	100	0.00
Total	100.00	30.39				

Table A.23. Air velocity experiments data for Khutala No. 2 seam coal from second stage Triboelectrostatic test at **2.5 m/sec,** 0 KV charging voltage & 12.5 KV separating voltage

Product collected	Fractional Yield (Wt) %	Ash content	Cumulative Weight %	Cumulative Ash content (%)	Combustible Recovery	Ash rejection %
1	6.54	9.17	6.54	9.17	8.62	98.07
2	9.64	15.10	16.18	12.70	20.49	93.38
3	8.77	16.91	24.95	14.18	31.07	88.61
4	31.43	26.63	56.39	21.12	64.52	61.66
5	2.93	26.67	59.31	21.39	67.63	59.15
6	3.64	31.46	62.95	21.98	71.25	55.47
7	11.59	38.53	74.54	24.55	81.58	41.09
8	17.00	45.88	91.54	28.51	94.93	15.98
9	8.46	58.70	100.00	31.06	100	0.00
Total	100.00	31.06				

Table A.24. Feed rate experiments data for Khutala No. 2 seam coal from second stage Tribo-electrostatic test at **17.32 g/min,** 0 KV charging voltage & 12.5 KV separating voltage

Product collected	Fractional Yield (Wt) %	Ash content	Cumulative Weight %	Cumulative Ash content (%)	Combustible Recovery	Ash rejection %
1	9.02	10.83	9.02	10.83	11.64	96.83
2	10.22	16.67	19.24	13.93	23.94	91.31
3	8.94	17.02	28.18	14.91	34.67	86.37
4	28.50	27.20	56.69	21.09	64.67	61.23
5	3.49	29.12	60.17	21.56	68.25	57.94
6	4.31	32.20	64.48	22.27	72.48	53.44
7	10.00	39.46	74.49	24.58	81.23	40.64
8	15.91	44.70	90.39	28.12	93.95	17.58
9	9.61	56.44	100.00	30.84	100	0.00
Total	100.00	30.84				

Table A.25. Feed rate experiments data for Khutala No. 2 seam coal from second stage Tribo-electrostatic test at **26.45 g/min,** 0 KV charging voltage & 12.5 KV separating voltage

Product collected	Fractional Yield (Wt) %	Ash content	Cumulative Weight %	Cumulative Ash content (%)	Combustible Recovery	Ash rejection %
1	6.90	10.21	6.90	10.21	8.89	97.68
2	10.52	17.04	17.42	14.34	21.42	91.77
3	8.05	17.39	25.47	15.30	30.96	87.15
4	32.74	27.07	58.21	21.92	65.24	57.93
5	3.25	28.89	61.46	22.29	68.56	54.83
6	2.16	31.67	63.62	22.61	70.67	52.58
7	13.04	39.06	76.66	25.41	82.08	35.78
8	14.43	42.38	91.09	28.09	94.01	15.62
9	8.91	53.17	100.00	30.33	100	0.00
Total	100.00	30.33				

Table A.26. Feed rate experiments data for Khutala No. 2 seam coal from second stage Tribo-electrostatic test at **33.40 g/min,** 0 KV charging voltage & 12.5 KV separating voltage

Product collected	Fractional Yield (Wt) %	Ash content	Cumulative Weight %	Cumulative Ash content (%)	Combustible Recovery	Ash rejection %
1	7.26	9.89	7.26	9.89	9.47	97.68
2	9.29	15.82	16.55	13.22	20.79	92.92
3	8.77	16.27	25.33	14.28	31.42	88.30
4	28.15	25.45	53.47	20.16	61.79	65.12
5	3.23	27.11	56.70	20.55	65.20	62.29
6	4.15	28.99	60.85	21.13	69.46	58.40
7	11.25	38.87	72.10	23.90	79.41	44.26
8	17.83	43.76	89.93	27.83	93.93	19.01
9	10.07	58.34	100.00	30.91	100	0.00
Total	100.00	30.91				

Table A.27. Rotary charger speed experiments data for Khutala No. 2 seam coal from second stage Tribo-electrostatic test at **2500 rpm,** 0 KV charging voltage & 12.5 KV separating voltage

Product collected	Fractional Yield (Wt) %	Ash content	Cumulative Weight %	Cumulative Ash content (%)	Combustible Recovery	Ash rejection %
1	7.30	8.90	7.30	8.90	9.56	97.86
2	9.00	14.39	16.31	11.93	20.63	93.60
3	8.32	15.44	24.62	13.12	30.74	89.37
4	26.18	24.27	50.81	18.86	59.22	68.46
5	3.04	25.22	53.84	19.22	62.48	65.94
6	3.78	29.59	57.62	19.90	66.31	62.26
7	11.99	36.21	69.62	22.71	77.30	47.97
8	18.63	42.59	88.25	26.91	92.67	21.86
9	11.75	56.55	100.00	30.39	100	0.00
Total	100.00	30.39				

Table A.28. Rotary charger speed experiments data for Khutala No. 2 seam from second stage Tribo-electrostatic test at **3000 rpm,** 0 KV charging voltage & 12.5 KV separating voltage

Product collected	Fractional Yield (Wt) %	Ash content	Cumulative Weight %	Cumulative Ash content (%)	Combustible Recovery	Ash rejection %
1	8.89	9.36	8.89	9.36	11.65	97.30
2	9.93	15.14	18.82	12.41	23.84	92.43
3	8.58	15.97	27.39	13.52	34.26	88.00
4	23.14	24.60	50.53	18.60	59.50	69.56
5	4.06	26.44	54.60	19.18	63.82	66.07
6	4.57	30.77	59.16	20.07	68.40	61.52
7	11.77	37.02	70.93	22.89	79.12	47.40
8	17.14	44.49	88.07	27.09	92.88	22.70
9	11.93	58.74	100.00	30.87	100	0.00
Total	100.00	30.87				

Table A.29. Rotary charger speed experiments data for Khutala No. 2 seam from second stage Tribo-electrostatic test at **4000 rpm,** 0 KV charging voltage & 12.5 KV separating voltage

Product collected	Fractional Yield (Wt) %	Ash content	Cumulative Weight %	Cumulative Ash content (%)	Combustible Recovery	Ash rejection %
1	10.73	9.93	10.73	9.93	13.97	96.54
2	9.85	15.23	20.58	12.47	26.04	91.68
3	9.57	16.42	30.15	13.72	37.61	86.58
4	19.33	24.97	49.48	18.12	58.57	70.92
5	4.94	25.70	54.42	18.80	63.87	66.80
6	5.87	29.44	60.28	19.84	69.86	61.20
7	9.73	37.54	70.01	22.30	78.64	49.35
8	16.95	44.08	86.97	26.54	92.35	25.10
9	13.03	59.37	100.00	30.82	100	0.00
Total	100.00	30.82				

Table A.30. Co-flow experiments data for Khutala No. 2 seam coal from second stage Tribo- electrostatic test at **2.5 m/sec,** 0 KV charging voltage & 12.5 KV separating voltage

Product collected	Fractional Yield (Wt) %	Ash content	Cumulative Weight %	Cumulative Ash content (%)	Combustible Recovery	Ash rejection %
1	7.37	8.75	7.37	8.75	9.67	97.89
2	8.57	14.21	15.93	11.69	20.25	93.90
3	8.51	15.51	24.44	13.02	30.60	89.57
4	26.35	25.72	50.79	19.61	58.76	67.36
5	3.00	24.55	53.79	19.88	62.02	64.95
6	4.18	28.41	57.97	20.50	66.33	61.06
7	12.77	35.14	70.74	23.14	78.24	46.35
8	17.79	42.48	88.53	27.03	92.97	21.58
9	11.47	57.41	100.00	30.51	100	0.00
Total	100.00	30.51				

Table A.31. Co-flow experiments data for Khutala No. 2 seam coal from second stage Tribo- electrostatic test at **3.0 m/sec,** 0 KV charging voltage & 12.5 KV separating voltage

Product collected	Fractional Yield (Wt) %	Ash content	Cumulative Weight %	Cumulative Ash content (%)	Combustible Recovery	Ash rejection %
1	7.30	8.95	7.30	8.95	9.56	97.85
2	9.00	14.39	16.31	11.95	20.63	93.59
3	8.32	15.44	24.62	13.13	30.73	89.36
4	26.18	24.27	50.81	18.87	59.22	68.45
5	3.04	25.22	53.84	19.23	62.48	65.94
6	3.78	29.59	57.62	19.91	66.31	62.26
7	11.99	36.21	69.62	22.72	77.30	47.97
8	18.63	42.59	88.25	26.91	92.67	21.86
9	11.75	56.55	100.00	30.40	100	0.00
Total	100.00	30.40				

Table A.32. Co-flow experiments data for Khutala No. 2 seam coal from second stage Tribo- electrostatic test at **3.5 m/sec,** 0 KV charging voltage & 12.5 KV separating voltage

Product collected	Fractional Yield (Wt) %	Ash content	Cumulative Weight %	Cumulative Ash content (%)	Combustible Recovery	Ash rejection %
1	6.58	9.41	6.58	9.41	8.62	98.00
2	7.95	14.63	14.53	12.27	18.45	94.24
3	8.60	16.48	23.13	13.83	28.85	89.65
4	27.06	23.72	50.19	19.16	58.73	68.89
5	2.75	25.43	52.94	19.49	61.70	66.63
6	3.76	26.22	56.70	19.94	65.72	63.44
7	12.23	36.41	68.93	22.86	76.97	49.04
8	19.52	43.24	88.45	27.36	93.01	21.74
9	11.55	58.19	100.00	30.92	100	0.00
Total	100.00	30.92				

Table A.33. Separating voltage experiments data for Khutala No. 2 seam coal from Single and Middling re-cycled electrostatic test at **10 KV,** 0 KV charging voltage & 1.9 m/sec velocity

Product collected	Fractional Yield (Wt) %	Ash content	Cumulative Weight %	Cumulative Ash content (%)	Combustible Recovery	Ash rejection %
1	19.19	15.07	19.19	15.07	23.73	90.77
2	8.36	17.75	27.55	15.88	33.74	86.03
3	30.24	27.02	57.79	21.71	65.87	59.94
4	11.85	39.08	69.64	24.67	76.39	45.15
5	30.36	46.58	100.00	31.32	100.00	0.00
Total	100.00	31.32				

Splitter distance: 0.6 cm from the negative electrode

Table A.34. Separating voltage experiments data for Khutala No. 2 seam coal from Single and Middling re-cycled electrostatic test at **12.5 KV,** 0 KV charging voltage & 1.9 m/sec velocity

Product collected	Fractional Yield (Wt) %	Ash content	Cumulative Weight %	Cumulative Ash content (%)	Combustible Recovery	Ash rejection %
1	21.66	14.74	21.66	14.74	26.85	89.78
2	9.29	17.38	30.94	15.53	38.00	84.61
3	26.83	26.78	57.77	20.76	66.57	61.60
4	10.77	40.17	68.54	23.81	75.94	47.74
5	31.46	47.40	100.00	31.23	100.00	0.00
Total	100.00	31.23				

Splitter distance: 0.6 cm from the negative electrode

Table A.35. Separating voltage experiments data for Khutala No. 2 seam coal from Single and Middling re-cycled electrostatic test at **10 KV,** 0 KV charging voltage & 1.9 m/sec velocity

Product collected	Fractional Yield (Wt) %	Ash content	Cumulative Weight %	Cumulative Ash content (%)	Combustible Recovery	Ash rejection %
1	24.27	15.22	24.27	15.22	29.83	88.09
2	9.97	19.02	34.24	16.33	41.54	81.98
3	24.85	29.19	59.10	21.74	67.05	58.59
4	10.72	40.04	69.82	24.55	76.37	44.75
5	30.18	45.99	100.00	31.02	100.00	0.00
Total	100.00	31.02				

Splitter distance: 1.0 cm from the negative electrode

Table A.36. Separating voltage experiments data for Khutala No. 2 seam coal from Single and Middling re-cycled electrostatic test at **12.5 KV,** 0 KV charging voltage & 1.9 m/sec velocity

Product collected	Fractional Yield (Wt) %	Ash content	Cumulative Weight %	Cumulative Ash content (%)	Combustible Recovery	Ash rejection %
1	25.36	14.77	25.36	14.77	31.36	87.94
2	10.27	17.94	35.63	15.68	43.58	82.02
3	21.54	28.52	57.17	20.52	65.92	62.24
4	10.60	39.67	67.77	23.52	75.20	48.71
5	32.23	46.96	100.00	31.07	100.00	0.00
Total	100.00	31.07				

Splitter distance: 1.0 cm from the negative electrode

Table A.37. Separating voltage experiments data for Koornfontein coal from second stage Tribo-electrostatic test at 1**0 KV**, 0 KV charging voltage & 2.5 m/sec air velocity

Product collected	Fractional Yield (Wt) %	Ash content	Cumulative Weight %	Cumulative Ash content (%)	Combustible Recovery	Ash rejection %
1	1.97	10.32	1.97	10.32	2.24	99.04
2	4.40	15.05	6.37	13.59	6.99	95.91
3	4.07	16.29	10.44	14.64	11.31	92.78
4	28.71	19.27	39.15	18.04	40.71	66.66
5	1.85	19.59	41.00	18.11	42.60	64.95
6	2.50	21.92	43.49	18.32	45.07	62.36
7	17.17	22.37	60.67	19.47	61.98	44.22
8	21.71	23.13	82.38	20.43	83.16	20.51
9	17.62	24.65	100.00	21.18	100	0.00
Total	100.00	21.18				

Table A.38. Separating voltage experiments data for Koornfontein coal from second stage Tribo-electrostatic test at 1**2.5 KV**, 0 KV charging voltage & 2.5 m/sec air velocity

Product collected	Fractional Yield (Wt) %	Ash content	Cumulative Weight %	Cumulative Ash content (%)	Combustible Recovery	Ash rejection %
1	3.60	10.50	3.60	10.50	4.10	98.24
2	6.55	14.24	10.15	12.91	11.25	93.89
3	5.11	16.12	15.25	13.99	16.70	90.04
4	28.35	19.44	43.61	17.53	45.77	64.33
5	2.80	20.80	46.41	17.73	48.59	61.61
6	2.67	22.53	49.08	17.99	51.23	58.79
7	15.40	23.54	64.49	19.32	66.22	41.87
8	19.57	24.56	84.05	20.54	85.01	19.45
9	15.95	26.14	100.00	21.43	100	0.00
Total	100.00	21.43				

Table A.39. Separating voltage experiments data for Koornfontein coal from second stage Tribo-electrostatic test at 15 **KV**, 0 KV charging voltage & 2.5 m/sec air velocity

Product collected	Fractional Yield (Wt) %	Ash content	Cumulative Weight %	Cumulative Ash content (%)	Combustible Recovery	Ash rejection %
1	4.38	10.88	4.38	10.88	4.96	97.76
2	6.39	13.47	10.77	12.42	11.98	93.71
3	7.33	15.85	18.10	13.81	19.81	88.25
4	1.58	18.20	19.68	14.16	21.46	86.90
5	27.45	19.20	47.13	17.10	49.63	62.12
6	2.89	22.80	50.02	17.43	52.46	59.01
7	15.46	23.78	65.48	18.93	67.43	41.73
8	19.15	24.96	84.63	20.29	85.68	19.25
9	15.37	26.64	100.00	21.27	100	0.00
Total	100.00	21.27				

Table A.40. Separating voltage experiments data for Koornfontein coal from second stage Tribo-electrostatic test at 20 **KV**, 0 KV charging voltage & 2.5 m/sec air velocity

Product collected	Fractional Yield (Wt) %	Ash content	Cumulative Weight %	Cumulative Ash content (%)	Combustible Recovery	Ash rejection %
1	5.65	11.46	5.65	11.46	6.34	96.93
2	8.54	14.44	14.19	13.25	15.60	91.10
3	7.14	15.40	21.32	13.97	23.26	85.90
4	25.13	19.05	46.46	16.72	49.05	63.24
5	3.32	20.98	49.78	17.00	52.38	59.94
6	3.25	22.57	53.03	17.35	55.58	56.46
7	12.47	23.92	65.50	18.60	67.60	42.35
8	18.30	24.90	83.79	19.97	85.02	20.79
9	16.21	27.10	100.00	21.13	100	0.00
Total	100.00	21.13				

Table A.41. Charging voltage experiments data for Koornfontein coal from second stage Tribo-electrostatic test at **0 KV**, 12.5 KV separating voltage & 2.5 m/sec air velocity

Product collected	Fractional Yield (Wt) %	Ash content	Cumulative Weight %	Cumulative Ash content (%)	Combustible Recovery	Ash rejection %
1	3.06	9.98	3.06	9.98	3.50	98.56
2	5.34	13.34	8.40	12.12	9.37	95.20
3	4.40	14.78	12.80	13.03	14.12	92.13
4	25.74	18.63	38.54	16.77	40.70	69.51
5	2.33	20.38	40.87	16.98	43.06	67.26
6	2.44	21.92	43.31	17.26	45.48	64.74
7	15.92	22.60	59.23	18.69	61.11	47.77
8	21.44	24.13	80.67	20.14	81.75	23.36
9	19.33	25.61	100.00	21.20	100	0.00
Total	100.00	21.20				

Table A.42. Charging voltage experiments data for Koornfontein coal from second stage Tribo-electrostatic test at **1.5 KV**, 12.5 KV separating voltage & 2.5 m/sec air velocity

Product collected	Fractional Yield (Wt) %	Ash content	Cumulative Weight %	Cumulative Ash content (%)	Combustible Recovery	Ash rejection %
1	7.30	11.66	7.30	11.66	8.20	96.00
2	10.64	15.57	17.95	13.98	19.61	88.21
3	9.05	17.49	27.00	15.16	29.10	80.77
4	2.71	21.11	29.70	15.70	31.81	78.09
5	33.52	21.14	63.23	18.58	65.39	44.78
6	3.00	24.18	66.23	18.84	68.28	41.37
7	11.34	24.67	77.56	19.69	79.13	28.23
8	15.07	26.13	92.64	20.74	93.28	9.72
9	7.36	28.10	100.00	21.28	100	0.00
Total	100.00	21.28				

Table A.43. Charging voltage experiments data for Koornfontein coal from second stage Tribo-electrostatic test at **2.5 KV**, 12.5 KV separating voltage & 2.5 m/sec air velocity

Product collected	Fractional Yield (Wt) %	Ash content	Cumulative Weight %	Cumulative Ash content (%)	Combustible Recovery	Ash rejection %
1	9.18	12.28	9.18	12.28	10.23	94.72
2	12.38	16.89	21.56	14.93	23.31	84.91
3	10.94	18.28	32.49	16.06	34.67	75.54
4	32.46	21.88	64.95	18.97	66.91	42.25
5	3.28	22.26	68.23	19.12	70.14	38.83
6	3.08	24.32	71.31	19.35	73.11	35.32
7	10.38	25.16	81.68	20.09	82.98	23.09
8	13.07	26.63	94.75	20.99	95.17	6.77
9	5.25	27.53	100.00	21.33	100	0.00
Total	100.00	21.33				

Table A.44. Charging voltage experiments data for Koornfontein coal from second stage Tribo-electrostatic test at **5.0 KV**, 12.5 KV separating voltage & 2.5 m/sec air velocity

Product collected	Fractional Yield (Wt) %	Ash content	Cumulative Weight %	Cumulative Ash content (%)	Combustible Recovery	Ash rejection %
1	14.81	13.93	14.81	13.93	16.18	90.26
2	14.08	18.06	28.89	15.94	30.82	78.26
3	15.76	19.68	44.65	17.26	46.88	63.63
4	2.86	22.37	47.51	17.57	49.69	60.61
5	29.42	23.13	76.93	19.70	78.39	28.49
6	3.55	24.47	80.48	19.91	81.79	24.39
7	6.80	25.19	87.28	20.32	88.24	16.31
8	9.24	26.92	96.52	20.95	96.81	4.57
9	3.48	27.81	100.00	21.19	100	0.00
Total	100.00	21.19				

Table A.45. Rotary charger speed experiments data for Koornfontein coal from second stage Tribo-electrostatic test at **2500 rpm**, 12.5 KV separating voltage & 2.5 m/sec air velocity

Product collected	Fractional Yield (Wt) %	Ash content	Cumulative Weight %	Cumulative Ash content (%)	Combustible Recovery	Ash rejection %
1	2.44	10.62	2.44	10.62	2.80	98.83
2	4.75	13.45	7.19	12.49	8.08	95.95
3	4.53	15.94	11.72	13.82	12.97	92.68
4	24.15	18.86	35.87	17.22	38.13	72.11
5	2.39	21.51	38.25	17.48	40.54	69.79
6	2.67	22.63	40.92	17.82	43.19	67.06
7	16.19	23.06	57.11	19.30	59.18	50.20
8	22.10	24.57	79.21	20.77	80.59	25.67
9	20.79	27.33	100.00	22.14	100	0.00
Total	100.00	22.14				

Table A.46. Rotary charger speed experiments data for Koornfontein coal from second stage Tribo-electrostatic test at **3000 rpm**, 12.5 KV separating voltage & 2.5 m/sec air velocity

Product collected	Fractional Yield (Wt) %	Ash content	Cumulative Weight %	Cumulative Ash content (%)	Combustible Recovery	Ash rejection %
1	3.16	11.11	3.16	11.11	3.59	98.38
2	5.84	14.22	9.00	13.13	9.98	94.54
3	4.97	15.02	13.97	13.80	15.37	91.09
4	23.14	18.43	37.11	16.69	39.46	71.39
5	2.99	21.90	40.10	17.08	42.44	68.37
6	2.83	21.90	42.93	17.39	45.26	65.51
7	15.08	22.93	58.00	18.83	60.09	49.54
8	19.08	24.67	77.08	20.28	78.43	27.79
9	22.92	26.25	100.00	21.65	100	0.00
Total	100.00	21.65				

Table A.47. Rotary charger speed experiments data for Koornfontein coal from second stage Tribo-electrostatic test at **4000 rpm**, 12.5 KV separating voltage & 2.5 m/sec air velocity

Product collected	Fractional Yield (Wt) %	Ash content	Cumulative Weight %	Cumulative Ash content (%)	Combustible Recovery	Ash rejection %
1	4.85	11.81	4.85	11.81	5.51	97.43
2	7.03	15.23	11.89	13.83	13.19	92.63
3	6.11	15.37	18.00	14.36	19.84	88.43
4	21.30	19.19	39.30	16.98	42.01	70.12
5	3.92	22.24	43.22	17.45	45.93	66.22
6	4.16	23.30	47.38	17.97	50.04	61.87
7	14.66	23.98	62.04	19.39	64.38	46.13
8	18.90	25.79	80.94	20.88	82.44	24.30
9	19.06	28.46	100.00	22.33	100	0.00
Total	100.00	22.33				

Table A.48. Rotary charger speed experiments data for Koornfontein coal from second stage Tribo-electrostatic test at **5000 rpm**, 12.5 KV separating voltage & 2.5 m/sec air velocity

Product collected	Fractional Yield (Wt) %	Ash content	Cumulative Weight %	Cumulative Ash content (%)	Combustible Recovery	Ash rejection %
1	5.12	10.90	5.12	10.90	5.84	97.45
2	7.35	14.21	12.47	12.85	13.91	92.68
3	6.39	15.08	18.86	13.61	20.86	88.28
4	20.94	19.15	39.80	16.52	42.53	69.96
5	4.10	21.98	43.90	17.03	46.63	65.84
6	3.75	22.09	47.65	17.43	50.37	62.06
7	15.01	24.60	62.66	19.15	64.86	45.19
8	18.47	25.37	81.13	20.56	82.51	23.79
9	18.87	27.60	100.00	21.89	100	0.00
Total	100.00	21.89				

Table A.49. Feed rate experiments data for Koornfontein coal from second stage Tribo-electrostatic test at **12 g/min**, 12.5 KV separating voltage & 2.5 m/sec air velocity

Product collected	Fractional Yield (Wt) %	Ash content	Cumulative Weight %	Cumulative Ash content (%)	Combustible Recovery	Ash rejection %
1	2.44	10.62	2.44	10.62	2.79	98.82
2	4.75	13.45	7.19	12.49	8.05	95.89
3	4.53	15.94	11.72	13.82	12.92	92.59
4	24.15	18.86	35.87	17.22	38.00	71.76
5	2.39	21.51	38.25	17.48	40.40	69.41
6	2.67	22.63	40.92	17.82	43.04	66.65
7	16.19	23.06	57.11	19.30	58.97	49.57
8	22.10	24.57	79.21	20.77	80.31	24.73
9	20.79	26.00	100.00	21.86	100	0.00
Total	100.00	21.86				

Table A.50. Feed rate experiments data for Koornfontein coal from second stage Tribo-electrostatic test at **17 g/min**, 12.5 KV separating voltage & 2.5 m/sec air velocity

Product collected	Fractional Yield (Wt) %	Ash content	Cumulative Weight %	Cumulative Ash content (%)	Combustible Recovery	Ash rejection %
1	4.19	11.11	4.19	11.11	4.70	97.78
2	7.95	13.94	12.14	12.96	13.36	92.47
3	5.57	15.44	17.71	13.74	19.32	88.36
4	27.43	18.91	45.14	16.88	47.43	63.55
5	3.90	20.71	49.04	17.19	51.35	59.69
6	2.83	22.04	51.87	17.45	54.14	56.70
7	15.14	23.18	67.01	18.75	68.84	39.92
8	18.52	24.58	85.53	20.01	86.50	18.15
9	14.47	26.22	100.00	20.91	100	0.00
Total	100.00	20.91				

Table A.51. Feed rate experiments data for Koornfontein coal from second stage Tribo-electrostatic test at **23 g/min**, 12.5 KV separating voltage & 2.5 m/sec air velocity

Product collected	Fractional Yield (Wt) %	Ash content	Cumulative Weight %	Cumulative Ash content (%)	Combustible Recovery	Ash rejection %
1	3.84	11.28	3.84	11.28	4.31	97.94
2	7.26	14.39	11.10	13.31	12.18	92.96
3	5.71	15.06	16.81	13.91	18.32	88.87
4	27.83	18.81	44.64	16.96	46.92	63.93
5	3.50	20.67	48.14	17.23	50.43	60.49
6	2.78	22.01	50.92	17.49	53.18	57.57
7	16.16	23.26	67.08	18.88	68.87	39.67
8	18.27	24.53	85.35	20.09	86.33	18.33
9	14.65	26.27	100.00	21.00	100	0.00
Total	100.00	21.00				

Table A.52. Air velocity experiments data for Koornfontein coal from second stage Tribo-electrostatic test at **2.5 m/sec**, 12.5 KV separating voltage & 0 KV charging voltage

Product collected	Fractional Yield (Wt) %	Ash content	Cumulative Weight %	Cumulative Ash content (%)	Combustible Recovery	Ash rejection %
1	2.44	10.62	2.44	10.62	2.80	98.83
2	4.75	13.45	7.19	12.49	8.08	95.95
3	4.53	15.94	11.72	13.82	12.97	92.68
4	24.15	18.86	35.87	17.22	38.13	72.11
5	2.39	21.51	38.25	17.48	40.54	69.79
6	2.67	22.63	40.92	17.82	43.19	67.06
7	16.19	23.06	57.11	19.30	59.18	50.20
8	22.10	24.57	79.21	20.77	80.59	25.67
9	20.79	27.33	100.00	22.14	100	0.00
Total	100.00	22.14				

Table A.53. Air velocity experiments data for Koornfontein coal from second stage Tribo-electrostatic test at **3.1 m/sec**, 12.5 KV separating voltage & 0 KV charging voltage

Product collected	Fractional Yield (Wt) %	Ash content	Cumulative Weight %	Cumulative Ash content (%)	Combustible Recovery	Ash rejection %
1	3.13	13.05	3.13	13.05	3.45	98.08
2	6.91	16.63	10.03	15.51	10.76	92.66
3	6.91	17.92	16.94	16.49	17.95	86.82
4	36.48	19.80	53.42	18.75	55.08	52.76
5	3.10	21.37	56.52	18.90	58.18	49.63
6	2.99	23.05	59.51	19.10	61.10	46.39
7	14.60	23.21	74.11	19.91	75.33	30.40
8	16.64	24.12	90.75	20.68	91.35	11.48
9	9.25	26.31	100.00	21.21	100	0.00
Total	100.00	21.21				

Table A.54. Air velocity experiments data for Koornfontein coal from second stage Tribo-electrostatic test at **3.7 m/sec**, 12.5 KV separating voltage & 0 KV charging voltage

Product collected	Fractional Yield (Wt) %	Ash content	Cumulative Weight %	Cumulative Ash content (%)	Combustible Recovery	Ash rejection %
1	3.81	14.51	3.81	14.51	4.12	97.37
2	7.67	17.98	11.48	16.83	12.09	90.81
3	7.54	18.66	19.02	17.56	19.86	84.12
4	39.75	19.85	58.78	19.11	60.21	46.59
5	3.18	22.32	61.96	19.27	63.34	43.21
6	3.01	22.90	64.97	19.44	66.28	39.94
7	13.89	23.41	78.86	20.14	79.75	24.48
8	14.85	23.84	93.71	20.73	94.07	7.64
9	6.29	25.55	100.00	21.03	100	0.00
Total	100.00	21.03				

Table A.55. Charging voltage experiments data for Koornfontein coal from Single and Middling re-cycled electrostatic test at **0 KV,** 12.5 KV separating voltage & 2.5 m/sec velocity

Product collected	Fractional Yield (Wt) %	Ash content	Cumulative Weight %	Cumulative Ash content (%)	Combustible Recovery	Ash rejection %
1	10.18	13.12	10.18	13.12	11.30	93.86
2	4.12	15.59	14.30	13.83	15.74	90.90
3	29.29	19.41	43.59	17.58	45.90	64.73
4	15.58	23.17	59.17	19.05	61.19	48.12
5	40.83	25.61	100.00	21.73	100.00	0.00
Total	100.00	21.73				

Splitter distance: 0.6 cm from the negative electrode

Table A.56. Charging voltage experiments data for Koornfontein coal from Single and Middling re-cycled electrostatic test at **1.5 KV,** 12.5 KV separating voltage & 2.5 m/sec velocity

Product collected	Fractional Yield (Wt) %	Ash content	Cumulative Weight %	Cumulative Ash content (%)	Combustible Recovery	Ash rejection %
1	17.25	14.04	17.25	14.04	18.95	88.86
2	7.32	17.99	24.57	15.22	26.62	82.80
3	38.01	21.34	62.58	18.94	64.83	45.51
4	11.20	24.86	73.78	19.83	75.58	32.71
5	26.22	27.12	100.00	21.75	100.00	0.00
Total	100.00	21.75				

Splitter distance: 0.6 cm from the negative electrode

Table A.57. Charging voltage experiments data for Koornfontein coal from Single and Middling re-cycled electrostatic test at **0 KV,** 12.5 KV separating voltage & 2.5 m/sec velocity

Product collected	Fractional Yield (Wt) %	Ash content	Cumulative Weight %	Cumulative Ash content (%)	Combustible Recovery	Ash rejection %
1	19.02	14.24	19.02	14.24	20.80	87.45
2	6.26	16.58	25.28	14.82	27.46	82.64
3	21.78	19.78	47.06	17.12	49.74	62.68
4	13.47	23.59	60.53	18.56	62.86	47.96
5	39.47	26.22	100.00	21.58	100.00	0.00
Total	100.00	21.58				

Splitter distance: 1.0 cm from the negative electrode

Table A.58. Charging voltage experiments data for Koornfontein coal from Single and Middling re-cycled electrostatic test at **1.5 KV,** 12.5 KV separating voltage & 2.5 m/sec velocity

Product collected	Fractional Yield (Wt) %	Ash content	Cumulative Weight %	Cumulative Ash content (%)	Combustible Recovery	Ash rejection %
1	28.24	15.42	28.24	15.42	30.41	79.71
2	10.33	18.66	38.57	16.29	41.12	70.73
3	24.07	21.84	62.65	18.42	65.07	46.24
4	9.80	25.34	72.45	19.36	74.39	34.67
5	27.55	27.01	100.00	21.47	100.00	0.00
Total	100.00	21.47				

Splitter distance: 1.0 cm from the negative electrode

Table A.59. Separating voltage experiments data for Liketh Townlands coal from second stage Tribo-electrostatic test at **10 KV**, 0 KV charging voltage & 2.5 m/sec air velocity

Product collected	Fractional Yield (Wt) %	Ash content	Cumulative Weight %	Cumulative Ash content (%)	Combustible Recovery	Ash rejection %
1	3.91	13.18	3.91	13.18	4.87	98.30
2	7.30	18.44	11.21	16.60	13.41	93.85
3	6.89	19.41	18.10	17.67	21.37	89.44
4	38.11	26.49	56.21	23.65	61.56	56.11
5	2.17	27.74	58.38	23.80	63.81	54.12
6	2.50	31.09	60.88	24.10	66.28	51.55
7	14.39	36.32	75.27	26.44	79.43	34.30
8	16.62	39.03	91.89	28.72	93.96	12.88
9	8.11	48.10	100.00	30.29	100	0.00
Total	100.00	30.29				

Table A.60. Separating voltage experiments data for Liketh Townlands coal from second stage Tribo-electrostatic test at **12.5 KV**, 0 KV charging voltage & 2.5 m/sec air velocity

Product collected	Fractional Yield (Wt) %	Ash content	Cumulative Weight %	Cumulative Ash content (%)	Combustible Recovery	Ash rejection %
1	5.27	12.55	5.27	12.55	6.72	97.89
2	7.79	17.29	13.05	15.38	16.11	93.61
3	7.23	18.72	20.28	16.57	24.67	89.30
4	32.67	25.65	52.95	22.17	60.08	62.63
5	2.64	30.49	55.59	22.57	62.76	60.06
6	3.06	32.87	58.65	23.10	65.75	56.86
7	13.21	37.20	71.86	25.70	77.85	41.21
8	17.15	42.17	89.02	28.87	92.31	18.18
9	10.98	52.00	100.00	31.41	100	0.00
Total	100.00	31.41				

Table A.61. Separating voltage experiments data for Liketh Townlands coal from second stage Tribo-electrostatic test at **15 KV**, 0 KV charging voltage & 2.5 m/sec air velocity

Product collected	Fractional Yield (Wt) %	Ash content	Cumulative Weight %	Cumulative Ash content (%)	Combustible Recovery	Ash rejection %
1	5.86	13.46	5.86	13.46	7.21	97.34
2	9.36	17.21	15.22	15.77	18.23	91.92
3	8.26	18.35	23.48	16.67	27.82	86.82
4	33.29	25.82	56.76	22.04	62.94	57.87
5	2.91	27.08	59.67	22.28	65.95	55.22
6	2.87	31.07	62.54	22.69	68.77	52.22
7	13.75	36.49	76.29	25.17	81.19	35.32
8	15.33	40.51	91.61	27.74	94.16	14.41
9	8.39	51.01	100.00	29.69	100	0.00
Total	100.00	29.69				

Table A.62. Separating voltage experiments data for Liketh Townlands coal from second stage Tribo-electrostatic test at **20 KV**, 0 KV charging voltage & 2.5 m/sec air velocity

Product collected	Fractional Yield (Wt) %	Ash content	Cumulative Weight %	Cumulative Ash content (%)	Combustible Recovery	Ash rejection %
1	7.03	13.80	7.03	13.80	8.63	96.74
2	10.47	17.85	17.50	16.22	20.88	90.47
3	9.07	18.18	26.56	16.89	31.44	84.93
4	29.79	25.07	56.35	21.21	63.22	59.86
5	3.05	27.77	59.40	21.55	66.36	57.02
6	3.22	31.09	62.62	22.04	69.52	53.66
7	12.58	36.81	75.20	24.51	80.84	38.10
8	14.68	41.03	89.88	27.21	93.17	17.89
9	10.12	52.61	100.00	29.78	100	0.00
Total	100.00	29.78				

Table A.63. Separating voltage experiments data for Liketh Townlands coal from second stage Tribo-electrostatic test at **22.5 KV**, 0 KV charging voltage & 2.5 m/sec air velocity

Product collected	Fractional Yield (Wt) %	Ash content	Cumulative Weight %	Cumulative Ash content (%)	Combustible Recovery	Ash rejection %
1	6.80	13.96	6.80	13.96	8.36	96.83
2	9.48	17.30	16.28	15.91	19.55	91.36
3	8.92	17.73	25.21	16.55	30.04	86.08
4	27.35	24.20	52.56	20.53	59.65	64.00
5	3.07	27.72	55.63	20.93	62.81	61.16
6	4.09	29.85	59.72	21.54	66.91	57.08
7	11.84	36.11	71.56	23.95	77.72	42.82
8	16.30	39.77	87.86	26.88	91.73	21.20
9	12.14	52.32	100.00	29.97	100	0.00
Total	100.00	29.97				

Table A.64. Charging voltage experiments data for Liketh Townlands coal from second stage Tribo-electrostatic test at **0 KV,** 12.5 KV separating voltage & 2.5 m/sec air velocity

Product collected	Fractional Yield (Wt) %	Ash content	Cumulative Weight %	Cumulative Ash content (%)	Combustible Recovery	Ash rejection %
1	5.27	12.55	5.27	12.55	6.72	97.89
2	7.79	17.29	13.05	15.38	16.11	93.61
3	7.23	18.72	20.28	16.57	24.67	89.30
4	32.67	25.65	52.95	22.17	60.08	62.63
5	2.64	30.49	55.59	22.57	62.76	60.06
6	3.06	32.87	58.65	23.10	65.75	56.86
7	13.21	37.20	71.86	25.70	77.85	41.21
8	17.15	42.17	89.02	28.87	92.31	18.18
9	10.98	52.00	100.00	31.41	100	0.00
Total	100.00	31.41				

Table A.65. Charging voltage experiments data for Liketh Townlands coal from second stage Tribo-electrostatic test at **1.5 KV,** 12.5 KV separating voltage & 2.5 m/sec air velocity

Product collected	Fractional Yield (Wt) %	Ash content	Cumulative Weight %	Cumulative Ash content (%)	Combustible Recovery	Ash rejection %
1	10.26	13.65	10.26	13.65	12.60	95.29
2	13.60	19.16	23.86	16.79	28.25	86.52
3	11.29	21.27	35.15	18.23	40.90	78.44
4	36.37	29.74	71.52	24.08	77.25	42.04
5	3.33	30.72	74.85	24.38	80.54	38.60
6	3.26	38.17	78.11	24.95	83.40	34.41
7	8.51	40.95	86.62	26.52	90.55	22.69
8	10.64	48.34	97.25	28.91	98.37	5.39
9	2.75	58.29	100.00	29.72	100	0.00
Total	100.00	29.72				

Table A.66. Charging voltage experiments data for Liketh Townlands coal from second stage Tribo-electrostatic test at **1.5 KV,** 12.5 KV separating voltage & 2.5 m/sec air velocity

Product collected	Fractional Yield (Wt) %	Ash content	Cumulative Weight %	Cumulative Ash content (%)	Combustible Recovery	Ash rejection %
1	10.26	13.65	10.26	13.65	12.60	95.29
2	13.60	19.16	23.86	16.79	28.25	86.52
3	11.29	21.27	35.15	18.23	40.90	78.44
4	36.37	29.74	71.52	24.08	77.25	42.04
5	3.33	30.72	74.85	24.38	80.54	38.60
6	3.26	38.17	78.11	24.95	83.40	34.41
7	8.51	40.95	86.62	26.52	90.55	22.69
8	10.64	48.34	97.25	28.91	98.37	5.39
9	2.75	58.29	100.00	29.72	100	0.00
Total	100.00	29.72				

Table A.67. Charging voltage experiments data for Liketh Townlands coal from second stage Tribo-electrostatic test at **2.5 KV,** 12.5 KV separating voltage & 2.5 m/sec air velocity

Product collected	Fractional Yield (Wt) %	Ash content	Cumulative Weight %	Cumulative Ash content (%)	Combustible Recovery	Ash rejection %
1	11.20	14.22	11.20	14.22	13.75	94.72
2	14.38	19.32	25.57	17.09	30.35	85.50
3	12.07	22.92	37.64	18.96	43.66	76.33
4	1.69	26.64	39.33	19.29	45.44	74.83
5	35.52	31.25	74.85	24.96	80.39	38.01
6	2.93	38.01	77.78	25.46	82.99	34.31
7	5.96	40.42	83.73	26.52	88.07	26.32
8	11.20	47.39	94.93	28.98	96.50	8.72
9	5.07	51.79	100.00	30.14	100	0.00
Total	100.00	30.14				

Table A.68. Charging voltage experiments data for Liketh Townlands coal from second stage Tribo-electrostatic test at **5.0 KV,** 12.5 KV separating voltage & 2.5 m/sec air velocity

Product collected	Fractional Yield (Wt) %	Ash content	Cumulative Weight %	Cumulative Ash content (%)	Combustible Recovery	Ash rejection %
1	16.47	15.36	16.47	15.36	19.82	91.47
2	16.30	20.91	32.78	18.12	38.16	79.98
3	15.44	24.93	48.22	20.30	54.64	67.01
4	3.04	30.02	51.26	20.88	57.67	63.94
5	29.10	34.28	80.36	25.73	84.86	30.32
6	2.85	39.51	83.21	26.20	87.31	26.52
7	8.52	48.22	91.72	28.25	93.58	12.68
8	5.84	42.18	97.56	29.08	98.38	4.39
9	2.44	53.34	100.00	29.67	100	0.00
Total	100.00	29.67				

Table A.69. Air velocity experiments data for Liketh Townlands coal from second stage Tribo-electrostatic test at **2.5 m/sec,** 12.5 KV separating voltage & 0 KV charging voltage

Product collected	Fractional Yield (Wt) %	Ash content	Cumulative Weight %	Cumulative Ash content (%)	Combustible Recovery	Ash rejection %
1	5.26	12.22	5.26	12.22	6.65	97.90
2	8.15	16.48	13.41	14.81	16.46	93.50
3	6.65	18.10	20.06	15.90	24.30	89.57
4	29.85	24.22	49.91	20.88	56.88	65.92
5	2.72	25.84	52.63	21.13	59.79	63.62
6	3.11	30.56	55.74	21.66	62.90	60.51
7	13.67	35.31	69.41	24.35	75.64	44.72
8	18.10	40.10	87.52	27.61	91.26	20.98
9	12.48	51.38	100.00	30.57	100	0.00
Total	100.00	30.57				

Table A.70. Air velocity experiments data for Liketh Townlands coal from second stage Tribo-electrostatic test at **3.1 m/sec,** 12.5 KV separating voltage & 0 KV charging voltage

Product collected	Fractional Yield (Wt) %	Ash content	Cumulative Weight %	Cumulative Ash content (%)	Combustible Recovery	Ash rejection %
1	4.02	14.03	4.02	14.03	4.98	98.16
2	7.50	18.88	11.52	17.19	13.75	93.53
3	6.89	19.93	18.42	18.21	21.70	89.04
4	35.85	26.47	54.26	23.67	59.69	58.04
5	2.76	28.98	57.02	23.92	62.51	55.42
6	2.94	32.34	59.96	24.34	65.37	52.32
7	14.80	35.77	74.76	26.60	79.07	35.02
8	16.60	39.54	91.36	28.95	93.53	13.57
9	8.64	48.07	100.00	30.60	100	0.00
Total	100.00	30.60				

Table A.71. Air velocity experiments data for Liketh Townlands coal from second stage Tribo-electrostatic test at **3.7 m/sec,** 12.5 KV separating voltage & 0 KV charging voltage

Product collected	Fractional Yield (Wt) %	Ash content	Cumulative Weight %	Cumulative Ash content (%)	Combustible Recovery	Ash rejection %
1	3.86	15.55	3.86	15.55	4.69	98.03
2	7.13	20.32	10.99	18.64	12.85	93.27
3	7.30	21.27	18.29	19.69	21.12	88.17
4	38.82	27.50	57.11	25.00	61.60	53.12
5	2.68	29.76	59.79	25.21	64.30	50.50
6	2.88	31.91	62.67	25.52	67.12	47.49
7	15.46	36.27	78.13	27.65	81.28	29.08
8	15.24	38.25	93.37	29.38	94.81	9.94
9	6.63	45.63	100.00	30.46	100	0.00
Total	100.00	30.46				

Table A.72. Air velocity experiments data for Liketh Townlands coal from second stage Tribo-electrostatic test at **4.2 m/sec,** 12.5 KV separating voltage & 0 KV charging voltage

Product collected	Fractional Yield (Wt) %	Ash content	Cumulative Weight %	Cumulative Ash content (%)	Combustible Recovery	Ash rejection %
1	3.48	17.61	3.48	17.61	4.17	98.03
2	6.49	22.27	9.98	20.64	11.50	93.39
3	8.62	23.24	18.60	21.85	21.12	86.96
4	35.92	28.47	54.52	26.21	58.44	54.14
5	3.46	30.94	57.98	26.49	61.91	50.70
6	4.60	32.46	62.58	26.93	66.42	45.91
7	12.32	35.61	74.89	28.36	77.94	31.84
8	17.84	37.59	92.73	30.13	94.11	10.32
9	7.27	44.22	100.00	31.16	100	0.00
Total	100.00	31.16				

Table A.73. Rotary charger speed experiments data for Liketh Townlands coal from second stage electrostatic test at **2500 rpm,** 12.5 KV separating voltage & 2.5 m/sec air velocity

Product collected	Fractional Yield (Wt) %	Ash content	Cumulative Weight %	Cumulative Ash content (%)	Combustible Recovery	Ash rejection %
1	5.27	12.55	5.27	12.55	6.72	97.89
2	7.79	17.29	13.05	15.38	16.11	93.61
3	7.23	18.72	20.28	16.57	24.67	89.30
4	32.67	25.65	52.95	22.17	60.08	62.63
5	2.64	30.49	55.59	22.57	62.76	60.06
6	3.06	32.87	58.65	23.10	65.75	56.86
7	13.21	37.20	71.86	25.70	77.85	41.21
8	17.15	42.17	89.02	28.87	92.31	18.18
9	10.98	52.00	100.00	31.41	100	0.00
Total	100.00	31.41				

Table A.74. Rotary charger speed experiments data for Liketh Townlands coal from second stage electrostatic test at **3000 rpm,** 12.5 KV separating voltage & 2.5 m/sec air velocity

Product collected	Fractional Yield (Wt) %	Ash content	Cumulative Weight %	Cumulative Ash content (%)	Combustible Recovery	Ash rejection %
1	5.87	12.83	5.87	12.83	7.35	97.51
2	8.19	16.62	14.07	15.04	17.15	93.03
3	7.35	18.64	21.41	16.27	25.73	88.51
4	29.50	24.35	50.92	20.95	57.77	64.82
5	3.08	27.88	53.99	21.35	60.95	62.00
6	3.04	32.74	57.03	21.96	63.89	58.71
7	13.72	34.74	70.75	24.43	76.74	43.00
8	17.21	41.02	87.96	27.68	91.31	19.72
9	12.04	49.69	100.00	30.33	100	0.00
Total	100.00	30.33				

Table A.75. Rotary charger speed experiments data for Liketh Townlands coal from second stage electrostatic test at **4000 rpm,** 12.5 KV separating voltage & 2.5 m/sec air velocity

Product collected	Fractional Yield (Wt) %	Ash content	Cumulative Weight %	Cumulative Ash content (%)	Combustible Recovery	Ash rejection %
1	7.34	13.06	7.34	13.06	9.29	96.93
2	9.04	17.54	16.39	15.53	20.13	91.86
3	7.37	18.36	23.75	16.41	28.88	87.53
4	25.42	24.14	49.17	20.41	56.92	67.89
5	3.95	32.69	53.12	21.32	60.79	63.76
6	12.46	34.88	65.59	23.90	72.60	49.84
7	4.02	36.95	69.61	24.65	76.29	45.09
8	16.62	41.62	86.23	27.92	90.40	22.95
9	13.77	52.07	100.00	31.25	100	0.00
Total	100.00	31.25				

Table A.76. Feed rate experiments data for Liketh Townlands coal from second stage electrostatic test at **12 g/min,** 12.5 KV separating voltage & 0 KV charging voltage

Product collected	Fractional Yield (Wt) %	Ash content	Cumulative Weight %	Cumulative Ash content (%)	Combustible Recovery	Ash rejection %
1	4.87	12.72	4.87	12.72	6.08	97.94
2	9.24	17.52	14.11	15.86	16.98	92.56
3	7.10	18.52	21.22	16.75	25.26	88.18
4	36.97	25.17	58.19	22.10	64.83	57.24
5	2.11	30.10	60.30	22.38	66.94	55.13
6	1.91	32.41	62.21	22.69	68.78	53.07
7	16.42	35.80	78.63	25.43	83.86	33.52
8	12.67	42.73	91.30	27.83	94.24	15.52
9	8.70	53.67	100.00	30.08	100	0.00
Total	100.00	30.08				

Table A.77. Feed rate experiments data for Liketh Townlands coal from second stage electrostatic test at **18 g/min,** 12.5 KV separating voltage & 0 KV charging voltage

Product collected	Fractional Yield (Wt) %	Ash content	Cumulative Weight %	Cumulative Ash content (%)	Combustible Recovery	Ash rejection %
1	4.72	11.95	4.72	11.95	6.11	98.24
2	8.15	15.89	12.87	14.44	16.19	94.19
3	6.56	17.02	19.42	15.31	24.19	90.70
4	2.70	26.26	22.12	16.65	27.11	88.49
5	31.34	29.37	53.46	24.11	59.66	59.72
6	2.81	29.90	56.27	24.40	62.56	57.09
7	13.88	34.46	70.16	26.39	75.94	42.14
8	18.14	40.68	88.30	29.32	91.76	19.06
9	11.70	52.13	100.00	31.99	100	0.00
Total	100.00	31.99				

Table A.78. Feed rate experiments data for Liketh Townlands coal from second stage electrostatic test at **25 g/min,** 12.5 KV separating voltage & 0 KV charging voltage

Product collected	Fractional Yield (Wt) %	Ash content	Cumulative Weight %	Cumulative Ash content (%)	Combustible Recovery	Ash rejection %
1	4.71	11.70	4.71	11.70	6.16	98.30
2	7.98	15.34	12.70	13.99	16.17	94.53
3	6.40	17.07	19.10	15.02	24.03	91.16
4	2.43	24.49	21.53	16.09	26.74	89.33
5	2.90	29.09	24.42	17.63	29.78	86.73
6	30.81	32.24	55.24	25.78	60.69	56.12
7	13.94	35.24	69.18	27.69	74.05	40.98
8	19.94	40.91	89.12	30.65	91.50	15.84
9	10.88	47.23	100.00	32.45	100	0.00
Total	100.00	32.45				

Table A.79. Charging voltage experiments data for Liketh Townlands coal from Single and Middling re-cycled electrostatic test at **0 KV,** 12.5KV separating voltage & 2.5 m/sec velocity

Product collected	Fractional Yield (Wt) %	Ash content	Cumulative Weight %	Cumulative Ash content (%)	Combustible Recovery	Ash rejection %
1	14.49	14.64	14.49	14.64	17.88	93.11
2	5.71	16.31	20.20	15.11	24.78	90.09
3	28.67	23.14	48.88	19.82	56.63	68.54
4	14.09	33.00	62.96	22.77	70.27	53.45
5	37.04	44.44	100.00	30.80	100.00	0.00
Total	100.00	30.80				

Splitter distance: 0.6 cm from the negative electrode

Table A.80. Charging voltage experiments data for Liketh Townlands coal from Single and Middling re-cycled electrostatic test at **1.5 KV,** 12.5KV separating voltage & 2.5 m/sec velocity

Product collected	Fractional Yield (Wt) %	Ash content	Cumulative Weight %	Cumulative Ash content (%)	Combustible Recovery	Ash rejection %
1	22.05	15.72	22.05	15.72	26.68	88.57
2	9.41	18.94	31.46	16.68	37.63	82.70
3	30.16	26.57	61.63	21.52	69.43	56.28
4	9.79	37.43	71.42	23.70	78.22	44.20
5	28.58	46.92	100.00	30.34	100.00	0.00
Total	100.00	30.34				

Splitter distance: 0.6 cm from the negative electrode

Table A.81. Charging voltage experiments data for Liketh Townlands coal from Single and Middling re-cycled electrostatic test at **0 KV,** 12.5KV separating voltage & 2.5 m/sec velocity

Product collected	Fractional Yield (Wt) %	Ash content	Cumulative Weight %	Cumulative Ash content (%)	Combustible Recovery	Ash rejection %
1	18.69	15.02	18.69	15.02	22.92	90.86
2	7.74	18.06	26.43	15.91	32.07	86.30
3	29.33	25.41	55.76	20.91	63.64	62.02
4	11.35	36.23	67.11	23.50	74.08	48.63
5	32.89	45.39	100.00	30.70	100.00	0.00
Total	100.00	30.70				

Splitter distance: 1.0 cm from the negative electrode

Table A.82. Charging voltage experiments data for Liketh Townlands coal from Single and Middling re-cycled electrostatic test at **1.5 KV,** 12.5KV separating voltage & 2.5 m/sec velocity

Product collected	Fractional Yield (Wt) %	Ash content	Cumulative Weight %	Cumulative Ash content (%)	Combustible Recovery	Ash rejection %
1	30.11	17.00	30.11	17.00	35.88	83.13
2	12.11	21.97	42.22	18.43	49.45	74.36
3	27.50	30.63	69.72	23.24	76.84	46.61
4	8.17	41.71	77.89	25.18	83.68	35.38
5	22.11	48.57	100.00	30.35	100.00	0.00
Total	100.00	30.35				

Splitter distance: 1.0 cm from the negative electrode

Table A.83. Separating voltage experiments data for Majuba coal from second stage Trib-oelectrostatic test at **10 KV, 0** KV charging voltage & 1.9 m/sec air velocity

Product collected	Fractional Yield (Wt) %	Ash content	Cumulative Weight %	Cumulative Ash content (%)	Combustible Recovery	Ash rejection %
1	2.85	10.82	2.85	10.82	3.61	98.96
2	5.84	16.41	8.69	14.58	10.55	95.72
3	3.86	17.28	12.55	15.41	15.09	93.47
4	28.67	23.31	41.22	20.90	46.32	70.90
5	2.28	27.64	43.50	21.26	48.66	68.78
6	1.71	29.73	45.21	21.58	50.37	67.06
7	19.24	31.36	64.46	24.50	69.14	46.68
8	17.47	34.96	81.93	26.73	85.29	26.05
9	18.07	42.69	100.00	29.61	100	0.00
Total	100.00	29.61				

Table A.84. Separating voltage experiments data for Majuba coal from second stage Tribo-electrostatic test at **12.5 KV, 0** KV charging voltage & 1.9 m/sec air velocity

Product collected	Fractional Yield (Wt) %	Ash content	Cumulative Weight %	Cumulative Ash content (%)	Combustible Recovery	Ash rejection %
1	5.00	11.53	5.00	11.53	6.28	98.05
2	7.68	16.23	12.67	14.38	15.41	93.84
3	5.71	17.00	18.38	15.19	22.14	90.56
4	28.29	23.94	46.67	20.49	52.70	67.68
5	2.86	27.88	49.53	20.92	55.63	64.98
6	2.16	29.01	51.69	21.26	57.80	62.87
7	14.41	32.33	66.09	23.67	71.65	47.13
8	17.85	36.64	83.94	26.43	87.71	25.03
9	16.06	46.11	100.00	29.59	100	0.00
Total	100.00	29.59				

Table A.85. Separating voltage experiments data for Majuba coal from second stage Tribo-electrostatic test at **15 KV, 0** KV charging voltage & 1.9 m/sec air velocity

Product collected	Fractional Yield (Wt) %	Ash content	Cumulative Weight %	Cumulative Ash content (%)	Combustible Recovery	Ash rejection %
1	6.31	11.81	6.31	11.81	7.92	97.50
2	9.08	16.61	15.39	14.64	18.71	92.43
3	6.12	17.62	21.51	15.49	25.89	88.80
4	25.81	24.08	47.32	20.17	53.78	67.92
5	2.94	26.34	50.26	20.53	56.86	65.32
6	2.66	29.72	52.92	21.00	59.53	62.66
7	14.93	32.86	67.85	23.61	73.79	46.18
8	16.38	38.15	84.23	26.44	88.22	25.18
9	15.77	47.52	100.00	29.76	100	0.00
Total	100.00	29.76				

Table A.86. Separating voltage experiments data for Majuba coal from second stage Tribo- electrostatic test at **20 KV, 0** KV charging voltage & 1.9 m/sec air velocity

Product collected	Fractional Yield (Wt) %	Ash content	Cumulative Weight %	Cumulative Ash content (%)	Combustible Recovery	Ash rejection %
1	7.41	12.74	7.41	12.74	9.19	96.81
2	9.61	17.05	17.01	15.17	20.51	91.28
3	6.81	17.36	23.83	15.80	28.51	87.29
4	22.24	23.68	46.06	19.60	52.62	69.52
5	4.02	25.78	50.08	20.10	56.86	66.02
6	3.17	28.71	53.25	20.61	60.07	62.95
7	14.30	32.62	67.55	23.15	73.76	47.20
8	15.38	37.31	82.93	25.78	87.46	27.83
9	17.07	48.30	100.00	29.62	100	0.00
Total	100.00	29.62				

Table A.87. Charging voltage experiments data for Majuba coal from second stage Tribo-electrostatic test at **0 KV,** 12.5 KV separating voltage & 1.9 m/sec air velocity

Product collected	Fractional Yield (Wt) %	Ash content	Cumulative Weight %	Cumulative Ash content (%)	Combustible Recovery	Ash rejection %
1	3.88	11.40	3.88	11.40	4.92	98.53
2	4.50	17.06	8.37	14.44	10.25	95.99
3	7.33	18.66	15.71	16.41	18.79	91.44
4	25.99	23.39	41.70	20.76	47.28	71.26
5	2.92	28.41	44.62	21.26	50.27	68.51
6	2.45	28.48	47.07	21.64	52.78	66.19
7	15.85	31.76	62.92	24.19	68.26	49.48
8	19.17	35.81	82.08	26.90	85.87	26.69
9	17.92	44.88	100.00	30.12	100	0.00
Total	100.00	30.12				

Table A.88. Charging voltage experiments data for Majuba coal from second stage Tribo-electrostatic test at **1.5 KV,** 12.5 KV separating voltage & 1.9 m/sec air velocity

Product collected	Fractional Yield (Wt) %	Ash content	Cumulative Weight %	Cumulative Ash content (%)	Combustible Recovery	Ash rejection %
1	4.37	11.29	4.37	11.29	5.53	98.35
2	7.70	16.38	12.07	14.54	14.70	94.13
3	4.67	16.84	16.73	15.18	20.24	91.50
4	27.39	23.74	44.13	20.49	50.02	69.72
5	2.84	26.41	46.96	20.85	53.00	67.21
6	1.97	28.78	48.93	21.17	55.00	65.32
7	16.06	32.31	64.99	23.92	70.50	47.94
8	18.56	36.45	83.55	26.71	87.32	25.29
9	16.45	45.92	100.00	29.87	100	0.00
Total	100.00	29.87				

Table A.89. Charging voltage experiments data for Majuba coal from second stage Tribo-electrostatic test at **2.5 KV,** 12.5 KV separating voltage & 1.9 m/sec air velocity

Product collected	Fractional Yield (Wt) %	Ash content	Cumulative Weight %	Cumulative Ash content (%)	Combustible Recovery	Ash rejection %
1	4.84	11.67	4.84	11.67	6.09	98.11
2	7.40	16.60	12.24	14.65	14.88	93.98
3	5.08	17.13	17.32	15.38	20.89	91.06
4	27.85	23.67	45.17	20.49	51.17	68.96
5	2.64	26.89	47.81	20.84	53.92	66.58
6	2.11	29.39	49.92	21.20	56.04	64.50
7	17.36	32.43	67.27	24.10	72.75	45.62
8	16.92	36.97	84.19	26.69	87.94	24.64
9	15.81	46.47	100.00	29.81	100	0.00
Total	100.00	29.81				

Table A.90. Charging voltage experiments data for Majuba coal from second stage Tribo-electrostatic test at **5.0 KV,** 12.5 KV separating voltage & 1.9 m/sec air velocity

Product collected	Fractional Yield (Wt) %	Ash content	Cumulative Weight %	Cumulative Ash content (%)	Combustible Recovery	Ash rejection %
1	4.91	11.55	4.91	11.55	6.18	98.10
2	7.65	16.37	12.56	14.49	15.29	93.89
3	5.42	17.31	17.98	15.34	21.67	90.74
4	28.58	23.88	46.56	20.58	52.65	67.81
5	2.81	27.12	49.37	20.95	55.56	65.25
6	2.10	29.08	51.47	21.28	57.68	63.20
7	16.59	33.12	68.06	24.17	73.48	44.73
8	16.77	36.94	84.83	26.70	88.54	23.92
9	15.17	46.94	100.00	29.77	100	0.00
Total	100.00	29.77				

Table A.91. Air velocity experiments data for Majuba coal from second stage Tribo-electrostatic test at **1.3 m/sec,** 12.5 KV separating voltage & 1.5 KV charging voltage

Product collected	Fractional Yield (Wt) %	Ash content	Cumulative Weight %	Cumulative Ash content (%)	Combustible Recovery	Ash rejection %
1	4.11	10.76	4.11	10.76	5.21	98.50
2	6.32	15.60	10.44	13.69	12.79	95.17
3	4.78	16.19	15.21	14.48	18.47	92.55
4	19.94	21.64	35.16	18.54	40.66	77.95
5	3.75	24.32	38.90	19.10	44.68	74.87
6	2.77	26.47	41.67	19.59	47.57	72.39
7	17.10	29.64	58.77	22.51	64.66	55.24
8	18.36	33.78	77.13	25.19	81.91	34.26
9	22.87	44.29	100.00	29.56	100	0.00
Total	100.00	29.56				

Table A.92. Air velocity experiments data for Majuba coal from second stage Tribo-electrostatic test at **1.9 m/sec,** 12.5 KV separating voltage & 1.5 KV charging voltage

Product collected	Fractional Yield (Wt) %	Ash content	Cumulative Weight %	Cumulative Ash content (%)	Combustible Recovery	Ash rejection %
1	4.05	10.92	4.05	10.92	5.15	98.52
2	6.57	15.42	10.62	13.70	13.07	95.13
3	4.61	16.62	15.23	14.59	18.55	92.56
4	25.06	23.22	40.29	19.96	45.99	73.08
5	2.36	24.58	42.65	20.21	48.52	71.14
6	2.46	27.43	45.11	20.61	51.07	68.88
7	16.31	30.99	61.43	23.36	67.12	51.95
8	19.62	35.35	81.05	26.27	85.21	28.72
9	18.95	45.27	100.00	29.87	100	0.00
Total	100.00	29.87				

Table A.93. Air velocity experiments data for Majuba coal from second stage Tribo-electrostatic test at **2.5 m/sec,** 12.5 KV separating voltage & 1.5 KV charging voltage

Product collected	Fractional Yield (Wt) %	Ash content	Cumulative Weight %	Cumulative Ash content (%)	Combustible Recovery	Ash rejection %
1	3.25	12.21	3.25	12.21	4.04	98.65
2	6.61	17.18	9.86	15.54	11.79	94.78
3	5.28	17.64	15.13	16.27	17.94	91.62
4	29.07	24.77	44.20	21.86	48.90	67.10
5	2.97	27.38	47.17	22.21	51.95	64.33
6	2.38	28.42	49.55	22.51	54.36	62.03
7	18.22	32.32	67.76	25.14	71.82	41.99
8	17.67	34.85	85.44	27.15	88.12	21.02
9	14.56	42.39	100.00	29.37	100	0.00
Total	100.00	29.37				

Table A.94. Feed rate experiments data for Majuba coal from second stage Tribo-electrostatic test at **12 g/min,** 12.5 KV separating voltage & 1.5 KV charging voltage

Product collected	Fractional Yield (Wt) %	Ash content	Cumulative Weight %	Cumulative Ash content (%)	Combustible Recovery	Ash rejection %
1	4.62	11.09	4.62	11.09	5.83	98.26
2	7.62	16.36	12.24	14.37	14.86	94.03
3	5.08	16.55	17.32	15.01	20.87	91.18
4	27.60	23.61	44.92	20.29	50.76	69.07
5	2.32	25.68	47.23	20.56	53.21	67.06
6	2.25	28.63	49.48	20.92	55.48	64.87
7	16.29	31.92	65.77	23.65	71.21	47.23
8	18.02	36.42	83.79	26.39	87.45	24.97
9	16.21	45.40	100.00	29.48	100	0.00
Total	100.00	29.48				

Table A.95. Feed rate experiments data for Majuba coal from second stage Tribo-electrostatic test at **17 g/min,** 12.5 KV separating voltage & 1.5 KV charging voltage

Product collected	Fractional Yield (Wt) %	Ash content	Cumulative Weight %	Cumulative Ash content (%)	Combustible Recovery	Ash rejection %
1	4.41	10.91	4.41	10.91	5.58	98.38
2	7.69	16.04	12.10	14.17	14.75	94.21
3	4.25	16.29	16.35	14.72	19.81	91.88
4	27.00	23.17	43.34	19.98	49.28	70.76
5	3.26	24.23	46.61	20.28	52.79	68.10
6	2.09	27.41	48.70	20.59	54.95	66.16
7	17.20	31.84	65.90	23.52	71.61	47.67
8	17.23	36.27	83.12	26.17	87.21	26.58
9	16.88	46.67	100.00	29.63	100	0.00
Total	100.00	29.63				

Table A.96. Feed rate experiments data for Majuba coal from second stage Tribo-electrostatic test at **24 g/min,** 12.5 KV separating voltage & 1.5 KV charging voltage

Product collected	Fractional Yield (Wt) %	Ash content	Cumulative Weight %	Cumulative Ash content (%)	Combustible Recovery	Ash rejection %
1	4.00	10.47	4.00	10.47	5.07	98.58
2	7.25	15.24	11.24	13.54	13.77	94.82
3	3.90	15.32	15.15	14.00	18.45	92.78
4	25.09	21.92	40.24	18.94	46.19	74.08
5	3.30	24.91	43.53	19.39	49.70	71.28
6	2.17	25.35	45.70	19.67	51.99	69.41
7	16.79	30.53	62.49	22.59	68.51	51.97
8	18.91	35.12	81.40	25.50	85.89	29.38
9	18.60	46.43	100.00	29.39	100	0.00
Total	100.00	29.39				

Table A.97. Rotary charger speed experiments data for Majuba coal from second stage Tribo-electrostatic test at **2500 rpm,** 12.5 KV separating voltage & 1.5 KV charging voltage

Product collected	Fractional Yield (Wt) %	Ash content	Cumulative Weight %	Cumulative Ash content (%)	Combustible Recovery	Ash rejection %
1	4.62	11.09	4.62	11.09	5.83	98.26
2	7.62	16.36	12.24	14.37	14.86	94.03
3	5.08	16.55	17.32	15.01	20.87	91.18
4	27.60	23.61	44.92	20.29	50.76	69.07
5	2.32	25.68	47.23	20.56	53.21	67.06
6	2.25	28.63	49.48	20.92	55.48	64.87
7	16.29	31.92	65.77	23.65	71.21	47.23
8	18.02	36.42	83.79	26.39	87.45	24.97
9	16.21	45.40	100.00	29.48	100	0.00
Total	100.00	29.48				

Table A.98. Rotary charger speed experiments data for Majuba coal from second stage Tribo-electrostatic test at **3000 rpm,** 12.5 KV separating voltage & 1.5 KV charging voltage

Product collected	Fractional Yield (Wt) %	Ash content	Cumulative Weight %	Cumulative Ash content (%)	Combustible Recovery	Ash rejection %
1	6.35	11.96	6.35	11.96	7.93	97.43
2	9.09	16.56	15.44	14.67	18.70	92.34
3	6.28	17.12	21.71	15.38	26.09	88.71
4	27.09	24.76	48.80	20.59	55.03	66.02
5	3.18	26.40	51.98	20.94	58.35	63.18
6	2.44	29.70	54.42	21.33	60.78	60.73
7	15.40	33.68	69.82	24.06	75.29	43.19
8	15.12	37.72	84.95	26.49	88.66	23.90
9	15.05	46.93	100.00	29.57	100	0.00
Total	100.00	29.57				

Table A.99. Rotary charger speed experiments data for Majuba coal from second stage Tribo-electrostatic test at **4000 rpm,** 12.5 KV separating voltage & 1.5 KV charging voltage

Product collected	Fractional Yield (Wt) %	Ash content	Cumulative Weight %	Cumulative Ash content (%)	Combustible Recovery	Ash rejection %
1	8.83	12.27	8.83	12.27	11.00	96.34
2	7.30	17.47	16.14	14.62	19.56	92.02
3	9.73	17.71	25.86	15.78	30.93	86.20
4	22.81	24.95	48.67	20.08	55.24	66.96
5	3.84	27.57	52.51	20.63	59.19	63.38
6	3.32	29.68	55.83	21.17	62.50	60.04
7	14.23	33.51	70.06	23.67	75.94	43.92
8	15.15	38.78	85.21	26.36	89.11	24.06
9	14.79	48.12	100.00	29.58	100	0.00
Total	100.00	29.58				

Table A.100. Co-flow velocity experiments data for Majuba coal from second stage Tribo-electrostatic test at **2.5 m/sec,** 12.5 KV separating voltage & 1.9 m/sec inlet air velocity

Product collected	Fractional Yield (Wt) %	Ash content	Cumulative Weight %	Cumulative Ash content (%)	Combustible Recovery	Ash rejection %
1	5.00	11.23	5.00	11.23	6.24	98.06
2	8.33	16.49	13.33	14.52	16.03	93.30
3	5.95	18.22	19.28	15.66	22.87	89.55
4	3.15	24.02	22.43	16.83	26.24	86.93
5	28.68	25.64	51.11	21.78	56.23	61.48
6	2.94	28.25	54.06	22.13	59.20	58.61
7	15.46	31.87	69.52	24.29	74.02	41.56
8	17.34	35.66	86.85	26.56	89.71	20.16
9	13.15	44.32	100.00	28.90	100	0.00
Total	100.00	28.90				

Table A.101. Co-flow velocity experiments data for Majuba coal from second stage Tribo-electrostatic test at **3.0 m/sec,** 12.5 KV separating voltage & 1.9 m/sec inlet air velocity

Product collected	Fractional Yield (Wt) %	Ash content	Cumulative Weight %	Cumulative Ash content (%)	Combustible Recovery	Ash rejection %
1	4.49	11.26	4.49	11.26	5.67	98.30
2	8.18	16.67	12.67	14.75	15.37	93.72
3	5.25	18.15	17.91	15.75	21.48	90.51
4	2.98	24.69	20.90	17.03	24.68	88.04
5	29.89	25.44	50.79	21.98	56.40	62.47
6	2.32	29.43	53.11	22.30	58.73	60.18
7	16.67	32.94	69.78	24.84	74.64	41.72
8	16.96	37.77	86.73	27.37	89.66	20.18
9	13.27	45.25	100.00	29.74	100	0.00
Total	100.00	29.74				

Table A.102. Co-flow velocity experiments data for Majuba coal from second stage Tribo-electrostatic test at **3.5 m/sec,** 12.5 KV separating voltage & 1.9 m/sec inlet air velocity

Product collected	Fractional Yield (Wt) %	Ash content	Cumulative Weight %	Cumulative Ash content (%)	Combustible Recovery	Ash rejection %
1	3.42	11.72	3.42	11.72	4.36	98.69
2	6.76	16.64	10.18	14.99	12.50	95.03
3	5.00	17.11	15.19	15.69	18.48	92.25
4	2.57	24.90	17.76	17.02	21.27	90.17
5	31.11	25.99	48.87	22.73	54.51	63.85
6	2.08	28.43	50.95	22.96	56.66	61.92
7	17.40	33.14	68.35	25.55	73.45	43.16
8	17.56	38.42	85.91	28.18	89.06	21.20
9	14.09	46.21	100.00	30.72	100	0.00
Total	100.00	30.72				

Table A.103. Co-flow velocity experiments data for Majuba coal from second stage Tribo-electrostatic test at **3.5 m/sec,** 12.5 KV separating voltage & 1.9 m/sec inlet air velocity

Product collected	Fractional Yield (Wt) %	Ash content	Cumulative Weight %	Cumulative Ash content (%)	Combustible Recovery	Ash rejection %
1	3.42	11.72	3.42	11.72	4.36	98.69
2	6.76	16.64	10.18	14.99	12.50	95.03
3	5.00	17.11	15.19	15.69	18.48	92.25
4	2.57	24.90	17.76	17.02	21.27	90.17
5	31.11	25.99	48.87	22.73	54.51	63.85
6	2.08	28.43	50.95	22.96	56.66	61.92
7	17.40	33.14	68.35	25.55	73.45	43.16
8	17.56	38.42	85.91	28.18	89.06	21.20
9	14.09	46.21	100.00	30.72	100	0.00
Total	100.00	30.72				

Table A.104. Separating voltage experiments data for Majuba from Single and Middling re-cycled electrostatic test at **12.5 KV,** 1.5 KV charging voltage & 1.9 m/sec velocity

Product collected	Fractional Yield (Wt) %	Ash content	Cumulative Weight %	Cumulative Ash content (%)	Combustible Recovery	Ash rejection %
1	14.91	15.07	14.91	15.07	18.07	92.49
2	4.83	16.31	19.74	15.37	23.84	89.86
3	22.87	22.34	42.61	19.11	49.19	72.79
4	15.83	31.25	58.44	22.40	64.71	56.26
5	41.56	40.51	100.00	29.93	100.00	0.00
Total	100.00	29.93				

Splitter distance: 0.6 cm from the negative electrode

Table A.105. Separating voltage experiments data for Majuba from Single and Middling re-cycled electrostatic test at **15 KV,** 1.5 KV charging voltage & 1.9 m/sec velocity

Product collected	Fractional Yield (Wt) %	Ash content	Cumulative Weight %	Cumulative Ash content (%)	Combustible Recovery	Ash rejection %
1	16.82	15.27	16.82	15.27	20.29	91.36
2	5.39	16.11	22.21	15.47	26.73	88.45
3	21.07	22.00	43.29	18.65	50.13	72.86
4	14.95	31.07	58.24	21.84	64.80	57.25
5	41.76	40.78	100.00	29.75	100.00	0.00
Total	100.00	29.75				

Splitter distance: 0.6 cm from the negative electrode

Table A.106. Separating voltage experiments data for Majuba from Single and Middling re-cycled electrostatic test at **20 KV,** 1.5 KV charging voltage & 1.9 m/sec velocity

Product collected	Fractional Yield (Wt) %	Ash content	Cumulative Weight %	Cumulative Ash content (%)	Combustible Recovery	Ash rejection %
1	17.53	15.58	17.53	15.58	21.13	90.89
2	6.10	16.82	23.63	15.90	28.38	87.46
3	18.83	22.12	42.47	18.66	49.32	73.56
4	13.29	30.15	55.76	21.40	62.58	60.18
5	44.24	40.76	100.00	29.96	100.00	0.00
Total	100.00	29.96				

Splitter distance: 0.6 cm from the negative electrode

Table A.107. Separating voltage experiments data for Majuba from Single and Middling re-cycled electrostatic test at **25 KV,** 1.5 KV charging voltage & 1.9 m/sec velocity

Product collected	Fractional Yield (Wt) %	Ash content	Cumulative Weight %	Cumulative Ash content (%)	Combustible Recovery	Ash rejection %
1	25.36	14.77	25.36	14.77	31.36	87.94
2	10.27	17.94	35.63	15.68	43.58	82.02
3	21.54	28.52	57.17	20.52	65.92	62.24
4	10.60	39.67	67.77	23.52	75.20	48.71
5	32.23	46.96	100.00	31.07	100.00	0.00
Total	100.00	31.07				

Splitter distance: 0.6 cm from the negative electrode

Table A.108. Separating voltage experiments data for Majuba from Single and Middling re-cycled electrostatic test at **12.5 KV,** 1.5 KV charging voltage & 1.9 m/sec velocity

Product collected	Fractional Yield (Wt) %	Ash content	Cumulative Weight %	Cumulative Ash content (%)	Combustible Recovery	Ash rejection %
1	22.96	16.14	22.96	16.14	27.45	87.58
2	7.83	18.96	30.79	16.86	36.49	82.61
3	28.39	27.92	59.19	22.16	65.67	56.05
4	11.77	36.12	70.95	24.48	76.38	41.81
5	29.05	42.96	100.00	29.85	100.00	0.00
Total	100.00	29.85				

Splitter distance: 1.0 cm from the negative electrode

Table A.109. Separating voltage experiments data for Majuba from Single and Middling re-cycled electrostatic test at **15 KV,** 1.5 KV charging voltage & 1.9 m/sec velocity

Product collected	Fractional Yield (Wt) %	Ash content	Cumulative Weight %	Cumulative Ash content (%)	Combustible Recovery	Ash rejection %
1	24.21	16.09	24.21	16.09	28.99	86.98
2	7.68	18.84	31.89	16.75	37.89	82.15
3	26.10	27.52	57.99	21.60	64.88	58.14
4	11.32	36.00	69.31	23.95	75.22	44.53
5	30.69	43.42	100.00	29.93	100.00	0.00
Total	100.00	29.93				

Splitter distance: 1.0 cm from the negative electrode

Table A.110. Separating voltage experiments data for Majuba from Single and Middling re-cycled electrostatic test at **20 KV,** 1.5 KV charging voltage & 1.9 m/sec velocity

Product collected	Fractional Yield (Wt) %	Ash content	Cumulative Weight %	Cumulative Ash content (%)	Combustible Recovery	Ash rejection %
1	26.62	16.32	26.62	16.32	31.81	85.50
2	8.20	18.52	34.83	16.84	41.36	80.43
3	20.59	27.82	55.42	20.92	62.58	61.31
4	10.31	35.70	65.73	23.24	72.05	49.03
5	34.27	42.87	100.00	29.96	100.00	0.00
Total	100.00	29.96				

Splitter distance: 1.0 cm from the negative electrode

Table A.111. Splitter distance experiments data for Klipfontein coal from second stage Tribo-electrostatic test at **R=0.6, C=1.5, L= 2.7 cm,** 12.5 KV separating voltage & 1.9 m/sec air velocity

Product collected	Fractional Yield (Wt) %	Ash content	Cumulative Weight %	Cumulative Ash content (%)	Combustible Recovery	Ash rejection %
1	24.29	24.46	24.29	24.46	28.11	82.88
2	16.62	30.18	40.91	26.78	45.88	68.43
3	15.64	33.57	56.55	28.66	61.79	53.31
4	15.56	36.61	72.11	30.38	76.90	36.89
5	6.04	36.83	78.15	30.88	82.75	30.48
6	5.91	43.25	84.07	31.75	87.89	23.11
7	5.44	47.73	89.51	32.72	92.24	15.63
8	6.73	50.49	96.24	33.96	97.34	5.84
9	3.76	53.90	100.00	34.71	100	0.00
Total	100.00	34.71				

Table A.112. Splitter distance experiments data for Klipfontein coal from second stage Tribo-electrostatic test at **R=0.6, C=2.9, L= 1.3 cm,** 12.5 KV separating voltage & 1.9 m/sec air velocity

Product collected	Fractional Yield (Wt) %	Ash content	Cumulative Weight %	Cumulative Ash content (%)	Combustible Recovery	Ash rejection %
1	26.28	25.31	26.28	25.31	30.18	80.96
2	19.69	32.61	45.98	28.44	50.58	62.59
3	19.58	35.07	65.56	30.42	70.12	42.94
4	1.65	38.56	67.20	30.62	71.68	41.12
5	25.80	42.25	93.01	33.84	94.58	9.93
6	2.55	45.84	95.55	34.16	96.70	6.59
7	1.62	47.84	97.18	34.39	98.00	4.36
8	2.22	53.97	99.40	34.83	99.58	0.93
9	0.60	54.03	100.00	34.95	100	0.00
Total	100.00	34.95				

Table A.113. Splitter distance experiments data for Klipfontein coal from second stage Tribo-electrostatic test at **R=1.0, C=2.8, L= 1.0 cm,** 12.5 KV separating voltage & 1.9 m/sec air velocity

Product collected	Fractional Yield (Wt) %	Ash content	Cumulative Weight %	Cumulative Ash content (%)	Combustible Recovery	Ash rejection %
1	29.36	25.99	29.36	25.99	33.74	78.57
2	20.24	35.74	49.60	29.97	53.94	58.25
3	19.89	37.02	69.48	31.99	73.39	37.58
4	4.38	37.32	73.86	32.30	77.65	32.99
5	17.70	43.48	91.56	34.46	93.18	11.37
6	3.26	46.19	94.82	34.87	95.91	7.15
7	1.88	46.72	96.70	35.10	97.46	4.68
8	3.30	50.47	100.00	35.60	100	0.00
Total	100.00	35.60				

Table A.114. Splitter distance experiments data for Klipfontein coal from second stage Tribo-electrostatic test at **R=1.5, C=1.5, L= 1.8 cm,** 12.5 KV separating voltage & 1.9 m/sec air velocity

Product collected	Fractional Yield (Wt) %	Ash content	Cumulative Weight %	Cumulative Ash content (%)	Combustible Recovery	Ash rejection %
1	55.51	27.47	55.51	**27.47**	**61.24**	55.50
2	15.95	37.59	71.45	29.73	76.38	38.00
3	10.83	41.53	82.28	31.28	86.01	24.87
4	4.08	42.77	86.36	31.82	89.56	19.78
5	6.05	47.27	92.41	32.83	94.41	11.44
6	3.34	48.54	95.75	33.38	97.03	6.70
7	1.49	50.37	97.24	33.64	98.15	4.52
8	1.92	54.67	99.15	34.05	99.47	1.46
9	0.85	59.00	100.00	34.26	100	0.00
Total	100.00	34.26				

Table A.115. Charging voltage experiments data for Klipfontein coal from second stage Tribo-electrostatic test at **0 KV,** 22.5 KV separating voltage & 2.5 m/sec air velocity

Product collected	Fractional Yield (Wt) %	Ash content	Cumulative Weight %	Cumulative Ash content (%)	Combustible Recovery	Ash rejection %
1	6.42	15.77	6.42	15.77	8.58	97.27
2	6.90	19.60	13.31	17.75	17.38	93.61
3	10.08	23.76	23.39	20.34	29.58	87.14
4	21.54	27.57	44.94	23.81	54.36	71.09
5	3.76	37.18	48.70	24.84	58.11	67.31
6	12.56	38.96	61.26	27.73	70.28	54.10
7	16.80	46.82	78.06	31.84	84.46	32.84
8	4.78	47.21	82.83	32.73	88.46	26.75
9	17.17	57.67	100.00	37.01	100	0.00
Total	100.00	37.01				

Table A.116. Charging voltage experiments data for Klipfontein coal from second stage Tribo-electrostatic test at **1.5 KV,** 22.5 KV separating voltage & 2.5 m/sec air velocity

Product collected	Fractional Yield (Wt) %	Ash content	Cumulative Weight %	Cumulative Ash content (%)	Combustible Recovery	Ash rejection %
1	15.47	19.60	15.47	19.60	19.25	91.43
2	15.38	25.53	30.85	22.56	36.98	80.34
3	12.02	26.62	42.88	23.70	50.64	71.29
4	4.50	35.52	47.37	24.82	55.13	66.78
5	22.07	36.73	69.45	28.60	76.75	43.87
6	5.33	43.85	74.78	29.69	81.38	37.27
7	8.27	46.62	83.05	31.38	88.21	26.38
8	11.00	52.16	94.04	33.81	96.35	10.17
9	5.96	60.45	100.00	35.39	100	0.00
Total	100.00	35.39				

Table A.117. Charging voltage experiments data for Klipfontein coal from second stage Tribo-electrostatic test at **2.5 KV,** 22.5 KV separating voltage & 2.5 m/sec air velocity

Product collected	Fractional Yield (Wt) %	Ash content	Cumulative Weight %	Cumulative Ash content (%)	Combustible Recovery	Ash rejection %
1	16.20	20.91	16.20	20.91	20.03	90.60
2	14.07	27.11	30.27	23.79	36.06	80.01
3	13.60	27.94	43.87	25.08	51.38	69.47
4	4.95	37.47	48.82	26.33	56.21	64.32
5	20.75	37.63	69.57	29.70	76.45	42.64
6	5.73	42.11	75.30	30.65	81.63	35.95
7	7.95	48.09	83.25	32.31	88.08	25.33
8	10.78	51.86	94.03	34.55	96.20	9.82
9	5.97	59.24	100.00	36.03	100	0.00
Total	100.00	36.03				

Table A.118. Charging voltage experiments data for Klipfontein coal from second stage Tribo-electrostatic test at **3.5 KV,** 22.5 KV separating voltage & 2.5 m/sec air velocity

Product collected	Fractional Yield (Wt) %	Ash content	Cumulative Weight %	Cumulative Ash content (%)	Combustible Recovery	Ash rejection %
1	21.53	23.03	21.53	23.03	25.68	86.01
2	14.49	29.12	36.03	25.48	41.59	74.11
3	15.93	30.93	51.95	27.15	58.64	60.21
4	4.19	38.03	56.14	27.96	62.66	55.72
5	19.15	39.41	75.29	30.87	80.63	34.43
6	5.29	44.53	80.59	31.77	85.18	27.78
7	6.67	45.30	87.26	32.81	90.84	19.26
8	8.27	51.13	95.53	34.39	97.10	7.33
9	4.47	58.13	100.00	35.45	100	0.00
Total	100.00	35.45				

Table A.119. Charging voltage experiments data for Klipfontein coal from second stage Tribo-electrostatic test at **5.0 KV,** 22.5 KV separating voltage & 2.5 m/sec air velocity

Product collected	Fractional Yield (Wt) %	Ash content	Cumulative Weight %	Cumulative Ash content (%)	Combustible Recovery	Ash rejection %
1	22.19	25.72	22.19	25.72	25.59	83.97
2	17.73	30.90	39.91	28.02	44.61	68.58
3	15.84	32.17	55.75	29.20	61.29	54.26
4	16.89	39.23	72.64	31.53	77.22	35.65
5	4.75	39.52	77.39	32.02	81.68	30.37
6	4.95	43.26	82.34	32.70	86.04	24.36
7	6.05	45.35	88.39	33.56	91.18	16.65
8	7.46	49.13	95.85	34.77	97.07	6.35
9	4.15	54.49	100.00	35.59	100	0.00
Total	100.00	35.59				

Table A.120. Charging voltage experiments data for Klipfontein coal from second stage Tribo-electrostatic test at **6.0 KV,** 22.5 KV separating voltage & 2.5 m/sec air velocity

Product collected	Fractional Yield (Wt) %	Ash content	Cumulative Weight %	Cumulative Ash content (%)	Combustible Recovery	Ash rejection %
1	28.25	26.57	28.25	26.57	32.10	78.77
2	16.59	32.72	44.84	28.85	49.36	63.42
3	16.97	34.09	61.81	30.29	66.67	47.06
4	4.55	39.92	66.37	30.95	70.90	41.92
5	14.71	40.14	81.08	32.61	84.52	25.22
6	4.54	42.54	85.62	33.14	88.56	19.75
7	5.41	44.71	91.04	33.83	93.19	12.91
8	5.80	48.92	96.83	34.73	97.77	4.89
9	3.17	54.55	100.00	35.36	100	0.00
Total	100.00	35.36				

Table A.121. Charging voltage experiments data for Klipfontein coal from second stage Tribo-electrostatic test at **7.5 KV,** 22.5 KV separating voltage & 2.5 m/sec air velocity

Product collected	Fractional Yield (Wt) %	Ash content	Cumulative Weight %	Cumulative Ash content (%)	Combustible Recovery	Ash rejection %
1	28.93	27.04	28.93	27.04	32.66	77.89
2	16.08	33.63	45.01	29.39	49.18	62.60
3	14.67	34.03	59.68	30.53	64.16	48.50
4	16.70	39.08	76.37	32.40	79.90	30.06
5	4.69	40.24	81.07	32.86	84.24	24.72
6	4.53	42.71	85.60	33.38	88.26	19.25
7	5.28	44.34	90.88	34.01	92.80	12.64
8	5.72	47.08	96.60	34.79	97.49	5.03
9	3.40	52.28	100.00	35.38	100	0.00
Total	100.00	35.38				

Table A.122. Charging voltage experiments data for Klipfontein coal from second stage Tribo-electrostatic test at **8.5 KV,** 22.5 KV separating voltage & 2.5 m/sec air velocity

Product collected	Fractional Yield (Wt) %	Ash content	Cumulative Weight %	Cumulative Ash content (%)	Combustible Recovery	Ash rejection %
1	30.87	27.70	30.87	27.70	34.46	75.73
2	16.37	34.12	47.24	29.92	51.11	59.87
3	17.32	34.97	64.56	31.28	68.49	42.68
4	14.69	38.60	79.25	32.64	82.42	26.58
5	4.83	40.41	84.08	33.08	86.86	21.04
6	3.87	42.98	87.95	33.52	90.27	16.31
7	4.89	44.47	92.85	34.10	94.47	10.14
8	4.34	47.84	97.18	34.71	97.96	4.25
9	2.82	53.09	100.00	35.23	100	0.00
Total	100.00	35.23				

Table A.123. Rotary charging speed experiments data for Klipfontein coal from second stage Tribo-electrostatic test at **2500 rpm,** 22.5 KV separating voltage & 2.5 m/sec air velocity

Product collected	Fractional Yield (Wt) %	Ash content	Cumulative Weight %	Cumulative Ash content (%)	Combustible Recovery	Ash rejection %
1	6.59	14.52	6.59	14.52	8.69	97.28
2	6.33	19.41	12.92	16.91	16.55	93.78
3	10.16	19.80	23.08	18.19	29.12	88.05
4	24.94	27.60	48.02	23.07	56.95	68.46
5	3.30	31.64	51.32	23.62	60.43	65.49
6	2.41	36.54	53.73	24.20	62.78	62.99
7	14.26	39.51	67.98	27.41	76.08	46.96
8	15.87	45.82	83.85	30.90	89.33	26.26
9	16.15	57.15	100.00	35.14	100	0.00
Total	100.00	35.14				

Table A.124. Rotary charging speed experiments data for Klipfontein coal from second stage Tribo-electrostatic test at **3000 rpm,** 22.5 KV separating voltage & 2.5 m/sec air velocity

Product collected	Fractional Yield (Wt) %	Ash content	Cumulative Weight %	Cumulative Ash content (%)	Combustible Recovery	Ash rejection %
1	6.42	15.77	6.42	15.77	8.51	97.23
2	6.90	19.00	13.31	17.44	17.30	93.63
3	10.08	21.00	23.39	18.98	29.84	87.83
4	21.54	26.57	44.94	22.62	54.74	72.14
5	3.76	37.18	48.70	23.74	58.46	68.30
6	12.56	38.96	61.26	26.86	70.53	54.89
7	16.80	46.82	78.06	31.16	84.59	33.32
8	4.78	47.21	82.83	32.08	88.56	27.14
9	17.17	57.67	100.00	36.47	100	0.00
Total	100.00	36.47				

Table A.125. Rotary charging speed experiments data for Klipfontein coal from second stage Tribo-electrostatic test at **4000 rpm,** 22.5 KV separating voltage & 2.5 m/sec air velocity

Product collected	Fractional Yield (Wt) %	Ash content	Cumulative Weight %	Cumulative Ash content (%)	Combustible Recovery	Ash rejection %
1	8.37	15.70	8.37	15.70	11.01	96.35
2	6.98	20.00	15.35	17.66	19.73	92.47
3	10.27	20.06	25.62	18.62	32.55	86.73
4	19.80	27.95	45.42	22.69	54.83	71.34
5	4.46	34.00	49.88	23.70	59.43	67.12
6	3.98	37.10	53.86	24.69	63.34	63.02
7	12.65	39.45	66.51	27.50	75.30	49.14
8	15.47	46.04	81.98	31.00	88.33	29.33
9	18.02	58.53	100.00	35.96	100	0.00
Total	100.00	35.96				

Table A.126. Rotary charging speed experiments data for Klipfontein coal from second stage Tribo-electrostatic test at **5000 rpm,** 22.5 KV separating voltage & 2.5 m/sec air velocity

Product collected	Fractional Yield (Wt) %	Ash content	Cumulative Weight %	Cumulative Ash content (%)	Combustible Recovery	Ash rejection %
1	8.00	14.85	8.00	14.85	10.71	96.74
2	7.16	19.41	15.16	17.00	19.79	92.92
3	9.46	19.72	24.62	18.05	31.73	87.80
4	17.63	27.97	42.25	22.19	51.70	74.26
5	4.37	32.84	46.62	23.19	56.32	70.31
6	4.29	34.64	50.91	24.15	60.73	66.24
7	12.38	41.00	63.29	27.45	72.22	52.29
8	16.23	44.64	79.52	30.96	86.35	32.40
9	20.48	57.61	100.00	36.42	100	0.00
Total	100.00	36.42				

Table A.127. Rotary charging speed experiments data for Klipfontein coal from second stage Tribo-electrostatic test at **5000 rpm,** 22.5 KV separating voltage & 2.5 m/sec air velocity

Product collected	Fractional Yield (Wt) %	Ash content	Cumulative Weight %	Cumulative Ash content (%)	Combustible Recovery	Ash rejection %
1	8.00	14.85	8.00	14.85	10.71	96.74
2	7.16	19.41	15.16	17.00	19.79	92.92
3	9.46	19.72	24.62	18.05	31.73	87.80
4	17.63	27.97	42.25	22.19	51.70	74.26
5	4.37	32.84	46.62	23.19	56.32	70.31
6	4.29	34.64	50.91	24.15	60.73	66.24
7	12.38	41.00	63.29	27.45	72.22	52.29
8	16.23	44.64	79.52	30.96	86.35	32.40
9	20.48	57.61	100.00	36.42	100	0.00
Total	100.00	36.42				

Table A.128. Separating voltage experiments data for Klipfontein coal from second stage Tribo-electrostatic test at **10 KV,** 0 KV charging voltage & 2.5 m/sec air velocity

Product collected	Fractional Yield (Wt) %	Ash content	Cumulative Weight %	Cumulative Ash content (%)	Combustible Recovery	Ash rejection %
1	8.00	14.85	8.00	14.85	10.71	96.74
2	7.16	19.41	15.16	17.00	19.79	92.92
3	9.46	19.72	24.62	18.05	31.73	87.80
4	17.63	27.97	42.25	22.19	51.70	74.26
5	4.37	32.84	46.62	23.19	56.32	70.31
6	4.29	34.64	50.91	24.15	60.73	66.24
7	12.38	41.00	63.29	27.45	72.22	52.29
8	16.23	44.64	79.52	30.96	86.35	32.40
9	20.48	57.61	100.00	36.42	100	0.00
Total	100.00	36.42				

Table A.129. Separating voltage experiments data for Klipfontein coal from second stage Tribo-electrostatic test at **12.5 KV,** 0 KV charging voltage & 2.5 m/sec air velocity

Product collected	Fractional Yield (Wt) %	Ash content	Cumulative Weight %	Cumulative Ash content (%)	Combustible Recovery	Ash rejection %
1	5.76	14.68	5.76	14.68	7.61	97.62
2	9.21	21.04	14.96	18.59	18.88	92.15
3	5.93	21.09	20.89	19.30	26.13	88.63
4	26.23	28.87	47.13	24.63	55.04	67.27
5	3.67	33.16	50.80	25.24	58.84	63.84
6	2.92	35.96	53.72	25.83	61.75	60.87
7	15.13	40.43	68.86	29.04	75.71	43.62
8	17.17	45.38	86.03	32.30	90.25	21.64
9	13.97	54.95	100.00	35.46	100	0.00
Total	100.00	35.46				

Table A.130. Separating voltage experiments data for Klipfontein coal from second stage Tribo-electrostatic test at **15 KV,** 0 KV charging voltage & 2.5 m/sec air velocity

Product collected	Fractional Yield (Wt) %	Ash content	Cumulative Weight %	Cumulative Ash content (%)	Combustible Recovery	Ash rejection %
1	6.08	15.25	6.08	15.25	7.99	97.39
2	9.03	19.17	15.11	17.59	19.31	92.52
3	7.37	21.83	22.47	18.98	28.24	87.99
4	25.80	29.59	48.27	24.65	56.41	66.50
5	3.79	33.02	52.07	25.26	60.35	62.97
6	3.34	37.95	55.40	26.03	63.56	59.41
7	13.71	40.35	69.12	28.87	76.25	43.83
8	16.84	46.01	85.96	32.23	90.35	22.01
9	14.04	55.69	100.00	35.52	100	0.00
Total	100.00	35.52				

Table A.131. Separating voltage experiments data for Klipfontein coal from second stage Tribo-electrostatic test at **20 KV,** 0 KV charging voltage & 2.5 m/sec air velocity

Product collected	Fractional Yield (Wt) %	Ash content	Cumulative Weight %	Cumulative Ash content (%)	Combustible Recovery	Ash rejection %
1	7.12	16.59	7.12	16.59	9.14	96.63
2	10.32	19.43	17.45	18.27	21.94	90.90
3	8.65	21.96	26.10	19.49	32.33	85.47
4	23.02	28.01	49.12	23.48	57.84	67.06
5	4.07	32.20	53.19	24.15	62.08	63.32
6	4.11	37.02	57.29	25.07	66.06	58.98
7	11.55	39.67	68.84	27.52	76.79	45.90
8	16.22	46.33	85.06	31.11	90.18	24.44
9	14.94	57.29	100.00	35.02	100	0.00
Total	100.00	35.02				

Table A.132. Air velocity experiments data for Klipfontein coal from second stage Tribo-electrostatic test at **2.5 m/sec,** 0 KV charging voltage & 12.5 KV separating voltage

Product collected	Fractional Yield (Wt) %	Ash content	Cumulative Weight %	Cumulative Ash content (%)	Combustible Recovery	Ash rejection %
1	5.24	14.90	5.24	14.90	6.89	97.79
2	8.21	20.16	13.45	18.11	17.01	93.10
3	6.44	21.46	19.88	19.19	24.82	89.18
4	27.25	29.09	47.13	24.92	54.68	66.71
5	2.77	32.13	49.90	25.32	57.58	64.19
6	2.92	34.67	52.82	25.83	60.52	61.32
7	15.14	39.92	67.96	28.97	74.58	44.18
8	16.95	44.41	84.91	32.05	89.14	22.84
9	15.09	53.41	100.00	35.28	100	0.00
Total	100.00	35.28				

Table A.133. Air velocity experiments data for Klipfontein coal from second stage Tribo-electrostatic test at **3.1 m/sec,** 0 KV charging voltage & 12.5 KV separating voltage

Product collected	Fractional Yield (Wt) %	Ash content	Cumulative Weight %	Cumulative Ash content (%)	Combustible Recovery	Ash rejection %
1	4.64	16.53	4.64	16.53	6.00	97.83
2	7.38	22.93	12.02	20.46	14.80	93.06
3	7.23	24.86	19.25	22.11	23.21	87.98
4	33.51	31.69	52.76	28.20	58.66	58.00
5	3.22	34.20	55.98	28.54	61.94	54.89
6	2.96	36.91	58.94	28.96	64.83	51.81
7	15.50	40.95	74.44	31.46	79.00	33.88
8	16.35	44.47	90.78	33.80	93.06	13.36
9	9.22	51.33	100.00	35.42	100	0.00
Total	100.00	35.42				

Table A.134. Air velocity experiments data for Klipfontein coal from second stage Tribo-electrostatic test at **3.7 m/sec,** 0 KV charging voltage & 12.5 KV separating voltage

Product collected	Fractional Yield (Wt) %	Ash content	Cumulative Weight %	Cumulative Ash content (%)	Combustible Recovery	Ash rejection %
1	4.91	19.16	4.91	19.16	6.16	97.36
2	8.05	26.33	12.95	23.61	15.36	91.41
3	7.74	26.66	20.69	24.75	24.17	85.61
4	34.73	32.54	55.42	29.63	60.55	53.86
5	3.25	35.03	58.67	29.93	63.83	50.65
6	3.41	37.08	62.08	30.32	67.16	47.10
7	14.49	41.25	76.58	32.39	80.38	30.30
8	15.30	43.92	91.88	34.31	93.70	11.43
9	8.12	50.05	100.00	35.59	100	0.00
Total	100.00	35.59				

Table A.135. Air velocity experiments data for Klipfontein coal from second stage Tribo-electrostatic test at **4.3 m/sec,** 0 KV charging voltage & 12.5 KV separating voltage

Product collected	Fractional Yield (Wt) %	Ash content	Cumulative Weight %	Cumulative Ash content (%)	Combustible Recovery	Ash rejection %
1	5.58	21.61	5.58	21.61	6.81	96.62
2	8.16	27.15	13.74	24.90	16.05	90.42
3	8.82	28.33	22.56	26.24	25.88	83.42
4	34.41	33.75	56.97	30.78	61.35	50.90
5	3.51	35.30	60.48	31.04	64.88	47.43
6	3.58	37.25	64.07	31.39	68.38	43.70
7	14.21	41.36	78.27	33.20	81.33	27.25
8	14.39	43.10	92.66	34.73	94.07	9.88
9	7.34	48.07	100.00	35.71	100	0.00
Total	100.00	35.71				

Table A.136. Feed rate experiments data for Klipfontein coal from second stage Tribo-electrostatic test at **12 g/min,** 0 KV charging voltage & 12.5 KV separating voltage

Product collected	Fractional Yield (Wt) %	Ash content	Cumulative Weight %	Cumulative Ash content (%)	Combustible Recovery	Ash rejection %
1	5.24	14.90	5.24	14.90	6.89	97.79
2	8.21	20.16	13.45	18.11	17.01	93.10
3	6.44	21.46	19.88	19.19	24.82	89.18
4	27.25	29.09	47.13	24.92	54.68	66.71
5	2.77	32.13	49.90	25.32	57.58	64.19
6	2.92	34.67	52.82	25.83	60.52	61.32
7	15.14	39.92	67.96	28.97	74.58	44.18
8	16.95	44.41	84.91	32.05	89.14	22.84
9	15.09	53.41	100.00	35.28	100	0.00
Total	100.00	35.28				

Table A.137. Feed rate experiments data for Klipfontein coal from second stage Tribo-electrostatic test at **18 g/min,** 0 KV charging voltage & 12.5 KV separating voltage

Product collected	Fractional Yield (Wt) %	Ash content	Cumulative Weight %	Cumulative Ash content (%)	Combustible Recovery	Ash rejection %
1	4.35	13.22	4.35	13.22	5.80	98.35
2	7.79	17.90	12.13	16.22	15.62	94.36
3	5.31	20.59	17.45	17.55	22.09	91.22
4	29.40	28.32	46.84	24.31	54.46	67.37
5	2.75	28.80	49.60	24.56	57.47	65.09
6	2.30	36.07	51.90	25.07	59.73	62.71
7	16.35	38.15	68.25	28.20	75.27	44.84
8	17.59	45.29	85.84	31.70	90.05	22.01
9	14.16	54.25	100.00	34.90	100	0.00
Total	100.00	34.90				

Table A.138. Feed rate experiments data for Klipfontein coal from second stage Tribo-electrostatic test at **26 g/min,** 0 KV charging voltage & 12.5 KV separating voltage

Product collected	Fractional Yield (Wt) %	Ash content	Cumulative Weight %	Cumulative Ash content (%)	Combustible Recovery	Ash rejection %
1	3.72	12.62	3.72	12.62	5.01	98.67
2	7.57	18.48	11.29	16.55	14.53	94.68
3	4.92	19.08	16.21	17.32	20.66	92.01
4	28.72	27.60	44.93	23.89	52.72	69.46
5	2.92	31.44	47.84	24.35	55.80	66.85
6	2.33	33.89	50.17	24.79	58.18	64.61
7	15.74	38.65	65.91	28.10	73.06	47.30
8	18.11	43.91	84.02	31.51	88.73	24.67
9	15.98	54.25	100.00	35.14	100	0.00
Total	100.00	35.14				

Table A.139. Charging voltage experiments data for Klipfontein coal from Single and Middling re-cycled electrostatic test at **0 KV,** 12.5 KV separating voltage & 2.5 m/sec velocity

Product collected	Fractional Yield (Wt) %	Ash content	Cumulative Weight %	Cumulative Ash content (%)	Combustible Recovery	Ash rejection %
1	15.37	17.42	15.37	17.42	19.58	92.39
2	5.36	20.19	20.73	18.14	26.18	89.32
3	24.25	27.50	44.98	23.18	53.31	70.36
4	15.52	37.82	60.51	26.94	68.20	53.67
5	39.49	47.82	100.00	35.19	100.00	0.00
Total	100.00	35.19				

Splitter distance: 0.6 cm from the negative electrode

Table A.140. Charging voltage experiments data for Klipfontein coal from Single and Middling re-cycled electrostatic test at **1.5 KV,** 12.5 KV separating voltage & 2.5 m/sec velocity

Product collected	Fractional Yield (Wt) %	Ash content	Cumulative Weight %	Cumulative Ash content (%)	Combustible Recovery	Ash rejection %
1	26.01	20.79	26.01	20.79	31.80	84.64
2	10.46	24.90	36.47	21.97	43.92	77.24
3	25.81	33.65	62.28	26.81	70.35	52.57
4	10.07	43.34	72.36	29.11	79.16	40.17
5	27.64	51.16	100.00	35.21	100.00	0.00
Total	100.00	35.21				

Splitter distance: 0.6 cm from the negative electrode

Table A.141. Charging voltage experiments data for Klipfontein coal from Single and Middling re-cycled electrostatic test at **0 KV,** 12.5 KV separating voltage & 2.5 m/sec velocity

Product collected	Fractional Yield (Wt) %	Ash content	Cumulative Weight %	Cumulative Ash content (%)	Combustible Recovery	Ash rejection %
1	20.85	19.46	20.85	19.46	26.10	88.62
2	8.03	23.86	28.88	20.68	35.61	83.25
3	27.76	32.54	56.65	26.49	64.72	57.92
4	12.42	42.08	69.07	29.30	75.91	43.27
5	30.93	49.89	100.00	35.67	100.00	0.00
Total	100.00	35.67				

Splitter distance: 1.0 cm from the negative electrode

Table A.142. Charging voltage experiments data for Klipfontein coal from Single and Middling re-cycled electrostatic test at **1.5 KV,** 12.5 KV separating voltage & 2.5 m/sec velocity

Product collected	Fractional Yield (Wt) %	Ash content	Cumulative Weight %	Cumulative Ash content (%)	Combustible Recovery	Ash rejection %
1	31.65	21.76	31.65	21.76	38.13	80.35
2	12.33	27.94	43.98	23.49	51.81	70.52
3	26.41	38.05	70.40	28.95	77.01	41.85
4	8.07	47.08	78.47	30.82	83.58	31.01
5	21.53	50.48	100.00	35.05	100.00	0.00
Total	100.00	35.05				

Splitter distance: 1.0 cm from the negative electrode

Table A.143. Charging voltage experiments data for Khutala No. 4 seam coal from second stage Tribo-electrostatic test at **0 KV,** 12.5 KV separating voltage & 1.9 m/sec air velocity

Product collected	Fractional Yield (Wt) %	Ash content	Cumulative Weight %	Cumulative Ash content (%)	Combustible Recovery	Ash rejection %
1	2.38	10.63	2.38	10.63	3.30	99.29
2	4.79	17.47	7.16	15.20	9.45	96.95
3	4.22	18.55	11.39	16.44	14.80	94.76
4	27.67	28.38	39.05	24.90	45.63	72.78
5	1.76	29.02	40.82	25.08	47.58	71.35
6	1.95	32.93	42.77	25.44	49.62	69.55
7	17.25	39.29	60.02	29.42	65.91	50.58
8	22.12	41.21	82.13	32.59	86.14	25.08
9	17.87	50.14	100.00	35.73	100	0.00
Total	100.00	35.73				

Table A.144. Charging voltage experiments data for Khutala No. 4 seam coal from second stage Tribo-electrostatic test at **1.5 KV,** 12.5 KV separating voltage & 1.9 m/sec air velocity

Product collected	Fractional Yield (Wt) %	Ash content	Cumulative Weight %	Cumulative Ash content (%)	Combustible Recovery	Ash rejection %
1	3.35	12.66	3.35	12.66	4.56	98.82
2	6.29	18.44	9.63	16.43	12.55	95.58
3	4.65	19.02	14.28	17.27	18.42	93.12
4	30.62	28.69	44.90	25.06	52.45	68.61
5	2.37	30.99	47.27	25.36	55.00	66.56
6	2.08	34.01	49.35	25.72	57.14	64.59
7	15.75	40.73	65.10	29.35	71.69	46.69
8	20.77	44.24	85.87	32.95	89.74	21.06
9	14.13	53.42	100.00	35.84	100	0.00
Total	100.00	35.84				

Table A.145. Charging voltage experiments data for Khutala No. 4 seam coal from second stage Tribo-electrostatic test at **2.5 KV,** 12.5 KV separating voltage & 1.9 m/sec air velocity

Product collected	Fractional Yield (Wt) %	Ash content	Cumulative Weight %	Cumulative Ash content (%)	Combustible Recovery	Ash rejection %
1	3.46	10.76	3.46	10.76	4.80	98.96
2	6.62	18.11	10.08	15.59	13.25	95.61
3	5.24	18.88	15.32	16.71	19.87	92.84
4	31.72	29.92	47.04	25.62	54.48	66.30
5	2.52	30.82	49.57	25.88	57.19	64.13
6	2.28	33.58	51.84	26.22	59.55	61.99
7	15.51	41.81	67.35	29.81	73.60	43.86
8	19.52	44.22	86.88	33.05	90.55	19.73
9	13.12	53.76	100.00	35.77	100	0.00
Total	100.00	35.77				

Table A.146. Charging voltage experiments data for Khutala No. 4 seam coal from second stage Tribo-electrostatic test at **5.0 KV,** 12.5 KV separating voltage & 1.9 m/sec air velocity

Product collected	Fractional Yield (Wt) %	Ash content	Cumulative Weight %	Cumulative Ash content (%)	Combustible Recovery	Ash rejection %
1	3.80	11.30	3.80	11.30	5.26	98.80
2	6.92	18.55	10.72	15.98	14.04	95.22
3	5.22	18.73	15.94	16.88	20.65	92.49
4	31.36	29.39	47.30	25.17	55.16	66.78
5	2.47	31.84	49.76	25.50	57.78	64.59
6	1.95	33.09	51.72	25.79	59.82	62.78
7	14.96	41.74	66.68	29.37	73.40	45.36
8	20.21	44.90	86.89	32.98	90.76	20.04
9	13.11	54.78	100.00	35.84	100	0.00
Total	100.00	35.84				

Table A.147. Separating voltage experiments data for Khutala No. 4 seam coal from second stage Tribo-electrostatic test at **12.5 KV,** 0 KV charging voltage & 1.9 m/sec air velocity

Product collected	Fractional Yield (Wt) %	Ash content	Cumulative Weight %	Cumulative Ash content (%)	Combustible Recovery	Ash rejection %
1	2.38	10.63	2.38	10.63	3.30	99.29
2	4.79	17.47	7.16	15.20	9.45	96.95
3	4.22	18.55	11.39	16.44	14.80	94.76
4	27.67	28.38	39.05	24.90	45.63	72.78
5	1.76	29.02	40.82	25.08	47.58	71.35
6	1.95	32.93	42.77	25.44	49.62	69.55
7	17.25	39.29	60.02	29.42	65.91	50.58
8	22.12	41.21	82.13	32.59	86.14	25.08
9	17.87	50.14	100.00	35.73	100	0.00
Total	100.00	35.73				

Table A.148. Separating voltage experiments data for Khutala No. 4 seam coal from second stage Tribo-electrostatic test at **15 KV,** 0 KV charging voltage & 1.9 m/sec air velocity

Product collected	Fractional Yield (Wt) %	Ash content	Cumulative Weight %	Cumulative Ash content (%)	Combustible Recovery	Ash rejection %
1	4.18	10.81	4.18	10.81	5.83	98.75
2	7.15	17.15	11.33	14.81	15.10	95.34
3	5.25	17.78	16.58	15.75	21.84	92.76
4	25.29	27.28	41.87	22.71	50.60	73.62
5	3.00	30.75	44.87	23.25	53.85	71.06
6	2.34	32.75	47.21	23.72	56.30	68.94
7	15.21	40.25	62.41	27.75	70.51	51.96
8	20.58	44.54	82.99	31.91	88.36	26.53
9	17.01	56.23	100.00	36.05	100	0.00
Total	100.00	36.05				

Table A.149. Separating voltage experiments data for Khutala No. 4 seam coal from second stage Tribo-electrostatic test at **20 KV,** 0 KV charging voltage & 1.9 m/sec air velocity

Product collected	Fractional Yield (Wt) %	Ash content	Cumulative Weight %	Cumulative Ash content (%)	Combustible Recovery	Ash rejection %
1	5.17	11.62	5.17	11.62	7.11	98.32
2	5.70	16.90	10.86	14.39	14.47	95.63
3	7.26	17.38	18.12	15.59	23.81	92.10
4	21.79	25.95	39.91	21.24	48.92	76.28
5	3.19	29.99	43.10	21.89	52.39	73.60
6	2.88	30.39	45.98	22.42	55.52	71.15
7	14.22	38.97	60.20	26.33	69.02	55.66
8	20.40	43.73	80.60	30.73	86.88	30.70
9	19.40	56.56	100.00	35.75	100	0.00
Total	100.00	35.75				

Table A.150. Separating voltage experiments data for Khutala No. 4 seam coal from second stage Tribo-electrostatic test at **25 KV,** 0 KV charging voltage & 1.9 m/sec air velocity

Product collected	Fractional Yield (Wt) %	Ash content	Cumulative Weight %	Cumulative Ash content (%)	Combustible Recovery	Ash rejection %
1	5.17	12.81	5.17	12.81	7.04	98.16
2	5.81	17.05	10.98	15.05	14.57	95.41
3	6.74	17.27	17.71	15.90	23.28	92.18
4	19.08	25.16	36.79	20.70	45.60	78.86
5	3.47	30.34	40.26	21.53	49.37	75.94
6	3.61	30.74	43.86	22.29	53.27	72.86
7	13.76	38.65	57.62	26.19	66.46	58.09
8	20.39	42.04	78.01	30.34	84.94	34.29
9	21.99	56.17	100.00	36.02	100	0.00
Total	100.00	36.02				

Table A.151. Rotary charger speed experiments data for Khutala No. 4 seam coal from second stage Tribo-electrostatic test at **2500 rpm,** 0 KV charging voltage & 1.9 m/sec air velocity

Product collected	Fractional Yield (Wt) %	Ash content	Cumulative Weight %	Cumulative Ash content (%)	Combustible Recovery	Ash rejection %
1	2.38	10.63	2.38	10.63	3.30	99.29
2	4.79	17.47	7.16	15.20	9.45	96.95
3	4.22	18.55	11.39	16.44	14.80	94.76
4	27.67	28.38	39.05	24.90	45.63	72.78
5	1.76	29.02	40.82	25.08	47.58	71.35
6	1.95	32.93	42.77	25.44	49.62	69.55
7	17.25	39.29	60.02	29.42	65.91	50.58
8	22.12	41.21	82.13	32.59	86.14	25.08
9	17.87	50.14	100.00	35.73	100	0.00
Total	100.00	35.73				

Table A.152. Rotary charger speed experiments data for Khutala No. 4 seam coal from second stage Tribo-electrostatic test at **3000 rpm,** 0 KV charging voltage & 1.9 m/sec air velocity

Product collected	Fractional Yield (Wt) %	Ash content	Cumulative Weight %	Cumulative Ash content (%)	Combustible Recovery	Ash rejection %
1	4.34	10.98	4.34	10.98	6.01	98.67
2	7.43	18.22	11.76	15.55	15.46	94.89
3	5.82	18.71	17.58	16.60	22.83	91.84
4	25.63	27.97	43.21	23.34	51.57	71.80
5	3.14	31.06	46.35	23.87	54.94	69.07
6	2.70	33.61	49.05	24.40	57.73	66.54
7	15.52	40.85	64.57	28.35	72.02	48.82
8	19.47	44.13	84.04	32.01	88.95	24.80
9	15.96	55.56	100.00	35.77	100	0.00
Total	100.00	35.77				

Table A.153. Rotary charger speed experiments data for Khutala No. 4 seam coal from second stage Tribo-electrostatic test at **4000 rpm,** 0 KV charging voltage & 1.9 m/sec air velocity

Product collected	Fractional Yield (Wt) %	Ash content	Cumulative Weight %	Cumulative Ash content (%)	Combustible Recovery	Ash rejection %
1	5.56	11.38	5.56	11.38	7.65	98.22
2	7.68	17.96	13.24	15.20	17.43	94.34
3	6.55	18.53	19.80	16.30	25.71	90.92
4	22.86	28.06	42.65	22.60	51.23	72.89
5	3.86	31.03	46.52	23.30	55.36	69.51
6	2.91	32.17	49.43	23.82	58.43	66.88
7	15.15	40.43	64.58	27.72	72.43	49.65
8	19.51	44.51	84.09	31.62	89.23	25.23
9	15.91	56.38	100.00	35.56	100	0.00
Total	100.00	35.56				

Table A.154. Air velocity experiments data for Khutala No. 4 seam coal from second stage Tribo-electrostatic test at **1.3 m/sec,** 0 KV charging voltage & 12.5 KV separating voltage

Product collected	Fractional Yield (Wt) %	Ash content	Cumulative Weight %	Cumulative Ash content (%)	Combustible Recovery	Ash rejection %
1	3.43	11.48	3.43	11.48	4.71	98.90
2	5.85	17.25	9.28	15.12	12.24	96.06
3	4.16	17.39	13.44	15.82	17.58	94.03
4	18.55	25.70	31.99	21.55	38.99	80.65
5	3.36	29.53	35.35	22.31	42.66	77.86
6	3.58	32.68	38.93	23.26	46.41	74.58
7	13.90	36.74	52.83	26.81	60.06	60.25
8	22.43	39.91	75.26	30.71	81.00	35.11
9	24.74	50.56	100.00	35.62	100	0.00
Total	100.00	35.62				

Table A.155. Air velocity experiments data for Khutala No. 4 seam coal from second stage Tribo-electrostatic test at **1.9 m/sec,** 0 KV charging voltage & 12.5 KV separating voltage

Product collected	Fractional Yield (Wt) %	Ash content	Cumulative Weight %	Cumulative Ash content (%)	Combustible Recovery	Ash rejection %
1	4.02	11.45	4.02	11.45	5.49	98.69
2	8.04	17.12	12.06	15.23	15.78	94.78
3	6.09	17.94	18.16	16.14	23.50	91.67
4	28.31	26.90	46.47	22.70	55.44	70.04
5	3.45	29.34	49.92	23.15	59.20	67.16
6	1.71	33.41	51.62	23.49	60.95	65.55
7	17.06	39.20	68.69	27.40	76.96	46.54
8	16.99	44.15	85.67	30.72	91.60	25.24
9	14.33	62.00	100.00	35.20	100	0.00
Total	100.00	35.20				

Table A.156. Air velocity experiments data for Khutala No. 4 seam coal from second stage Tribo-electrostatic test at **2.5 m/sec,** 0 KV charging voltage & 12.5 KV separating voltage

Product collected	Fractional Yield (Wt) %	Ash content	Cumulative Weight %	Cumulative Ash content (%)	Combustible Recovery	Ash rejection %
1	2.97	12.15	2.97	12.15	4.08	98.99
2	6.70	17.69	9.68	15.99	12.69	95.69
3	5.56	18.37	15.24	16.86	19.76	92.85
4	28.48	27.75	43.72	23.95	51.87	70.84
5	2.55	30.16	46.26	24.30	54.65	68.70
6	2.25	33.38	48.52	24.72	56.99	66.60
7	15.39	40.27	63.91	28.46	71.33	49.35
8	21.02	44.91	84.93	32.53	89.40	23.06
9	15.07	54.93	100.00	35.91	100	0.00
Total	100.00	35.91				

Table A.157. Feed rate experiments data for Khutala No. 4 seam coal from second stage Tribo-electrostatic test at **12.84 g/min,** 0 KV charging voltage & 12.5 KV separating voltage

Product collected	Fractional Yield (Wt) %	Ash content	Cumulative Weight %	Cumulative Ash content (%)	Combustible Recovery	Ash rejection %
1	4.27	12.08	4.27	12.08	5.85	98.56
2	7.48	17.92	11.75	15.80	15.42	94.81
3	6.12	18.72	17.88	16.80	23.17	91.61
4	27.05	28.19	44.93	23.66	53.44	70.32
5	2.69	31.46	47.62	24.10	56.31	67.96
6	2.65	34.64	50.27	24.65	59.01	65.39
7	14.55	40.72	64.83	28.26	72.45	48.84
8	20.07	45.31	84.90	32.29	89.56	23.45
9	15.10	55.61	100.00	35.81	100	0.00
Total	100.00	35.81				

Table A.158. Feed rate experiments data for Khutala No. 4 seam coal from second stage Tribo-electrostatic test at **20.08 g/min,** 0 KV charging voltage & 12.5 KV separating voltage

Product collected	Fractional Yield (Wt) %	Ash content	Cumulative Weight %	Cumulative Ash content (%)	Combustible Recovery	Ash rejection %
1	4.18	10.81	4.18	10.81	5.83	98.75
2	7.15	17.15	11.33	14.81	15.10	95.34
3	5.25	17.78	16.58	15.75	21.84	92.76
4	25.29	27.28	41.87	22.71	50.60	73.62
5	3.00	30.75	44.87	23.25	53.85	71.06
6	2.34	32.75	47.21	23.72	56.30	68.94
7	15.21	40.25	62.41	27.75	70.51	51.96
8	20.58	44.54	82.99	31.91	88.36	26.53
9	17.01	56.23	100.00	36.05	100	0.00
Total	100.00	36.05				

Table A.159. Feed rate experiments data for Khutala No. 4 seam coal from second stage Tribo-electrostatic test at **29.30 g/min,** 0 KV charging voltage & 12.5 KV separating voltage

Product collected	Fractional Yield (Wt) %	Ash content	Cumulative Weight %	Cumulative Ash content (%)	Combustible Recovery	Ash rejection %
1	4.85	11.71	4.85	11.71	6.68	98.42
2	7.84	17.57	12.69	15.33	16.77	94.58
3	5.72	18.22	18.41	16.23	24.07	91.69
4	26.31	27.18	44.72	22.67	53.98	71.79
5	2.61	33.37	47.33	23.26	56.69	69.37
6	2.75	29.98	50.08	23.63	59.70	67.07
7	13.87	41.06	63.95	27.41	72.46	51.22
8	20.47	45.58	84.42	31.82	89.85	25.25
9	15.58	58.25	100.00	35.93	100	0.00
Total	100.00	35.93				

Table A.160. Charging voltage experiments data for Khutala No. 4 seam coal from Single and Middling re-cycled electrostatic test at **0 KV,** 12.5 KV separating voltage & 1.9 m/sec velocity

Product collected	Fractional Yield (Wt) %	Ash content	Cumulative Weight %	Cumulative Ash content (%)	Combustible Recovery	Ash rejection %
1	12.32	17.51	12.32	17.51	15.87	94.01
2	6.38	20.53	18.70	18.54	23.80	90.37
3	27.36	28.89	46.06	24.69	54.20	68.40
4	15.27	40.71	61.34	28.68	68.34	51.12
5	38.66	47.59	100.00	35.99	100.00	0.00
Total	100.00	35.99				

Splitter distance: 0.6 cm from the negative electrode

Table A.161. Charging voltage experiments data for Khutala No. 4 seam coal from Single and Middling re-cycled electrostatic test at **1.5 KV,** 12.5 KV separating voltage & 1.9 m/sec velocity

Product collected	Fractional Yield (Wt) %	Ash content	Cumulative Weight %	Cumulative Ash content (%)	Combustible Recovery	Ash rejection %
1	14.00	18.18	14.00	18.18	17.86	92.91
2	6.23	20.03	20.22	18.75	25.63	89.44
3	29.11	28.97	49.33	24.78	57.88	65.94
4	14.60	41.26	63.93	28.54	71.26	49.16
5	36.07	48.92	100.00	35.89	100.00	0.00
Total	100.00	35.89				

Splitter distance: 0.6 cm from the negative electrode

Table A.162. Charging voltage experiments data for Khutala No. 4 seam coal from Single and Middling re-cycled electrostatic test at **0 KV,** 12.5 KV separating voltage & 1.9 m/sec velocity

Product collected	Fractional Yield (Wt) %	Ash content	Cumulative Weight %	Cumulative Ash content (%)	Combustible Recovery	Ash rejection %
1	22.21	18.42	22.21	18.42	28.20	88.56
2	9.51	22.61	31.72	19.68	39.65	82.54
3	22.93	33.92	54.65	25.65	63.23	60.78
4	13.87	44.74	68.51	29.52	75.15	43.43
5	31.49	49.30	100.00	35.75	100.00	0.00
Total	100.00	35.75				

Splitter distance: 1.0 cm from the negative electrode

Table A.163. Charging voltage experiments data for Khutala No. 4 seam coal from Single and Middling re-cycled electrostatic test at **1.5 KV,** 12.5 KV separating voltage & 1.9 m/sec velocity

Product collected	Fractional Yield (Wt) %	Ash content	Cumulative Weight %	Cumulative Ash content (%)	Combustible Recovery	Ash rejection %
1	23.12	18.50	23.12	18.50	29.63	88.25
2	7.79	25.53	30.91	20.27	38.75	82.78
3	22.22	33.30	53.14	25.72	62.06	62.45
4	12.06	44.21	65.19	29.14	72.63	47.81
5	34.81	50.00	100.00	36.40	100.00	0.00
Total	100.00	36.40				

Splitter distance: 1.0 cm from the negative electrode

Table A.164. Charging voltage experiments data for Polmaise coal from second stage Tribo-electrostatic test at **0 KV,** 12.5 KV separating voltage & 2.5 m/sec air velocity

Product collected	Fractional Yield (Wt) %	Ash content	Cumulative Weight %	Cumulative Ash content (%)	Combustible Recovery	Ash rejection %
1	2.55	14.99	2.55	14.99	3.19	98.81
2	5.58	21.51	8.13	19.47	9.65	95.08
3	4.23	22.34	12.35	20.45	14.49	92.15
4	28.95	29.19	41.30	26.58	44.71	65.89
5	2.27	29.76	43.57	26.74	47.07	63.78
6	2.22	31.67	45.80	26.98	49.31	61.59
7	16.52	35.37	62.32	29.20	65.05	43.44
8	21.97	35.47	84.29	30.84	85.95	19.21
9	15.71	39.35	100.00	32.18	100	0.00
Total	100.00	32.18				

Table A.165. Charging voltage experiments data for Polmaise coal from second stage Tribo-electrostatic test at **1.5 KV,** 12.5 KV separating voltage & 2.5 m/sec air velocity

Product collected	Fractional Yield (Wt) %	Ash content	Cumulative Weight %	Cumulative Ash content (%)	Combustible Recovery	Ash rejection %
1	5.56	16.86	5.56	16.86	6.79	97.06
2	9.01	23.34	14.57	20.87	16.94	90.47
3	7.85	24.58	22.42	22.17	25.64	84.43
4	2.47	30.59	24.89	23.00	28.16	82.06
5	2.59	31.30	27.48	23.78	30.77	79.53
6	34.06	31.93	61.54	28.29	64.82	45.47
7	17.15	36.90	78.68	30.17	80.72	25.65
8	12.43	37.09	91.11	31.11	92.20	11.22
9	8.89	40.29	100.00	31.93	100	0.00
Total	100.00	31.93				

Table A.166. Charging voltage experiments data for Polmaise coal from second stage Tribo-electrostatic test at **2.5 KV,** 12.5 KV separating voltage & 2.5 m/sec air velocity

Product collected	Fractional Yield (Wt) %	Ash content	Cumulative Weight %	Cumulative Ash content (%)	Combustible Recovery	Ash rejection %
1	6.90	18.27	6.90	18.27	8.30	96.07
2	10.24	24.91	17.13	22.24	19.61	88.11
3	8.46	25.21	25.60	23.22	28.92	81.45
4	2.38	30.89	27.98	23.87	31.35	79.16
5	2.22	31.66	30.20	24.45	33.58	76.97
6	34.63	32.94	64.83	28.98	67.76	41.37
7	12.50	37.01	77.33	30.28	79.34	26.94
8	15.30	37.26	92.63	31.43	93.47	9.15
9	7.37	39.80	100.00	32.05	100	0.00
Total	100.00	32.05				

Table A.167. Charging voltage experiments data for Polmaise coal from second stage Tribo-electrostatic test at **5.0 KV,** 12.5 KV separating voltage & 2.5 m/sec air velocity

Product collected	Fractional Yield (Wt) %	Ash content	Cumulative Weight %	Cumulative Ash content (%)	Combustible Recovery	Ash rejection %
1	10.12	20.45	10.12	20.45	11.84	93.54
2	11.73	26.42	21.84	23.66	24.54	83.87
3	11.89	27.52	33.73	25.02	37.22	73.66
4	2.63	31.94	36.36	25.52	39.85	71.04
5	2.84	33.20	39.21	26.08	42.65	68.09
6	33.63	34.47	72.84	29.95	75.08	31.90
7	10.44	36.97	83.28	30.83	84.75	19.86
8	11.51	37.53	94.78	31.64	95.33	6.38
9	5.22	39.19	100.00	32.04	100	0.00
Total	100.00	32.04				

Table A.168. Separating voltage experiments data for Polmaise coal from second stage Tribo-electrostatic test at **12.5 KV,** 0 KV charging voltage & 2.5 m/sec air velocity

Product collected	Fractional Yield (Wt) %	Ash content	Cumulative Weight %	Cumulative Ash content (%)	Combustible Recovery	Ash rejection %
1	3.00	14.60	3.00	14.60	3.78	98.64
2	5.75	20.17	8.75	18.26	10.54	95.04
3	4.42	21.36	13.17	19.30	15.67	92.10
4	2.41	26.91	15.58	20.48	18.27	90.08
5	23.07	28.66	38.65	25.36	42.54	69.53
6	2.90	29.26	41.56	25.63	45.57	66.89
7	15.19	34.60	56.75	28.03	60.22	50.55
8	22.14	35.66	78.89	30.17	81.22	26.01
9	21.11	39.65	100.00	32.17	100	0.00
Total	100.00	32.17				

Table A.169. Separating voltage experiments data for Polmaise coal from second stage Tribo-electrostatic test at **15 KV,** 0 KV charging voltage & 2.5 m/sec air velocity

Product collected	Fractional Yield (Wt) %	Ash content	Cumulative Weight %	Cumulative Ash content (%)	Combustible Recovery	Ash rejection %
1	3.85	15.44	3.85	15.44	4.79	98.15
2	6.47	20.12	10.32	18.37	12.41	94.10
3	4.44	20.69	14.76	19.07	17.60	91.24
4	21.18	28.43	35.94	24.59	39.94	72.51
5	3.20	29.04	39.14	24.95	43.29	69.62
6	2.97	29.04	42.12	25.24	46.40	66.93
7	14.54	35.22	56.66	27.80	60.28	51.00
8	22.21	35.73	78.87	30.03	81.32	26.31
9	21.13	40.02	100.00	32.14	100	0.00
Total	100.00	32.14				

Table A.170. Separating voltage experiments data for Polmaise coal from second stage Tribo-electrostatic test at **20 KV,** 0 KV charging voltage & 2.5 m/sec air velocity

Product collected	Fractional Yield (Wt) %	Ash content	Cumulative Weight %	Cumulative Ash content (%)	Combustible Recovery	Ash rejection %
1	4.65	16.56	4.65	16.56	5.71	97.60
2	7.46	20.59	12.11	19.04	14.44	92.82
3	5.80	21.09	17.91	19.71	21.19	89.01
4	3.24	28.25	21.15	21.01	24.61	86.16
5	19.26	28.37	40.41	24.52	44.93	69.15
6	4.10	29.46	44.51	24.98	49.19	65.39
7	12.27	35.30	56.78	27.21	60.88	51.90
8	20.76	36.01	77.54	29.56	80.45	28.63
9	22.46	40.93	100.00	32.12	100	0.00
Total	100.00	32.12				

Table A.171. Separating voltage experiments data for Polmaise coal from second stage Tribo-electrostatic test at **25 KV,** 0 KV charging voltage & 2.5 m/sec air velocity

Product collected	Fractional Yield (Wt) %	Ash content	Cumulative Weight %	Cumulative Ash content (%)	Combustible Recovery	Ash rejection %
1	5.37	17.27	5.37	17.27	6.56	97.13
2	7.90	21.23	13.26	19.63	15.74	91.93
3	5.71	21.38	18.98	20.16	22.37	88.15
4	15.90	28.27	34.87	23.85	39.21	74.22
5	5.24	29.10	40.11	24.54	44.69	69.49
6	3.95	29.25	44.07	24.96	48.82	65.91
7	10.36	35.26	54.43	26.92	58.73	54.59
8	21.26	35.73	75.69	29.40	78.90	31.04
9	24.31	41.21	100.00	32.27	100	0.00
Total	100.00	32.27				

Table A.172. Air velocity experiments data for Polmaise coal from second stage Tribo-electrostatic test at **2.5 m/sec,** 0 KV charging voltage & 12.5 KV separating voltage

Product collected	Fractional Yield (Wt) %	Ash content	Cumulative Weight %	Cumulative Ash content (%)	Combustible Recovery	Ash rejection %
1	2.36	13.98	2.36	13.98	3.00	98.97
2	5.57	18.50	7.93	17.15	9.69	95.77
3	3.36	20.31	11.30	18.09	13.64	93.64
4	2.21	26.23	13.50	19.42	16.04	91.84
5	22.55	27.72	36.06	24.61	40.07	72.40
6	2.42	29.14	38.48	24.90	42.60	70.20
7	15.44	33.89	53.92	27.47	57.64	53.93
8	22.35	35.40	76.27	29.80	78.92	29.33
9	23.73	39.74	100.00	32.16	100	0.00
Total	100.00	32.16				

Table A.173. Air velocity experiments data for Polmaise coal from second stage Tribo-electrostatic test at **3.1 m/sec,** 0 KV charging voltage & 12.5 KV separating voltage

Product collected	Fractional Yield (Wt) %	Ash content	Cumulative Weight %	Cumulative Ash content (%)	Combustible Recovery	Ash rejection %
1	2.19	15.86	2.19	15.86	2.71	98.92
2	5.11	20.99	7.30	19.45	8.66	95.58
3	5.02	22.63	12.32	20.75	14.38	92.03
4	28.19	28.87	40.51	26.40	43.90	66.67
5	2.33	29.50	42.83	26.57	46.31	64.53
6	3.45	30.70	46.28	26.88	49.83	61.23
7	14.92	34.86	61.20	28.82	64.14	45.03
8	23.28	35.76	84.48	30.73	86.16	19.08
9	15.52	39.45	100.00	32.09	100	0.00
Total	100.00	32.09				

Table A.174. Air velocity experiments data for Polmaise coal from second stage Tribo-electrostatic test at **3.7 m/sec,** 0 KV charging voltage & 12.5 KV separating voltage

Product collected	Fractional Yield (Wt) %	Ash content	Cumulative Weight %	Cumulative Ash content (%)	Combustible Recovery	Ash rejection %
1	2.63	19.63	2.63	19.63	3.11	98.39
2	6.41	24.72	9.04	23.24	10.21	93.45
3	7.05	25.87	16.08	24.39	17.90	87.77
4	2.88	30.14	18.96	25.27	20.87	85.06
5	33.30	30.23	52.26	28.43	55.07	53.68
6	4.10	32.21	56.36	28.70	59.16	49.56
7	14.62	35.04	70.99	30.01	73.15	33.59
8	18.93	36.03	89.91	31.28	90.97	12.33
9	10.09	39.20	100.00	32.08	100	0.00
Total	100.00	32.08				

Table A.175. Air velocity experiments data for Polmaise coal from second stage Tribo-electrostatic test at **4.3 m/sec,** 0 KV charging voltage & 12.5 KV separating voltage

Product collected	Fractional Yield (Wt) %	Ash content	Cumulative Weight %	Cumulative Ash content (%)	Combustible Recovery	Ash rejection %
1	3.44	22.29	3.44	22.29	3.95	97.63
2	7.75	26.79	11.19	25.41	12.33	91.20
3	8.81	27.23	20.00	26.21	21.80	83.78
4	35.60	30.97	55.60	29.26	58.10	49.64
5	3.51	32.57	59.11	29.45	61.60	46.11
6	4.24	32.64	63.35	29.67	65.82	41.82
7	13.40	36.01	76.75	30.78	78.48	26.88
8	14.04	36.31	90.78	31.63	91.69	11.11
9	9.22	38.94	100.00	32.30	100	0.00
Total	100.00	32.30				

Table A.176. Rotary charger speed experiments data for Polmaise coal from second stage Tribo-electrostatic test at **2500 rpm,** 0 KV charging voltage & 12.5 KV separating voltage

Product collected	Fractional Yield (Wt) %	Ash content	Cumulative Weight %	Cumulative Ash content (%)	Combustible Recovery	Ash rejection %
1	2.36	13.98	2.36	13.98	3.00	98.97
2	5.57	18.50	7.93	17.15	9.69	95.77
3	3.36	20.31	11.30	18.09	13.64	93.64
4	2.21	26.23	13.50	19.42	16.04	91.84
5	22.55	27.72	36.06	24.61	40.07	72.40
6	2.42	29.14	38.48	24.90	42.60	70.20
7	15.44	33.89	53.92	27.47	57.64	53.93
8	22.35	35.40	76.27	29.80	78.92	29.33
9	23.73	39.74	100.00	32.16	100	0.00
Total	100.00	32.16				

Table A.177. Rotary charger speed experiments data for Polmaise coal from second stage Tribo-electrostatic test at **3000 rpm,** 0 KV charging voltage & 12.5 KV separating voltage

Product collected	Fractional Yield (Wt) %	Ash content	Cumulative Weight %	Cumulative Ash content (%)	Combustible Recovery	Ash rejection %
1	3.43	15.40	3.43	15.40	4.27	98.36
2	6.44	20.37	9.86	18.64	11.82	94.28
3	4.11	20.83	13.98	19.29	16.62	91.61
4	22.01	27.86	35.99	24.53	40.02	72.52
5	2.56	28.24	38.55	24.78	42.73	70.26
6	2.75	29.25	41.31	25.08	45.60	67.76
7	15.02	34.64	56.33	27.63	60.07	51.56
8	21.56	35.60	77.89	29.83	80.52	27.67
9	22.11	40.20	100.00	32.13	100	0.00
Total	100.00	32.13				

Table A.178. Rotary charger speed experiments data for Polmaise coal from second stage Tribo-electrostatic test at **4000 rpm,** 0 KV charging voltage & 12.5 KV separating voltage

Product collected	Fractional Yield (Wt) %	Ash content	Cumulative Weight %	Cumulative Ash content (%)	Combustible Recovery	Ash rejection %
1	5.09	15.27	5.09	15.27	6.37	97.59
2	6.72	20.58	11.82	18.29	14.24	93.29
3	5.44	21.12	17.26	19.18	20.58	89.72
4	1.51	28.03	18.76	19.89	22.18	88.41
5	20.88	28.50	39.65	24.43	44.21	69.94
6	3.93	29.59	43.57	24.89	48.28	66.33
7	13.25	35.26	56.82	27.31	60.94	51.84
8	21.56	36.28	78.38	29.78	81.20	27.56
9	21.62	41.07	100.00	32.22	100	0.00
Total	100.00	32.22				

Table A.179. Separating voltage experiments data for Polmaise coal from Single and Middling re-cycled electrostatic test at **10 KV,** 0 KV charging voltage & 2.5 m/sec velocity

Product collected	Fractional Yield (Wt) %	Ash content	Cumulative Weight %	Cumulative Ash content (%)	Combustible Recovery	Ash rejection %
1	10.52	19.71	10.52	19.71	12.47	93.57
2	4.58	22.18	15.10	20.46	17.73	90.42
3	29.04	29.35	44.14	26.31	48.01	63.99
4	14.69	35.42	58.83	28.58	62.01	47.86
5	41.17	37.49	100.00	32.25	100.00	0.00
Total	100.00	32.25				

Splitter distance: 0.6 cm from the negative electrode

Table A.180. Separating voltage experiments data for Polmaise coal from Single and Middling re-cycled electrostatic test at **12.5 KV,** 0 KV charging voltage & 2.5 m/sec velocity

Product collected	Fractional Yield (Wt) %	Ash content	Cumulative Weight %	Cumulative Ash content (%)	Combustible Recovery	Ash rejection %
1	11.86	19.57	11.86	19.57	14.10	92.83
2	4.99	21.91	16.84	20.26	19.86	89.45
3	28.31	29.65	45.15	26.15	49.30	63.52
4	14.06	35.82	59.21	28.44	62.64	47.96
5	40.79	38.05	100.00	32.36	100.00	0.00
Total	100.00	32.36				

Splitter distance: 0.6 cm from the negative electrode

Table A.181. Separating voltage experiments data for Polmaise coal from Single and Middling re-cycled electrostatic test at **15 KV,** 0 KV charging voltage & 2.5 m/sec velocity

Product collected	Fractional Yield (Wt) %	Ash content	Cumulative Weight %	Cumulative Ash content (%)	Combustible Recovery	Ash rejection %
1	13.06	19.87	13.06	19.87	15.50	92.01
2	5.48	21.44	18.54	20.33	21.87	88.39
3	24.24	29.11	42.78	25.31	47.32	66.66
4	12.38	35.88	55.16	27.68	59.07	52.98
5	44.84	38.36	100.00	32.47	100.00	0.00
Total	100.00	32.47				

Splitter distance: 0.6 cm from the negative electrode

Table A.182. Charging voltage experiments data for Polmaise coal from Single and Middling re-cycled electrostatic test at **0 KV,** 12.5 KV separating voltage & 2.5 m/sec velocity

Product collected	Fractional Yield (Wt) %	Ash content	Cumulative Weight %	Cumulative Ash content (%)	Combustible Recovery	Ash rejection %
1	17.92	21.10	17.92	21.10	20.90	88.30
2	6.71	24.44	24.63	22.01	28.39	83.23
3	23.60	30.95	48.24	26.38	52.47	60.63
4	12.43	36.77	60.67	28.51	64.08	46.49
5	39.33	38.20	100.00	32.32	100.00	0.00
Total	100.00	32.32				

Splitter distance: 1.0 cm from the negative electrode

Table A.183. Charging voltage experiments data for Polmaise coal from Single and Middling re-cycled electrostatic test at **1.5 KV,** 12.5 KV separating voltage & 2.5 m/sec velocity

Product collected	Fractional Yield (Wt) %	Ash content	Cumulative Weight %	Cumulative Ash content (%)	Combustible Recovery	Ash rejection %
1	25.14	22.70	25.14	22.70	28.67	82.29
2	9.76	26.79	34.90	23.84	39.21	74.18
3	24.48	33.68	59.38	27.90	63.17	48.59
4	9.81	38.07	69.18	29.34	72.13	37.01
5	30.82	38.70	100.00	32.23	100.00	0.00
Total	100.00	32.23				

Splitter distance: 1.0 cm from the negative electrode

Table A.184. Air velocity experiments data for New Vaal coal from second stage Tribo-electrostatic test at **1.3 m/sec,** 0 KV charging voltage & 12.5 KV separating voltage

Product collected	Fractional Yield (Wt) %	Ash content	Cumulative Weight %	Cumulative Ash content (%)	Combustible Recovery	Ash rejection %
1	3.49	16.10	3.49	16.10	4.95	98.62
2	2.42	22.58	5.91	18.75	8.11	97.28
3	4.71	23.77	10.62	20.98	14.16	94.53
4	7.26	31.26	17.88	25.15	22.58	88.96
5	4.56	34.27	22.43	27.00	27.63	85.13
6	5.80	34.09	28.23	28.46	34.08	80.28
7	8.29	38.68	36.52	30.78	42.66	72.40
8	23.13	41.45	59.65	34.92	65.51	48.87
9	40.35	49.34	100.00	40.74	100	0.00
Total	100.00	40.74				

Table A.185. Air velocity experiments data for New Vaal coal from second stage Tribo-electrostatic test at **1.9 m/sec,** 0 KV charging voltage & 12.5 KV separating voltage

Product collected	Fractional Yield (Wt) %	Ash content	Cumulative Weight %	Cumulative Ash content (%)	Combustible Recovery	Ash rejection %
1	3.09	15.80	3.09	15.80	4.37	98.80
2	3.45	21.91	6.53	19.02	8.90	96.93
3	4.79	24.10	11.32	21.17	15.01	94.09
4	11.69	31.55	23.01	26.44	28.47	84.99
5	3.92	34.31	26.93	27.59	32.80	81.67
6	4.11	34.46	31.04	28.50	37.32	78.18
7	11.86	40.11	42.90	31.71	49.27	66.45
8	21.92	42.36	64.81	35.31	70.51	43.55
9	35.19	50.17	100.00	40.54	100	0.00
Total	100.00	40.54				

Table A.186. Air velocity experiments data for New Vaal coal from second stage Tribo-electrostatic test at **2.5 m/sec,** 0 KV charging voltage & 12.5 KV separating voltage

Product collected	Fractional Yield (Wt) %	Ash content	Cumulative Weight %	Cumulative Ash content (%)	Combustible Recovery	Ash rejection %
1	2.33	16.60	2.33	16.60	3.27	99.05
2	3.61	23.14	5.94	20.57	7.94	96.99
3	4.14	23.74	10.09	21.87	13.26	94.56
4	13.01	32.04	23.10	27.60	28.13	84.28
5	3.30	32.10	26.40	28.16	31.90	81.67
6	3.38	35.35	29.77	28.98	35.58	78.73
7	14.49	40.04	44.26	32.60	50.19	64.43
8	23.68	43.00	67.94	36.22	72.89	39.33
9	32.06	49.75	100.00	40.56	100	0.00
Total	100.00	40.56				

Table A.187. Air velocity experiments data for New Vaal coal from second stage Tribo-electrostatic test at **3.1 m/sec,** 0 KV charging voltage & 12.5 KV separating voltage

Product collected	Fractional Yield (Wt) %	Ash content	Cumulative Weight %	Cumulative Ash content (%)	Combustible Recovery	Ash rejection %
1	2.20	19.74	2.20	19.74	2.97	98.93
2	4.38	26.28	6.58	24.09	8.40	96.09
3	3.91	26.36	10.49	24.94	13.24	93.55
4	17.00	33.85	27.48	30.45	32.15	79.36
5	3.55	36.66	31.04	31.16	35.94	76.15
6	3.81	38.23	34.85	31.93	39.90	72.55
7	16.53	41.48	51.38	35.01	56.17	55.64
8	22.34	43.38	73.72	37.54	77.44	31.74
9	26.28	48.97	100.00	40.55	100	0.00
Total	100.00	40.55				

Table A.188. Charging voltage experiments data for New Vaal coal from second stage Tribo-electrostatic test at **0 KV,** 12.5 KV separating voltage & 2.5 m/sec air velocity

Product collected	Fractional Yield (Wt) %	Ash content	Cumulative Weight %	Cumulative Ash content (%)	Combustible Recovery	Ash rejection %
1	0.94	20.45	0.94	20.45	1.23	99.51
2	2.62	27.97	3.56	25.99	4.34	97.65
3	3.41	27.98	6.97	26.96	8.39	95.22
4	3.06	35.03	10.03	29.42	11.67	92.49
5	20.23	35.91	30.26	33.76	33.03	74.02
6	2.06	38.13	32.32	34.04	35.13	72.02
7	19.12	41.26	51.44	36.72	53.64	51.96
8	24.19	40.10	75.63	37.80	77.52	27.29
9	24.37	44.02	100.00	39.32	100	0.00
Total	100.00	39.32				

Table A.189. Charging voltage experiments data for New Vaal coal from second stage Tribo-electrostatic test at **1.5 KV,** 12.5 KV separating voltage & 2.5 m/sec air velocity

Product collected	Fractional Yield (Wt) %	Ash content	Cumulative Weight %	Cumulative Ash content (%)	Combustible Recovery	Ash rejection %
1	3.45	23.78	3.45	23.78	4.35	97.93
2	8.65	31.59	12.10	29.36	14.14	91.02
3	7.41	31.78	19.51	30.28	22.51	85.07
4	32.47	38.33	51.98	35.31	55.64	53.61
5	4.15	39.22	56.14	35.60	59.82	49.49
6	3.40	40.45	59.54	35.88	63.17	46.01
7	16.85	43.96	76.38	37.66	78.79	27.29
8	15.31	44.41	91.69	38.79	92.87	10.10
9	8.31	48.13	100.00	39.56	100	0.00
Total	100.00	39.56				

Table A.190. Charging voltage experiments data for New Vaal coal from second stage Tribo-electrostatic test at **2.5 KV,** 12.5 KV separating voltage & 2.5 m/sec air velocity

Product collected	Fractional Yield (Wt) %	Ash content	Cumulative Weight %	Cumulative Ash content (%)	Combustible Recovery	Ash rejection %
1	5.35	25.51	5.35	25.51	6.58	96.54
2	11.36	33.09	16.70	30.66	19.14	87.03
3	10.13	33.52	26.83	31.74	30.27	78.42
4	36.05	39.70	62.88	36.30	66.18	42.18
5	3.65	39.97	66.53	36.50	69.80	38.48
6	3.55	41.34	70.08	36.75	73.24	34.77
7	12.42	44.84	82.49	37.97	84.56	20.67
8	12.35	45.29	94.84	38.92	95.72	6.50
9	5.16	49.76	100.00	39.48	100	0.00
Total	100.00	39.48				

Table A.191. Charging voltage experiments data for New Vaal coal from second stage Tribo-electrostatic test at **5.0 KV,** 12.5 KV separating voltage & 2.5 m/sec air velocity

Product collected	Fractional Yield (Wt) %	Ash content	Cumulative Weight %	Cumulative Ash content (%)	Combustible Recovery	Ash rejection %
1	10.46	29.54	10.46	29.54	12.07	92.06
2	17.14	35.32	27.61	33.13	30.22	76.50
3	14.76	35.62	42.37	34.00	45.77	62.98
4	30.79	40.76	73.15	36.84	75.63	30.73
5	4.78	40.97	77.94	37.10	80.25	25.70
6	4.32	42.37	82.26	37.37	84.33	20.99
7	6.85	45.45	89.11	37.99	90.44	12.99
8	9.65	46.09	98.76	38.79	98.96	1.56
9	1.24	48.86	100.00	38.91	100	0.00
Total	100.00	38.91				

Table A.192. Charge reverser experiments data for New Vaal coal from second stage Tribo-electrostatic test at **+2.5 KV charging voltage,** 12.5 KV separating voltage & 2.5 m/sec air velocity

Product collected	Fractional Yield (Wt) %	Ash content	Cumulative Weight %	Cumulative Ash content (%)	Combustible Recovery	Ash rejection %
1	20.56	28.18	20.56	28.18	24.70	85.61
2	12.11	31.68	32.66	29.48	38.54	76.07
3	24.54	41.17	57.20	34.49	62.70	50.97
4	11.26	47.77	68.46	36.68	72.54	37.60
5	31.54	47.97	100.00	40.24	100.00	0.00
Total	100.00	40.24				

Splitter distance: 0.6 cm from the negative electrode

Table A.193. Charge reverser experiments data for New Vaal coal from second stage Tribo-electrostatic test at **+1.5 KV charging voltage,** 12.5 KV separating voltage & 2.5 m/sec air velocity

Product collected	Fractional Yield (Wt) %	Ash content	Cumulative Weight %	Cumulative Ash content (%)	Combustible Recovery	Ash rejection %
1	17.55	24.92	17.55	24.92	22.23	89.27
2	7.94	28.50	25.49	26.04	31.82	83.72
3	20.09	38.52	45.57	31.54	52.66	64.73
4	10.09	46.54	55.66	34.26	61.77	53.21
5	44.34	48.91	100.00	40.75	100.00	0.00
Total	100.00	40.75				

Splitter distance: 0.6 cm from the negative electrode

Table A.194. Charge reverser experiments data for New Vaal coal from second stage Tribo-electrostatic test at **0 KV charging voltage,** 12.5 KV separating voltage & 2.5 m/sec air velocity

Product collected	Fractional Yield (Wt) %	Ash content	Cumulative Weight %	Cumulative Ash content (%)	Combustible Recovery	Ash rejection %
1	10.71	22.83	10.71	22.83	14.06	94.07
2	3.54	25.13	14.24	23.40	18.56	91.91
3	12.11	33.32	26.35	27.96	32.30	82.13
4	11.60	40.96	37.95	31.93	43.95	70.60
5	62.05	46.90	100.00	41.22	100.00	0.00
Total	100.00	41.22				

Splitter distance: 0.6 cm from the negative electrode

Table A.195. Charge reverser experiments data for New Vaal coal from second stage Tribo-electrostatic test at **-1.5 KV charging voltage,** 12.5 KV separating voltage & 2.5 m/sec air velocity

Product collected	Fractional Yield (Wt) %	Ash content	Cumulative Weight %	Cumulative Ash content (%)	Combustible Recovery	Ash rejection %
1	6.80	23.03	6.80	23.03	8.87	96.18
2	3.10	29.71	9.91	25.12	12.57	93.93
3	9.25	33.57	19.16	29.20	22.98	86.35
4	10.80	38.92	29.96	32.71	34.16	76.09
5	70.04	44.52	100.00	40.98	100.00	0.00
Total	100.00	40.98				

Splitter distance: 0.6 cm from the negative electrode

Table A.196. Charge reverser experiments data for New Vaal coal from second stage Tribo-electrostatic test at **-2.5 KV charging voltage,** 12.5 KV separating voltage & 2.5 m/sec air velocity

Product collected	Fractional Yield (Wt) %	Ash content	Cumulative Weight %	Cumulative Ash content (%)	Combustible Recovery	Ash rejection %
1	7.67	27.23	7.67	27.23	9.42	94.89
2	2.18	28.20	9.84	27.44	12.06	93.38
3	7.45	34.45	17.30	30.46	20.32	87.09
4	9.91	38.22	27.20	33.29	30.66	77.81
5	72.80	43.62	100.00	40.81	100.00	0.00
Total	100.00	40.81				

Splitter distance: 0.6 cm from the negative electrode

Table A.197. Summary data for **Majuba coal** at single stage Tribo-electrostatic test for different splitter distance at 1.5 KV charging voltage, 12.5 KV separating voltage & 2.5 m/sec air velocity

Splitter distance at **single stage separation (cm)**	Ash content	Cumulative Ash content (%)	Combustible Recovery
R=0.6; C=1.5 & L=2.7	30.01	14.67	16.27
R=1.0; C=1.5 & L=2.3	30.00	16.24	27.16
Splitter distance at **second stage separation** (cm)	Ash content	Cumulative Ash content (%)	Combustible Recovery
R=0.6; C=1.5 & L=2.7	30.01	11.10	5.83
R=1.0; C=1.5 & L=2.3	30.00	13.26	11.18

Table A.198. Summary data for **Koorfontein coal** at single stage Tribo-electrostatic test for different splitter distance at 0 KV charging voltage, 12.5 KV separating voltage & 2.5 m/sec air velocity

Splitter distance at **single stage separation** (cm)	Ash content	Cumulative Ash content (%)	Combustible Recovery
R=0.6; C=1.5 & L=2.7	30.01	13.12	11.30
R=1.0; C=1.5 & L=2.3	30.00	14.24	20.83
Splitter distance at **second stage separation** (cm)	Ash content	Cumulative Ash content (%)	Combustible Recovery
R=0.6; C=1.5 & L=2.7	30.01	9.98	3.51
R=1.0; C=1.5 & L=2.3	30.00	11.66	6.68

APPENDIX B

APPENDIX B

Washability, Froth rate and Tribo-electrostatic Plots

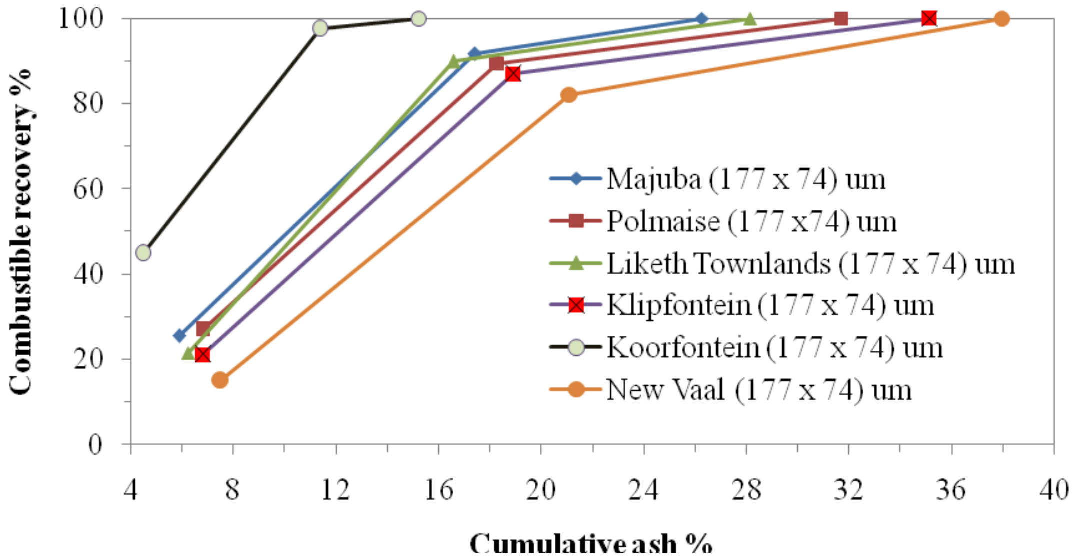

Figure B.1 Performance washability curve for coal samples at relative density: 1.4 and 1.8

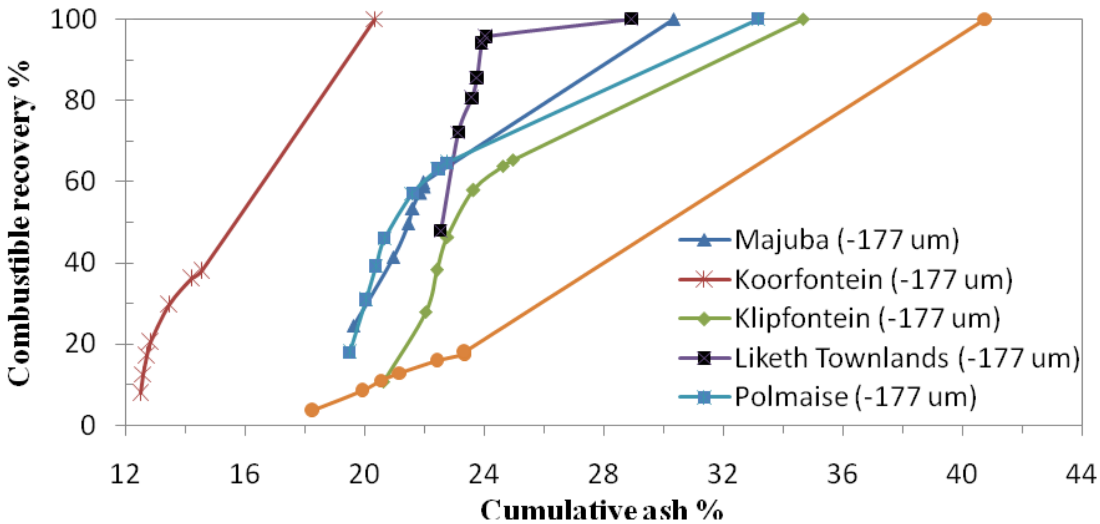

Figure B.2 Combustible recovery/cumulative ash curve obtained using "froth flotation rate test" at 910 g/ton, 15 ppm and 1200 rpm.

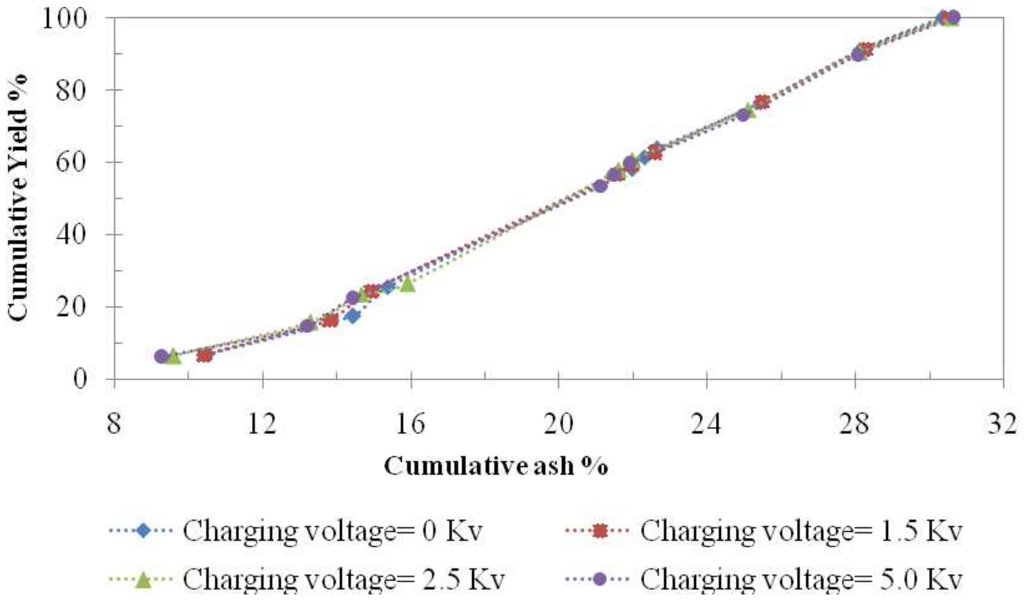

Figure B.3 Effect of charging voltage on Khutala No. 2 seam coal under second stage test at a constant splitter distance, air velocity, feed rate and separating voltage

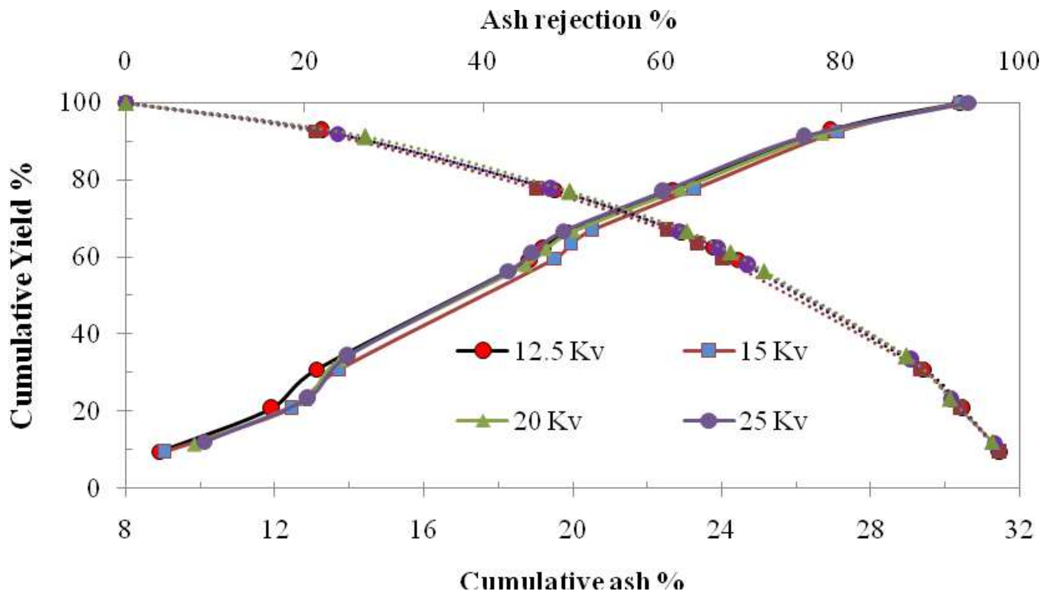

Figure B.4 Effect of separating voltage on Khutala No. 2 seam coal under second stage test at a constant splitter distance, air velocity, feed rate and charging voltage

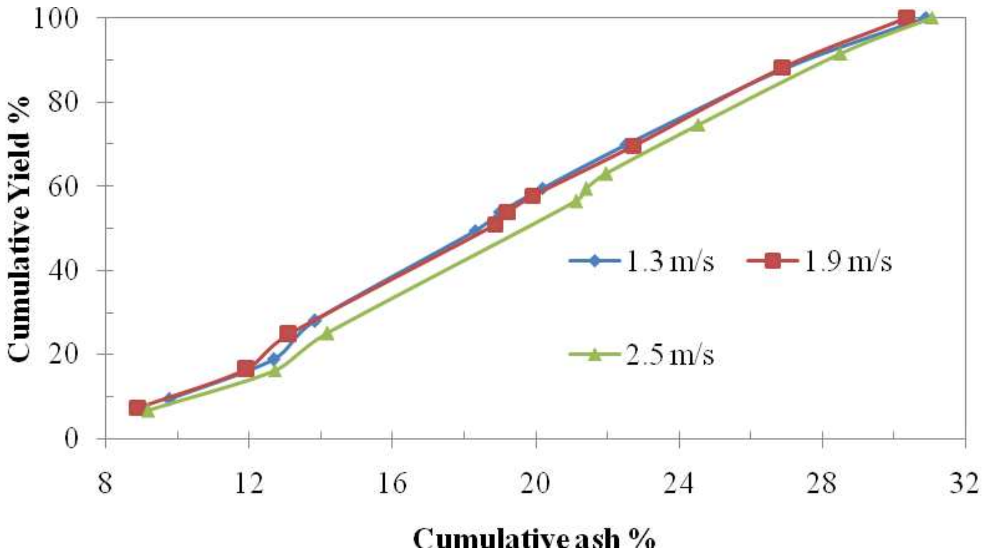

Figure B.5 Effect of air velocity on Khutala No. 2 seam coal under second stage test at a constant splitter distance, separating voltage, feed rate and charging voltage

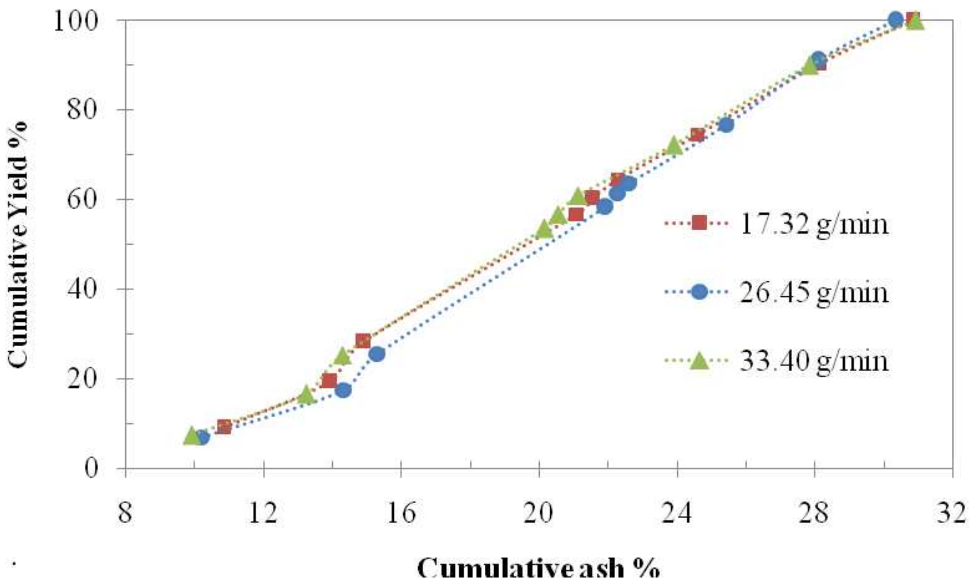

Figure B.6 Effect of feed rate on Khutala No. 2 seam coal under second stage test at a constant splitter distance, separating voltage, air velocity and charging voltage

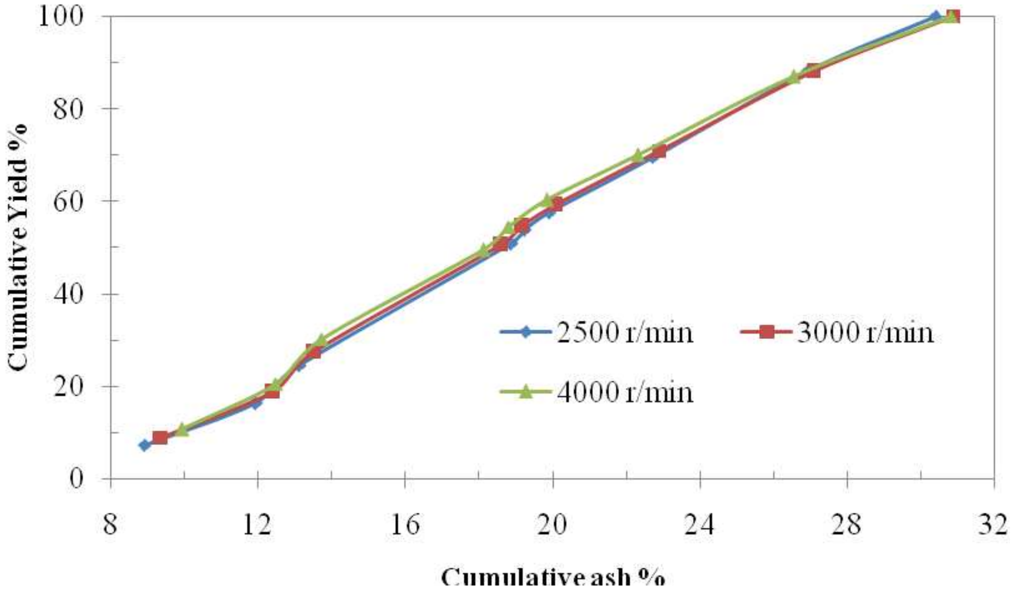

Figure B.7 Effect of rotary charger speed on Khutala No. 2 seam coal under second stage test at a constant splitter distance, separating voltage, air velocity and charging voltage

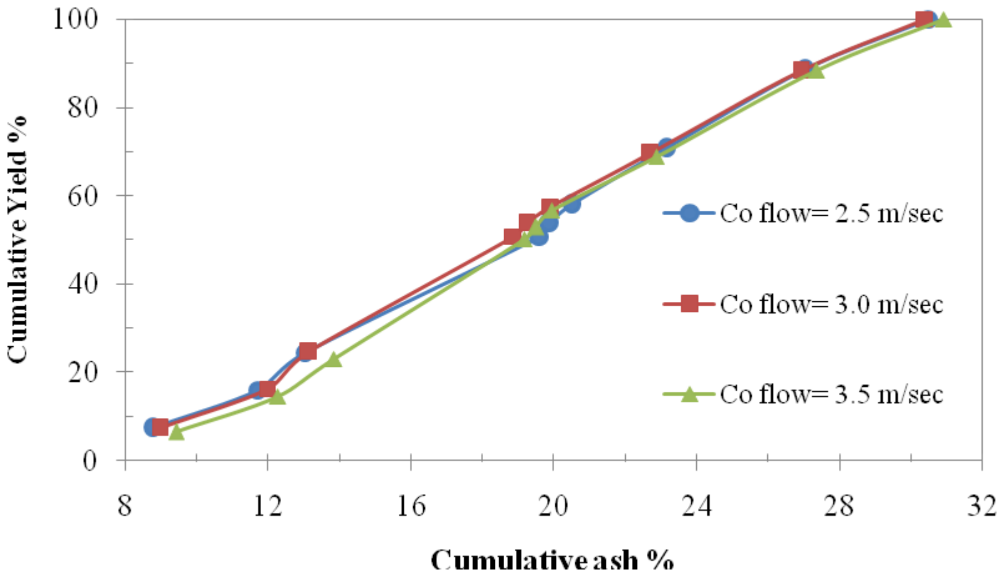

Figure B.8 Effect of Co-flow velocity on Khutala No. 2 seam coal under second stage test at a constant splitter distance, separating voltage, air velocity and charging voltage

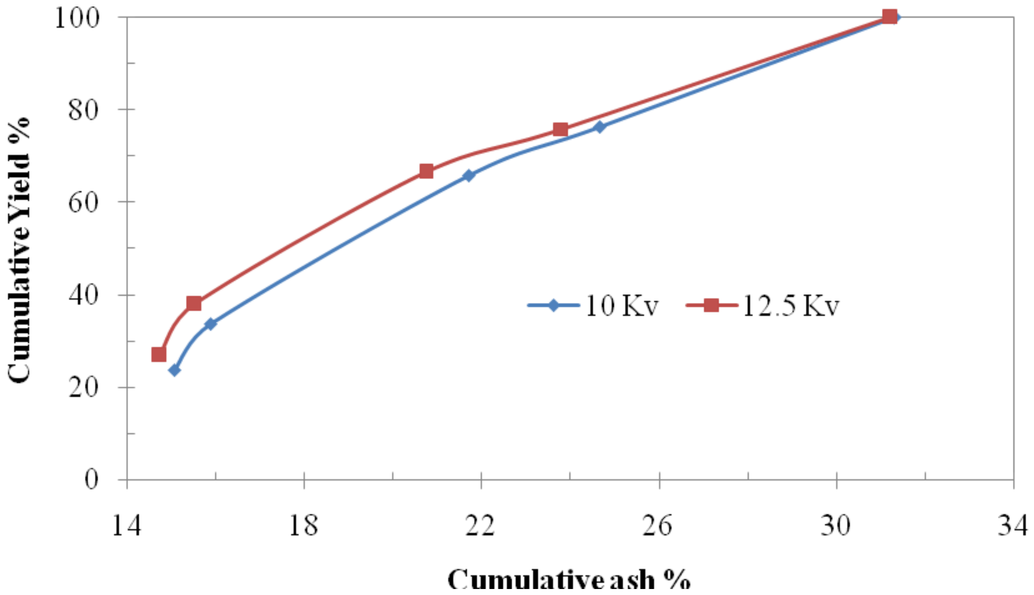

Figure B.9 Effect of separating voltage on single and two stage test with Khutala No. 2 seam coal at a constant charging voltage of 0 KV, air velocity of 1.9 m/sec, rotary speed of 2500 rpm, and splitter distance: R =0.6 cm

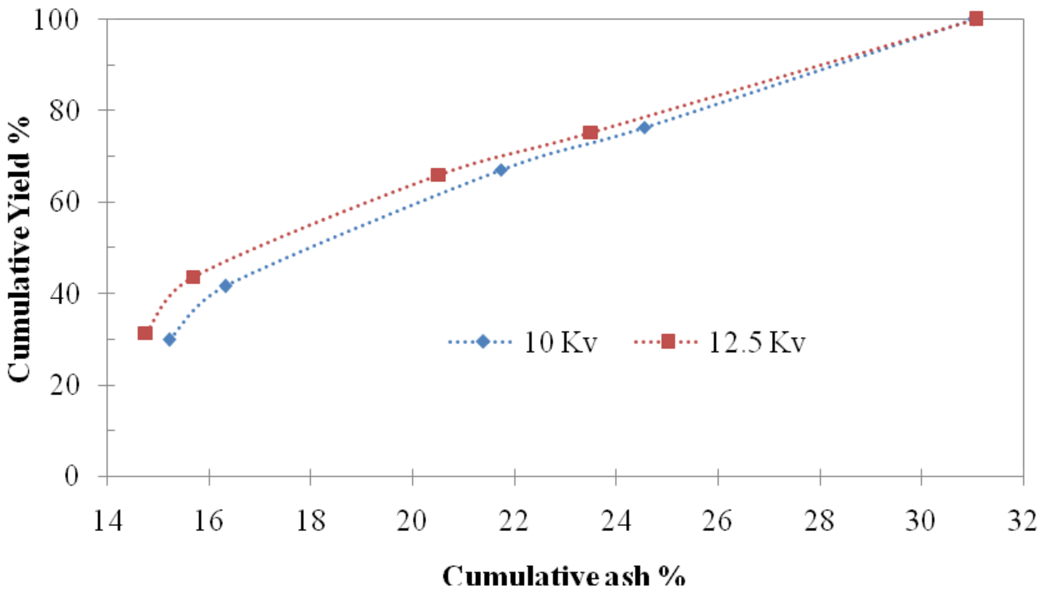

Figure B.10 Effect of separating voltage on single and two stage test with Khutala No. 2 seam coal at a constant charging voltage of 0 KV, air velocity of 1.9 m/sec, rotary speed of 2500 rpm, and splitter distance: R =1.0 cm

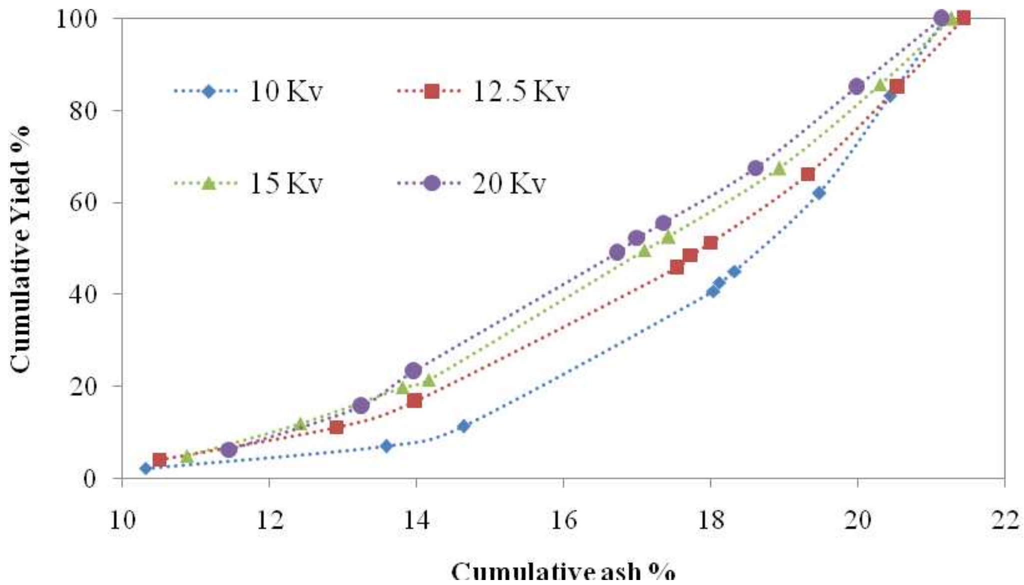

Figure B.11 Effect of separating voltage on Koorfontein coal under second stage test at a constant splitter distance, rotary charger speed, air velocity and charging voltage

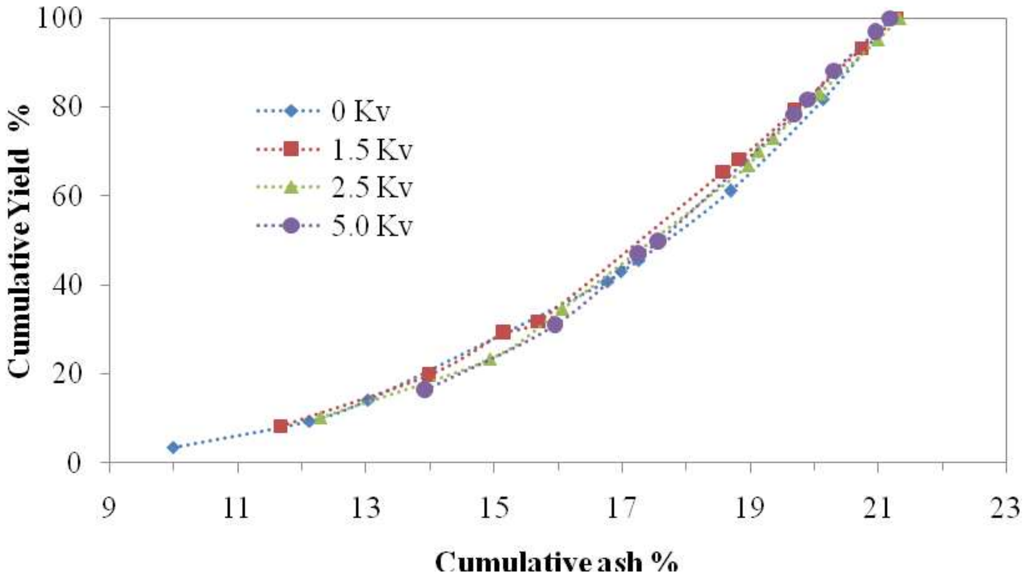

Figure B.12 Effect of charging voltage on Koorfontein coal under second stage test at a constant splitter distance, rotary charger speed, air velocity and separating voltage

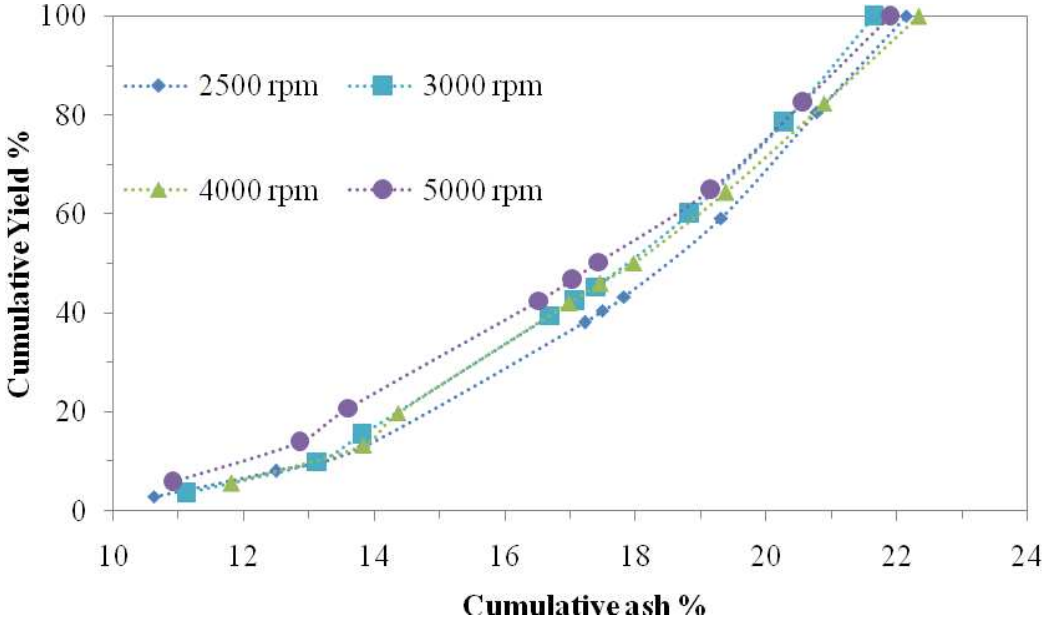

Figure B.13 Effect of rotary charger speed on Koorfontein coal under second stage test at a constant splitter distance, charging voltage, air velocity and separating voltage

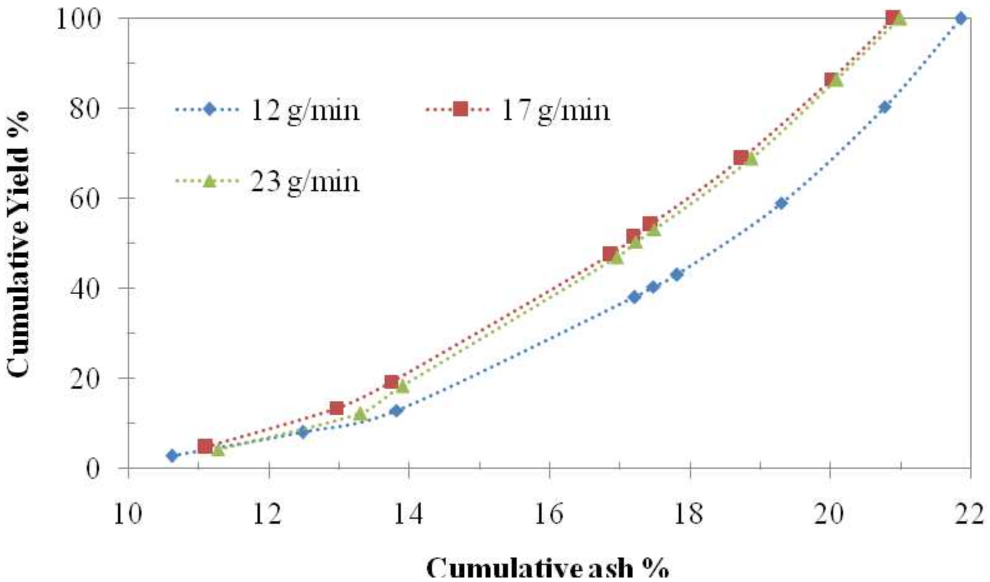

Figure B.14 Effect of feed rate on Koorfontein coal under second stage test at a constant splitter distance, charging voltage, air velocity and separating voltage

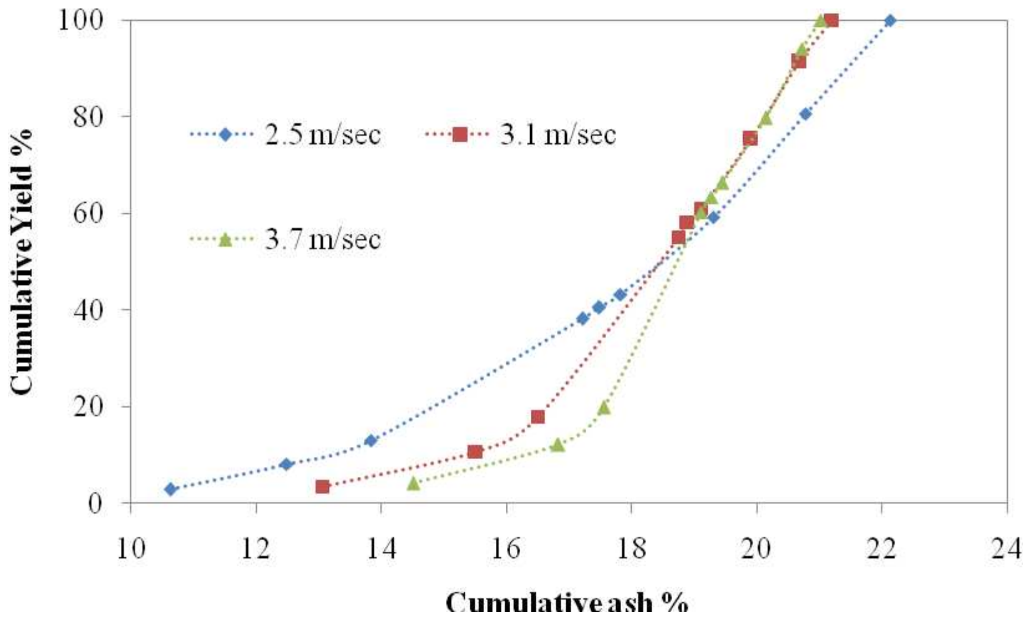

Figure B.15 Effect of air velocity on Koorfontein coal under second stage test at a constant splitter distance, charging voltage, feed rate and separating voltage

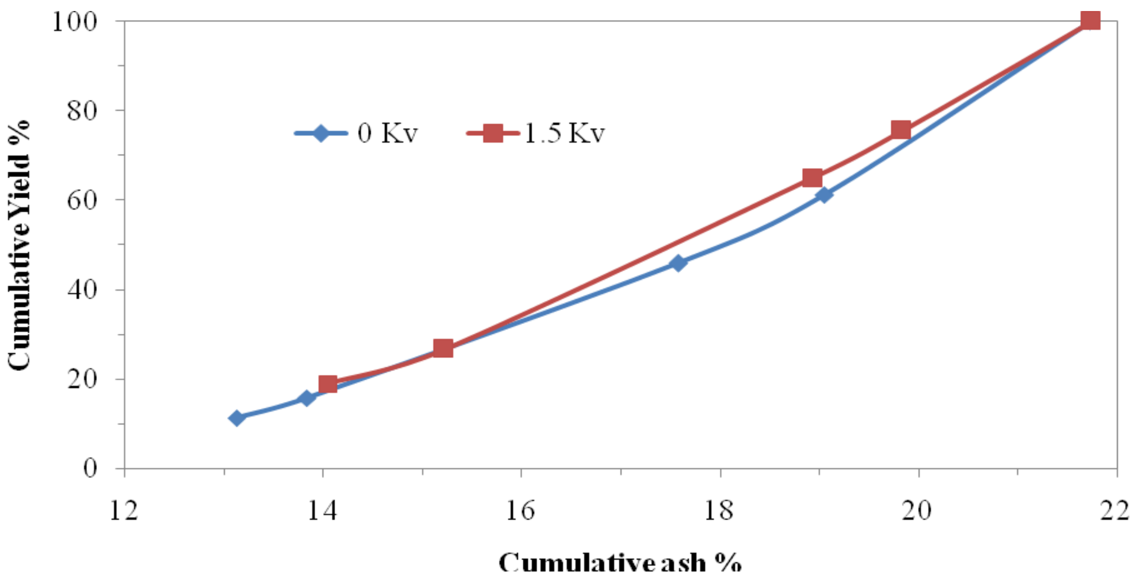

Figure B.16 Effect of charging voltage on single and two stage test with Koorfontein coal at a constant separating voltage of 12.5 KV, air velocity of 1.9 m/sec, rotary speed of 2500 rpm, and splitter distance: R =0.6 cm

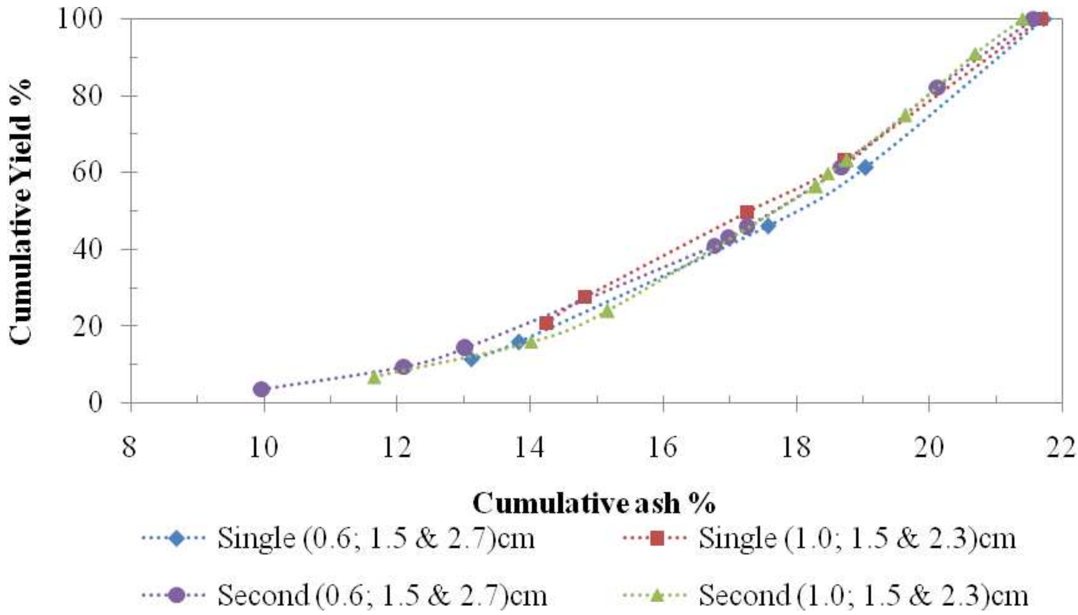

Figure B.17 Effect of charging voltage on single and two stage test with Koorfontein coal at a constant separating voltage of 12.5 KV, air velocity of 1.9 m/sec, rotary speed of 2500 rpm, and splitter distance: R =1.0 cm

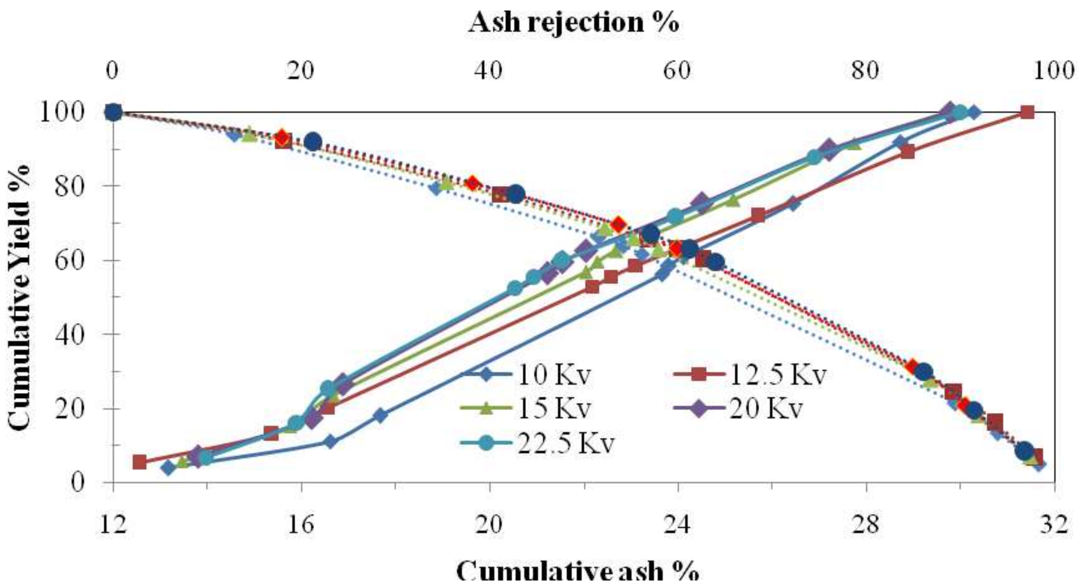

Figure B.18 Effect of separating voltage on Liketh Townlands coal under second stage test at a constant splitter distance, charging voltage, feed rate and air velocity

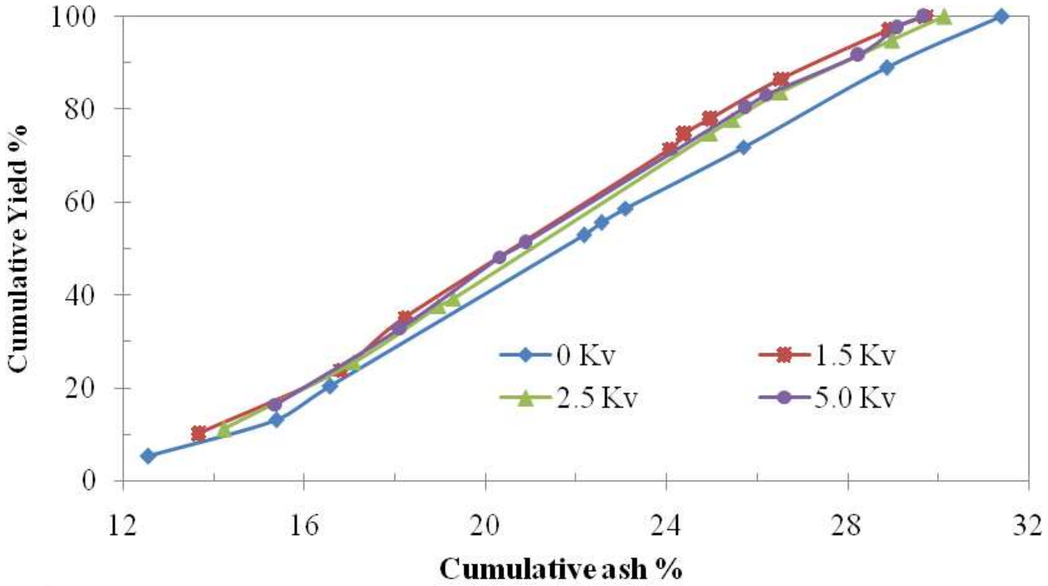

Figure B.19 Effect of charging voltage on Liketh Townlands coal under second stage test at a constant splitter distance, separating voltage, feed rate and air velocity

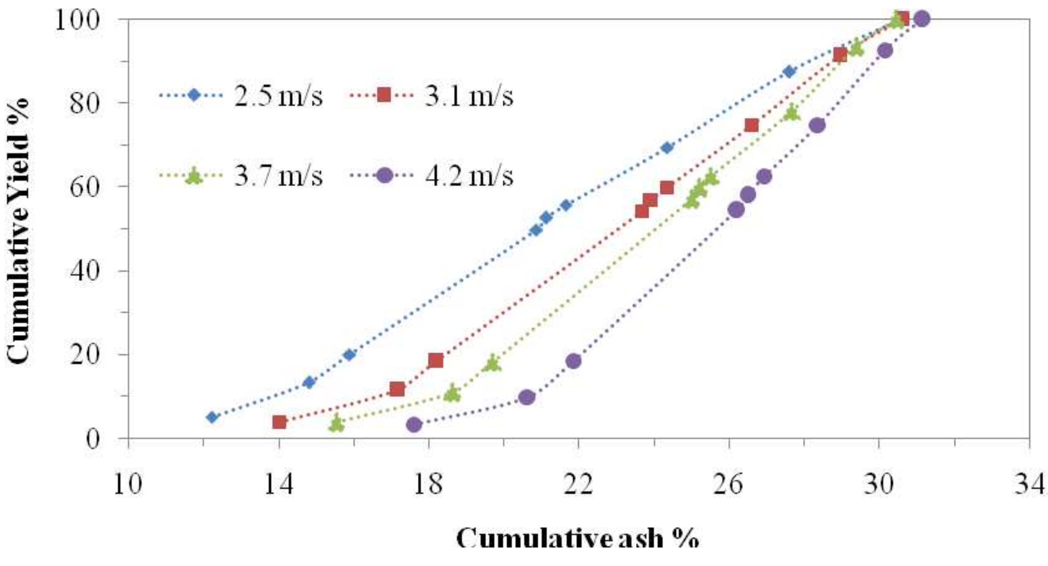

Figure B.20 Effect of air velocity on Liketh Townlands coal under second stage test at a constant splitter distance, separating voltage, feed rate and air velocity

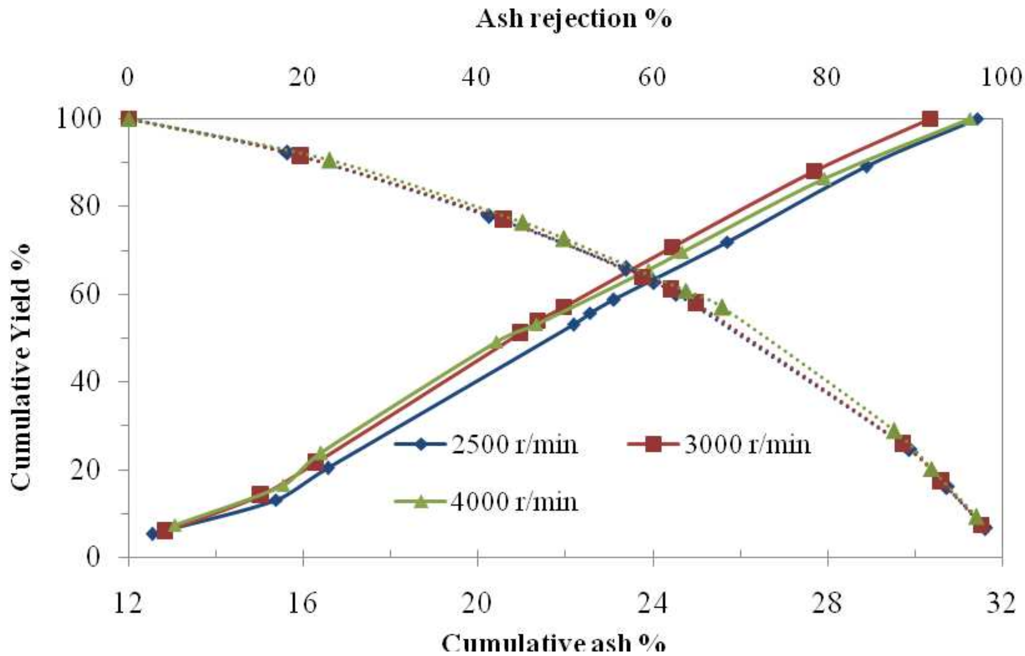

Figure B.21 Effect of rotary charger speed on Liketh Townlands coal under second stage test at a constant splitter distance, separating voltage, feed rate and air velocity

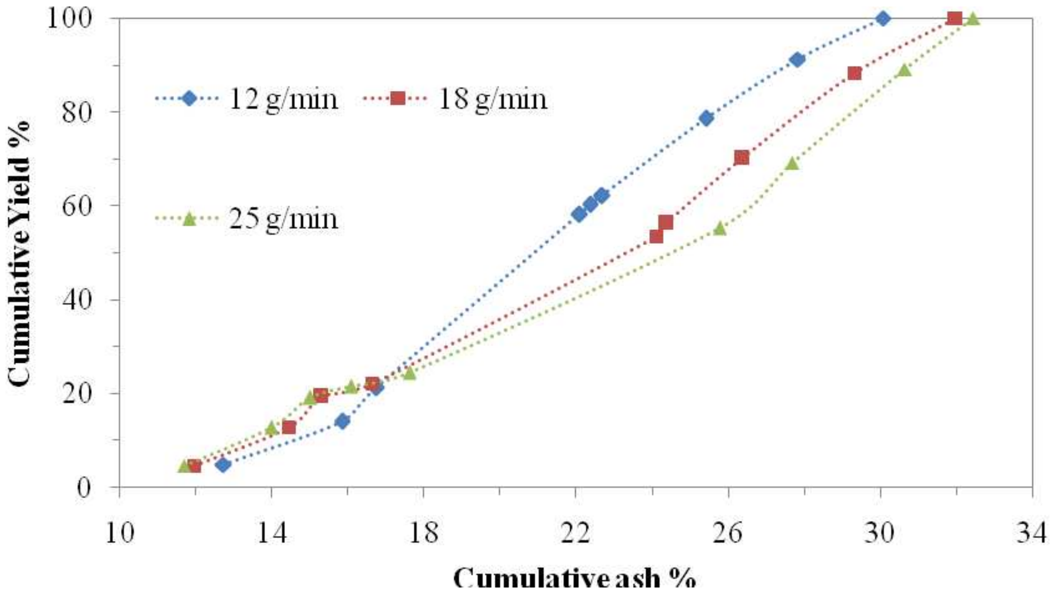

Figure B.22 Effect of feed rate on Liketh Townlands coal under second stage test at a constant splitter distance, separating voltage, rotary charger speed and air velocity

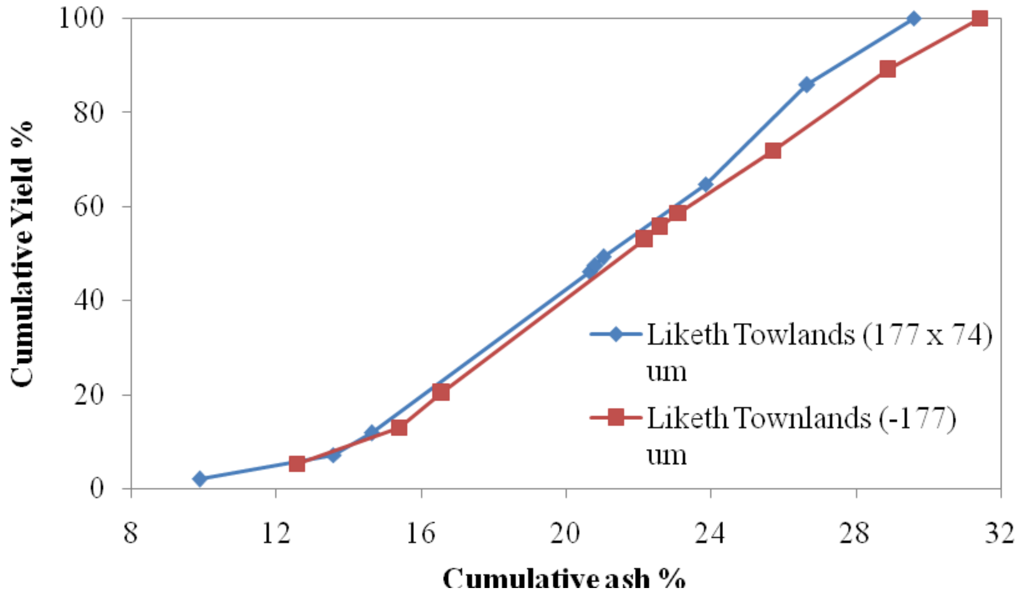

Figure B.23 Effect of particle size on Liketh Townlands coal under second stage test at a constant splitter distance, separating voltage, rotary charger speed and air velocity

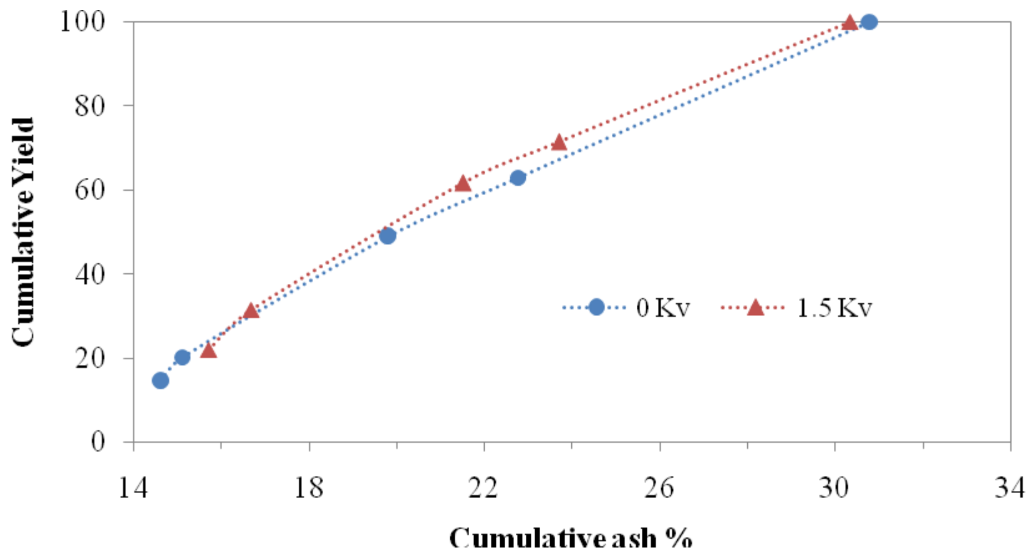

Figure B.24 Effect of charging voltage on single and two stage test with Liketh Townlands coal **(-177) um** at a constant separating voltage of 12.5 KV, air velocity of 1.9 m/sec, rotary speed of 2500 rpm, and splitter distance: R =0.6 cm

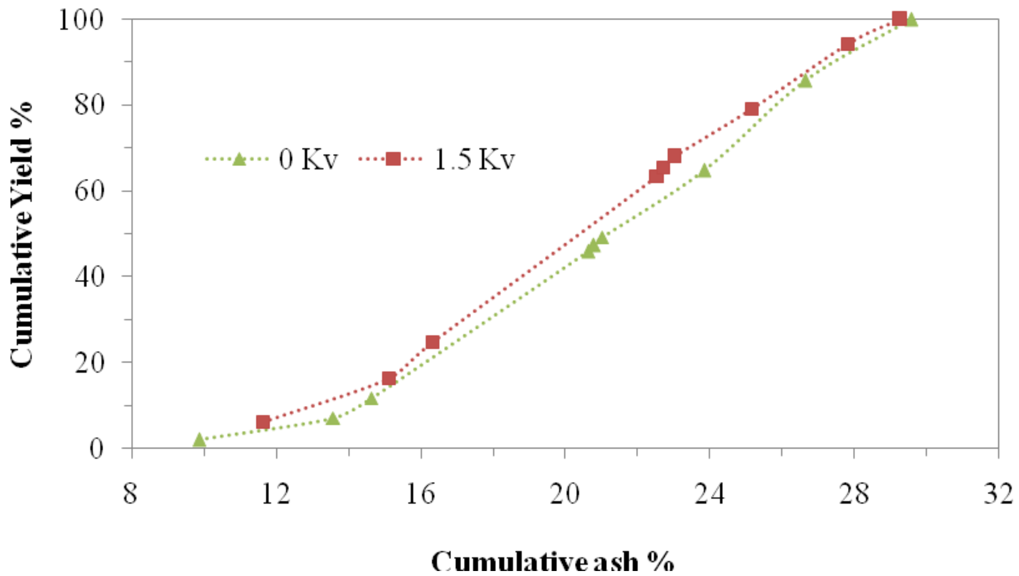

Figure B.25 Effect of charging voltage on single and two stage test with Liketh Townlands coal **(177 X 74) um** at a constant separating voltage of 12.5 KV, air velocity of 1.9 m/sec, rotary speed of 2500 rpm, and splitter distance: R =0.6 cm

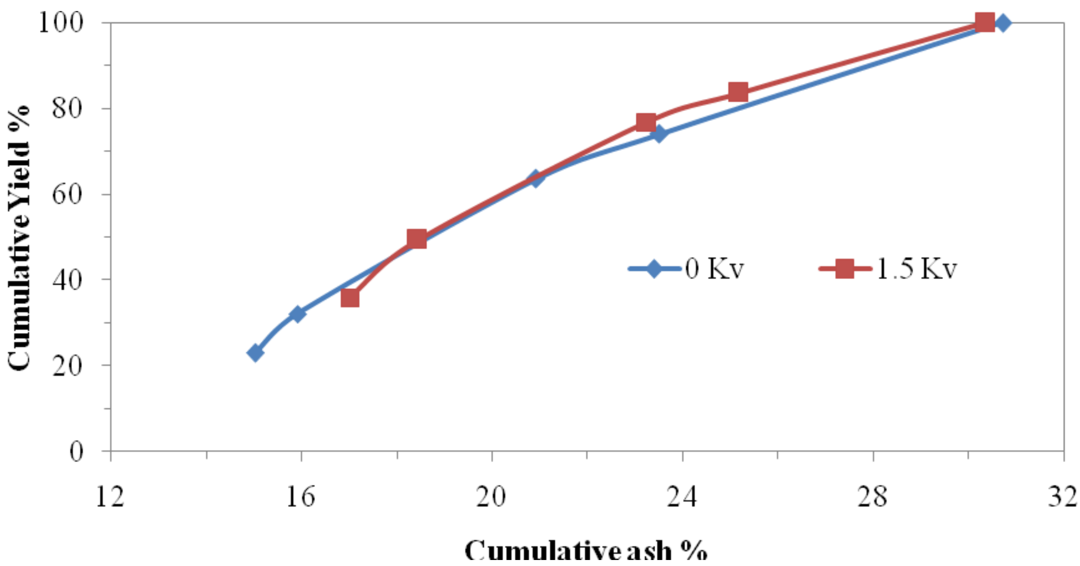

Figure B.26 Effect of charging voltage on single and two stage test with Liketh Townlands coal at a constant separating voltage of 12.5 KV, air velocity of 1.9 m/sec, rotary speed of 2500 rpm, and splitter distance: R =1.0 cm

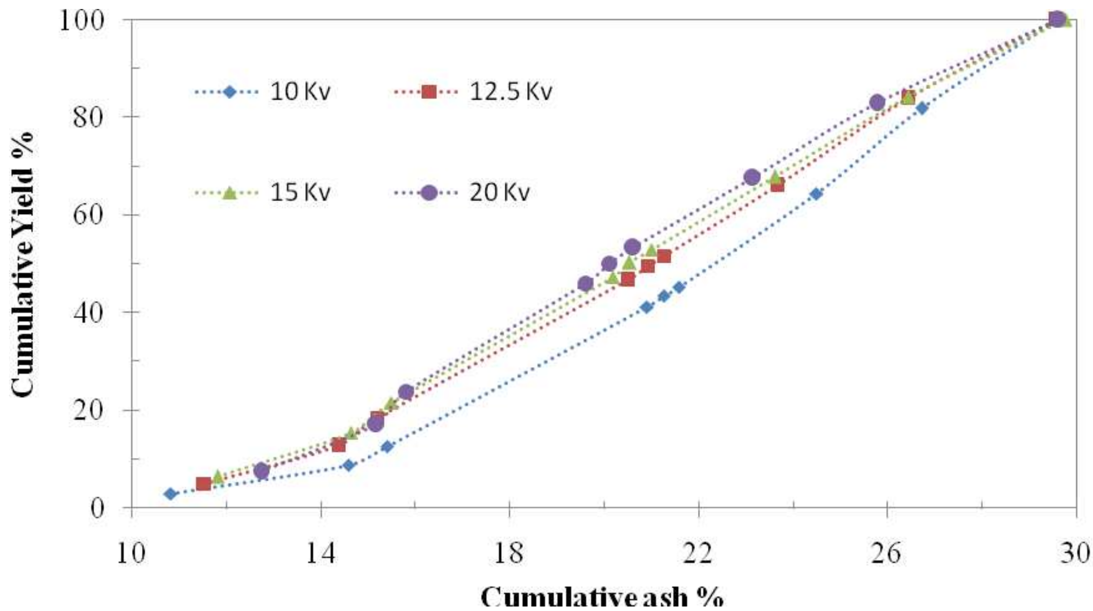

Figure B.27 Effect of separating voltage on Majuba coal under second stage test at a constant splitter distance, charging voltage, feed rate and air velocity

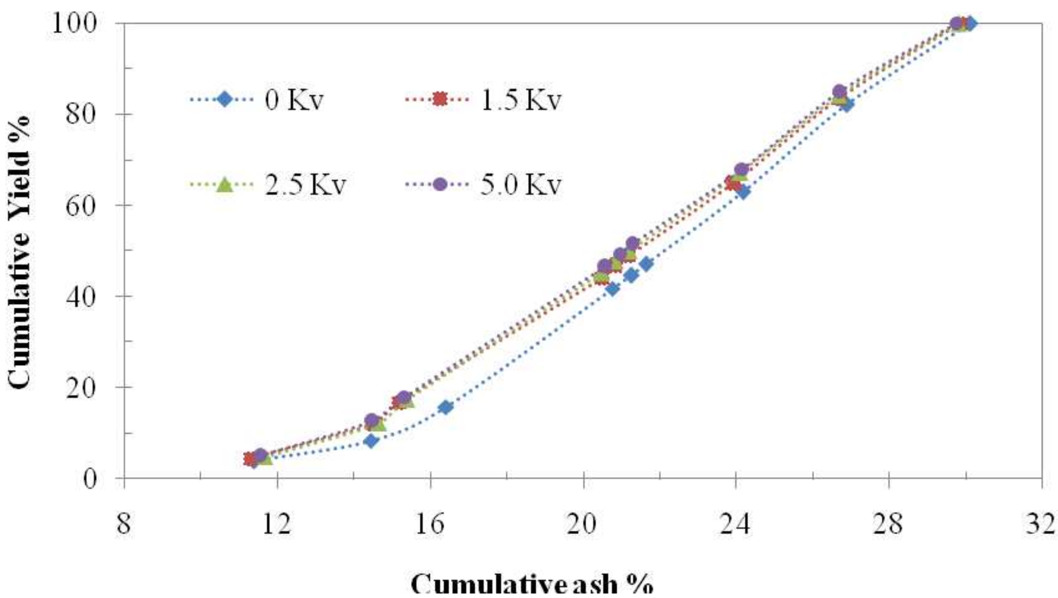

Figure B.28 Effect of charging voltage on Majuba coal under second stage test at a constant splitter distance, separating voltage, feed rate and air velocity

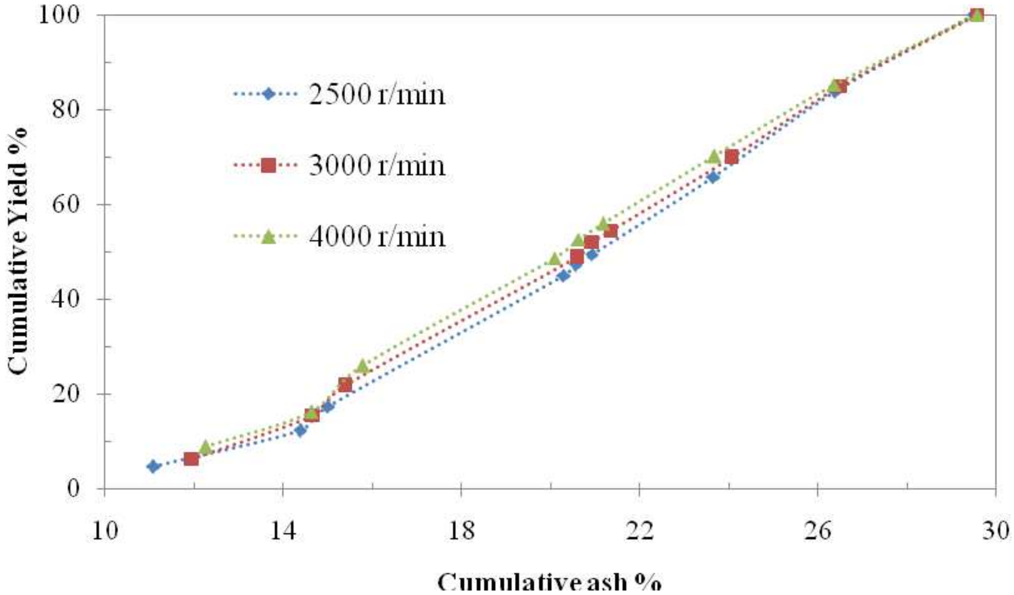

Figure B.29 Effect of rotary charger speed on Majuba coal under second stage test at a constant splitter distance, separating voltage, feed rate and charging voltage

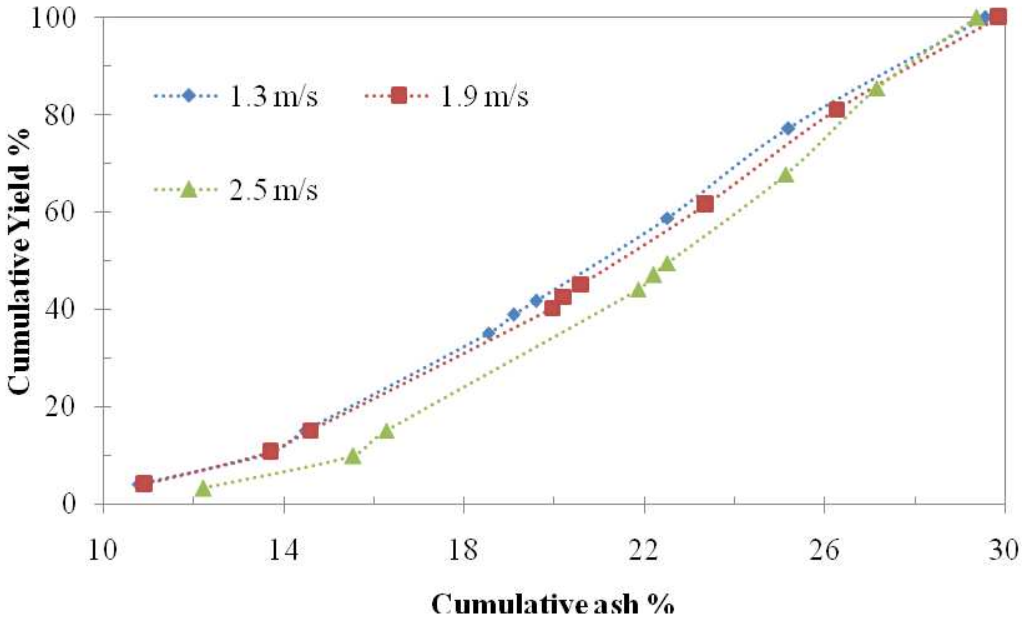

Figure B.30 Effect of air velocity on Majuba coal under second stage test at a constant splitter distance, separating voltage, feed rate and charging voltage.

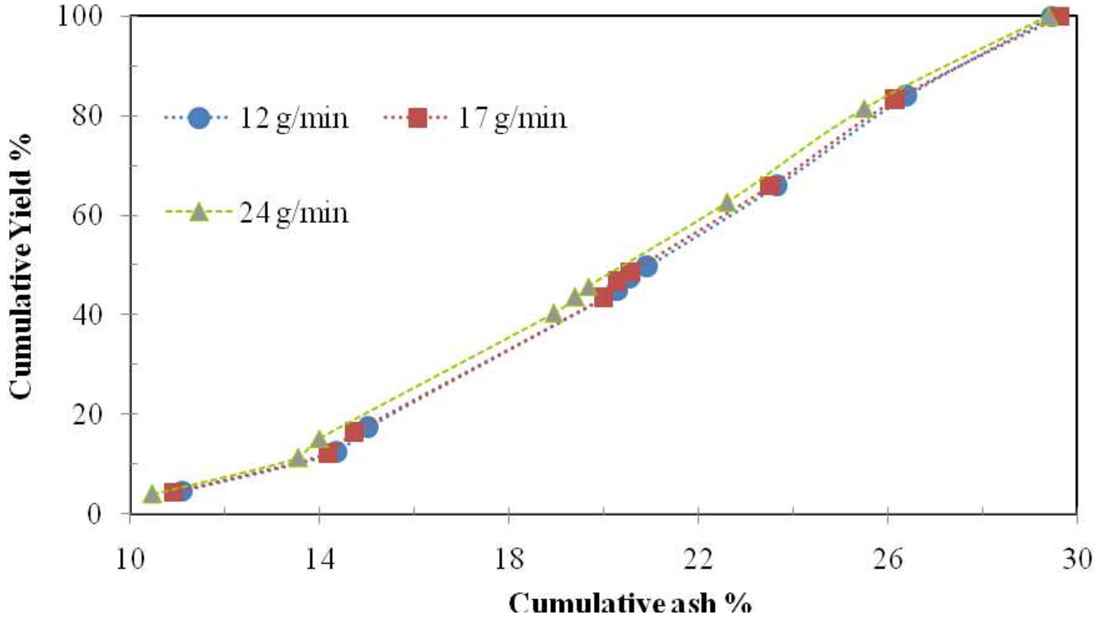

Figure B.31 Effect of feed rate on Majuba coal under second stage test at a constant splitter distance, separating voltage, air velocity and charging voltage.

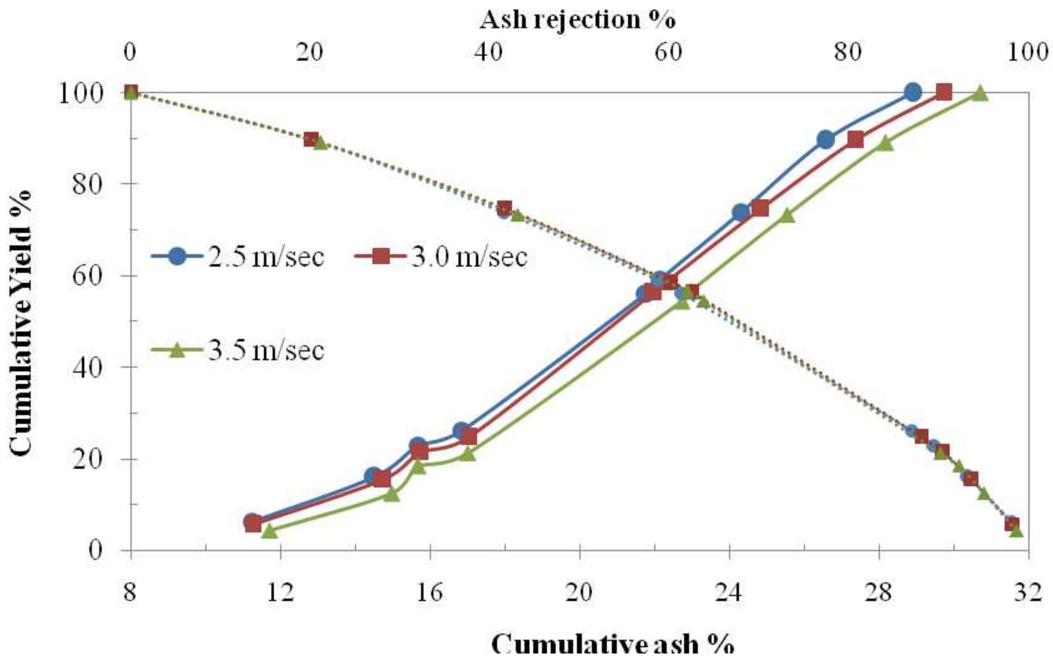

Figure B.32 Effect of Co-flow on Majuba coal under second stage test at a constant splitter distance, separating voltage, air velocity and charging voltage.

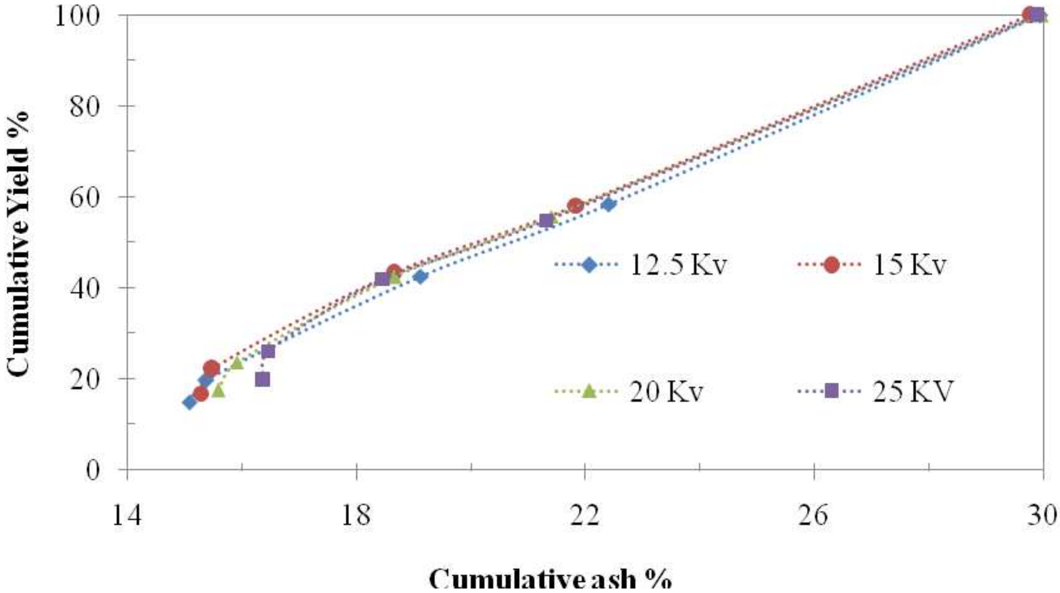

Figure B.33 Effect of separating voltage on single and two stage test with Majuba coal at a constant separating voltage of 12.5 KV, air velocity of 1.9 m/sec, rotary speed of 2500 rpm, and splitter distance: R =0.6 cm

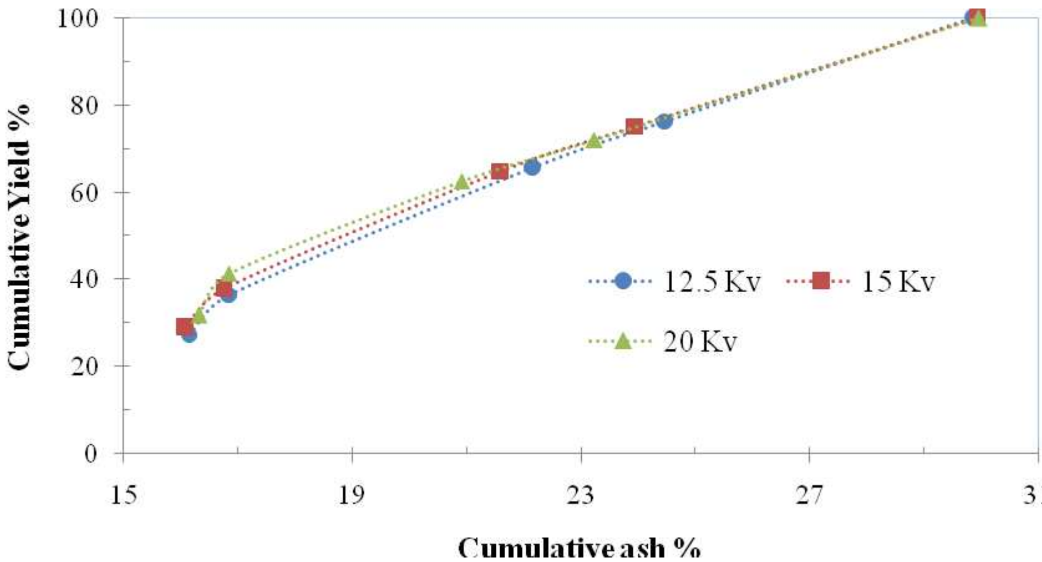

Figure B.34 Effect of separating voltage on single and two stage test with Majuba coal at a constant separating voltage of 12.5 KV, air velocity of 1.9 m/sec, rotary speed of 2500 rpm, and splitter distance: R =1.0 cm

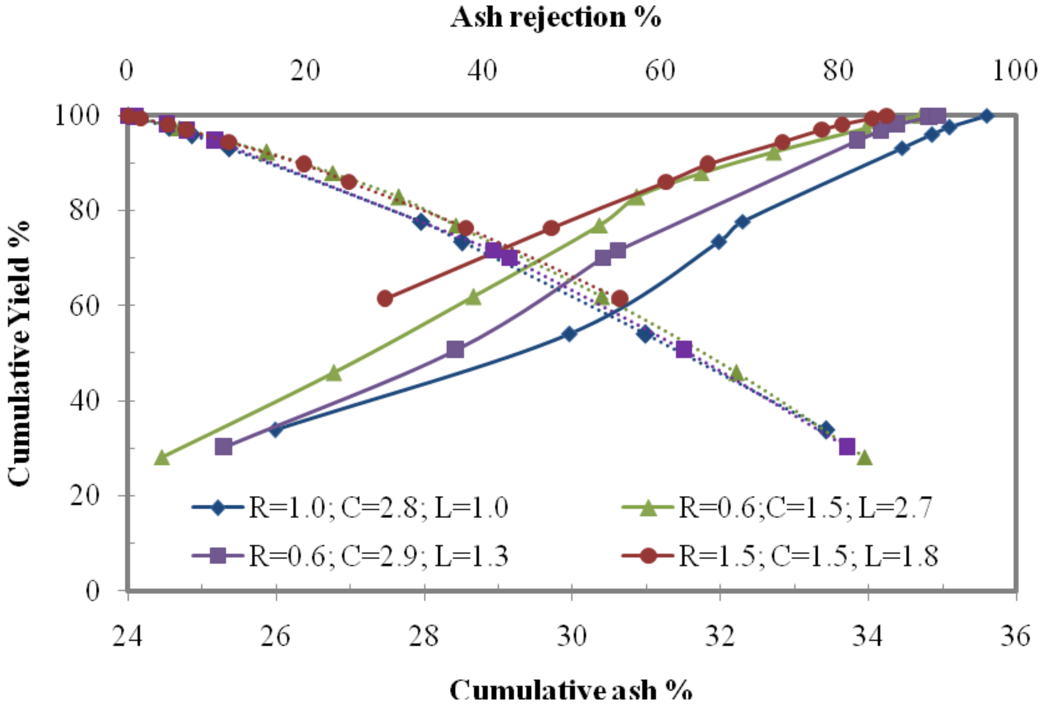

Figure B.35. The effect of splitter distance on recovery and grade of Klipfontein coal at constant charging voltage: 5 KV; separating voltage: 22.5 KV; and air velocity: 2.5 m/sec;

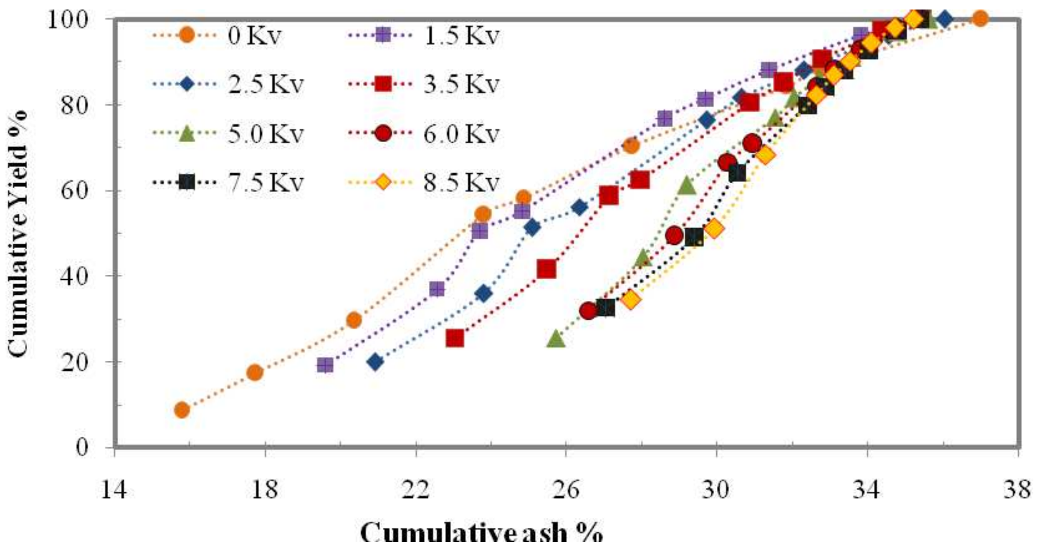

Figure B.36. The effect of charging voltage on recovery and grade of Klipfontein coal at constant rotary charger speed: 3000 rpm; separating voltage: 22.5 KV; air velocity: 2.5 m/sec; and separating voltage: 22.5 KV

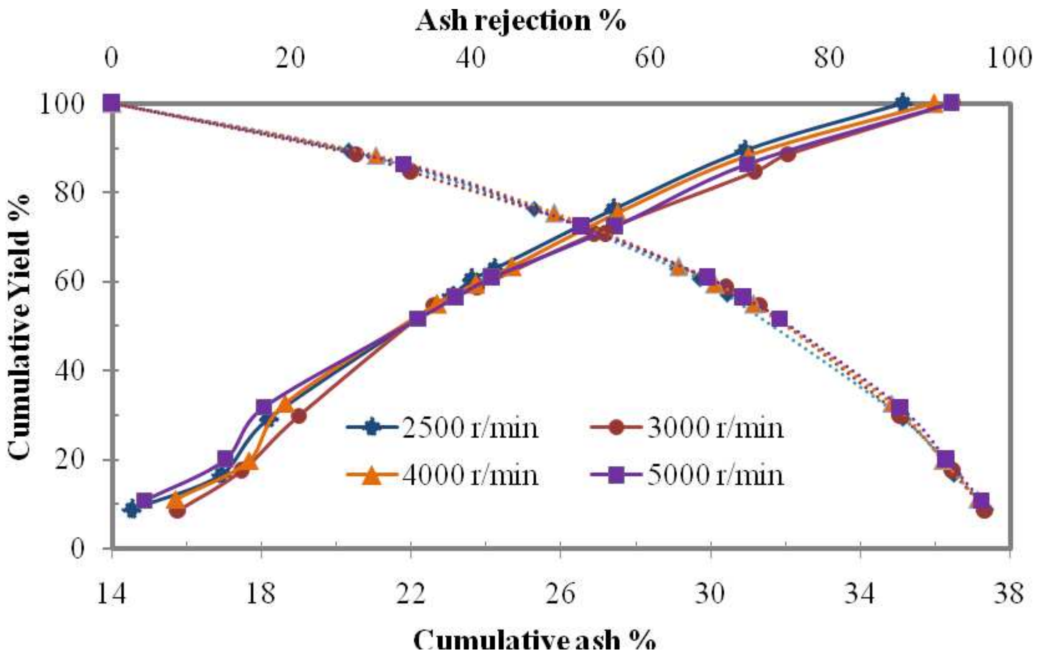

Figure B.37. The effect of rotary charger speed on recovery and grade of Klipfontein coal at constant separating voltage: 22.5 KV; charging voltage: 0 KV; air velocity: 2.5 m/sec; and separating voltage: 22.5 KV

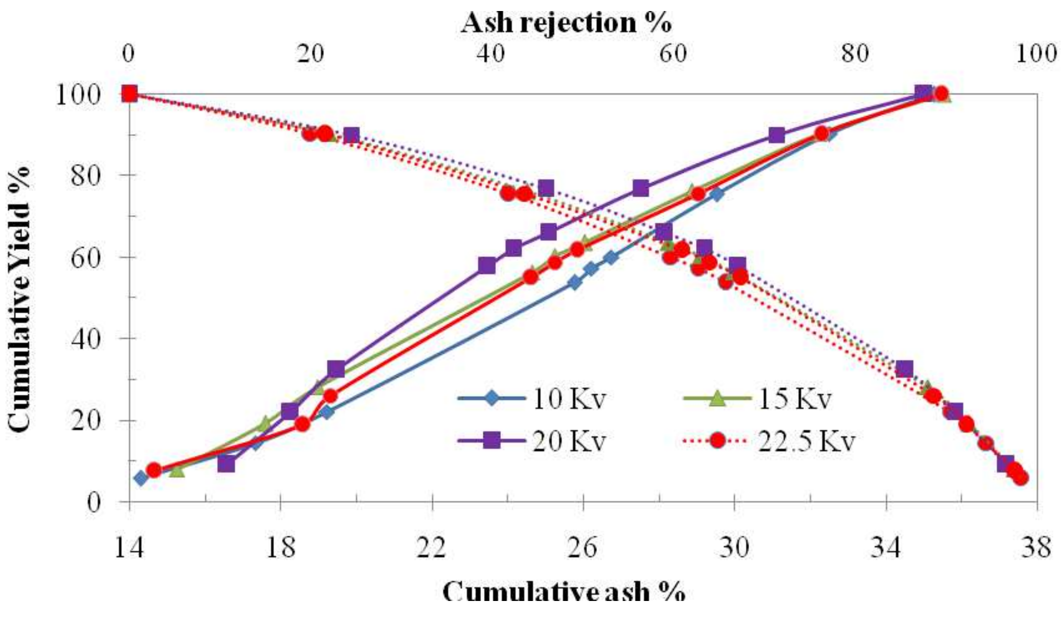

Figure B.38. The effect of separating voltage on recovery and grade of Klipfontein coal at constant charging voltage: 0 KV; air velocity: 2.5 m/sec; rotary charger speed: 3000; and separating voltage: 22.5 KV

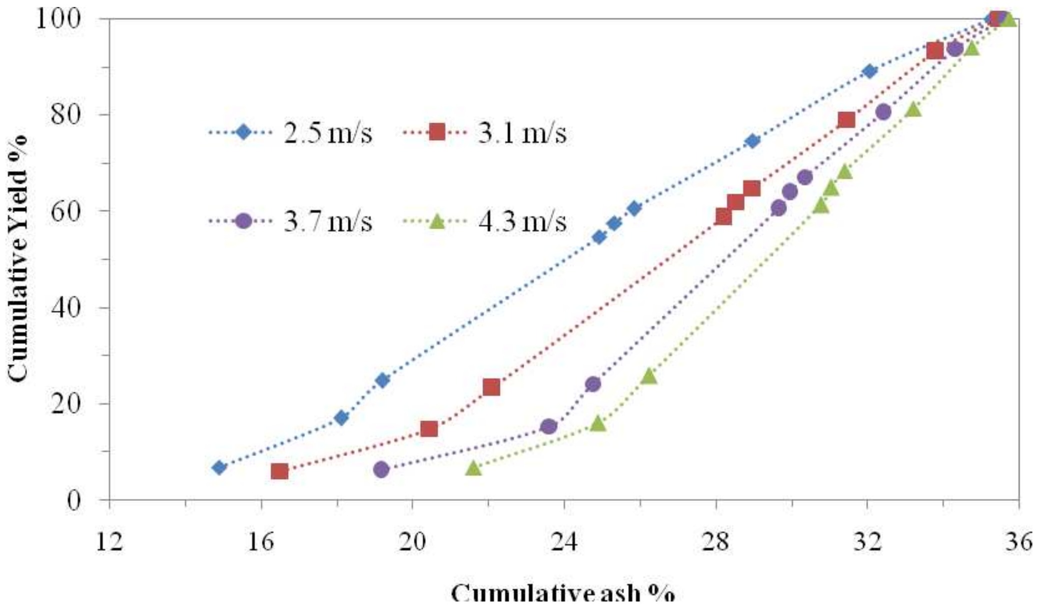

Figure B.39. The effect of air velocity on recovery and grade of Klipfontein coal at constant charging voltage: 0 KV; air velocity: 2.5 m/sec; rotary charger speed: 2500; and separating voltage: 12.5 KV

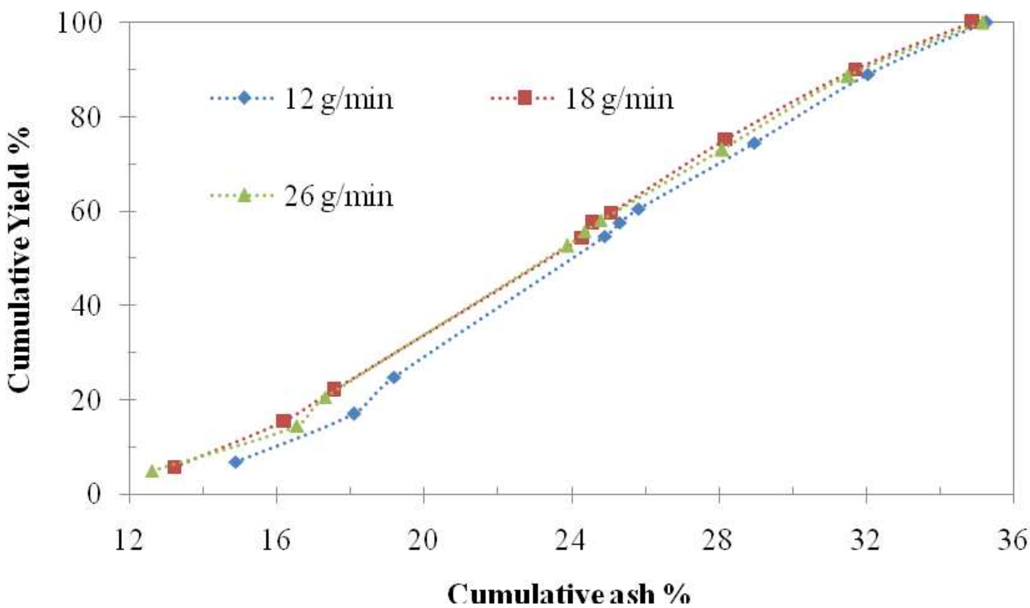

Figure B.40. The effect of feed rate on recovery and grade of Klipfontein coal at constant charging voltage: 0 KV; air velocity: 2.5 m/sec; rotary charger speed: 2500; and separating voltage: 12.5 KV

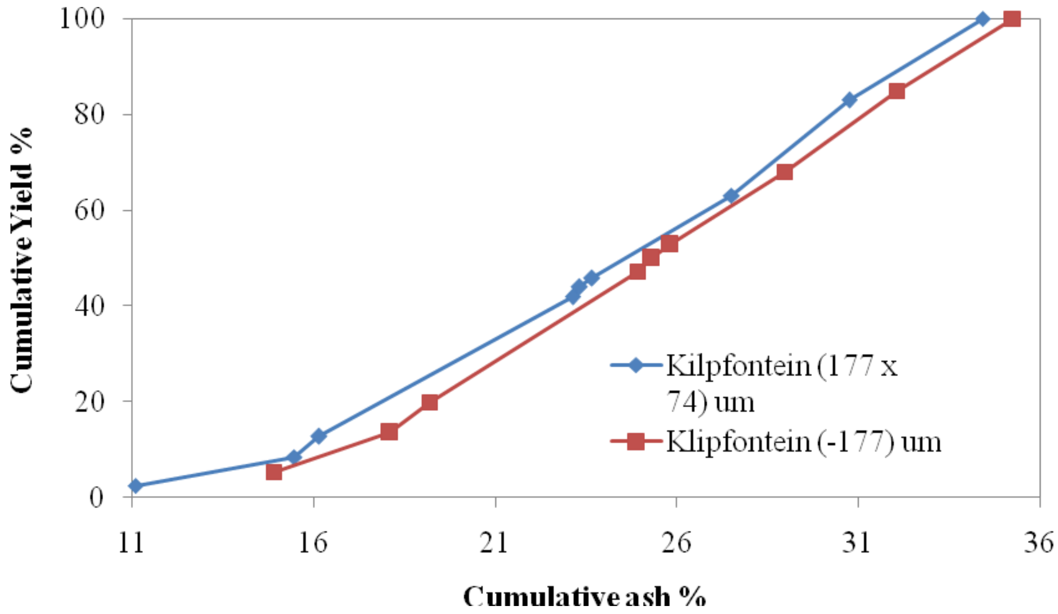

Figure B.41. The effect of particle size on recovery and grade of Klipfontein coal at constant charging voltage: 0 KV; air velocity: 2.5 m/sec; rotary charger speed: 2500; and separating voltage: 12.5 KV

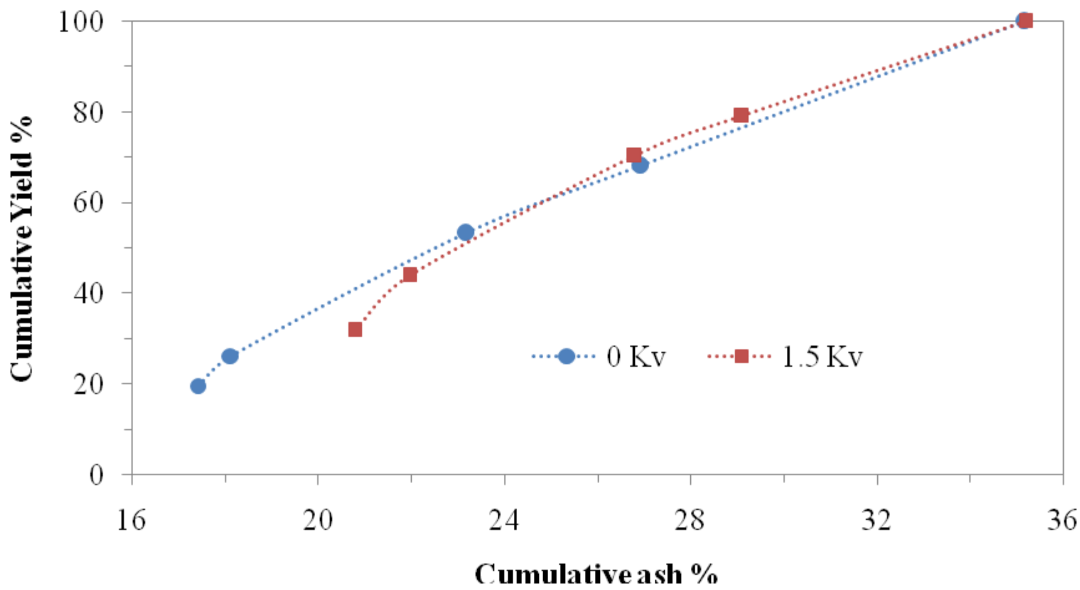

Figure B.42. Effect of charging voltage on single and two stage test with Klipfontein coal at a constant separating voltage of 12.5 KV, air velocity of 2.5 m/sec, rotary speed of 2500 rpm, and splitter distance: R =0.6 cm

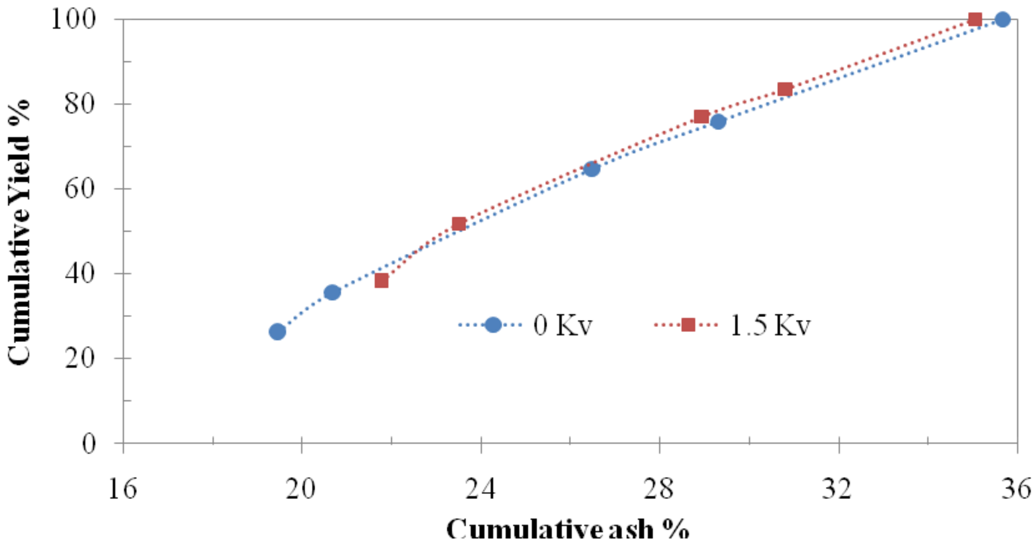

Figure B.43. Effect of charging voltage on single and two stage test with Klipfontein coal at a constant separating voltage of 12.5 KV, air velocity of 2.5 m/sec, rotary speed of 2500 rpm, and splitter distance: R =1.0 cm

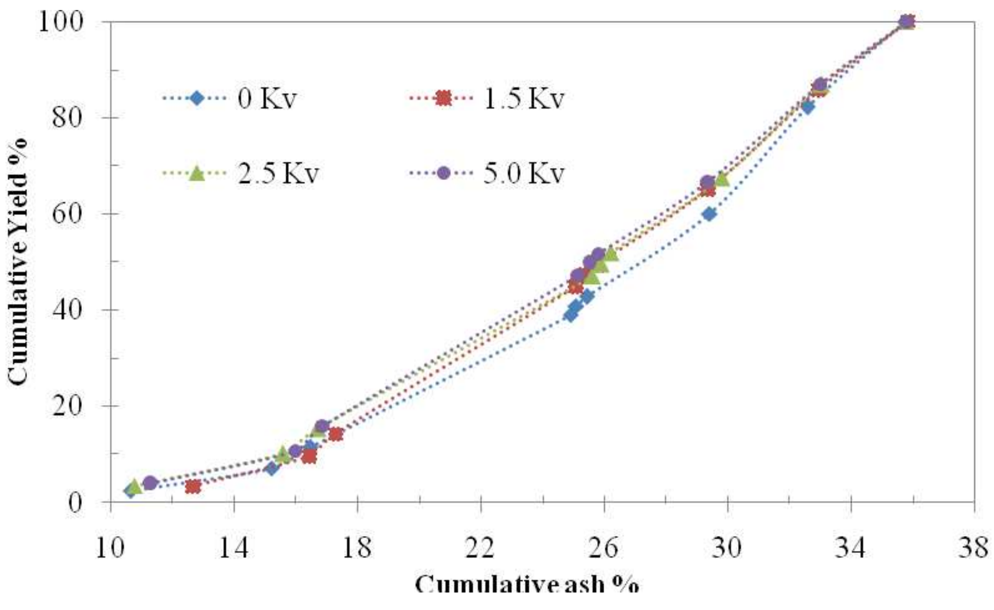

Figure B.44. The effect of charging voltage on recovery and grade of Khutala No. 4 seam coal at constant air velocity: 1.9 m/sec; rotary charger speed: 2500; and separating voltage: 12.5 KV

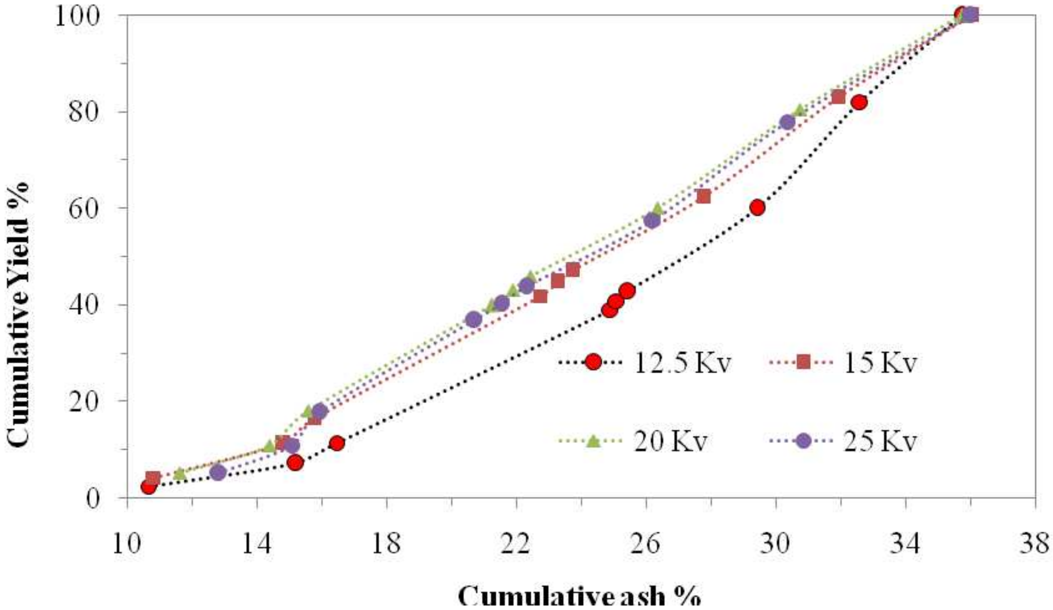

Figure B.45. The effect of separating voltage on recovery and grade of Khutala No. 4 seam coal at constant air velocity: 1.9 m/sec; rotary charger speed: 2500; and separating voltage: 12.5 KV

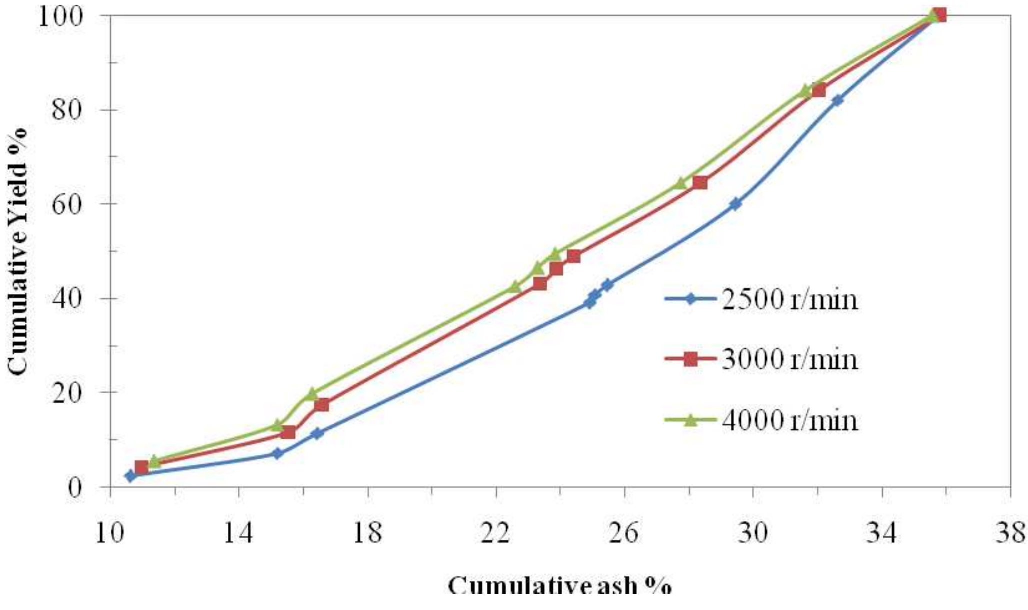

Figure B.46. The effect of rotary charger speed on recovery and grade of Khutala No. 4 seam coal at constant air velocity: 1.9 m/sec; charging voltage: 0 KV; and separating voltage: 12.5 KV

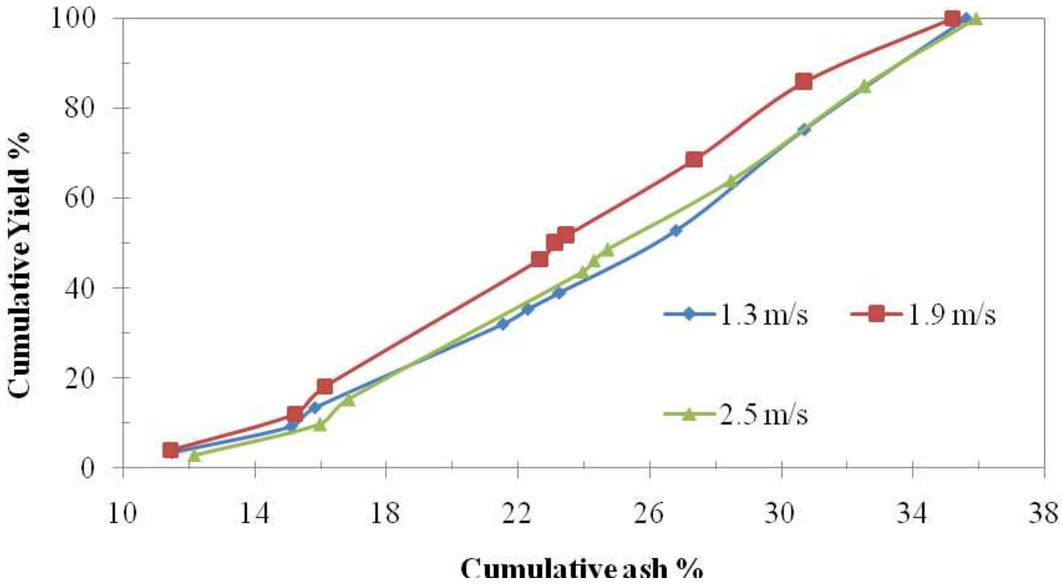

Figure B.47. The effect of air velocity on recovery and grade of Khutala No. 4 seam coal at constant rotary charger speed: 2500 rpm; charging voltage: 0 KV; and separating voltage: 12.5 KV

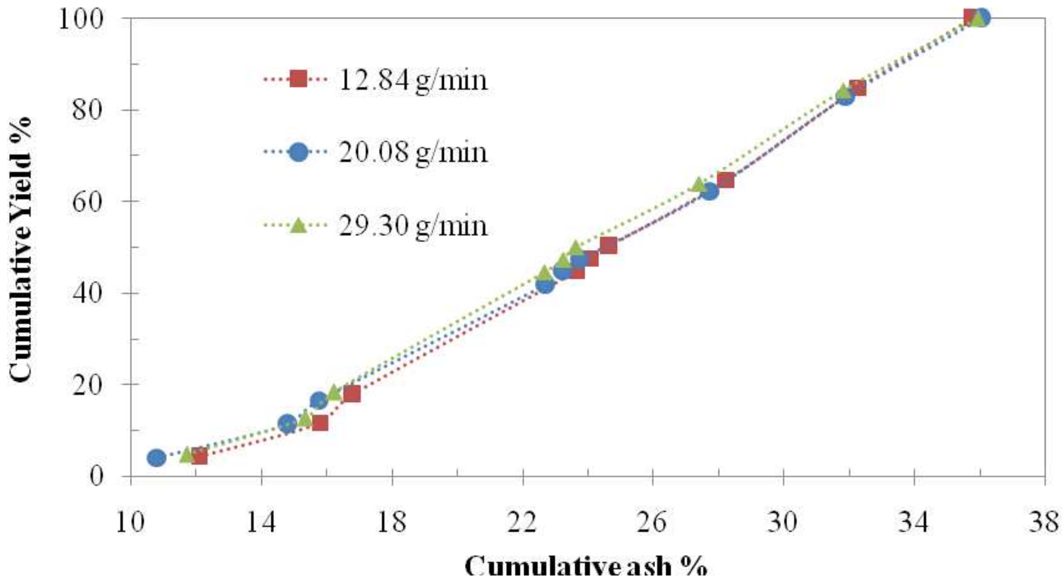

Figure B.48. The effect of feed rate on recovery and grade of Khutala No. 4 seam coal at constant air velocity: 1.9 m/sec; charging voltage: 0 KV; and separating voltage: 12.5 KV

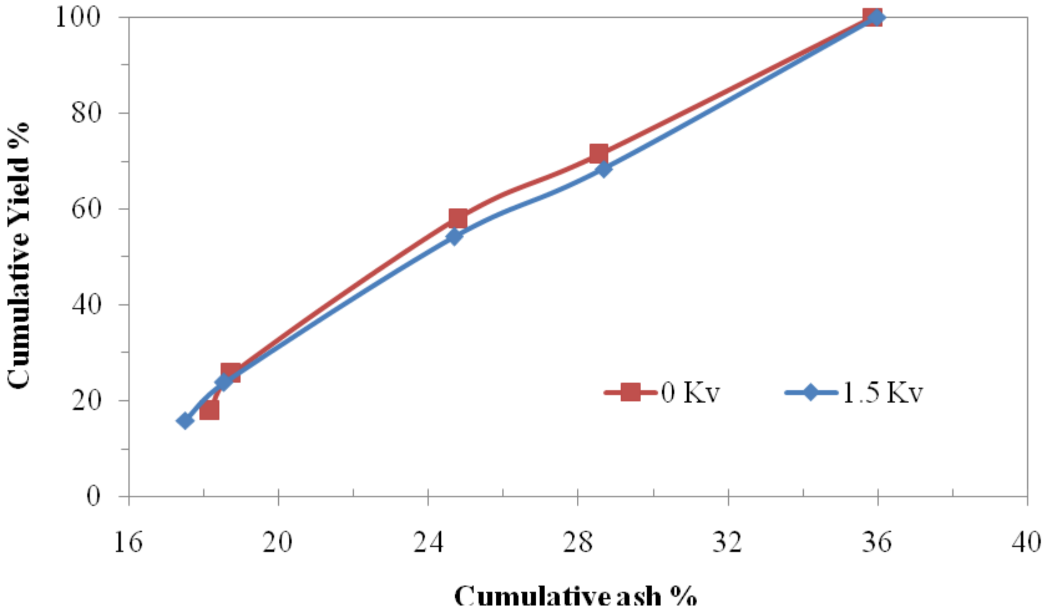

Figure B.49. Effect of charging voltage on single and two stage test with Khutala No. 4 seam coal at a constant separating voltage of 12.5 KV, air velocity of 1.9 m/sec, rotary speed of 2500 rpm, and splitter distance: R =0.6 cm

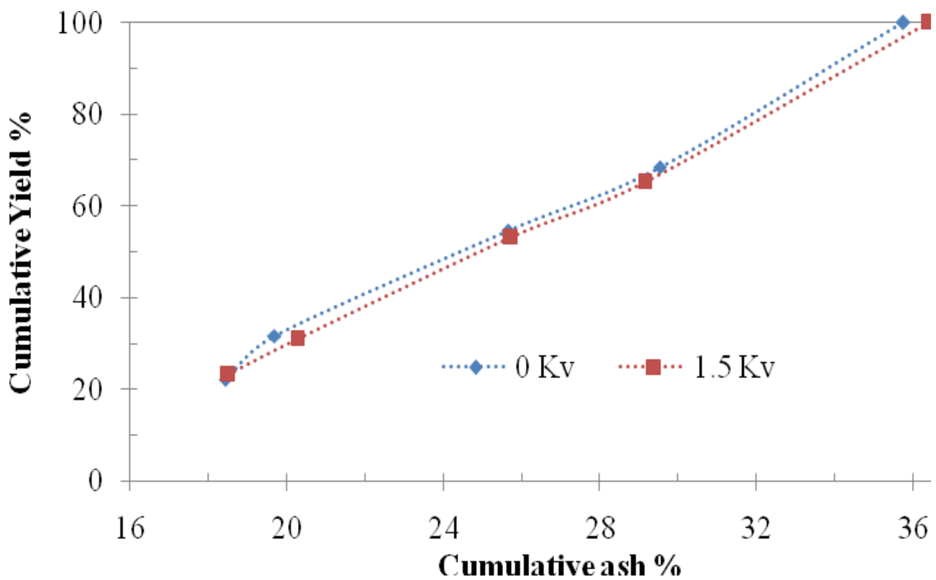

Figure B.50. Effect of charging voltage on single and two stage test with Khutala No. 4 seam coal at a constant separating voltage of 12.5 KV, air velocity of 1.9 m/sec, rotary speed of 2500 rpm, and splitter distance: R =1.0 cm

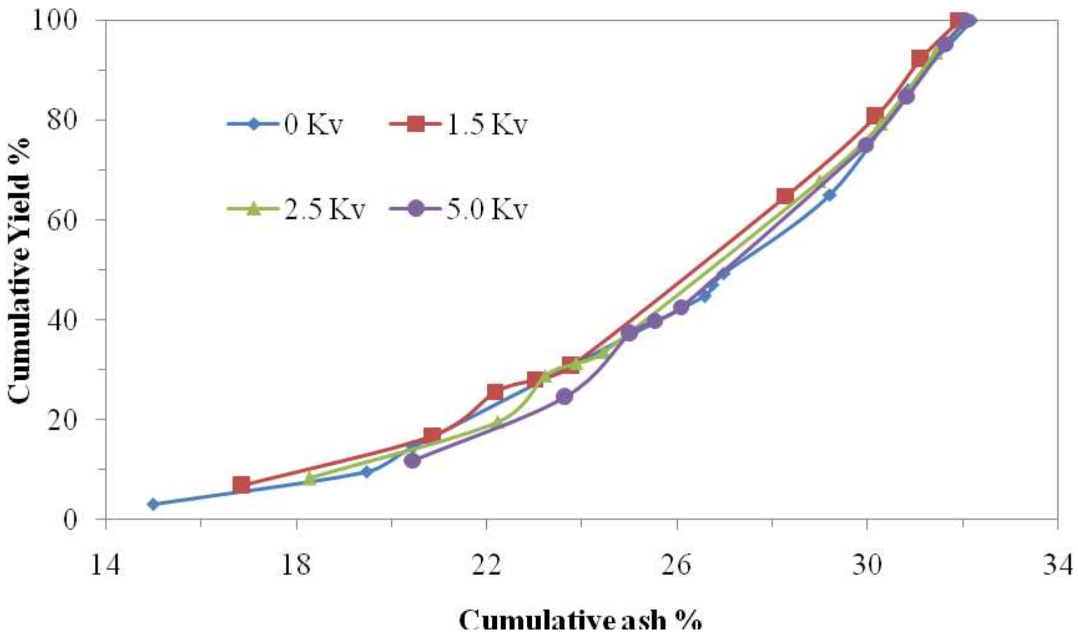

Figure B.51. The effect of charging voltage on recovery and grade of Polmaise coal at constant rotary charger speed: 2500 rpm; charging voltage: 0 KV; and separating voltage: 12.5 KV

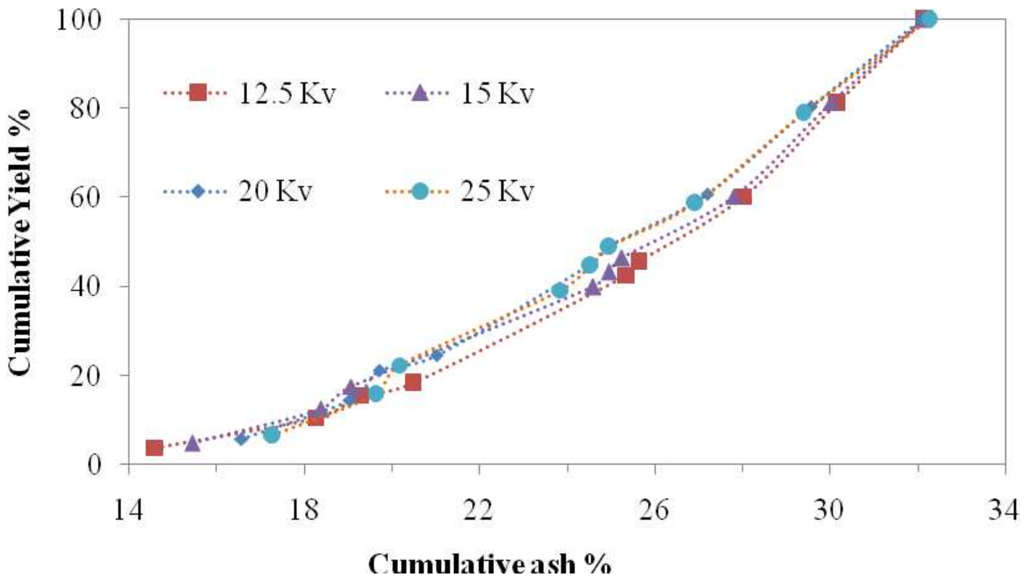

Figure B.52. The effect of separating voltage on recovery and grade of Polmaise coal at constant rotary charger speed: 2500 rpm; charging voltage: 0 KV; and separating voltage: 12.5 KV

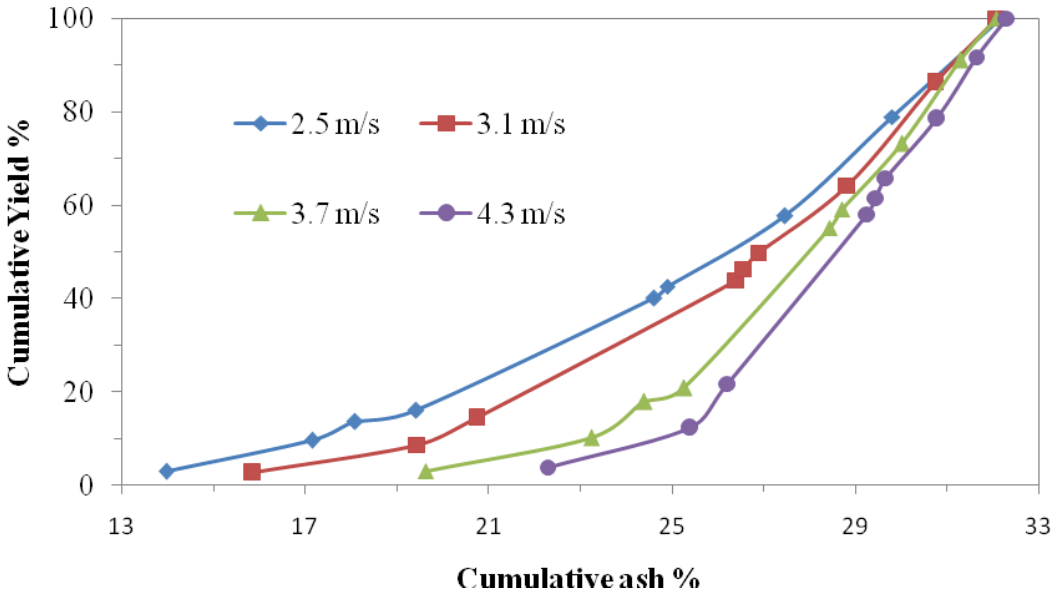

Figure B.53. The effect of separating voltage on recovery and grade of Polmaise coal at constant rotary charger speed: 2500 rpm; charging voltage: 0 KV; and separating voltage: 12.5 KV

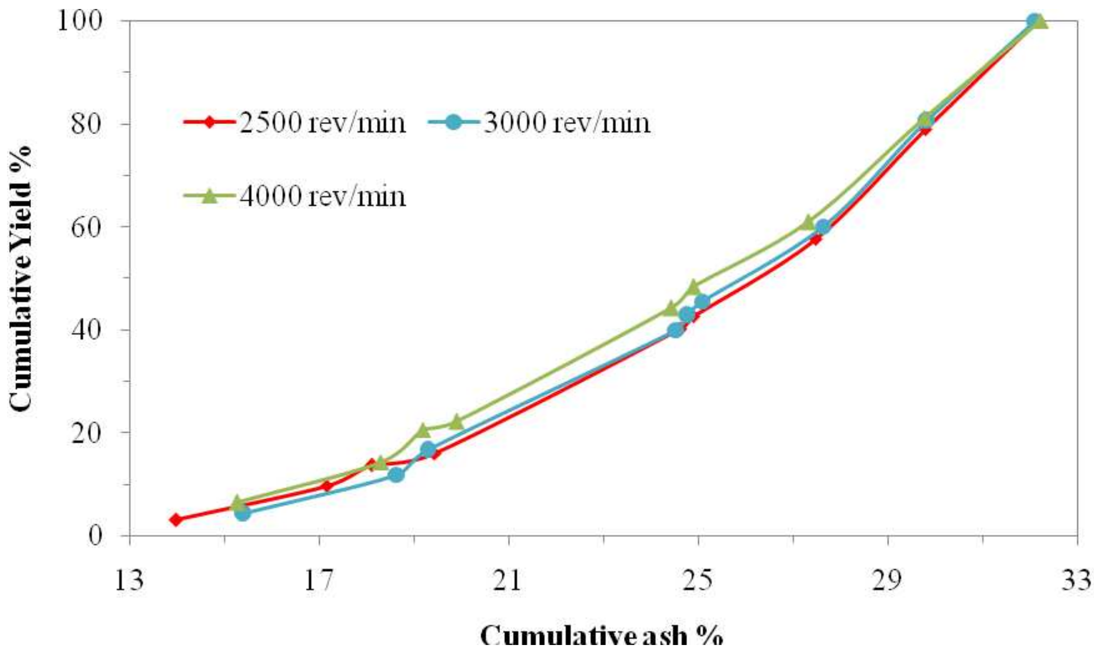

Figure B.54. The effect of rotary charger speed on recovery and grade of Polmaise coal at constant rotary charger speed: 2500 rpm; charging voltage: 0 KV; and separating voltage: 12.5 KV

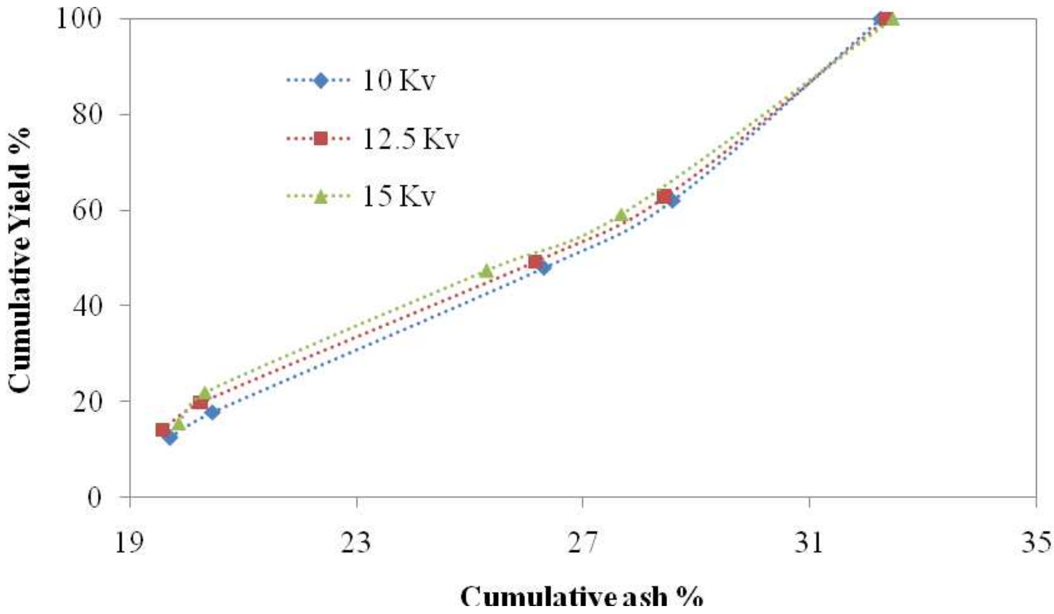

Figure B.55. Effect of separating voltage on single and two stage test with Polmaise coal at a constant charging voltage of 0 KV, air velocity of 1.9 m/sec, rotary speed of 2500 rpm, and splitter distance: R =0.6 cm

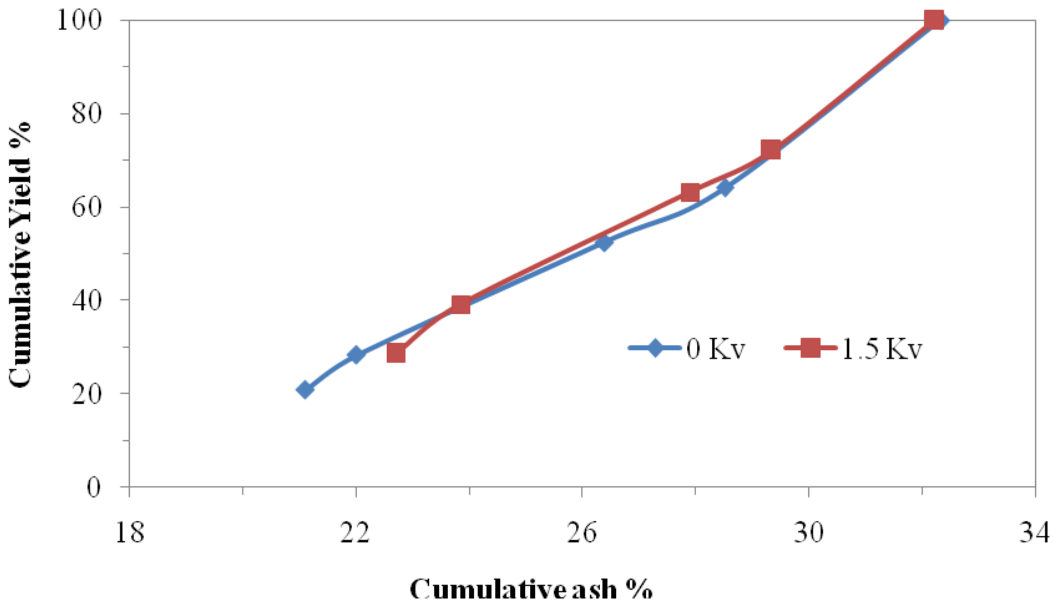

Figure B.56. Effect of separating voltage on single and two stage test with Polmaise coal at a constant charging voltage of 0 KV, air velocity of 1.9 m/sec, rotary speed of 2500 rpm, and splitter distance: R =1.0 cm

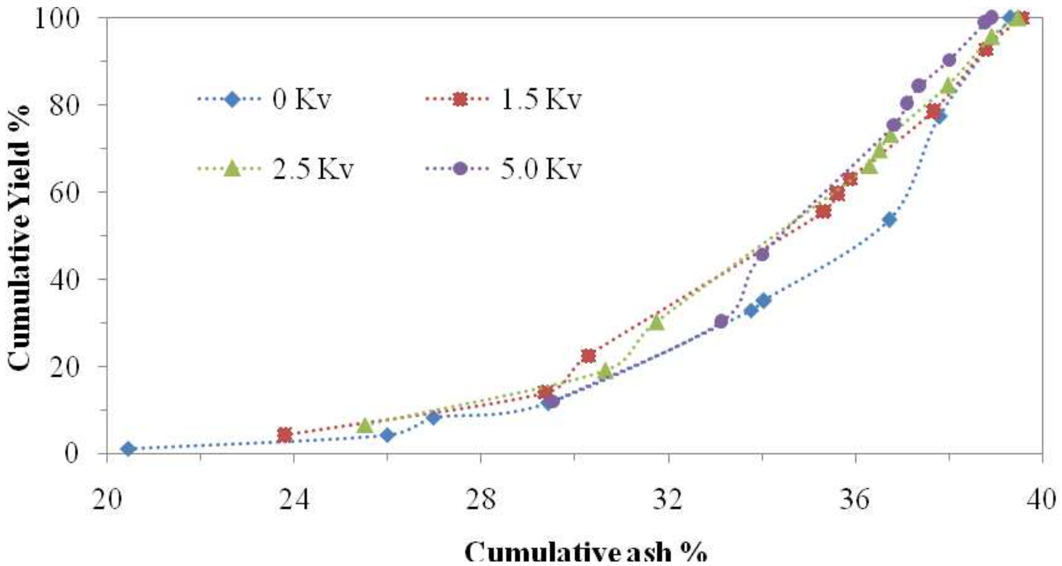

Figure B.57. The effect of charging voltage on recovery and grade of New Vaal coal at constant rotary charger speed: 2500 rpm; separating voltage: 12.5 KV; and air velocity: 2.5 m/sec

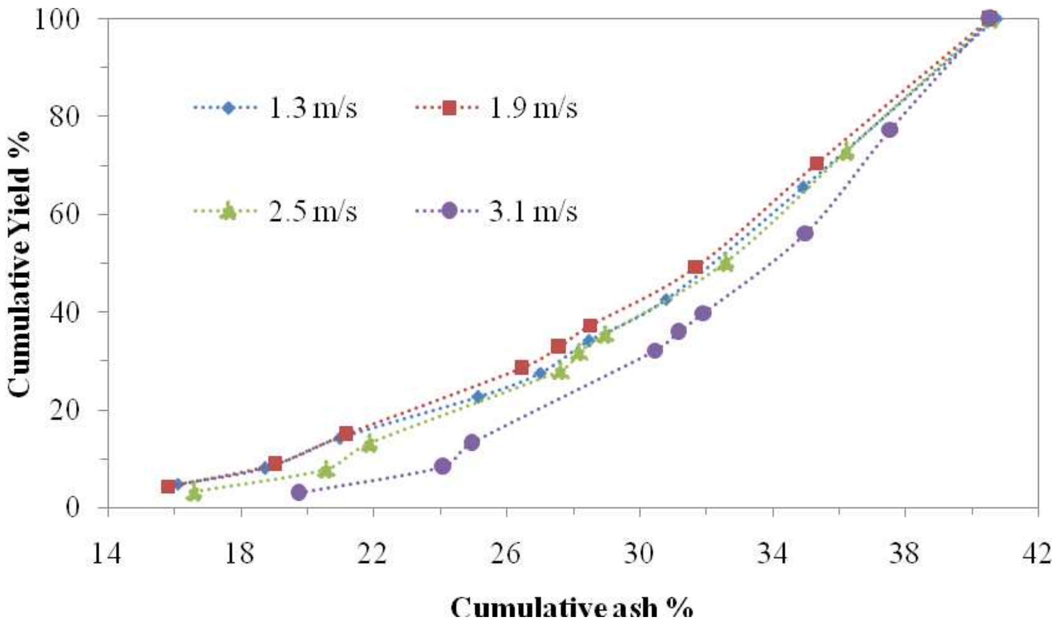

Figure B.58. The effect of air velocity on recovery and grade of New Vaal coal at constant rotary charger speed: 2500 rpm; separating voltage: 12.5 KV; and charging voltage: 0 KV

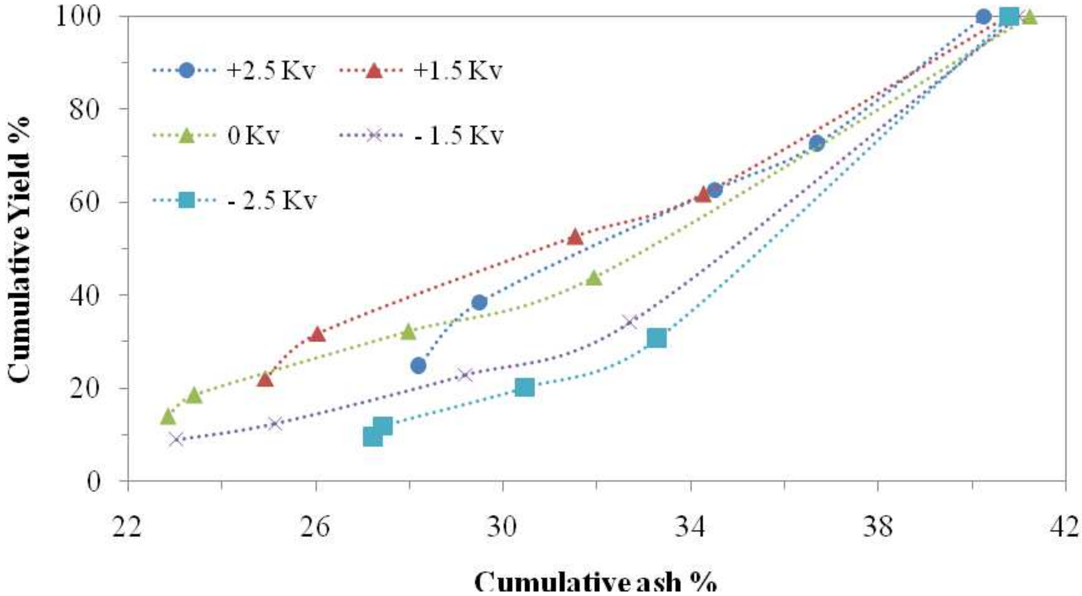

Figure B.59. The effect of charging voltage (charge reversal) on recovery and grade of New Vaal coal at constant rotary charger speed: 2500 rpm; separating voltage: 12.5 KV; and charging voltage: 0 KV; and splitter distance: R =0.6 cm